

**Selective Carbon-Carbon Bond Activation of Ethers
by Rhodium Porphyrins**

LAI, Tsz Ho

A Thesis Submitted in Partial Fulfillment
of the Requirements for the Degree of
Doctor of Philosophy
in
Chemistry

The Chinese University of Hong Kong

May 2010

UMI Number: 3445949

All rights reserved

INFORMATION TO ALL USERS

The quality of this reproduction is dependent upon the quality of the copy submitted.

In the unlikely event that the author did not send a complete manuscript and there are missing pages, these will be noted. Also, if material had to be removed, a note will indicate the deletion.



UMI 3445949

Copyright 2011 by ProQuest LLC.

All rights reserved. This edition of the work is protected against unauthorized copying under Title 17, United States Code.



ProQuest LLC
789 East Eisenhower Parkway
P.O. Box 1346
Ann Arbor, MI 48106-1346

Thesis/Assessment Committee

Professor SHING, Tony Kung Ming (Chair)

Professor CHAN, Kin Shing (Thesis Supervisor)

Professor LEUNG, Wing Por (Committee Member)

Professor LAU, Chak-Po (External Examiner)

Table of Contents

	Page
Table of Contents	i
Acknowledgement	v
Abbreviations	vi
Structural Abbreviations of Porphyrin	vii
Abstract	viii
Chapter 1 Introduction to Carbon-Carbon Bond Activation	1
1.1 Carbon-Carbon Bond Cleavages by Organic Reagent	1
1.1.2 Intramolecular Carbon-Carbon Bond Cleavage	1
1.1.2.1 Radical Rearrangement	2
1.1.2.2 Carbocation Rearrangement	3
1.1.3 Intermolecular Carbon-Carbon Bond Cleavage	4
1.1.3.1 Carbon-Carbon Bond Cleavage by Halogen Radical	4
1.1.3.2 Electrophilic Cleavage of Hydrocarbons by Strong Acids	5
1.2 Carbon-Carbon Bond Activation (CCA) by Transition Metal Complexes	7
1.2.1 Electrophilic Activation of Hydrocarbon by Transition Metal Complexes	7
1.2.2 Thermodynamic and Kinetic Considerations in CCA and CHA	9
1.2.3 Protocols of CCA by Transition Metal Complexes	10
1.2.3.1 CCA in Strained System	10
1.2.3.2 CCA Driven by Aromatization	12
1.2.3.3 Chelation-Assisted CCA	13
1.2.3.4 CCA through β -Carbon Elimination	17
1.2.3.5 CCA through Formal Alkane Metathesis	19
1.2.4 CCA by High Valent Transition Metal Complexes	22
1.3 Classification of CCA of Organic Substrates	25
Chapter 2 Introduction to Metalloporphyrin	29
2.1 Porphyrin Ligands and Metalloporphyrins	29
2.2 Chemistry of Rhodium(III) Porphyrins	30

2.2.1 Bond Activation Reactions by Rhodium(III) Porphyrins	31
2.3 Chemistry of Rhodium(II) Porphyrins	33
2.3.1 Carbon-Carbon Bond Activation by Rhodium(II) Porphyrin Complex	35
2.4 Carbon-Carbon Bond Activation of Ethers by Rh(por)CH ₂ CH ₂ OH	36
2.5 Chemistry of Transition Metal Hydroxide	37
2.6 Chemistry of Metalloporphyrin Hydroxide	39
2.6.1 Examples of Metalloporphyrin Hydroxide	39
2.6.2 Redox of Metalloporphyrin Hydroxide	42
2.7 Scope of the Thesis	44
Chapter 3 Carbon-Carbon Bond Activation of Ethers by Rhodium(II) Porphyrin	45
3.1 Introduction	45
3.2 Preparation of starting materials	45
3.2.1 Synthesis of Porphyrins	45
3.2.2 Synthesis of Rhodium Porphyrins	46
3.3 Carbon-Carbon Bond Activation of Ethers by Rhodium(II) Porphyrin	47
3.3.1 Ligand Effects	47
3.3.2 Porphyrin Effects	49
3.3.3 Scope of Reaction	50
3.4 Mechanistic Investigation of CCA of Ether with Rh ^{II} (tmp)	51
3.4.1 Possible Mechanism for the CCA of Ether with Rh ^{II} (tmp)	51
3.4.2 NMR Monitoring of CCA Reaction	52
3.4.3 Fate of Organic Coproducts	53
3.4.3.1 Phosphine Effect - Observation of Suspected (PPh ₃)Rh(tmp)OR	55
3.4.3.2 Intramolecular Trapping with Cyclic Ether	56
3.4.4 Energetic Consideration of C-C Bond Cleavage with Rh ^{II} (tmp)	58
3.4.5 Alternative CCA Mechanism by Rh(tmp)OH	59
3.4.5.1 Disproportionation of (PPh ₃)Rh(tmp)(H ₂ O)	59
3.4.5.2 Energetic Consideration of C-C Bond Cleavage with Rh(tmp)OH	61

3.4.5.3 Base and Water Effects	62
3.5 Summary	64
Chapter 4 Base-Promoted Carbon-Carbon Bond Activation of Ethers by Rhodium(III) Porphyrins	65
4.1 Introduction	65
4.2 Attempted Synthesis of Rhodium(III) Porphyrin Hydroxide	65
4.3 Carbon-Carbon Bond Activation of Ethers by Rhodium(III) Porphyrin Hydroxide	68
4.3.1 Base Effects	68
4.3.2 Counter Anion Effects	69
4.3.3 Porphyrin Effects	70
4.3.4 Temperature Effects	71
4.3.5 Scope of Symmetrical Ethers	72
4.3.6 Scope of Unsymmetrical Ethers	73
4.4 X-Ray Structures of Rh(tmp) ^I Bu, Rh(ttp) ^I Bu and Rh(t ₄ -CF ₃ pp)Bu	75
4.5 Mechanistic Investigation	79
4.5.1 NMR Monitoring of CCA of Ether	79
4.5.2 Reaction Intermediates: Rh(tmp)H, [Rh ^I (tmp)] ⁻ and Rh ^{II} (tmp)	83
4.5.2.1 Rh(tmp)H	83
4.5.2.2 [Rh ^I (tmp)] ⁻	85
4.5.2.3 Rh ^{II} (tmp)	86
4.5.3 Rh(tmp)OH	87
4.5.4 Promoting Roles of KOH in Interconversion of Rhodium Porphyrin Species	88
4.5.4.1 Ligand Substitution	88
4.5.4.2 Reducing Agent	90
4.5.4.3 Based-Promoted Dehydrogenation of Rh(tmp)H	93
4.5.4.4 Hydroxide-Induced Disproportionation of Rh ^{II} (tmp)	98
4.6 Thermodynamic and Kinetic Considerations of Selective CCA on Bu ₂ O	98
4.7 Summary of Reaction Mechanism	100
4.8 Potential Catalytic CCA of Ether	101
4.9 Conclusion	103

Chapter 5	Experimental Section	105
Reference		161
Appendix		173
X-Ray Crystallography Data		174
NMR Spectra		188
List of Publications		197

Acknowledgement

First and foremost, I would like to express my most sincere gratitude to my supervisor, Prof. Kin Shing Chan, for his invaluable advice, patient guidance, and enthusiasm in my postgraduate studies throughout my research work and the preparation of this thesis.

I would also like to give thanks to all members of the Department of Chemistry for their help and technical support in all circumstances.

Special thanks are given to all my seniors: Dr. Siu Kwan Yeung, Dr. Lirong Zhang, Dr. Xinzhu Li and Ms. Cheuk Man Lau for their support and encouragement when I started my research.

Last but not least, I want to thank all my dear former and current group members: Mr. Peng Fai Chiu, Mr. Yun Wai Chan, Ms. Baozhu Li, Mr. Chi Wai Cheung, Ms. Xu Song, Mr. Kwong Shing Choi, Mr. Man Ho Lee, Mr. Hong Sang Fung, Ms. Ching Chi Au, Dr. Jenkins Yin Ki Tsang, Ms. Siu Yin Lee and Ms. Yingying Qian for their encouragement and helpful discussion. I wish them continued success in their research and career.

December, 2009.

Tsz Ho Lai

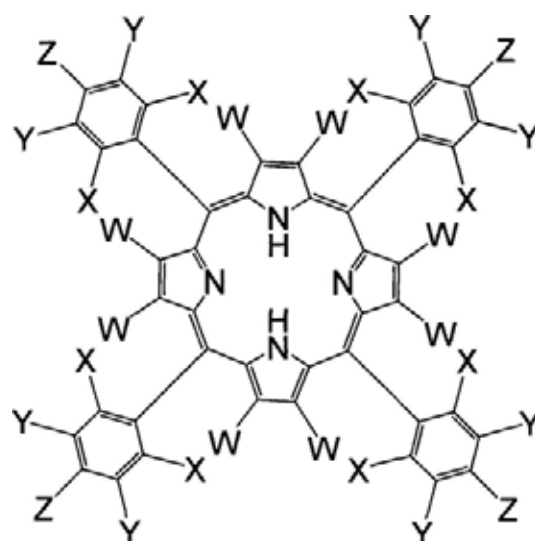
Department of Chemistry

The Chinese University of Hong Kong

Abbreviations

δ	: chemical shift	M^+	: molecular ion
Anal	: analytical	Me	: methyl
BDE	: bond dissociation energy	mg	: milligram (s)
Bn	: benzyl	MHz	: megahertz
ⁱ Bu	: <i>iso</i> -butyl	min	: minute (s)
ⁿ Bu	: <i>n</i> -butyl	mL	: milliliter (s)
^t Bu	: <i>tert</i> -butyl	mmol	: millimole (s)
Calcd.	: calculated	MS	: mass spectrometry
CCA	: C-C bond activation	NMR	: nuclear magnetic resonance
CHA	: C-H bond activation	OEt	: ethoxide
COA	: C-O bond activation	OPr	: propoxide
d	: day (s)	por	: porphyrin dianion
d	: doublet (NMR)	ⁿ Pr	: <i>n</i> -propyl
dd	: doublet of doublets (NMR)	ppm	: part per million
dt	: doublet of triplets (NMR)	P(Cy) ₃	: tricyclohexylphosphine
e	: electron	P(ⁱ Pr) ₃	: tri(<i>isopropyl</i>)phosphine
E.A.	: ethyl acetate	PPh ₃	: triphenylphosphine
ESI (MS)	: electrospray ionization(MS)	P(<i>toly</i>) ₃	: tri(<i>p-toly</i>)phosphine
Et	: ethyl	P(4-MeO-Ph) ₃	: tri(4-methoxyphenyl)- phosphine
FAB (MS)	: fast atom bombardment (MS)	Ph	: phenyl
GC-MS	: gas chromatography (MS)	PhCN	: benzonitrile
g	: gram (s)	ⁱ Pr	: <i>isopropyl</i>
h	: hour (s)	q	: quartet (NMR)
HOMO	: highest occupied molecular orbital	qu	: quintet (NMR)
HRMS	: high resolution mass spectrometry	R	: alkyl group
Hz	: hertz	RDS	: rate determining step
IR	: infrared	r.t.	: room temperature
J	: coupling constant	s	: singlet (NMR)
L	: ligand	t	: triplet (NMR)
LUMO	: lowest unoccupied molecular orbital	TLC	: thin-layer chromatography
m	: multiplet (NMR)	THF	: tetrahydrofuran
M	: molarity	TMS	: tetramethylsilane
		μ L	: microliter (s)

Structural Abbreviations of Porphyrins



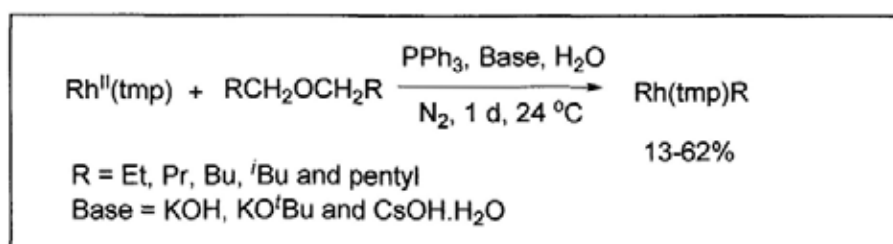
Nomenclature of Porphyrins

Abbreviations	Porphyrin	Substituents			
		W	X	Y	Z
H ₂ tmp	5,10,15,20-tetramesitylporphyrin	H	Me	H	Me
H ₂ ttp	5,10,15,20-tetratolylporphyrin	H	H	H	Me
H ₂ t ₄ -CF ₃ pp	5,10,15,20-tetra(4-trifluoromethylphenyl)- porphyrin	H	H	H	CF ₃
H ₂ tdbpp	5,10,15,20-tetra(3,5-di- <i>t</i> -butylphenyl)- porphyrin	H	H	^t Bu	H
H ₂ oep	2,3,7,8,12,13,17,18-octaethylporphyrin	Et	-	-	-
H ₂ tspp	5,10,15,20-tetra(<i>p</i> -sulfonatophenyl)- porphyrin	H	H	H	SO ₃ ⁻

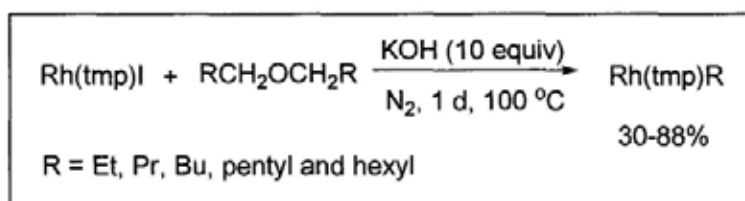
Abstract

The objective of this thesis focuses on studies of selective, base-promoted aliphatic carbon(α)-carbon(β) bond activation (CCA) of ethers with rhodium(II) and rhodium(III) meso-tetramesitylporphyrin complexes ($\text{Rh}^{\text{II}}(\text{tmp})$ and $\text{Rh}(\text{tmp})\text{I}$). The roles of potassium hydroxide in promoting the interconversions of rhodium porphyrin species ($\text{Rh}^{\text{II}}(\text{tmp})$, $\text{Rh}(\text{tmp})\text{I}$, $\text{Rh}(\text{tmp})\text{OH}$ and $\text{Rh}(\text{tmp})\text{H}$) will also be discussed.

Part 1 describes the selective C(α)-C(β) bonds cleavage of a series of aliphatic ethers ($\text{RCH}_2\text{OCH}_2\text{R}$: R = Et, Pr, Bu, ^iBu and pentyl) by $\text{Rh}^{\text{II}}(\text{tmp})$ using PPh_3 as the promoting ligand to give $\text{Rh}(\text{tmp})$ -alkyls bearing the C(β)-substituent in 13-40% yields at 24 °C. The rate and the yields of $\text{Rh}(\text{tmp})$ -alkyls decreased with increasing steric hindrance of ethers. Addition of bases such as KO^iBu , $\text{CsOH}\cdot\text{H}_2\text{O}$ and KOH as well as H_2O further promoted the product yields of the reactions with *n*-butyl ether to 56-62%. The reaction between $\text{Rh}^{\text{II}}(\text{tmp})$ and the cyclic ether, oxepane, at 24 °C for 1 day gave $\text{Rh}(\text{tmp})(\text{CH}_2)_5\text{OCHO}$ in 17% yield suggesting that $\text{Rh}(\text{tmp})\text{OH}$ is the key intermediate in the C-C cleavage step and presumably generated via the PPh_3^- , H_2O -, and OH^- -assisted disproportionation of $\text{Rh}^{\text{II}}(\text{tmp})$.

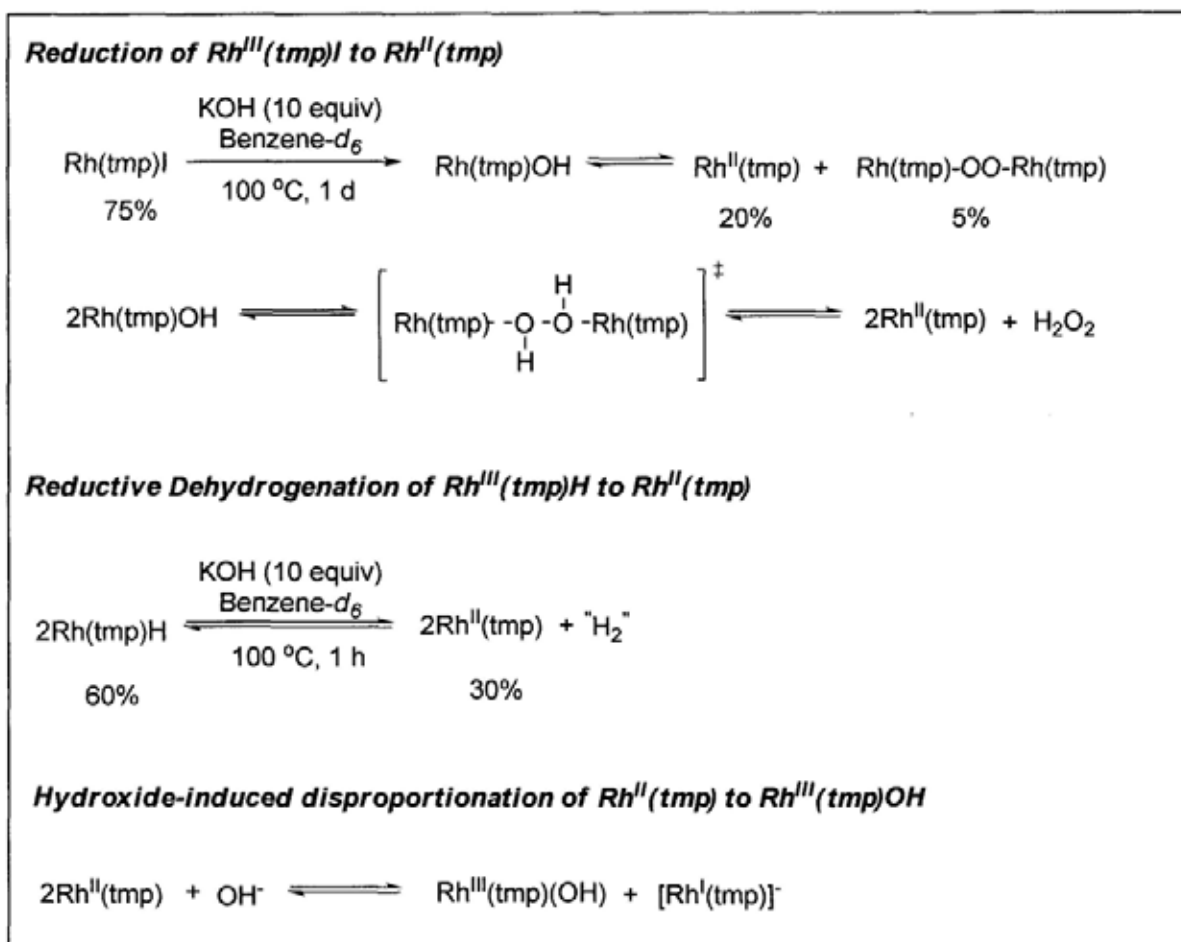


Part 2 describes the *in-situ* preparation of highly reactive Rh(tmp)OH directly from Rh(tmp)I and KOH at 100 °C for subsequent CCA with ethers. Rh(tmp)I was reacted with a series of aliphatic ethers (RCH₂OCH₂R: R = Et, Pr, Bu, pentyl and hexyl) in the presence of KOH (10 equiv) at 100 °C for 1 day to give Rh(tmp)alkyls in 30-88% yields. Rh^{II}(tmp) and Rh(tmp)H were observed throughout the course of reaction but reactivity studies suggested that they are the non-productive intermediates. Rather Rh(tmp)OH is the most probable species for the C-C bond cleavage.



Mechanistic investigation also revealed the promoting roles of KOH in the interconversions of Rh(tmp)-species. Firstly, the reduction of Rh(tmp)I to Rh^{II}(tmp) was observed. Rh(tmp)I reacted with KOH in benzene-*d*₆ at 100 °C for 1 day to give the reduction product of Rh^{II}(tmp) in 20% yield. Rh(tmp)OH intermediate is proposed to form via ligand substitution between Rh(tmp)I and KOH. Rh(tmp)OH can undergo bimolecular reductive elimination to give Rh^{II}(tmp) and H₂O₂. The formation of Rh(tmp)OH and H₂O₂ were supported by the observation of Rh(tmp)-OO-Rh(tmp) in 5% yield which is formed via the reaction between Rh^{II}(tmp) and trace amount of O₂, generated from the KI-, KOH- and Rh(tmp)-catalyzed decomposition of H₂O₂.

Secondly, the reductive dehydrogenation of $\text{Rh}(\text{tmp})\text{H}$ to $\text{Rh}^{\text{II}}(\text{tmp})$ was also observed. $\text{Rh}(\text{tmp})\text{H}$ reacted with KOH in benzene- d_6 at 100 °C for 1 hour to give $\text{Rh}^{\text{II}}(\text{tmp})$ in 30% yield. $[\text{Rh}^{\text{I}}(\text{tmp})]^-$ is proposed to form initially via the deprotonation of $\text{Rh}(\text{tmp})\text{H}$ with KOH and then reacts with the unreacted $\text{Rh}(\text{tmp})\text{H}$ to give $\text{Rh}^{\text{II}}(\text{tmp})$ via electron transfer. Thirdly, the hydroxide-induced disproportionation of $\text{Rh}^{\text{II}}(\text{tmp})$ to $\text{Rh}^{\text{III}}(\text{tmp})\text{OH}$ and $[\text{Rh}^{\text{I}}(\text{tmp})]^-$ has also been proposed.



摘要

本論文主要研究了二價銦和三價銦的間-四均三甲基苯基卟啉絡合物 ($\text{Rh}^{\text{II}}(\text{tmp})$ 和 $\text{Rh}^{\text{III}}(\text{tmp})\text{I}$) 與脂肪醚的反應，發現鹼可以促進 (α)-碳和(β)-碳鍵的選擇性活化。同時，討論了氫氧化鉀在各種銦卟啉絡合物($\text{Rh}^{\text{II}}(\text{tmp})$, $\text{Rh}(\text{tmp})\text{I}$, $\text{Rh}(\text{tmp})\text{OH}$ 和 $\text{Rh}(\text{tmp})\text{H}$) 之間相互轉化的作用。

第一部分介紹了在 24 °C 條件下， $\text{Rh}^{\text{II}}(\text{tmp})$ 與一系列脂肪醚 ($\text{RCH}_2\text{OCH}_2\text{R}$: $\text{R} =$ 乙基，丙基，丁基，異丁基和戊基) 的反應，發現添加三苯基膦 (PPh_3) 作為配體可以促進 α -碳和 β -碳鍵的選擇性活化，得到 β -碳與金屬銦相連的銦卟啉烷基絡合物，產率為 13-40%。隨著醚的空間位阻的增加，反應的速度以及銦卟啉烷基絡合物的產率都將隨之降低。在與正丁基醚的反應中發現，鹼性添加劑，例如叔丁基鉀，一水合氫氧化銣，氫氧化鉀和水，可以將產率進一步提高至 56-62%。在 24 °C 條件下， $\text{Rh}^{\text{II}}(\text{tmp})$ 與脂環醚 (環氧己烷) 反應一天，可以得到 $\text{Rh}(\text{tmp})(\text{CH}_2)_5\text{OCHO}$ ，產率為 17%。這說明 $\text{Rh}(\text{tmp})\text{OH}$ 是 C-C 鍵斷裂的關鍵性中間體，同時我們推測 $\text{Rh}^{\text{II}}(\text{tmp})$ 可以在三苯基膦，水或者氫氧根的促進下進行歧化反應得到 $\text{Rh}(\text{tmp})\text{OH}$ 。

第二部分描述了在 100 °C 的條件下， $\text{Rh}(\text{tmp})\text{I}$ 與氫氧化鉀直接反應，現場形成高活性的 $\text{Rh}(\text{tmp})\text{OH}$ ，然後進一步與醚進行碳-碳鍵活化反應。在 100 °C 條件下， $\text{Rh}(\text{tmp})\text{I}$ 與一系列脂肪醚 ($\text{RCH}_2\text{OCH}_2\text{R}$: $\text{R} =$ 乙基，丙基，丁基，戊基和己基) 反應一天，可以得到相應的銦卟啉烷基絡合物，產率為 30-88%。在反應過程中，觀察到了 $\text{Rh}^{\text{II}}(\text{tmp})$ 和 $\text{Rh}(\text{tmp})\text{H}$ ，但是對其反應的活性研究表明，它們不是活性中間體。相反， $\text{Rh}(\text{tmp})\text{OH}$ 則是最可能的斷裂碳-碳鍵的中間體。

機理研究顯示了氫氧化鉀在銦卟啉絡合物的相互轉化中的促進作用。首先， $\text{Rh}(\text{tmp})\text{I}$ 被還原成 $\text{Rh}^{\text{II}}(\text{tmp})$ 。在 100 °C，以氘代苯做溶劑的條件下， $\text{Rh}(\text{tmp})\text{I}$ 與氫氧化鉀反應一天，得到 20%的還原產物 $\text{Rh}^{\text{II}}(\text{tmp})$ 。我們推測 $\text{Rh}(\text{tmp})\text{I}$ 與氫氧化鉀經過配體的取代反應，得到 $\text{Rh}(\text{tmp})\text{OH}$ ， $\text{Rh}(\text{tmp})\text{OH}$ 可以進行雙分子的還

原消除形成 $\text{Rh}^{\text{II}}(\text{tmp})$ 和雙氧水。推測 $\text{Rh}^{\text{II}}(\text{tmp})$ 和雙氧水的形成，主要是在實驗上觀察到了 $\text{Rh}(\text{tmp})\text{-OO-Rh}(\text{tmp})$ ，產率為 5%。 $\text{Rh}(\text{tmp})\text{-OO-Rh}(\text{tmp})$ 的形成，可能是由于雙氧水在碘化鉀，氫氧化鉀以及銻卟啉的催化作用下分解，產生微量的氧氣，氧氣進一步與 $\text{Rh}^{\text{II}}(\text{tmp})$ 反應，從而形成 $\text{Rh}(\text{tmp})\text{-OO-Rh}(\text{tmp})$ 。其次， $\text{Rh}(\text{tmp})\text{H}$ 還原脫氫形成 $\text{Rh}^{\text{II}}(\text{tmp})$ 。在 $100\text{ }^{\circ}\text{C}$ ，以氘苯為溶劑的條件下， $\text{Rh}(\text{tmp})\text{H}$ 與氫氧化鉀反應一個小時，得到 $\text{Rh}^{\text{II}}(\text{tmp})$ ，產率為 30%。我們推測，在反應初期， $\text{Rh}(\text{tmp})\text{H}$ 在氫氧化鉀的作用下脫氫，形成 $[\text{Rh}^{\text{I}}(\text{tmp})]^{-}$ ，然後 $[\text{Rh}^{\text{I}}(\text{tmp})]^{-}$ 與未反應的 $\text{Rh}(\text{tmp})\text{H}$ 進一步進行電子轉移，得到 $\text{Rh}^{\text{II}}(\text{tmp})$ 。最后， $\text{Rh}^{\text{II}}(\text{tmp})$ 在氫氧根的誘導作用下，進行歧化反應，形成 $\text{Rh}^{\text{III}}(\text{tmp})\text{OH}$ 和 $[\text{Rh}^{\text{I}}(\text{tmp})]^{-}$ 。

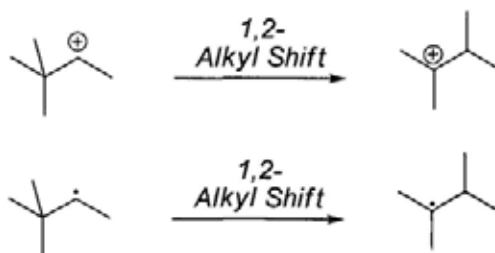
Chapter 1 Introduction to Carbon-Carbon Bond Activation

1.1 Carbon-Carbon Bond Cleavage By Organic Reagent

Chemical transformations that involve either the intramolecular or intermolecular cleavage of carbon-carbon bond are important and mechanistically interesting. Development and mechanistic understanding of the carbon-carbon bond cleavage of hydrocarbons can usher a new era in organic synthesis and hydrocarbon refinery.

1.1.2 Intramolecular Carbon-Carbon Bond Cleavage

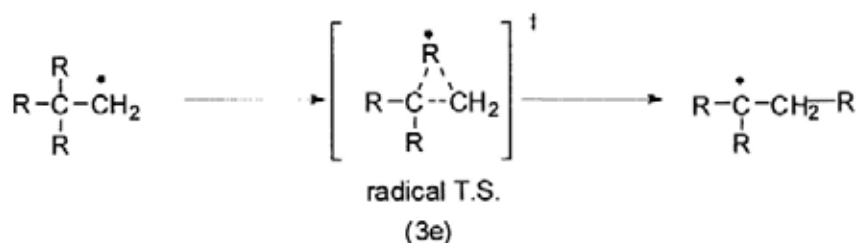
Examples of intramolecular carbon-carbon bond cleavage were reported in a variety of classic organic chemical transformations, reactive species such as carbocation and carbon center radical are usually proposed as the reaction intermediates. Those reactive intermediates are known to undergo skeletal rearrangement through hydride shift or alkyl shift (C-C bond cleavage) to generate a more stable intermediate (Scheme 1.1).¹⁻⁴



Scheme 1.1 Intramolecular Carbocation/Radical Rearrangement

1.1.2.1 Radical Rearrangement

1,2-alkyl shift in radicals is found to be less common than the analogous rearrangement in carbocations which is due to its less stable three electrons transition state in radical rearrangement (Scheme 1.2)¹⁻² because electrons in excess of two can be accommodated only in anti-bonding molecular orbital of much higher energy.

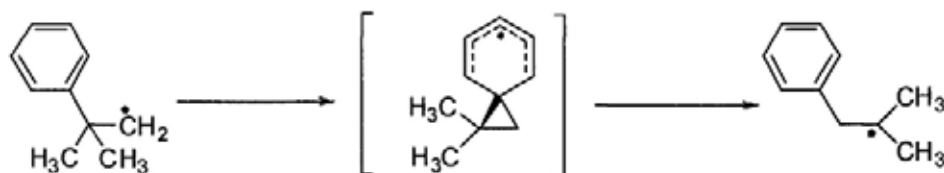


Scheme 1.2 1,2-Alkyl shift involving 3e Transition State

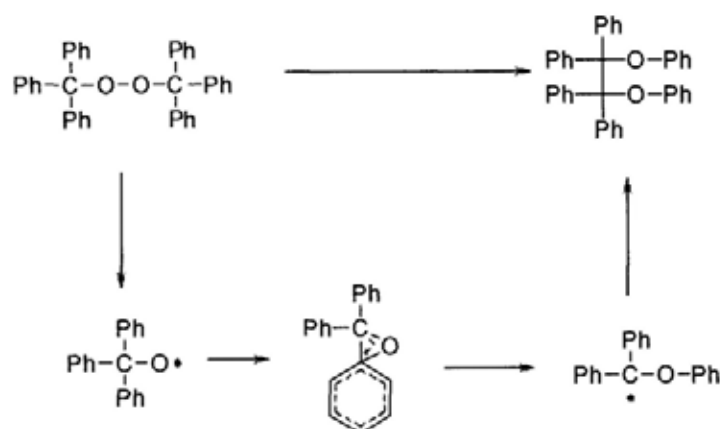
Specifically, the facile 1,2-vinyl and 1,2-aryl shifts are known to occur in the system of cyclopropylcarbinyl radical (Scheme 1.3), cyclohexadienyl radical (Scheme 1.4) and benzylic radical (Scheme 1.5), respectively.¹⁻²



Scheme 1.3 Rearrangement of Cyclopropylcarbinyl Radical to Butenyl Radical



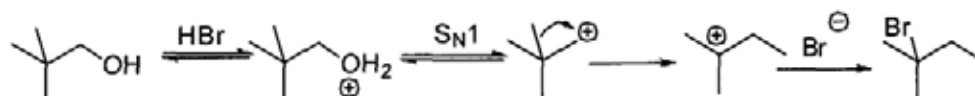
Scheme 1.4 1,2-Aryl Shifts Involving Cyclohexadienyl Radical Intermediate



Scheme 1.5 Conversion of *Bis*(triphenylmethylperoxide) to Tetraphenylethane via Radical Rearrangement

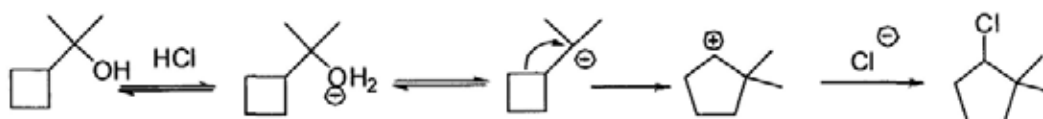
1.1.2.2 Carbocation Rearrangement

The most common carbocation rearrangement involving carbon-carbon bond clipping is the $\text{S}_{\text{N}}1$ reaction between the alcohol and acid. For example, in the bromination of neopentyl alcohol, a primary carbocation formed initially would undergo Wagner-Meerwein shift³ (1,2-methyl shift), in which the methyl group is rapidly migrated to the adjacent carbon, to generate a more stable tertiary carbocation before bromination takes place (Scheme 1.6).²



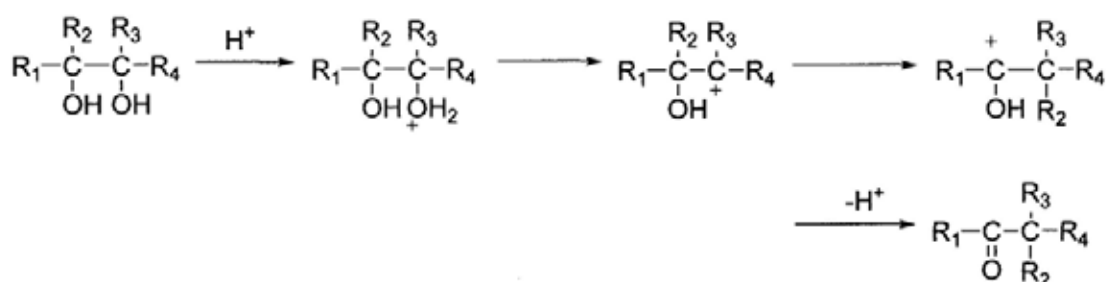
Scheme 1.6 Carbocation Rearrangement in Bromination of Primary Alcohol

This type of carbocation rearrangement is also driven by the relief of ring strain such as cyclobutane (Scheme 1.7).²



Scheme 1.7 Expansions of Cyclobutane to Cyclopentane via Carbocation Rearrangement

Similar carbocation rearrangement is also found in the conversion of glycol to aldehyde/ketone under acidic conditions via the Pinacol rearrangement^{1,5}(Scheme 1.8).



Scheme 1.8 Pinacol Rearrangement of Glycols

1.1.3 Intermolecular Carbon-Carbon Bond Cleavage

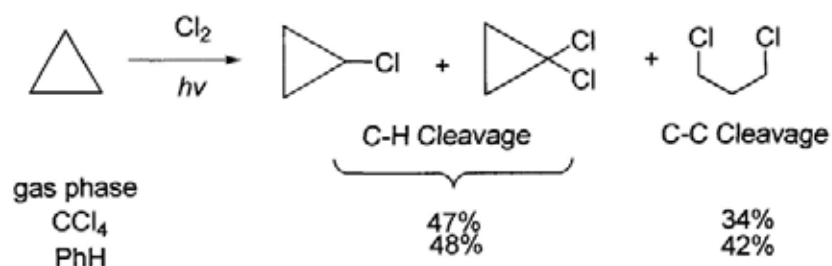
The non-polar bond nature of hydrocarbons makes the direct intermolecular cleavage of C-C bond more difficult and challenging. Traditionally, C-C bond is thermally cracked in very harsh conditions at high temperature (>500 °C) and high pressure in the presence of acid catalysts.⁶

1.1.3.1 Carbon-Carbon Bond Cleavage by Halogen Radical

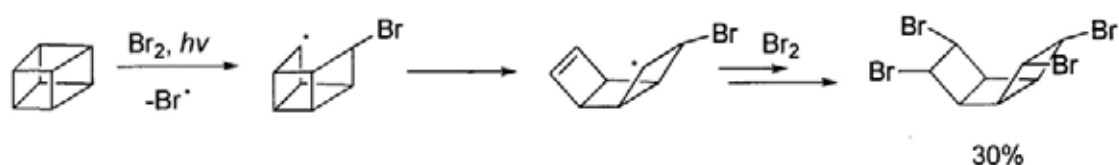
Intermolecular carbon-carbon cleavage by radical is rarely reported. Special examples include free-radical halogenation of ring strained hydrocarbons such as

cyclopropane (Scheme 1.9), cubane (Scheme 1.10), and propellane (Scheme 1.11)

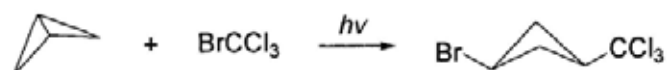
under illuminating conditions.⁷



Scheme 1.9 C-H and C-C Chlorination of Cyclopropane in Different Solvents



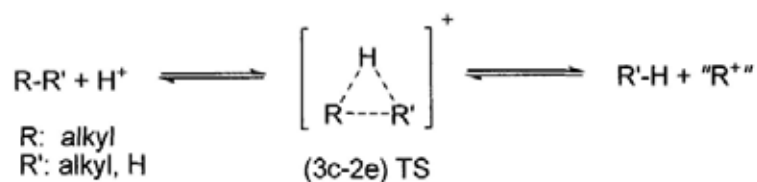
Scheme 1.10 Ring-Opening Bromination of Cubane



Scheme 1.11 Radical Cleavage of [1.1.1]Propellane

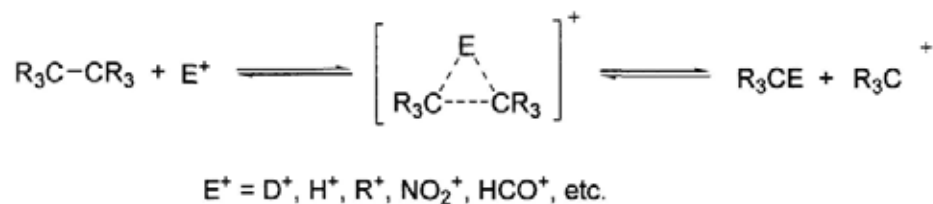
1.1.3.2 Electrophilic Cleavage of Hydrocarbon by Strong Acids

Strong Lewis and Bronsted acid can sufficiently protonate alkane to give a pentacoordinated carbonium ion, $[\text{R}_4\text{CH}]^+$, followed by the scission of the C-C bond into a lower alkane and another carbocations (Scheme 1.12).⁸ Olah reported a series of remarkable hydrocarbon activation in superacidic media.⁹



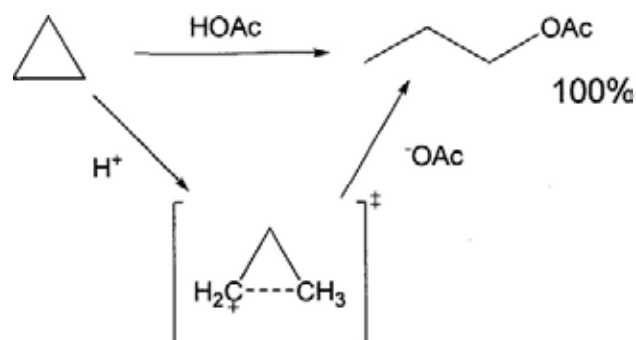
Scheme 1.12 A three-center two-electron transition state of protolysis of alkane

Superacid such as HF/BF₃, HF/SbF₅, HF/TaF₅, FSO₃H/SbF₅ were firstly reported to catalyze C-C bond cleavage in the liquid phase. For example, neopentane reacts with the extremely strong acid FSO₃H-SbF₅ to give methane and *t*-butyl cation.¹⁰ Solid acid catalyst systems, such as those based on Nafion H, longer-chain perfluorinated alkanesulfonic acids, and fluorinated graphite intercalates, were subsequently developed and utilized for heterogeneous reactions.¹⁰ Furthermore, a broad range of reactions with varied electrophiles were also found to be feasible when superacidic, low-nucleophilic reaction conditions were used (Scheme 1.13).¹⁰



Scheme 1.13 Electrophilic C-C Bond Cleavage

Wiberg *et al.* also reported the examples of electrophilic cleavage of cycloalkanes or bicycloalkanes with acetic acid (Scheme 1.14). The especially high reactivity of those cycloalkanes over other hydrocarbons is most likely due to their high strain energy that making it more reactive.



Scheme 1.14 Acetolysis of Alkylcyclopropane

However, the C-C bond activation of hydrocarbon by super acids is usually not selective and practical as the rearrangement of the reactive carbocation intermediate commonly occurs in an uncontrollable manner.

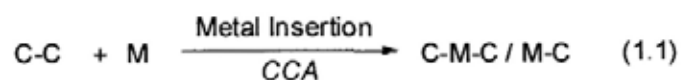
1.2 Carbon-Carbon Bond Activation (CCA) by Transition Metal Complexes

1.2.1 Electrophilic Activation by Transition Metal Complexes

Besides strong acids, the high valent transition metals, species that have multiple vacant lobe-shaped d orbitals, are also strong electrophiles and Lewis acids.⁸ Due to their strong Lewis acidities, it is reasonable that the highly electrophilic transition metal $[M^{n+}]$ can also activate a C-C bond via a 3-center-2-electron transition state in a similar manner (Scheme 1.15).¹²



Scheme 1.15 Electrophilic clipping of alkane by a transition metal complex



Selective carbon-carbon bond activation (CCA) of unreactive hydrocarbon by a transition metal complex in mild conditions is one of the most important subjects in the field of organometallic chemistry due to its basic chemistry and potential industrial applications (eq 1.1).¹³ However, selective cleavage of a non-polar single C-C σ -bond in organic substrates is usually less competitive than the facile carbon-hydrogen bond activation (CHA) as a C-H bond is sterically more accessible and statistically more abundant over a C-C bond. The energy barrier for the C-C insertion is found to be 14 – 20 kcal/mol¹⁴ higher than that for the C-H clipping, although C-C bonds have lower bond dissociation energies (Table 1.1).

Table 1.1 Bond Dissociation Energies of C-C Bond and C-H Bond of Selected Organic Compounds¹⁵

	Organic Compound	C-C Bond (kcal/mol)	C(α)-H Bond (kcal/mol)
1	CH ₃ -CH ₃	90	100
2	CH ₃ -CH ₂ OH	87	95
3	C ₂ H ₅ -CH ₂ OCH ₃	83	93
4	CH ₃ C(O)CH ₃	84	96

1.2.2 Thermodynamic and Kinetic Considerations in CCA and CHA

In fact, CCA reaction of hydrocarbon by transition metal complexes is thermodynamic feasible, especially for 2nd and 3rd row transition metal. The normal C-C bond strength is 85-90 kcal/mol¹⁵ while the M-C bond strength is around 30-40 kcal/mol for 1st row transition metal¹⁶ and 50-70 kcal/mol for 2nd and 3rd row transition metal¹⁷ and therefore C-C bond activation is much more exothermic and thermodynamic feasible for 2nd and 3rd row transition metal complexes (Table 1.2). Furthermore, formation of two M-C bonds (~120 kcal/mol) can compensate the energy required for cleavage of one C-C bond (~90 kcal/mol) cleavage ($2M + C-C \rightarrow 2M-C$ or $M + C-C \rightarrow C-M-C$).

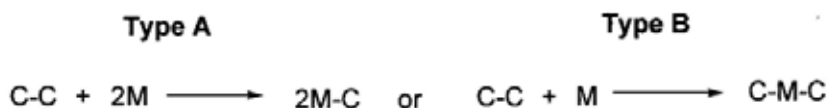


Table 1.2 Thermodynamic Estimation of CCA with Transition Metal

	$\Delta H/\text{kcal/mol}^a$	$T\Delta S_{298K}^{18}/\text{kcal/mol}$	$\Delta G/\text{kcal/mol}$
$C-C + 2M \rightarrow 2M-C/C-M-C$			
For 1 st row TM	$(-35) + (-35) + (90)$ = 20	-10	~30
For 2 nd and 3 rd TM	$(-55) + (-55) + (90)$ = -20	-10	~-10

^a Using BDE of CH₃-CH₃ (90 kcal/mol) as an example.

Where $\Delta H = (M-C) + (M-C) - (C-C)$

$$\Delta G = \Delta H - T\Delta S$$

$$T\Delta S_{298K} = (298K)(-35\text{eu})/1000$$

$$= \sim -10 \text{ kcal/mol}$$

Successful examples of CCA by transition metal complexes with various approaches will be reviewed in the following section (Section 1.2.3).

1.2.3 Protocols of CCA by Transition Metal Complexes

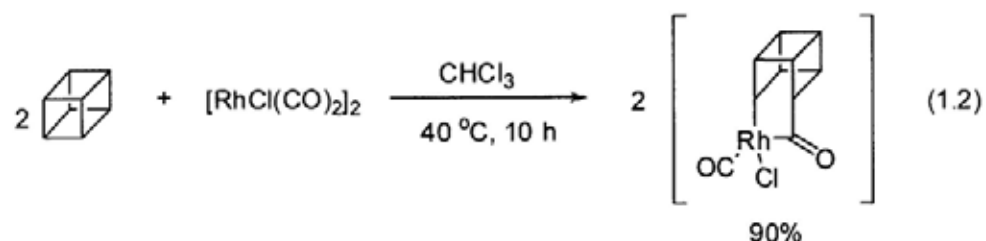
Although C-C bond cleavage is kinetically unfavorable and more challenging over C-H bond, different strategies and protocols have been developed in promoting CCA with transition metal complexes by the means of (i) ring strain relief and (ii) aromatization, (iii) chelation assistance of substrates, (iv) intramolecular β -carbon elimination and (v) formal alkane metathesis of simple alkanes.

1.2.3.1 CCA in Strained System

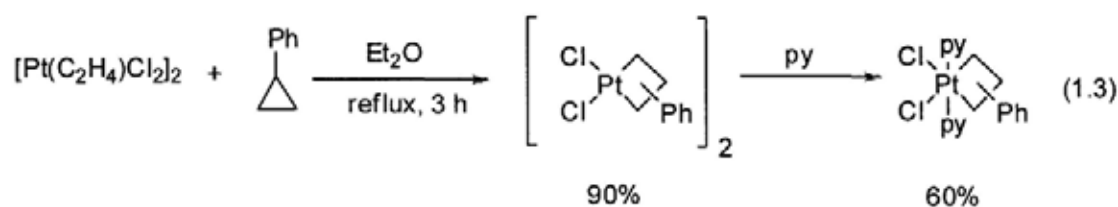
Carbon-carbon bond in severely strained hydrocarbons can be easily cleaved by the release of strain energy. The ring strain energy of cyclopropane and cyclobutane are around 25 kcal/mol to provide the thermodynamic driving force and therefore CCA is dominated in this class of substrates. Halpern, Tipper and Eisch reported early examples of CCA of highly ring strained systems with the activation of cubane (eq

1.2),¹⁹ cyclopropane²⁰ (eq 1.3) and biphenylene²¹ (eq 1.4), respectively.

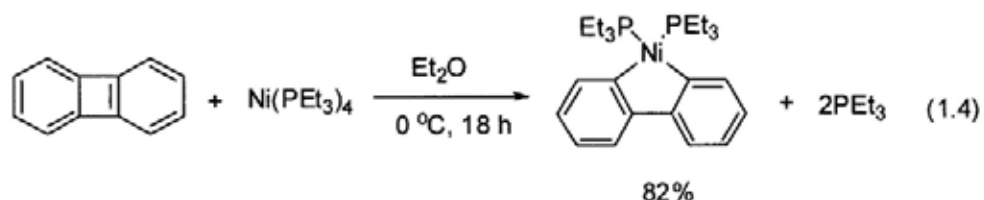
C(sp³)-C(sp³) activation of cubane



C(sp³)-C(sp³) activation of Cyclopropane



C(sp²)-C(sp²) activation of biphenylene



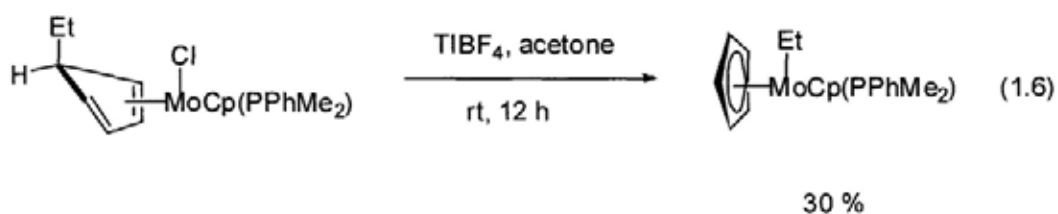
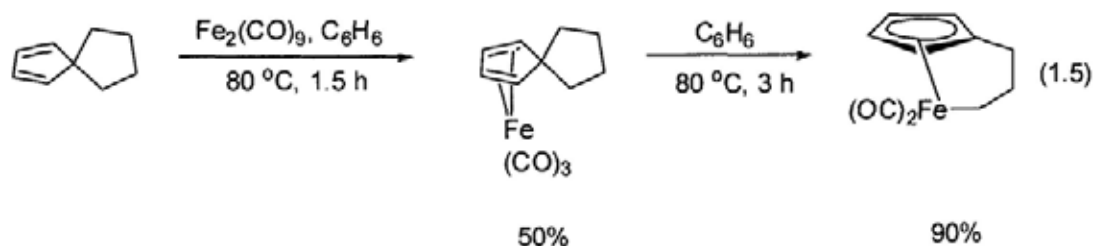
Other examples of strain released CCA include the use of low valent transition metal complexes such as Cp*Co(CH₂CH₂)₂,²² Cp*Rh(CH₂CH₂)₂,²² Pt(PPh₃)₂(C₂H₄),²³ and Cr(CO)₆,²⁴ [Ir(cod)Cl]₂.²⁵

1.2.3.2 CCA Driven by Aromatization

C-C bond cleavage can also be driven from the aromatization of the pre-aromatic compounds. The stabilization energy gained from aromatization is around 5 kcal/mol.^{1b}

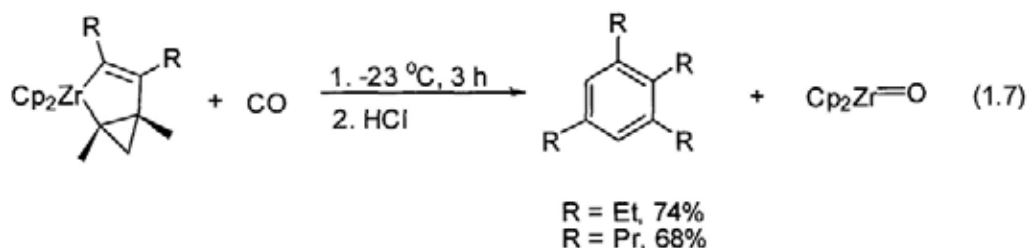
²⁶ Examples of CCA driven by aromatization mainly include the activation of the cyclopentadiene compounds with transition metals complexes to give the corresponding aromatic cyclopentadienyl metal complexes. Eilbracht and Benfield reported the activation of substituted cyclopentadiene derivatives to the corresponding cyclopentadienyl-iron complex²⁷ (eq 1.5) and cyclopentadienyl-molybdenum complex²⁸ (eq 1.6), respectively.

C(sp³)-C(sp³) activation of cyclopentadienes



Besides, Takahashi reported the C-C bond activation of substituted zirconocyclopentene derivative in the presence of carbon monoxide to give 1,2,3,5-tetrasubstituted benzenes in moderate yields²⁹ (eq 1.7).

CCA of zirconocyclopentene

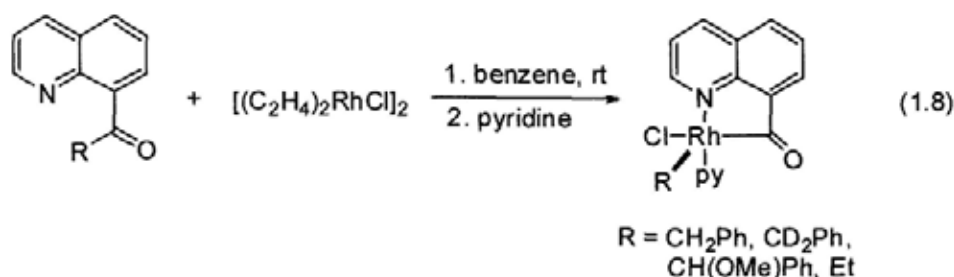


1.2.3.3 Chelation-Assisted CCA

Carbon-carbon bond activation of unstrained molecules could be achieved by utilizing the coordinating functionalities of the target molecules such as phosphine, carbonyl and imine containing substrates. The presences of chelating functionalities kinetically facilitate insertion of a transition metal to C-C bond in the close proximity. Besides, the C-C single bond between a carbonyl carbon and the α -carbon is relatively weaker than other aliphatic C-C bonds by around 5 kcal/mol.³⁰

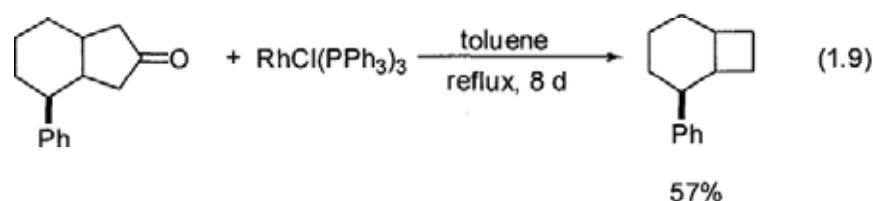
Suggs *et al.* reported the early examples of activation of C-C bond adjacent to a carbonyl group by low valent rhodium complexes.³⁰ $[(\text{CH}_2=\text{CH}_2)_2\text{RhCl}]_2$ activates 8-quinolyl alkyl ketones by oxidative addition between the carbonyl carbon and the α -carbon to form a five-membered cyclometalated complex (eq 1.8).

$C(sp^3)$ - $C(sp^2)$ activation of 8-quinoliny alkyl ketones



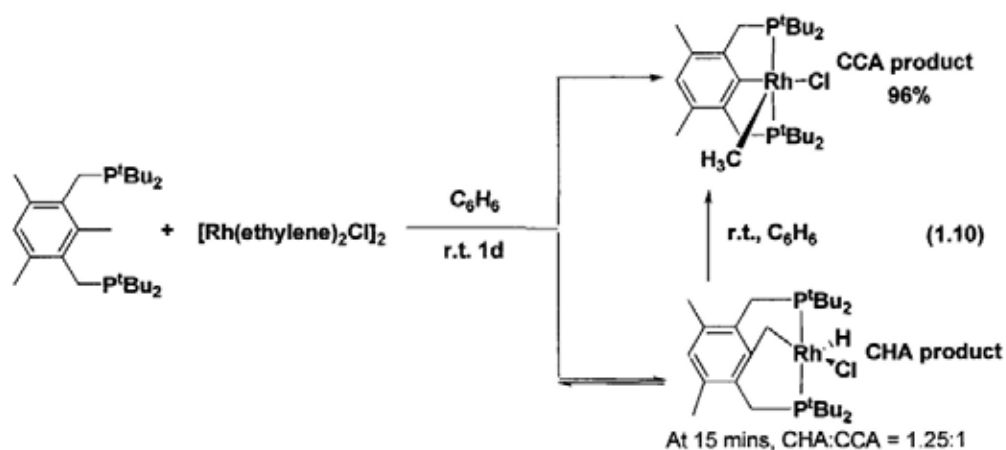
The C-C bond activation of cyclic ketone has been reported by Ito *et al.* using $\text{RhCl}(\text{PPh}_3)_3$.³¹ This reaction involves the oxidative addition of C-C bond of cyclic ketone into rhodium centre followed by decarbonylation and reductive elimination to generate cycloalkane (eq 1.9).

C(sp³)-C(sp²) activation of cyclopentanone



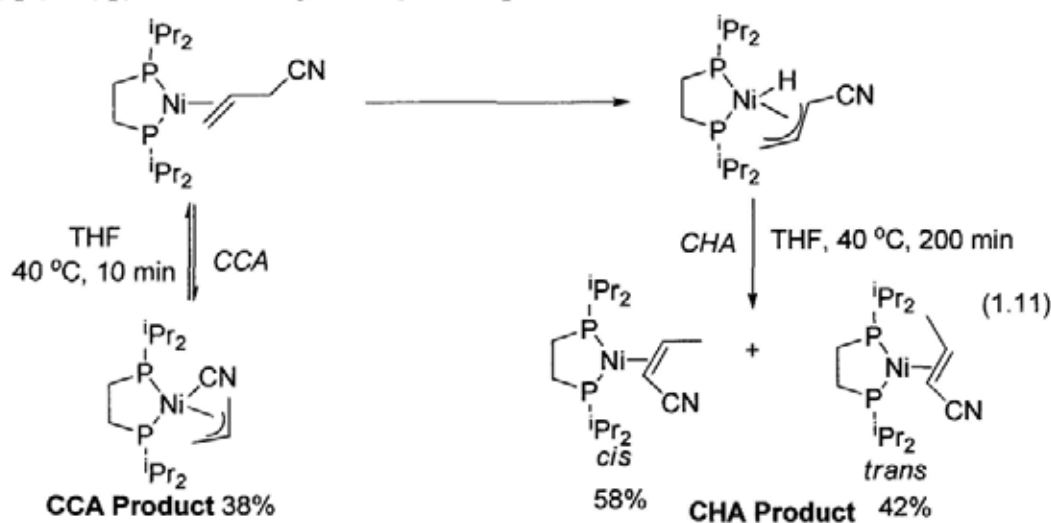
Milstein *et al.* reported the sp^3 - sp^2 intramolecular CCA reaction by using the diphosphine pincer-type chelating ligand with $[\text{Rh}(\text{C}_2\text{H}_4)\text{Cl}]_2$ ³² in which the rhodium metal is brought into the close proximity of the C(alkyl)-C(aryl) bond. This chemical transformation involves the parallel C-H activation of tolyl group to give the stable rhodium(III) complex followed by intramolecular aryl-methyl cleavage to give rhodium-aryl complexes (eq 1.10).

C(sp³)-C(sp²) activation of pincer ligand



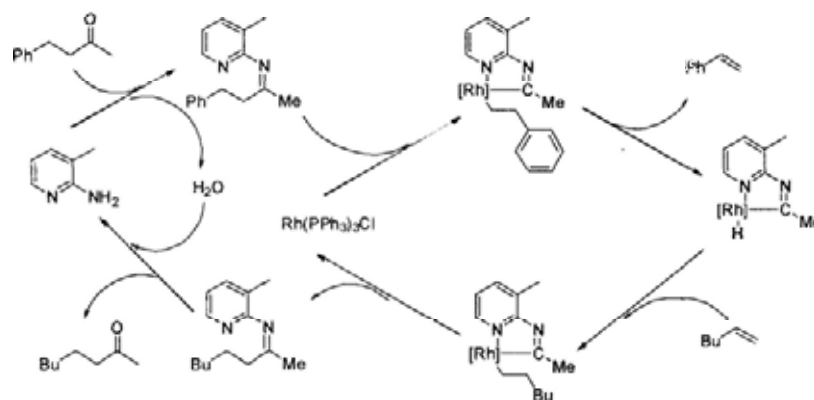
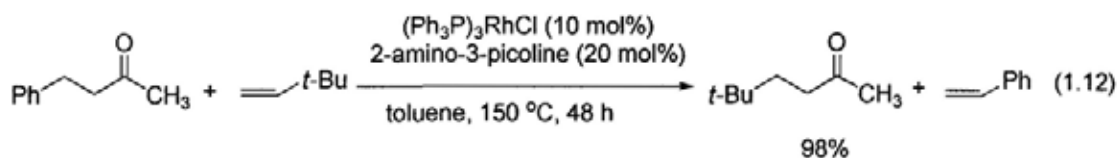
Another competitive CCA and CHA example of allyl cyanide with nickel complex has been reported by Jones *et al.*³³ Interconversion of $(\text{dippe})\text{Ni}(\eta^2\text{-CH}_2=\text{CHCH}_2\text{CN})$ gives a mixture of $(\text{dippe})\text{Ni}(\eta^3\text{-allyl})(\text{CN})$, the CCA product, and the olefin-isomerization products *cis* and *trans*- $(\text{dippe})\text{Ni}(\eta^2\text{-crotonitrile})$ via CHA (eq 1.11). The kinetically more favorable CCA reaction is reversible in which $(\text{dippe})\text{Ni}(\eta^3\text{-allyl})(\text{CN})$ is formed rapidly but then decreases with the concomitant increase of the crotonitrile complexes as the thermodynamic products.

***C(sp³)-C(sp)* activation of Ni-olefin complex**



Jun *et al.* developed the remarkable catalytic C-C bond activation of unstrained ketones with $\text{Rh}(\text{PPh}_3)_3\text{Cl}$ utilizing chelation-assisted protocol through the use of a temporary chelating auxiliary such as 2-amino-2-picoline which can be easily removed from the product by hydrolysis (eq 1.12 & Scheme 1.9).³⁴

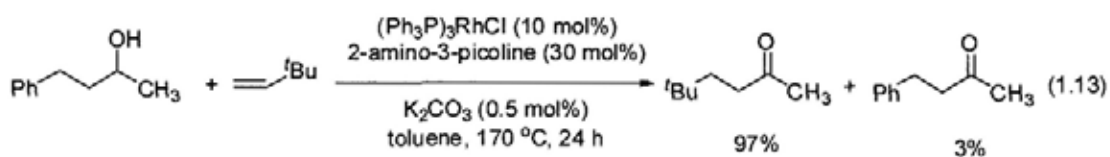
Catalytic $C(sp^3)$ - $C(sp^2)$ activation of ketone



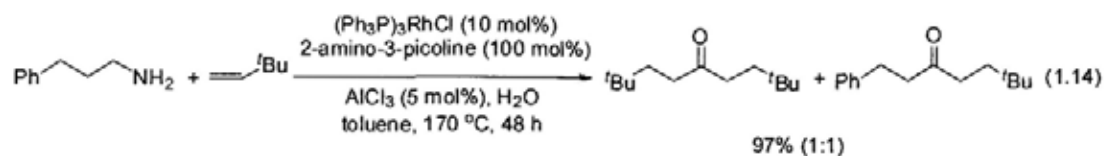
Scheme 1.16 Proposed Mechanism for Catalytic CCA of Unstrained Ketones

This strategy has been extended to the catalytic C-C bond activation of a variety of substrate scopes such as secondary alcohol (eq 1.13), primary amines (eq 1.14), allylamine, cycloalkanone imine and alkyne.³⁴

Catalytic $C(sp^3)$ - $C(sp^2)$ activation of secondary alcohol

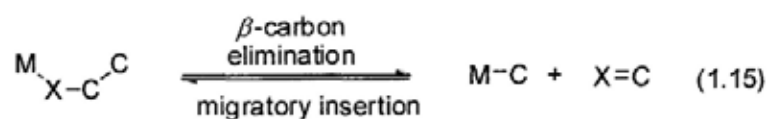


Catalytic $C(sp^3)$ - $C(sp^2)$ activation of primary amine



1.2.3.4 CCA through β -Carbon Elimination

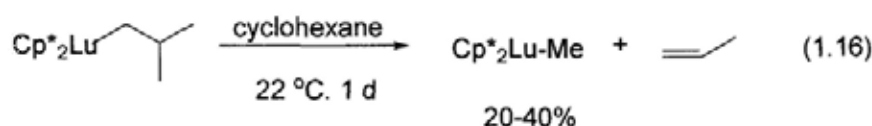
Besides direct intermolecular insertion of transition metal complex into a C-C single bond, CCA could also be achieved through intramolecular β -carbon elimination of transition-metal alkyls, alkoxides and amide (eq 1.15).



M= transition metal
X = C, O, N

Examples include the β -methyl elimination of $\text{Lu}(\eta^5\text{-C}_5\text{Me}_5)_2\text{CH}_2\text{CH}(\text{CH}_3)_2$ (eq 1.16),³⁵ $[\text{Me}_2\text{Si}(\eta^5\text{-C}_5\text{Me}_4)_2]\text{Sc}^i\text{Bu}$ complex (eq 1.17),³⁶ and the β -alkyl and β -aryl elimination of palladium cyclobutanolate complexes (eq 1.18).³⁷

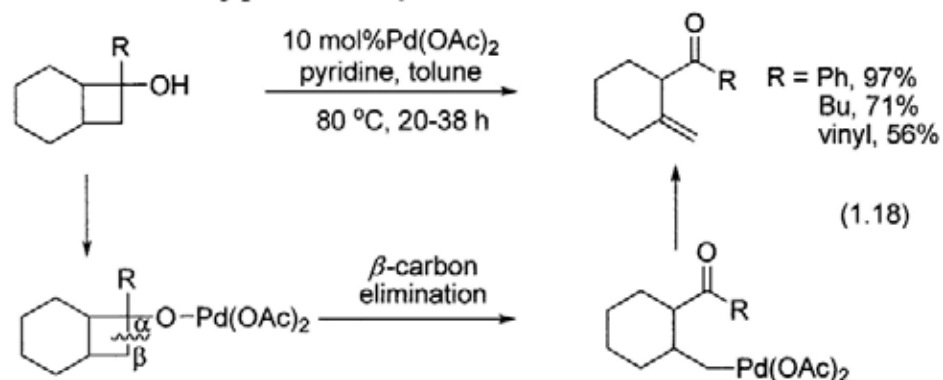
β -methyl elimination of Lu-alkyl complex



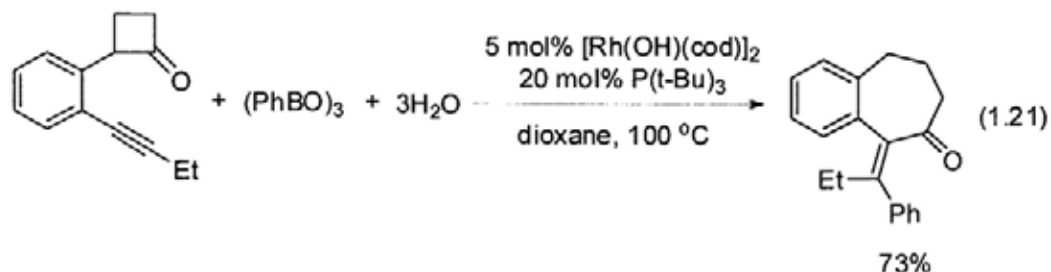
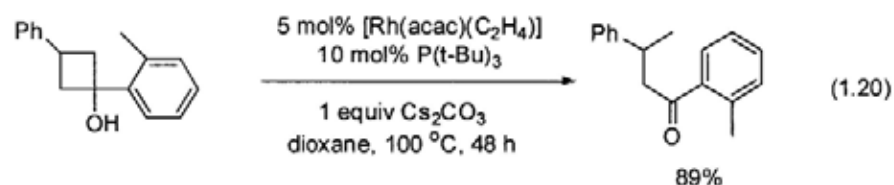
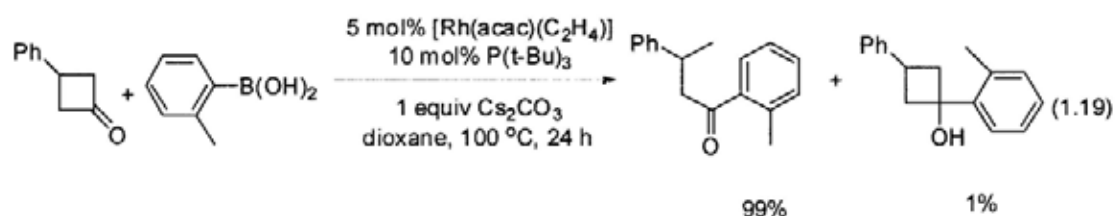
β -methyl elimination of Sc-alkyl complex



β -carbon elimination of palladium cyclobutanolate



Murakami *et al.* applied this protocol in developing the C-C bond activation with various synthetic perspectives such as arylation of cyclobutanones via ring opening and ring expansion of alkyne-substituted cyclobutanone catalyzed by rhodium(I) complexes.³⁸ In those chemical transformations, rhodium(I) cyclobutanolate was proposed as the reaction intermediate before β -carbon elimination step occurred. (eq 1.19 – 1.21)



1.2.3.5 CCA through Formal Alkane Metathesis

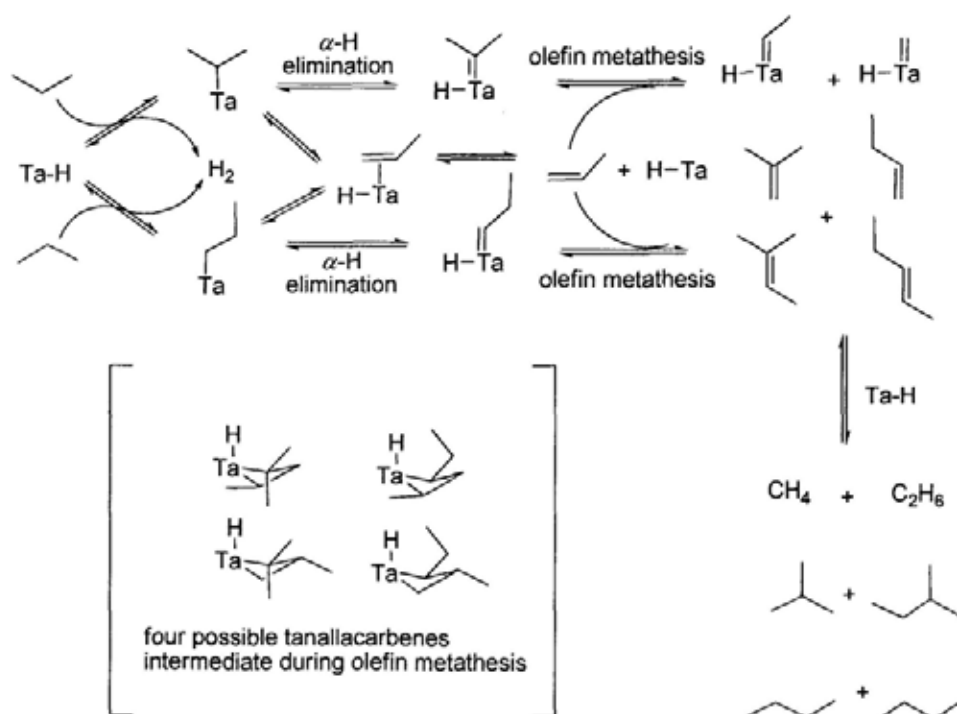
Activation of a carbon-carbon bond of the simplest and unreactive hydrocarbon, such as alkane, is the most challenging research area in the field of bond activation chemistry. The lacks of ring strain relief, chelation assistance and aromatization protocol of simplest hydrocarbon such as ethane lead to the difficulties in selective C-C bond activation of those substrates. In fact, direct C-C single bond alkane metathesis as the elementary step has not been reported. Two formal examples of alkane metathesis have been reported. Basset *et al.* earlier reported the first example of heterogeneous C-C bond activation of simple alkanes such as ethane, propane and butane etc. via a formal alkane metathesis to yield next higher and lower hydrocarbons catalyzed by silica-supported tantalum metal hydrides.³⁹

Table 1.3 Selected results of metathesis reaction of acyclic alkanes catalyzed by the [Ta]-H at 150 °C

Alkane	TON	Selectivity of alkanes produced (%)						
		Methane	Ethane	Propane	Butane	Isobutane	Pentane	Hexane
Ethane	46	53	-	44	2	<1	-	-
Propane	47	16	38	-	27	7	7	2
Butane	66	2	13	36	-	4	27	10
Isobutane	17	12	22	21	<1	-	-	-
Pentane	12	<1	4	17	32	<1	-	25

The C-C bonds of alkane were cleaved into the lower and higher hydrocarbons such as conversion of ethane to methane and propane with 53% and 44% selectivity respectively. However, for a higher alkane such as butane, the selectivity is relatively poor with only 36% propane and 27% pentane selectivity were obtained with cogeneration of other alkanes such as methane, ethane and hexane etc. Scheme 1.17 illustrates the proposed mechanism of the alkane metathesis of propane involving (1) C-H bond cleavage of alkane, (2) the α -H elimination to generate hydrido-tantalocarbenes, (3) olefin metathesis between hydrido-tantalocarbenes and another olefin to produce the next lower and higher hydrocarbons

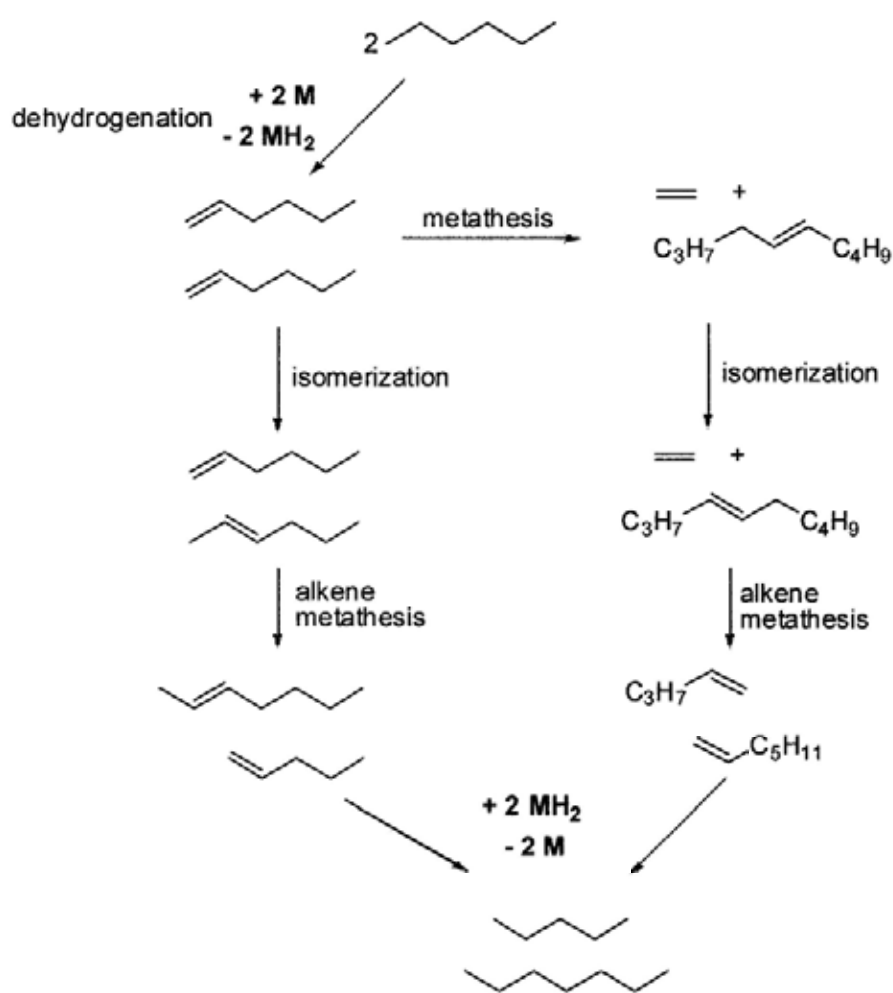
Formal alkane metathesis of propane



Scheme 1.17 Proposed Formal Alkane Metathesis with Silica-Supported Tantalum Hydride

Recently, Goldman and Brookhart *et al.*⁴⁰ reported the catalytic alkane metathesis via (i) tandem alkane dehydrogenation, (ii) olefin metathesis and (iii) olefin hydrogenation process with the combination of dehydrogenation iridium-based pincer complexes and molybdenum metathesis catalyst (Scheme 1.18).

Formal alkane metathesis of *n*-hexane



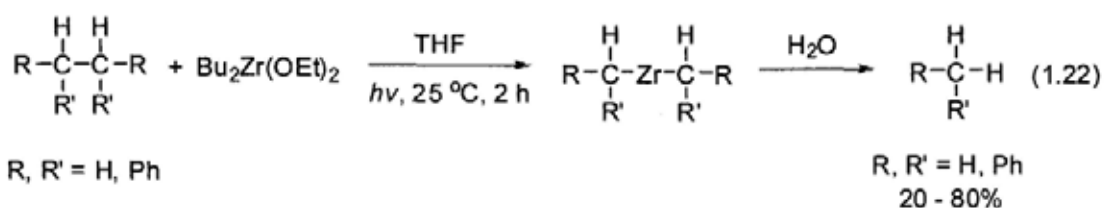
Scheme 1.18 Possible Pathways for the Metathesis of *n*-Hexane to *n*-Pentane and *n*-Heptane

1.2.4 CCA by High Valent Transition Metal Complexes

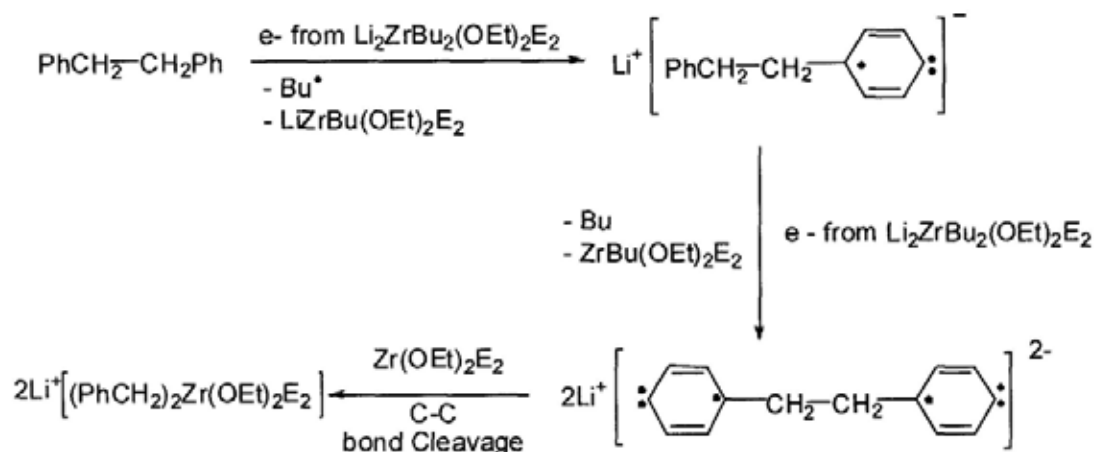
Carbon-carbon bond activation of hydrocarbons, including the ring strain relief, aromatization and chelation-assisted protocols, are mainly reported by using the low valent transition metal complexes as discussed in the previous section. The reaction mechanism usually involves the oxidative addition of C-C bond into the low valent transition metal complexes as the cleavage step. Examples of CCA by high valent transition metal complexes are still rare probably due to relatively unfavored formation of high valent transition metal complexes with oxidation state $> +5$. There are only a few examples of CCA with high valent transition metal complexes: (1) benzylic CCA of bibenzyl hydrocarbons by Zr(IV) complex,⁴¹ (2) CCA of nitrile by Rh(III) complex⁴² and (3) CCA of cyclopropane by Ir(III) complex.⁴³

In 2005, Eisch et al. reported the benzylic CCA of tetraphenylethane with zirconium(IV) complex in a donor solvent such as THF with moderate yields (eq 1.22).⁴¹ The ease of this reaction is probably due to the weaker benzylic C-C bond strength (63 kcal/mol)¹⁵ than the normal aliphatic hydrocarbons (~90 kcal/mol).

Benzylic CCA by zirconium(IV) complex



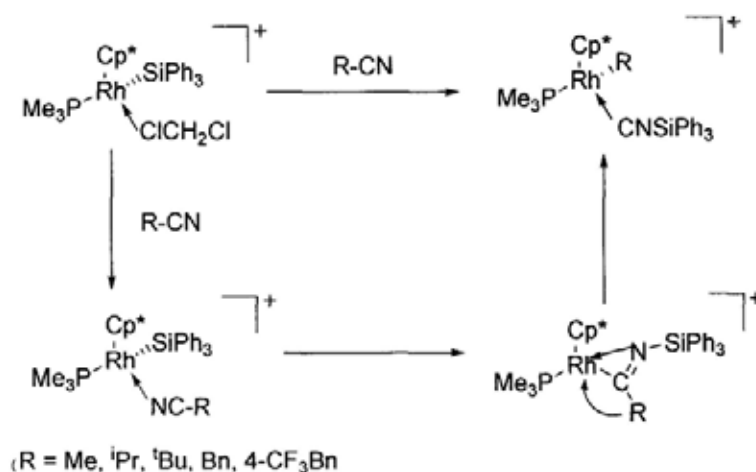
The proposed reaction mechanism involves the single electron transfer (SET) of $\text{Li}_2\text{ZrBu}_2(\text{OEt})_2\text{E}_2$ to the bibenzyl substrates under illumination of laboratory roof light with the concomitant butyl radical loss to yield the zirconated cleavage product as shown in Scheme 1.19



Scheme 1.19 Proposed SET Pathway for C-C Bond Cleavage of Bibenzyl Hydrocarbon

Besides, Bergman *et al.* published the results of two remarkable CCA by high valent group 9 transition metal complexes including the facile CCA of aryl- and alkyl-nitrile bond with cationic Rh(III) silyl complex⁴² and the CCA of cyclopropane with Ir(III) complexes.⁴³ In the activation of C-CN bond with Rh(III) silyl complexes, the proposed mechanism involves the migration of aryl or alkyl group of nitrile to Rh-center via the n^2 -iminoacyl intermediate and constitutes the key CCA step rather than oxidative addition as in most of the case with low valent rhodium complexes (Scheme 1.20).

CCA of nitrile with Rh(III) silyl complex

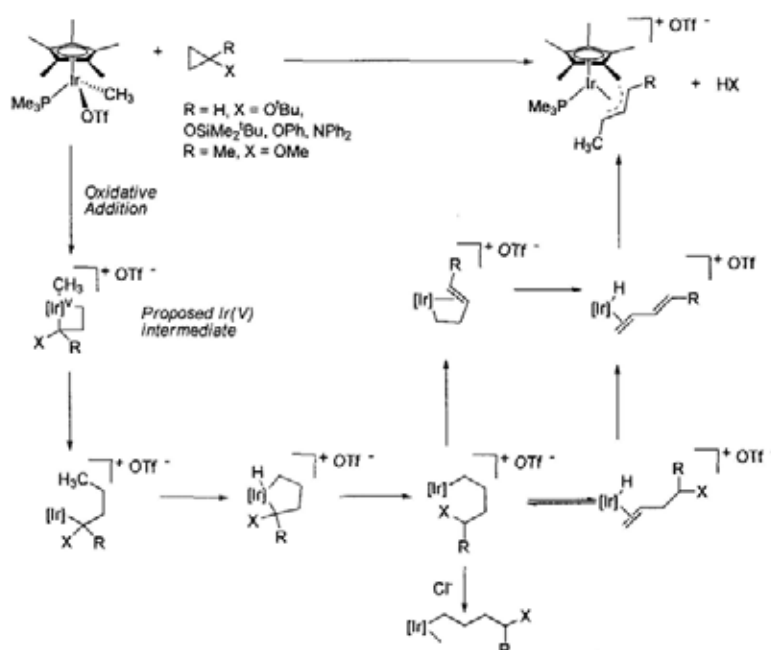


Scheme 1.20 Proposed CCA of Nitrile by Rh(III)-Silyl Complex

More recently, high valent Ir(III) complex was found to activate cyclopropane.

Cp*Ir(PMe₃)Ir(CH₃)OTf cleaves the carbon-carbon bond of both the alkoxy and siloxy cyclopropanes via oxidative addition to generate Ir(V) alkyl complex as the proposed intermediate. (Scheme 1.21).⁴³

CCA of cyclopropane with Ir(III) complex

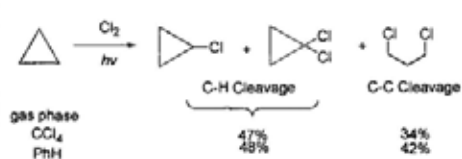

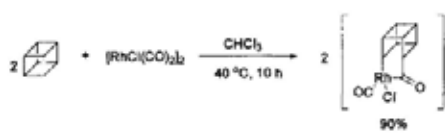
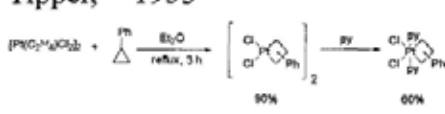
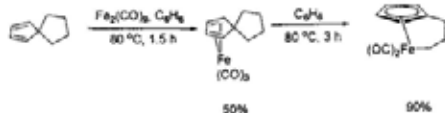
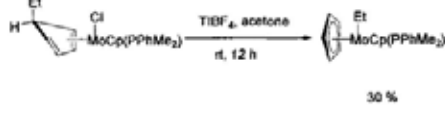


Scheme 1.21 Proposed CCA of Cyclopropane by Ir(III) Complex

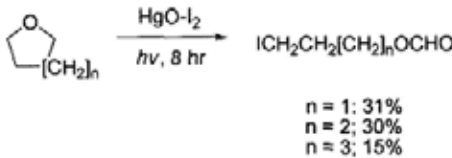
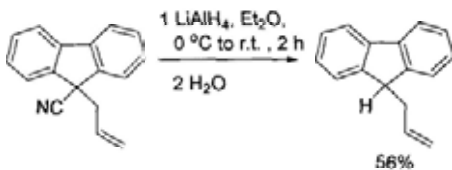
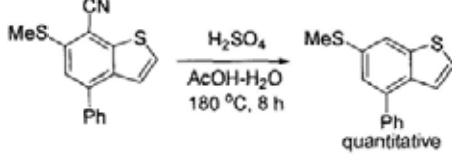
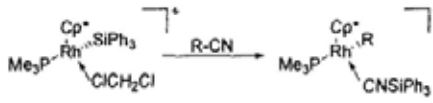
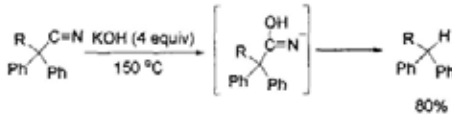
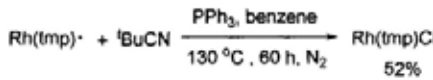
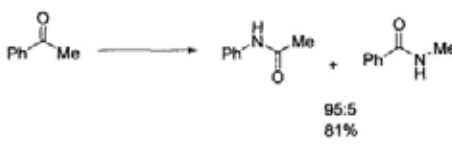
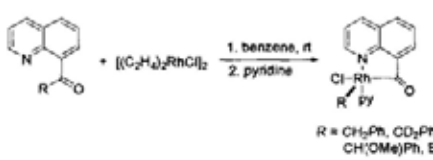
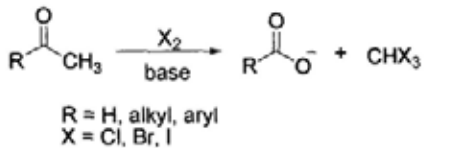
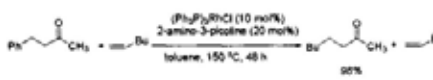
1.3 Classification of CCA of Organic Substrates

Carbon-carbon bond cleavage of a variety of substrate scopes with both organic reactions and transition metal assisted methods are summarized in Table 1.4

Table 1.4 Classification of CCA of Organic Substrates

	Type of Carbon-Carbon Bond Cleavage	
Organic Substrate	Organic Type	Transition Metal Type
Alkane	<p>Halogenation of Strained Hydrocarbon</p> <p>Roberts,⁷ 1945</p>  <p>gas phase CCl₄ PhH</p> <p>C-H Cleavage: 47% 48%</p> <p>C-C Cleavage: 34% 42%</p> <p>Protolysis of Alkane</p> <p>Olah,¹⁰ 1967</p> $R_3C-CR_3 + E^+ \longrightarrow \left[\begin{array}{c} R_3C \\ \\ R_3C \cdots CR_3 \\ \\ E \end{array} \right]^+ \longrightarrow R_3CE + R_3C^+$ <p>E = D⁺, H⁺, R⁺, NO₂⁺, HCO⁺, etc.</p> <p>Wiberg,¹¹ 1986</p> 	<p>Oxidative Addition of Strained Hydrocarbons</p> <p>Halpern,¹⁹ 1970</p>  <p>90%</p> <p>Tipper,²⁰ 1955</p>  <p>90% 60%</p> <p>Cleavage Driven by Aromatization</p> <p>Eilbracht,²⁷ 1980</p>  <p>50% 90%</p> <p>Benfield,²⁸ 1974</p>  <p>30%</p>

		<p>Bibenzyl Eisch,⁴¹ 2005</p> <p>$R, R' = H, Ph$ $R, R' = H, Ph$ 20 - 80%</p> <p>Formal Alkane Metathesis Bassets,³⁹ 1997</p> <p>Goldman,⁴⁰ 2006</p>
Alkyl- aromatics		<p>Chelation-Assisted Oxidative Addition Pincer Type Ligand Milstein,³² 1993</p> <p>96%</p>
Bipenylene		<p>Oxidative Addition of Strained C-C bond Eish,²¹ 1985</p> <p>82%</p>
Ether	<p>Cleavage of Homobenzylic Ether via Electron Transfer Floreancig,⁴⁴ 2001</p>	<p>Oxidative Cleavage of Cyclic Ether Lippard,⁴⁵ 2004</p> <p>Chan,⁴⁶ 2006</p> <p>36%</p>

	<p>Photolytic Cleavage Suginome,⁴⁷ 1990</p>  <p style="text-align: center;"> $n = 1; 31\%$ $n = 2; 30\%$ $n = 3; 15\%$ </p>	
Nitrile	<p>Reductive Decyanation Black,⁴⁸ 1978</p>  <p style="text-align: center;">56%</p>	<p>Oxidative Addition Miller,⁵¹ 2001</p> $\text{Ar-CN} + \text{R-M} \xrightarrow{\text{Ni cat.}} \text{Ar-R} + \text{R-CN}$
	<p>Acidic Decyanation Suresh,⁴⁹ 2000</p>  <p style="text-align: center;">quantitative</p>	<p>Deinsertion of silyl isocyanide Bergman,⁴² 2002</p> 
	<p>Base Promoted Decyanation Berkoff,⁵⁰ 1980</p>  <p style="text-align: center;">80%</p>	<p>Homolytic Cleavage by Rh^{II}(tmp) Chan,⁵¹ 2007</p>  <p style="text-align: center;">52%</p>
Ketone	<p>Schmidt Reaction Smith,⁵² 1950</p>  <p style="text-align: center;">95:5 81%</p>	<p>Oxidative Addition Suggs,³⁰ 1984</p>  <p style="text-align: center;"> $R = \text{CH}_2\text{Ph}, \text{CD}_3\text{Ph},$ $\text{CH}(\text{OMe})\text{Ph}, \text{Et}$ </p>
	<p>Haloform Reaction⁵³</p>  <p style="text-align: center;"> $R = \text{H, alkyl, aryl}$ $X = \text{Cl, Br, I}$ </p>	<p>Jun,³⁴ 1994</p>  <p style="text-align: center;">90%</p>

Ester	<p>Krapcho decarboxylation Krapcho,⁵⁴ 1967</p> $\text{CH}_3\text{CH}(\text{CO}_2\text{Et})_2 \xrightarrow[160\text{ }^\circ\text{C, 4 h}]{\text{NaCN, DMSO}} \text{CH}_3\text{CH}_2\text{CO}_2\text{Et}$ <p style="text-align: right;">75%</p>	<p>Homolytic Cleavage by Rh^{II}(tmp) Chan,⁵⁵ 2006</p> $\text{Rh(tmp)} + \text{Ph-CO-CH}_2\text{-CH}_3 \xrightarrow[130\text{ }^\circ\text{C, 24 h, N}_2]{\text{PPh}_3, \text{benzene}} \text{Rh(tmp)CH}_3$ <p style="text-align: right;">30%</p>
Carboxylic Acid	<p>Schmidt reaction Datta,⁵⁶ 1970</p> $\text{Ph-CH}_2\text{-CO}_2\text{H} \xrightarrow[40\text{ }^\circ\text{C, 1 h}]{\text{NaN}_3, \text{H}_2\text{SO}_4, \text{CHCl}_3} \text{Ph-CH}_2\text{-NH}_2$ <p style="text-align: right;">70%</p> <p>Hunsdiecker reaction Meyers,⁵⁷ 1979</p> $\text{C}_{13}\text{H}_{27}\text{COOH} \xrightarrow[\text{reflux, 3 hr}]{\text{Ti}_2\text{CO}_3, \text{Br}_2} \text{C}_{13}\text{H}_{27}\text{COOH}$ <p style="text-align: right;">91%</p>	
Alcohol	<p>Schmidt Reaction Pearson,⁵⁸ 1995</p> $\text{Cyclopentane-1,1-diol} \xrightarrow[2. \text{NaBH}_4]{1. n\text{-BuN}_3, 2.5 \text{ TfOH}} \text{N-Bu-piperidine}$ <p style="text-align: right;">95%</p> <p>Pinacol Rearrangement Bunton,⁵⁹ 1958</p> $\text{H}_3\text{C-C(CH}_3)_2\text{-C(CH}_3)_2\text{-CH}_3 \xrightarrow[73\text{ }^\circ\text{C, 55 h}]{\text{H}_2\text{SO}_4} \text{H}_3\text{C-C(CH}_3)_2\text{-C(CH}_3)_2\text{-CH}_3$ <p style="text-align: right;">70%</p>	<p>β-alkyl elimination of metal-alkoxide Kondo,⁶¹ 1998</p> $\text{Ph-CH(OH)-CH}_2\text{-CH}_3 \xrightarrow[180\text{ }^\circ\text{C, 15 h}]{\text{RhCl}_2(\text{PPh}_3)_2, \text{CO, CH}_2\text{CH}_2\text{OAc}} \text{Ph-CH=CH}_2 + \text{Me-CO-Ph}$ <p style="text-align: right;">91%</p> <p>CCA of secondary alcohol Jun,³⁴</p> $\text{Ph-CH(OH)-CH}_2\text{-CH}_3 \xrightarrow[\text{toluene, 170 }^\circ\text{C, 24 h}]{\text{(Ph}_3\text{P)}_2\text{RhCl (10 mol\%), 2-amino-3-picolone (30 mol\%), K}_2\text{CO}_3 \text{ (0.5 mol\%)}} \text{Ph-CO-CH}_2\text{-CH}_3 + \text{Ph-CH}_2\text{-CO-CH}_3$ <p style="text-align: right;">97% 5%</p>
Amide	<p>Hofmann Rearrangement Huang,⁶⁰ 1997</p> $\text{Ph-CO-NH}_2 \xrightarrow[\text{MeOH, reflux, 10 min}]{\text{NBS, NaOMe}} \text{Ph-NH-CO-Me}$ <p style="text-align: right;">91%</p>	<p>Homolytic Cleavage by Rh^{II}(tmp) Chan,⁵⁵ 2006</p> $\text{Rh(tmp)} + \text{Ph-CO-N(CH}_2\text{CH}_3)_2 \xrightarrow[130\text{ }^\circ\text{C, 6 h, N}_2]{\text{PPh}_3, \text{benzene}} \text{Rh(tmp)CH}_3$ <p style="text-align: right;">41%</p>
Amine		<p>CCA of Primary Amine Jun,³⁴</p> $\text{Ph-CH}_2\text{-NH}_2 \xrightarrow[\text{toluene, 170 }^\circ\text{C, 48 h}]{\text{(Ph}_3\text{P)}_2\text{RhCl (10 mol\%), 2-amino-3-picolone (10 mol\%), AgCl, 0.5 mol\% H}_2\text{O}} \text{Ph-CO-CH}_2\text{-CH}_3 + \text{Ph-CH}_2\text{-CO-CH}_3$ <p style="text-align: right;">97% (1:1)</p>

Chapter 2 Introduction to Metalloporphyrin

2.1 Porphyrin ligands and Metalloporphyrins

Porphyrin is a planar, tetradentate, dianionic and heterocyclic macrocycle assembled from four pyrroles and interconnected on opposite sides via four methine bridges. It contains an extensively 18 π -conjugated system in the inner 16-membered ring.⁶³⁻⁶⁶ Porphyrins in which the physical and chemical properties can be modified by peripheral substituents at meso or beta positions can serve as versatile robust ligands.⁶⁷

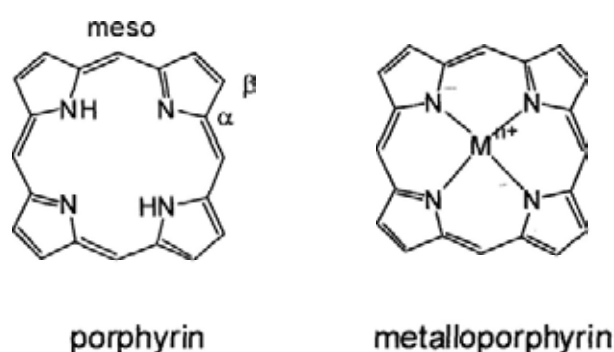


Figure 2.1 Structures of Porphyrin and Metalloporphyrin

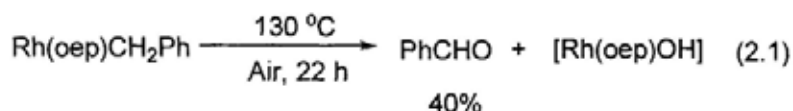
Porphyrins can form very stable tetradentate metal complexes by metalation with the replacement of two inner pyrrole protons by metal ions. Metalloporphyrins are characterized by an intense color of Soret band at around 400 nm. Metalloporphyrins are important model complexes for understanding the chemical and biological reactivities of important macromolecules such as cytochrome P450, coenzyme B_{12} and heme.⁶⁸⁻⁷¹ Early successful examples of catalytic reaction systems by

metalloporphyrins have been developed by Groves⁷² and Collman.⁷³ Metalloporphyrins have also been found to catalyze various reactions such as cyclopropanation of alkene,⁷⁴ epoxidation,⁷⁵ aziridination,⁷⁴ hydroxylation,⁷⁶ amidation of alkanes⁷⁷ and oxidation of alkene.⁷⁸

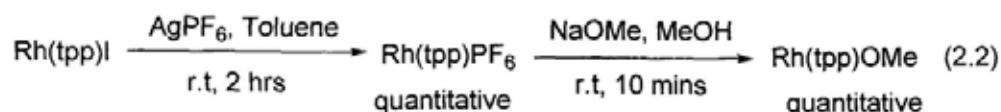
2.2 Chemistry Rhodium(III) Porphyrins

Group 9 diamagnetic rhodium(III) porphyrins play an important role in organometallic chemistry. The common five or six coordinate d^6 sigma-bonded alkyl, aryl and halides complexes of Rh(III) porphyrin are usually kinetically inert and air stable. Various chemical reactivities of Rh(III) porphyrin derivatives are reported such as (i) aerobic oxidation of rhodium porphyrin alkyls,⁷⁹ (ii) ligand substitution of rhodium porphyrin halide with alkoxide,⁸⁰ (iii) photolytic cleavage of Rh(por)-alkyls⁸¹ and (iv) thermal 1, 2-rearrangement of Rh(por)-alkyls.⁸²

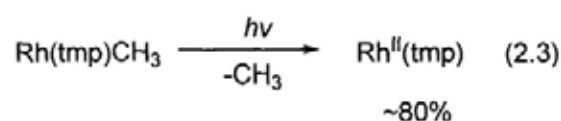
Oxidation of rhodium porphyrin alkyls



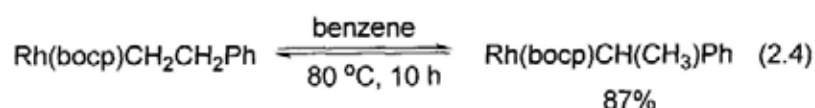
Ligand substitution of Rh(tpp)I to Rh(tpp)OMe with NaOMe



Photolytic cleavage of Rh(*por*)-alkyls



Alkyl 1,2-rearrangements



Rhodium(III) porphyrin complexes are also efficient catalysts in various type of reactions such as the cyclopropanation of alkene,⁸³ the aldol condensation of cyclic ketone,⁸⁴ and the cyclotrimerization of arylethylenes.⁸⁵

2.2.1 Bond Activation Reaction by Rhodium(III) Porphyrins

The unusual strong Rh-H (~60 kcal/mol) and Rh-C (~57 kcal/mol) bonds of rhodium porphyrin complexes (Table 2.1) provide the thermodynamic driving force in bond activation reactions of a variety of substrate scopes involving the breaking of the C-H bond and the C-C bond.

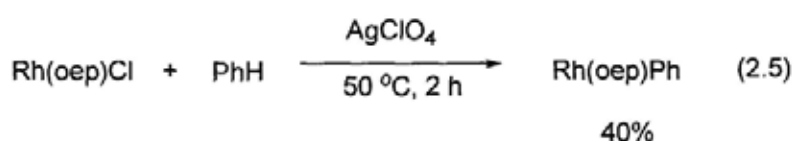
Table 2.1 Selected BDEs of Rhodium(III) Porphyrin Complexes⁸⁶

(<i>por</i>)Rh-C	BDE (kcal/mol)	(<i>por</i>)Rh-H	BDE (kcal/mol)
(tmp)Rh-CH ₃	57	(tmp)Rh-H	60
(ttp)Rh-CH ₃	57	(tpp)Rh-H	52 ^a
(oep)Rh-CH ₃	57	(oep)Rh-H	62
(oep)Rh-CH ₂ CH ₃	47		
(oep)Rh-CHO	58		

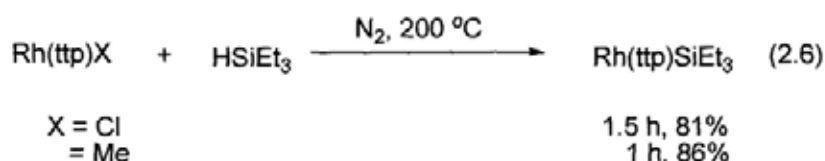
^a BDFE (change in free energy for dissociation of Rh-H bond)

Ogoshi *et al.* reported the aromatic carbon-hydrogen bond activation (CHA) of arenes by Rh(oep)Cl in the presence of AgClO₄.⁸⁷ More recently, Chan *et al.* reported the bond activation of a series of substrate scopes by rhodium(III) porphyrins such as the silicon-hydrogen bond activation of silane,⁸⁸ the CHA of aldehyde⁸⁹ and more recently the base promoted CHA of toluene^{90a} and alkane^{90b} by Rh(tp)Cl.

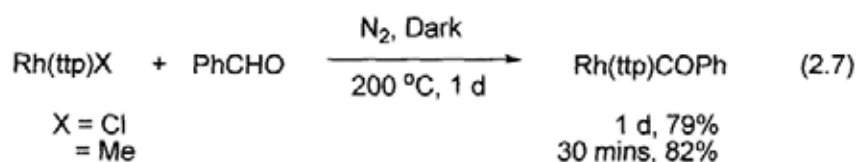
Aromatic C-H activation of arenes



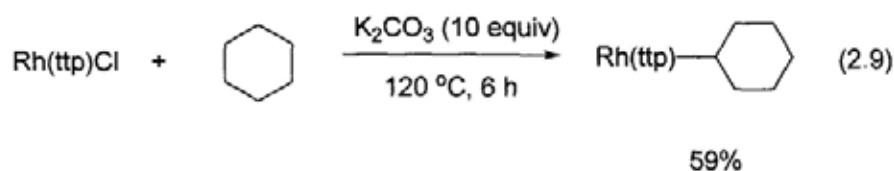
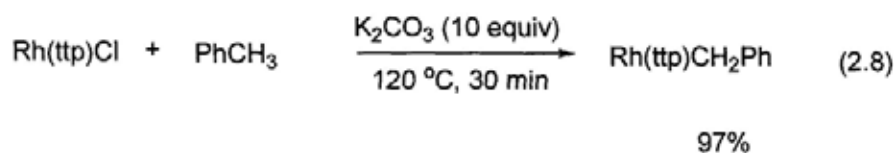
Activation of silicon-hydrogen bond



Aldehydic C-H activation



Base-promoted C-H activation



2.3 Chemistry of Rhodium(II) Porphyrins

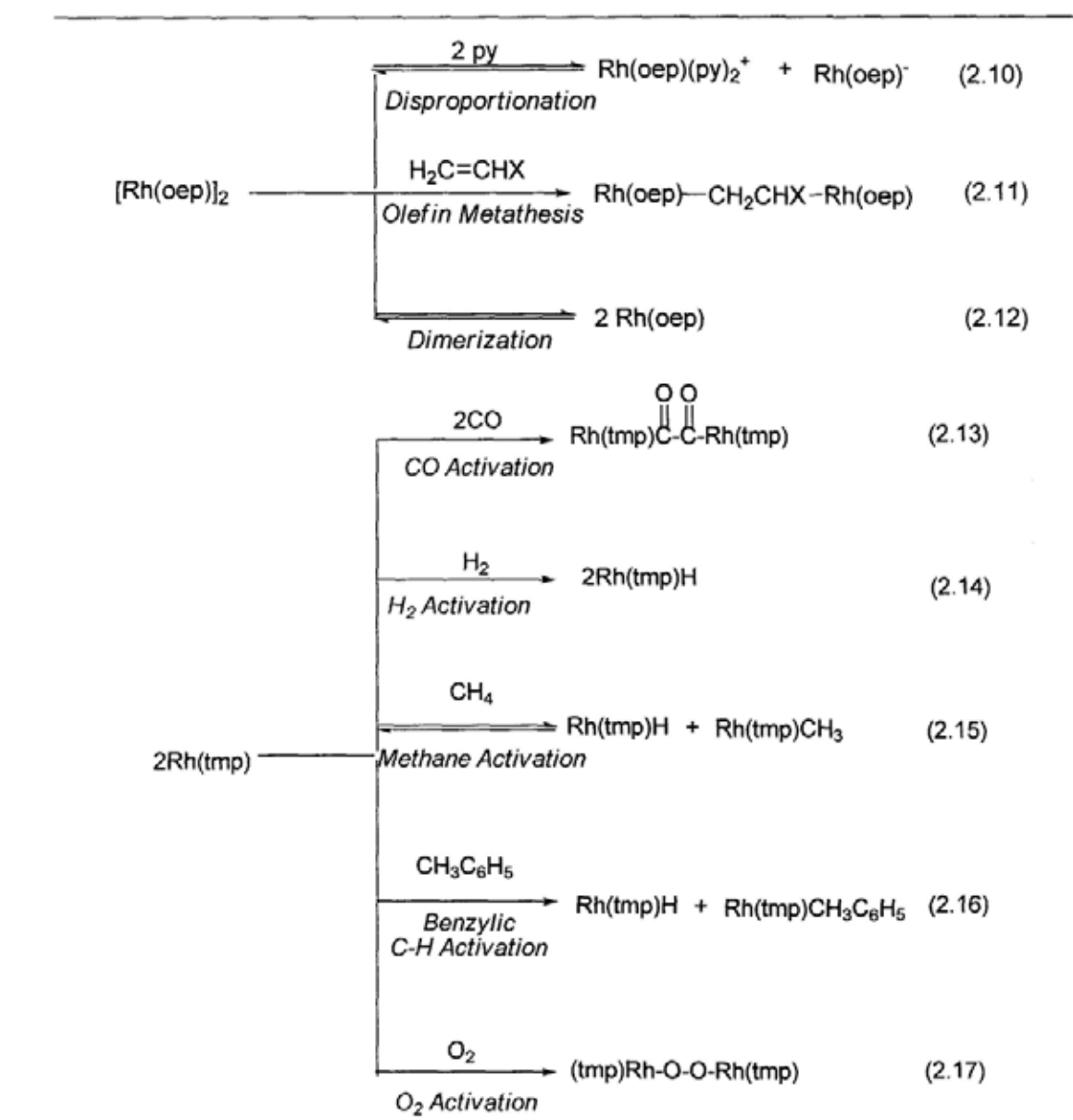
Rhodium(II) porphyrins with an odd d^7 electron configuration play important roles in organometallic chemistry. Rhodium(II) porphyrin species are usually generated from the photolysis of the corresponding rhodium porphyrin alkyl or rhodium porphyrin hydride. Rhodium(II) porphyrins can exist in the form of dimer or monomer. For the sterically hindered porphyrin such as tetramesitylporphyrin (tmp), its rhodium(II) porphyrin exists in the form of monomer, $[\text{Rh}^{\text{II}}(\text{tmp})]$. $[\text{Rh}^{\text{II}}(\text{tmp})]$ is paramagnetic due to one unpaired in dz^2 orbital which shows a broad peak signal in ^1H NMR⁸¹ and $[\text{Rh}^{\text{II}}(\text{tmp})]$ reacts like a radical and is very reactive. While for less hindered porphyrins such as tetraphenylporphyrin (tpp)⁹¹ and octaethylporphyrin (oep),⁹¹ the rhodium(II) porphyrins exist as dimers, $[\text{Rh}(\text{por})]_2$. The Rh-Rh bond strength of $[\text{Rh}(\text{por})]_2$ is around 12-16 kcal/mol.⁹¹ Therefore, rhodium(II) porphyrin dimer becomes less reactive than those monomeric rhodium(II) porphyrin.

Table 2.2 Selected BDEs of Rh-Rh Bond of Rhodium(II) Porphyrins

$\text{Rh}^{\text{II}}(\text{por}), d^7$	ΔH kcal/mol
$[\text{Rh}(\text{oep})]_2$ ^{75d}	15.5
$[\text{Rh}(\text{txp})]_2$ ^{74b}	12
$[\text{Rh}(\text{tmp})]$	Exists as monomer

Rhodium(II) porphyrins show various radical reactions with a wide variety of organic substrates. Wayland *et al.* reported a series of rhodium(II) porphyrin chemistry such as dimerization⁹¹ and disproportionation⁹² of Rh^{II}(por) complexes, the activation of dihydrogen,⁹³ oxygen,⁹⁴ carbon monoxide,⁹⁵ methane⁹⁶ and toluene.⁹⁷⁻⁹⁸

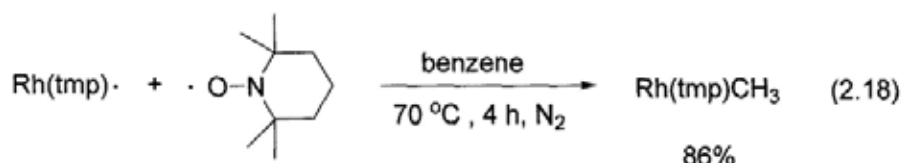
Table 2.3 Reactivity of Rhodium(II) Porphyrins



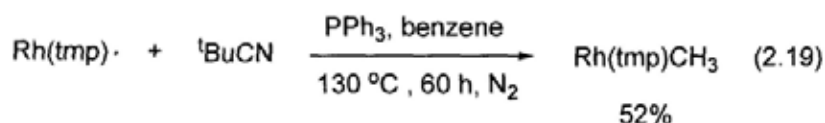
2.3.1 Carbon-Carbon Bond Activation by Rhodium(II) Porphyrin

Monomeric Rh(II) porphyrin, Rh^{II}(tmp), is also known to activate the carbon-carbon bond of a variety of substrates. Chan *et al.* reported a series of aliphatic sp^3 - sp^3 carbon-carbon bond activation by using Rh^{II}(tmp) in benzene solvent including nitroxide,⁶² nitrile,⁵¹ ketone,⁵⁵ ester⁵⁵ and amide⁵⁵ from moderate to good yields (eq 2.18 - 2.22). Mechanistic investigation showed that homolytic bimolecular substitution (S_H2) is the probable pathway in the C-C bond cleavage of nitroxide by Rh^{II}(tmp) (Scheme 2.1).⁶²

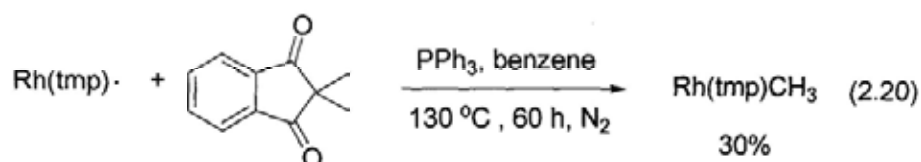
$C(sp^3)$ - $C(sp^3)$ bond activation of nitroxide



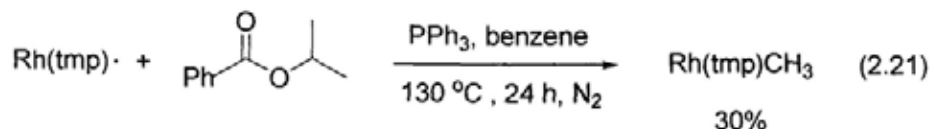
$C(sp^3)$ - $C(sp^3)$ bond activation of nitrile



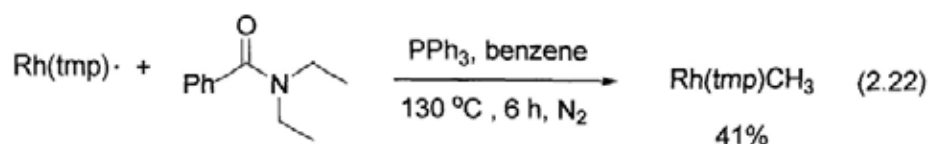
$C(sp^3)$ - $C(sp^3)$ bond activation of ketone

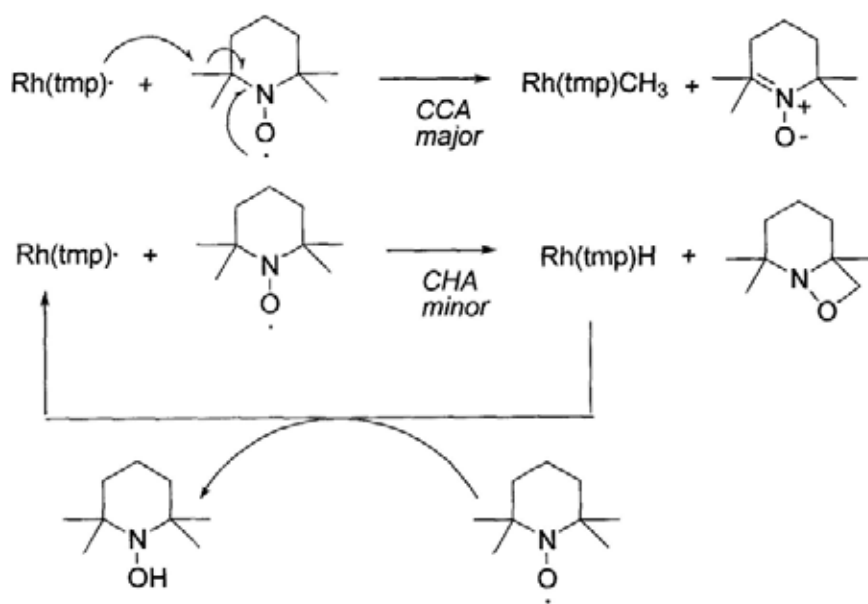


$C(sp^3)$ - $C(sp^3)$ bond activation of ester



$C(sp^3)$ - $C(sp^3)$ bond activation of amide

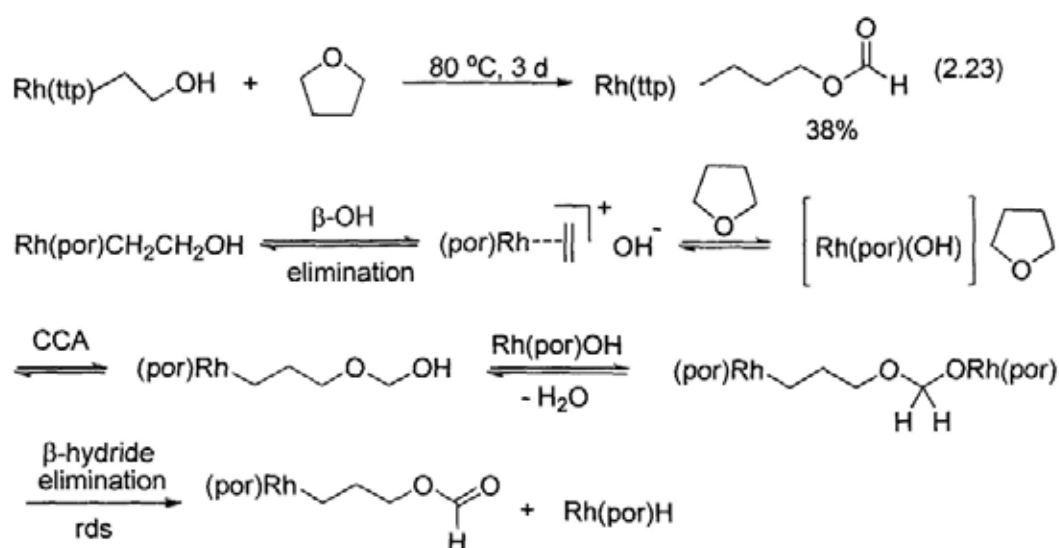




Scheme 2.1 Proposed Parallel CCA and CHA of TEMPO by $\text{Rh}^{\text{II}}(\text{tmp})$

2.4 Carbon-Carbon Bond Activation of Ethers by $\text{Rh}(\text{por})\text{CH}_2\text{CH}_2\text{OH}$

The activation of $\text{sp}^3\text{-sp}^3$ hybridized C-C bond of ether by $\text{Rh}(\text{por})\text{CH}_2\text{CH}_2\text{OH}$ was discovered by Dr. S. K. Yeung in Professor. K. S. Chan's group in 2005.⁴⁶ $\text{Rh}(\text{por})\text{OH}$ has been proposed as the key intermediate in the C-C bond cleavage step (Scheme 2.2, eq 2.23).



Scheme 2.2 Proposed Mechanism for the CCA of Ethers with $\text{Rh}(\text{tpp})\text{CH}_2\text{CH}_2\text{OH}$

2.5 Chemistry of Transition Metal Hydroxide, (L)_nM-OH

With the proposed Rh(por)OH as the key intermediate in the carbon-carbon bond activation of ethers with Rh(tp)CH₂CH₂OH, the chemistry of transition metal hydroxide is then briefly reviewed. Complexes with metal-hydroxide single bonds have been implicated in a wide range of biologically and synthetically important catalytic transformations.⁹⁹⁻¹⁰⁰ Late transition metal hydroxides have generated much interest because the reactivity of this combination of soft metal and hard ligand which is not well documented. Transition metal hydroxide bond is presumably very weak and reactive due to the p- π /d- π repulsion between the oxygen atom lone pair electrons and electrons in filled d shells on the metal center, resulting in a higher energy π -orbital (Figure 2.2).¹⁰¹

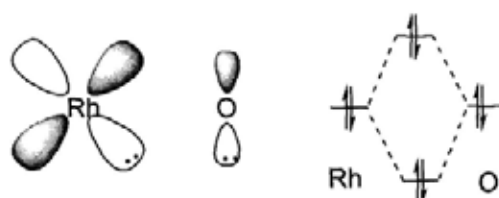
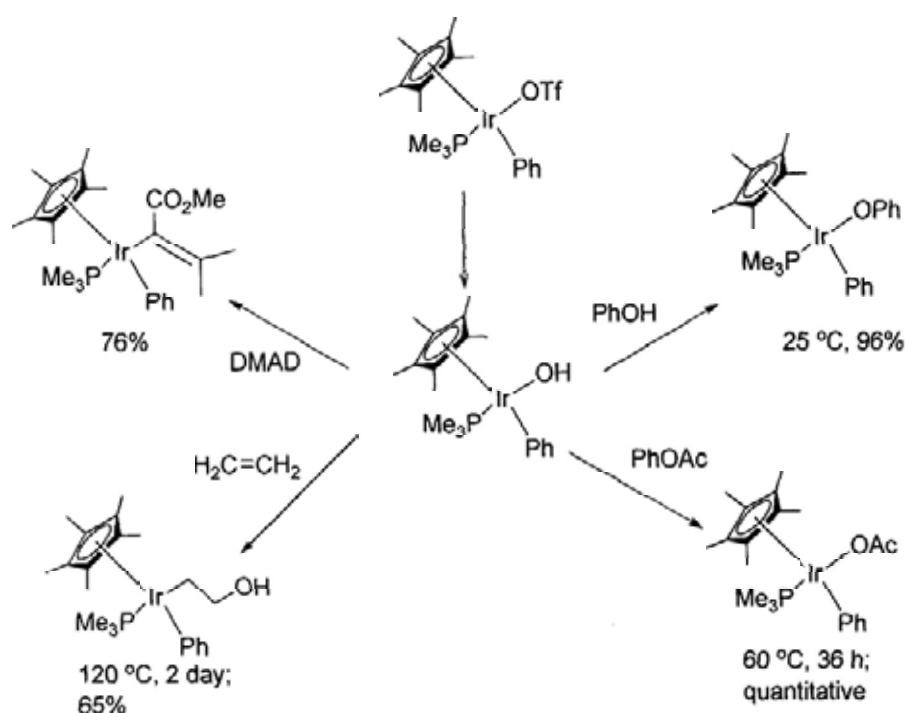


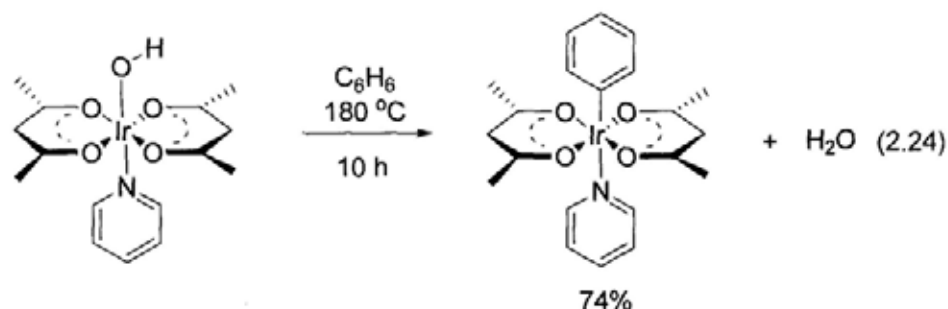
Figure 2.2 Interaction between a p-symmetry lone pair orbital on O-atom and the filled d-orbitals of a transition metal

Specifically, Bergman *et al.*¹⁰² reported that iridium hydroxo complex Cp*(PMe₃)Ir(Ph)OH undergoes insertion into both dimethyl acetylenedicarboxylate and ethylene. This iridium hydroxo complex also undergoes metathesis reaction with phenol to afford the corresponding phenoxide complex (Scheme 2.3).

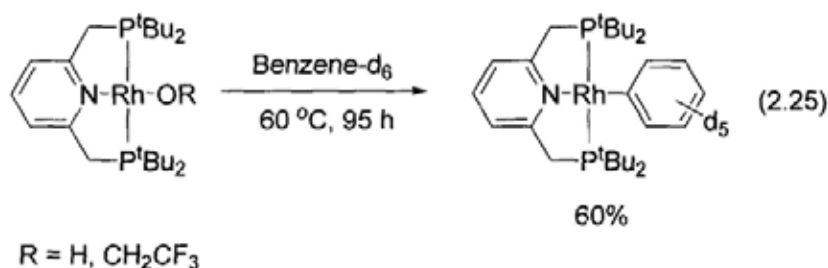


Scheme 2.3 Reactivity of $\text{Cp}^*(\text{PMe}_3)\text{Ir}(\text{Ph})\text{OH}$

Periana *et al.* discovered the catalytic, heterolytic carbon-hydrogen bond activation of benzene with an air- and heat-stable iridium-hydroxo complex, $(\text{acac-O,O})_2\text{Ir}^{\text{III}}(\text{OH})(\text{Py})$ to afford iridium-phenyl complexes with the cogeneration of H_2O molecule¹⁰³ (eq 2.24).



Later, Goldberg *et al.*¹⁰⁴ described another example of aromatic C-H bond activation of benzene with a rhodium hydroxo complex, $(\text{PNP})\text{Rh}(\text{OH})$ to afford $(\text{PNP})\text{Rh}(\text{phenyl})$ in moderate yield at mild conditions (eq 2.25).



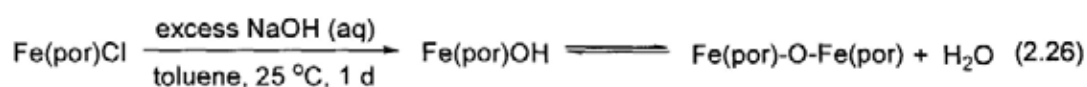
2.6 Chemistry of Metalloporphyrin Hydroxide

Transition metalloporphyrin hydroxide has rich chemistries because of their redox properties, the reported examples of M(por)OH mainly include the Fe^{III}(por)OH and Mn^{III}(por)OH.

2.6.1 Examples of Metalloporphyrin Hydroxide

2.6.1.2 Iron Porphyrin Hydroxide

Iron(III) porphyrin hydroxide, Fe(por)OH, prepared from the metathesis reaction between toluene solution of Fe(por)Cl and excess aqueous NaOH in which the sterically less hindered porphyrins, such as tpp (tpp = tetraphenylporphyrin), further dimerize to afford the μ -oxo-bridged complexes with the elimination of water molecule. While for the sterically more hindered porphyrin such as tetramesitylporphyrin, Fe(tmp)OH was obtained solely without further dimerization (eq 2.26, Figure 2.2).¹⁰⁵



por = tpp, tmp

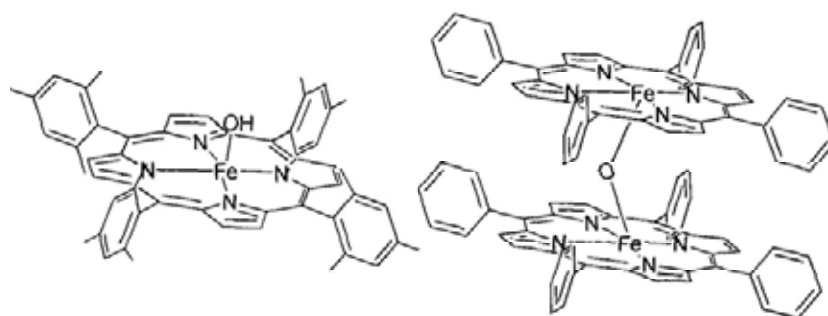
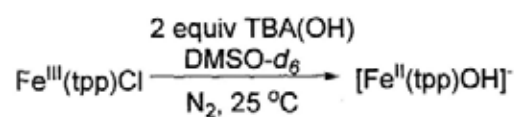


Figure 2.2 Structural features of $\text{Fe}(\text{tmp})\text{OH}$ and $[\text{Fe}(\text{tpb})]_2\text{O}$

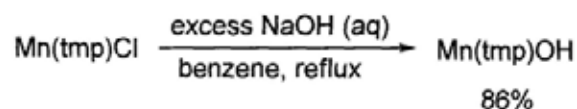
On the other hand, iron(II) porphyrin hydroxide, $[\text{Fe}^{\text{II}}(\text{por})\text{OH}]^-$ was proposed to be generated from the base-promoted reduction between iron(III) porphyrin complexes and excess tetrabutylammonium hydroxide in more polar solvents such as methanol and DMSO (Scheme 2.4).¹⁰⁶



Scheme 2.4 Reduction of $\text{Fe}^{\text{III}}(\text{tpp})\text{Cl}$ to $[\text{Fe}^{\text{II}}(\text{tpp})\text{OH}]^-$ with TBA(OH)

2.6.1.2 Manganese Porphyrin Hydroxide

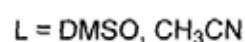
Similarly, Groves *et al.* describe the preparation of manganese(III) porphyrin hydroxide, $\text{Mn}^{\text{III}}(\text{tmp})\text{OH}$, from the benzene solution of $\text{Mn}^{\text{III}}(\text{tmp})\text{Cl}$ and NaOH under refluxing conditions (Scheme 2.5).¹⁰⁷



Scheme 2.5 Preparation of $\text{Mn}(\text{tmp})\text{OH}$ from $\text{Mn}(\text{tmp})\text{Cl}$

In contrast, Bruice *et al.* described an example of the autoreduction of manganese(III) porphyrin hydroxide in the presence of hydroxide and alkoxide in

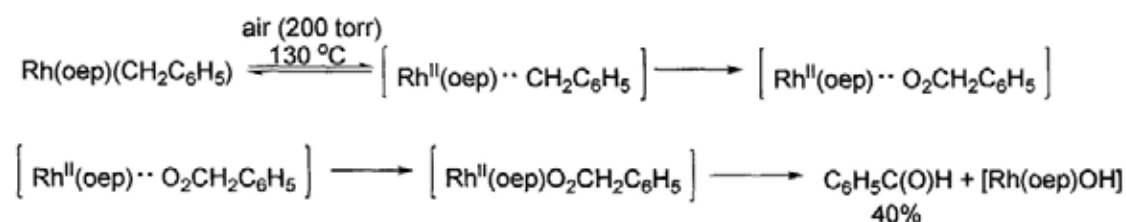
DMSO or acetonitrile via the proposed inner sphere electron transfer or nucleophilic attack on coordinated hydroxide by free OH⁻ to give manganese(II) complex (Scheme 2.6).¹⁰⁸



Scheme 2.6 Reduction of Mn^{III}(por) to Mn^{II}(por) via inner sphere electron transfer or nucleophilic attack

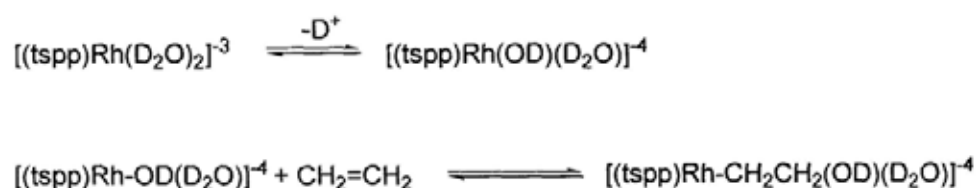
2.6.1.3 Rhodium Porphyrin Hydroxide

However, the chemistry of hydroxo rhodium porphyrin is less commonly reported. Wayland *et al.* proposed the first proposed example of [Rh(oep)OH] in the studies of the formation and thermal reactions of Rh-C bonds derived from the reactions of [Rh(oep)]₂ (oep = octaethylporphyrin) with alkyl C-H bonds in alkylaromatics. [Rh(oep)OH] was proposed as the coproduct together with benzaldehyde in the aerobic, thermal decomposition of Rh(oep)Bn (Scheme 2.7).¹⁰⁹



Scheme 2.7 Proposed generation of [Rh(oep)OH] from thermal decomposition of Rh(oep)Bn in the presence of O₂.

Later, in 2004, Wayland described a remarkable example of a water soluble hydroxo rhodium(III) porphyrin, $[\text{Rh}(\text{tspp})(\text{OD})(\text{D}_2\text{O})]^{-4}$ (tspp = tetra(*p*-sulfonato-phenyl) porphyrin dianion) and its regioselectivity and equilibrium thermodynamics of addition into olefins in aqueous media have been established (Scheme 2.8). The bond dissociation free energies of Rh-OD bond for $[(\text{tspp})\text{Rh-OD}(\text{D}_2\text{O})]^{-4}$ in water is estimated be around 62 kcal/mol.¹¹⁰



(tspp) = tetra(*p*-sulfonato phenyl) porphyrin

Scheme 2.8 Addition of Rh-OH to Olefin in Water

2.6.2 Redox of Metalloporphyrin Hydroxide

2.6.2.1 Redox of 1st row (Fe, Co, Mn) Metalloporphyrin Hydroxide

In addition, metalloporphyrin hydroxides show various redox properties especially under basic conditions, which will be discussed in the following section. Sawyer *et al.*¹¹¹ reported a series of remarkable oxidation of hydroxide ion with metalloporphyrin hydroxide including iron, manganese and cobalt. The selected redox reactions for the oxidation of HO⁻ with metalloporphyrin hydroxide in acetonitrile are shown in Table 2.4.

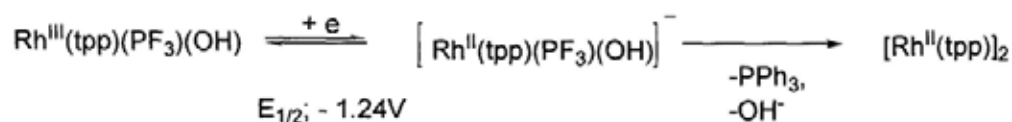
Table 2.4 Redox potentials for oxidation of OH⁻ of metalloporphyrin hydroxide

Electrode reaction	E _{1/2} ^a /V vs (SCE)
2OH ⁻ → O ²⁻ + H ₂ O + e ⁻	+0.35
H ₂ O → OH [•] + H ⁺ + e ⁻	+2.43
(tpp)Zn ^{II} (OH) ⁻ + OH ⁻ → (tpp)Zn ^{II} (O ⁻) ⁻ + H ₂ O + e ⁻	+0.49
(tpp)Fe ^{III} (OH) ⁻ → (tpp)Fe ^{III} (OH) ⁻ + e ⁻	+0.95
(tpp)Fe ^{III} (OH) ⁻ ₂ + OH ⁻ → (tpp)Fe ^{III} (O ⁻)(OH) ⁻ + H ₂ O + e ⁻	-0.89
(tpp)Mn ^{III} (OH) ⁻ ₂ + OH ⁻ → (tpp)Mn ^{III} (O ⁻)(OH) ⁻ + H ₂ O + e ⁻	-0.69
(tpp)Mn ^{III} (O ⁻)(OH) ⁻ + 2OH ⁻ → (tpp)Mn ^{III} (OH) ⁻ + O ₂ + H ₂ O + 3e ⁻	+0.19
Rh ^{III} (tpp)(PF ₃)(OH) + e ⁻ → [Rh ^{II} (tpp)(PF ₃)(OH)] ⁻	-1.24 ^b

^a in CH₃CN unless stated. ^b in THF

2.6.2.2 Redox Potential of Rhodium Porphyrin Hydroxide

Furthermore, the electrochemistry of (L)Rh(por)OH¹¹² was studied by Kadish *et al.*¹¹² (PF₃)Rh^{III}(tpp)(OH) was reported to undergo slow conversion of the electrogenerated π anion radical to dimeric [Rh^{II}(tpp)]₂. The first reduction potential of (PF₃)Rh^{III}(tpp)(OH) in THF was estimated as -1.24 V (Scheme 2.9).



Scheme 2.9 Proposed electron-transfer scheme for reduction of [Rh(tpp)(PF₃)(OH)]

2.7 Scope of the Thesis

The objectives of the research focus on the studies of the selective aliphatic carbon(α)-carbon(β) bond activation (CCA) of ether with rhodium porphyrin complexes and the promoting roles of bases in the interconversions of rhodium porphyrin species under different conditions. The thesis is outlined in the following sections:

- (i) ligand promoted, aliphatic carbon(α)-carbon(β) bond activation of ethers by rhodium(II) porphyrin radical under mild reaction conditions
- (ii) base-promoted, aliphatic carbon(α)-carbon(β) bond activation of ether by in-situ prepared rhodium porphyrin hydroxide from rhodium porphyrin iodide
- (iii) mechanistic investigation of the base-promoted interconversions of rhodium porphyrin species

Chapter 3 Carbon-Carbon Bond Activation of Ethers by Rhodium(II) Porphyrin

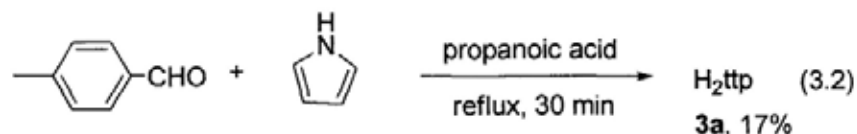
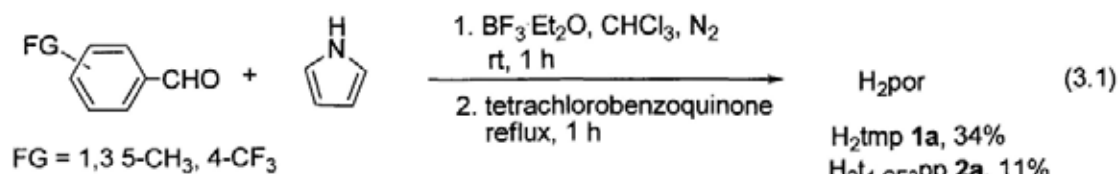
3.1 Introduction

Monomeric Rh(II) porphyrin, Rh^{II}(tmp), has been reported to activate the carbon-carbon bond of a variety of substrates. Chan *et al.* documented a series of aliphatic *sp*³-*sp*³ carbon-carbon bond activation by using Rh^{II}(tmp) in benzene solvent including nitroxide,⁶² nitrile,⁵¹ ketone,^{55a} ester^{55b} and amide^{55b} from moderate to good yields (see Chapter 2, Section 2.3). In exploring the substrate scopes in CCA with Rh^{II}(tmp), we discovered that the unstrained, aliphatic C(α)-C(β) bonds of ethers were cleaved to yield Rh(tmp)-alkyls bearing the C(β)-substituent in neat ethers. Mechanistic studies suggested that Rh(tmp)OH is more likely the active intermediate in the C-C bond cleavage step rather than the C-C bond cleavage with Rh^{II}(tmp) *via* S_H2 pathway.

3.2 Preparation of Starting Materials

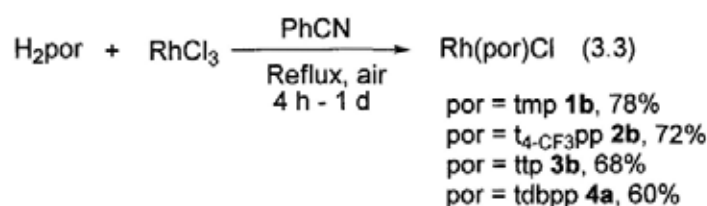
3.2.1 Synthesis of Porphyrins

The free base porphyrins, H₂por were synthesized from the co-tetramerization between pyrrole and substituted benzaldehydes according to the literature methods¹¹³ (eq 3.1 & 3.2).

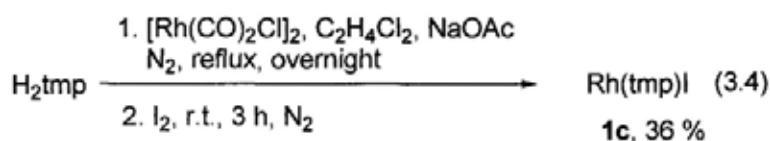


3.2.2 Synthesis of Rhodium Porphyrins

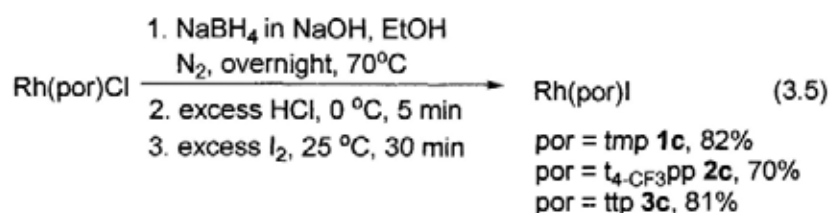
Rhodium porphyrin chlorides, Rh(por)Cl, were synthesized by refluxing H₂por and RhCl₃ in benzonitrile¹¹⁴ (eq 3.3).



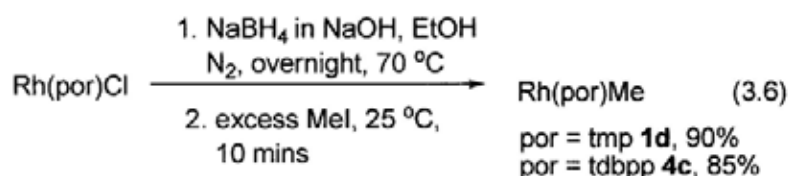
Rh(tmp)I, was prepared by the reaction between H₂tmp, [Rh(CO)₂Cl]₂ and NaOAc in dichloroethane followed by oxidation with I₂ to yield Rh(tmp)I⁸¹ (eq 3.4).



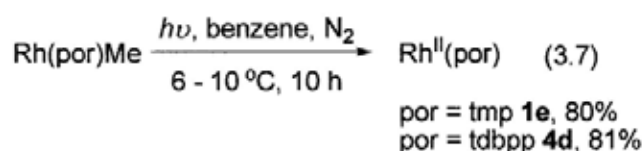
On the other hand, Rh(por)I was also prepared by reductive iodination of the Rh(por)Cl (eq 3.5).



Rhodium porphyrin methyls, Rh(por)Me were prepared from the reductive methylation of Rh(por)Cl with excess NaBH₄/MeI.⁸¹ (eq 3.6)



Rhodium(II) porphyrins, Rh^{II}(por), were prepared from the photolysis of Rh(por)Me in benzene according to the literature procedure (eq 3.7).⁸¹



3.3 Carbon-Carbon Bond Activation of Ethers with Rhodium(II) Porphyrin

3.3.1 Ligand Effects

Previously, the reactivity of Rh^{II}(tmp) towards the C-C bond cleavage was found to be enhanced with the addition of the promoter ligand such as triphenylphosphine.^{51,81b} Rh^{II}(tmp) is a square-planar, low-spin d⁷ complex with (dxy)²(dxy,yz)⁴(dz²)¹ configuration in which the HOMO of Rh^{II}(tmp) is dz². Rh(II) reacts with various ligands (L = σ donor and π acceptor) to form adducts⁹² (Figure 3.1). After coordination with a σ donor ligand, such as phosphine ligand, to form a five-coordinated (L)Rh^{II}(tmp) (L = Ar₃P), the complex becomes more electron-rich and higher in energy and therefore, more reactive.

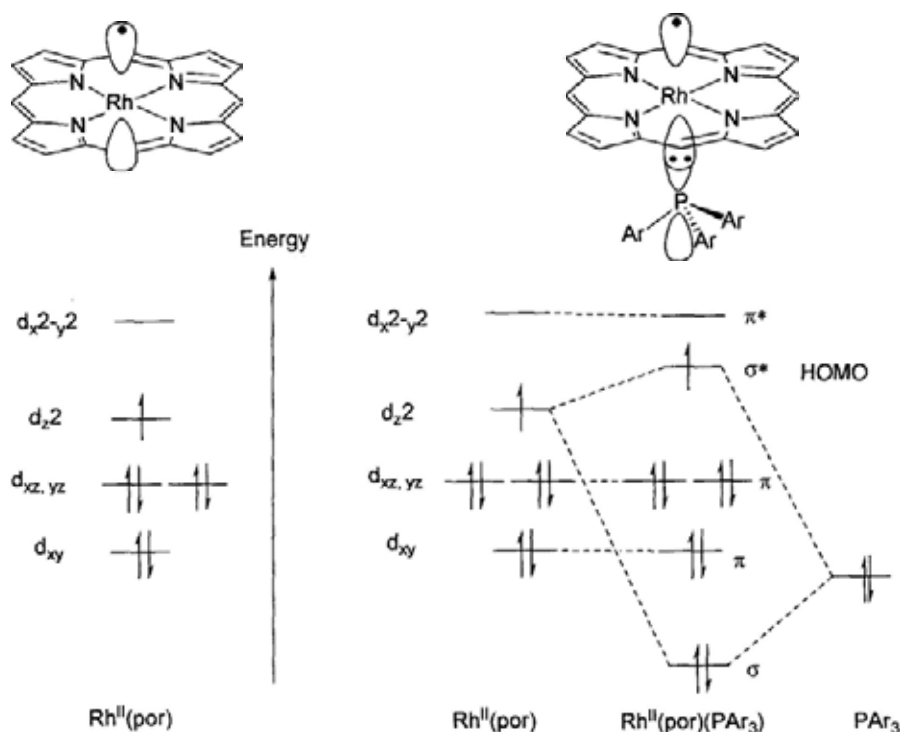


Figure 3.1 Energy diagram of molecular orbital for $(\text{PAr}_3)\text{Rh}^{\text{II}}(\text{por})$

Initially, $\text{Rh}^{\text{II}}(\text{tmp})$ reacted with neat *n*-butyl ether at room temperature for 1 day to give $\text{Rh}(\text{tmp})\text{Pr}$ in 15% yield only (Table 3.1, entry 1, eq 3.10). We then added one equivalent of various phosphine ligands such as $\text{P}(\text{Pr})_3$, $\text{P}(\text{Cy})_3$, $\text{P}(4\text{-MeOPh})_3$, $\text{P}(4\text{-toly})_3$ and PPh_3 as the promoter ligands in order to enhance the reactivity (Table 3.1, entries 2-7). Generally, phosphine ligands, except $\text{P}(\text{Pr})_3$ (Table 3.1, entry 2), promoted the reactivity of CCA in which PPh_3 ligand gave the best enhancement to 40% product yield (Table 3.1, entry 6). A higher loading of PPh_3 (2 equiv) did not enhance the CCA product yield (Table 3.1, entry 7). Most likely one equivalent of PPh_3 already converts most $\text{Rh}^{\text{II}}(\text{tmp})$ to $\text{Rh}^{\text{II}}(\text{tmp})(\text{PPh}_3)$ as the binding constant has been measured to be 2.34×10^3 at $25\text{ }^\circ\text{C}$.⁵¹ Therefore, $\text{Rh}^{\text{II}}(\text{tmp})$ exists in

approximately 80% in the form of $\text{Rh}^{\text{II}}(\text{tmp})(\text{PPh}_3)$.

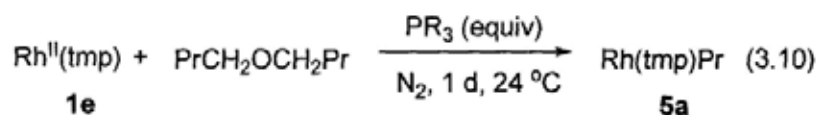


Table 3.1 Ligand Effects

Entry	PR ₃ / (equiv)	Rh(tmp)Pr 5a / yield %
1	Nil	15
2 ^a	P(^t Pr) ₃ (1)	5
3	P(Cy) ₃ (1)	18
4	P(4-MeOPh) ₃ (1)	16
5	P(4-toly) ₃ (1)	20
6	PPh ₃ (1)	40
7	PPh ₃ (2)	40

^a 5% of Rh(tmp)CH₃ was isolated, and was likely from the CCA of the isopropyl group of P(^tPr)₃.

3.3.2 Porphyrin Effects

The porphyrin effects on CCA were examined with monomeric $\text{Rh}^{\text{II}}(\text{tmp})$ and $\text{Rh}^{\text{II}}(\text{tdbpp})$ as well as $[\text{Rh}^{\text{II}}(\text{ttp})]_2$ dimer (Table 3.2, eq 3.11). The $\text{Rh}^{\text{II}}(\text{por})$ monomers gave the higher CCA yields than $[\text{Rh}(\text{ttp})]_2$ (Table 3.2 entries 1-2 vs entry 3). $\text{Rh}^{\text{II}}(\text{tmp})$ gave the highest yield in 40% (Table 3.2, entry 1) while $\text{Rh}^{\text{II}}(\text{tdbpp})$ gave slightly lower yield of 28% (Table 3.2, entry 2). Likely $\text{Rh}^{\text{II}}(\text{tdbpp})$ still exists in some extent as dimer. $[\text{Rh}(\text{ttp})]_2$ gave the lowest yield in only 7% (Table 3.2, entry 3). The low concentration of $\text{Rh}^{\text{II}}(\text{ttp})$ radical strongly reduces the product yield.

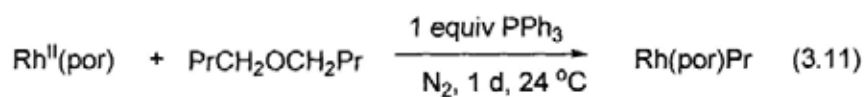


Table 3.2 Porphyrin Effects

Entry	Rh ^{II} (por)	Rh(por)Pr / Yield %
1	Rh ^{II} (tmp) 1e	Rh(tmp)Pr 5a (40)
2	Rh ^{II} (tdbpp) 4d	Rh(tdbpp)Pr 4e (28)
3	[Rh ^{II} (ttp)] ₂ 3e	Rh(ttp)Pr 3f (7)

3.3.3 Scope of Reaction

To explore the substrate scope, various ethers were then investigated using the optimal conditions at room temperature with the addition of PPh₃ (1 equiv) (Table 3.3, eq 3.12). Generally, higher yields were obtained for the straight chain aliphatic ethers than the branched one (Table 3.3, entries 1, 3 and 4 vs entries 5-6) probably due to steric reasons. The CCA reaction also took place even at 0 to 3 °C though requiring 5 days long (Table 3.3, entry 2). While for 2-ethoxyethyl ether, both the internal and terminal C(α)-C(β) bond were cleaved to give Rh(tmp)Me and Rh(tmp)CH₂OEt in around 1:1 ratio (Table 3.3, entries 7-8). Phenyl ethyl ether gave Rh(tmp)Et in 10% yield for 3 days as the carbon-oxygen activation (COA) product (Table 3.3, entry 9) probably due to the weaker PhO-Et bond (BDE of C-O bond of PhO-Et ~ 64 kcal/mol vs a typical BDE of the C(α)-C(β) bond of ether ~ 83 kcal/mol).¹⁵

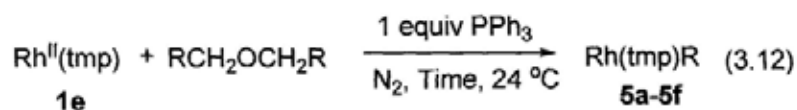


Table 3.3 Scopes of Ether

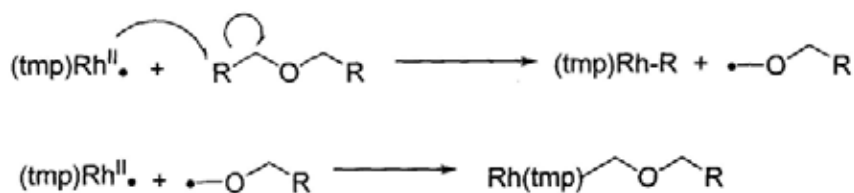
Entry	Ether	Time	Products/ Yield%
1	EtCH ₂ OCH ₂ Et	1d	Rh(tmp)Et 5b (41)
2 ^a	PrCH ₂ OCH ₂ Pr	5d	Rh(tmp)Pr 5a (38)
3	PrCH ₂ OCH ₂ Pr	1d	Rh(tmp)Pr 5a (40)
4	BuCH ₂ OCH ₂ Bu	5d	Rh(tmp)Bu 5c (30)
5	^t BuCH ₂ OCH ₂ ^t Bu	5d	Rh(tmp) ^t Bu 5d (13)
6	(CH ₂ O) ₂ CHPr	1d	Rh(tmp)Pr 5a (22)
7	(MeCH ₂ OCH ₂) ₂	4d	Rh(tmp)Me 1d (13) Rh(tmp)CH ₂ OEt 5f (12)
8 ^b	(MeCH ₂ OCH ₂) ₂	2d	Rh(tmp)Me 1d (16) Rh(tmp)CH ₂ OEt 5f (17)
9	PhOEt	3d	Rh(tmp)Et 5b (10)

a. reaction at 0 – 3 °C, *b.* reaction at 50 °C.

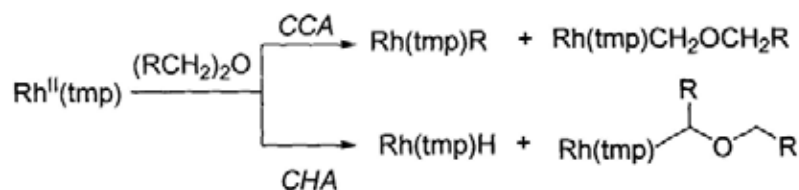
3.4 Mechanistic Investigation of CCA of Ether by Rh^{II}(tmp)

3.4.1 Possible Mechanism for the CCA of Ether with Rh^{II}(tmp) radical

Previously, the mechanism of the parallel CCA and CHA of nitroxide with Rh^{II}(tmp) radical has been proposed to operate via the homolytic bimolecular substitution pathway (S_H2) (Chapter 2, Section 2.2).⁶² Therefore, CCA and CHA of ethers by Rh^{II}(tmp) may concurrently occur (Schemes 3.1-3.2).



Scheme 3.1 Possible $\text{S}_{\text{H}2}$ pathway for the CCA of ether with $\text{Rh}^{\text{II}}(\text{tmp})$

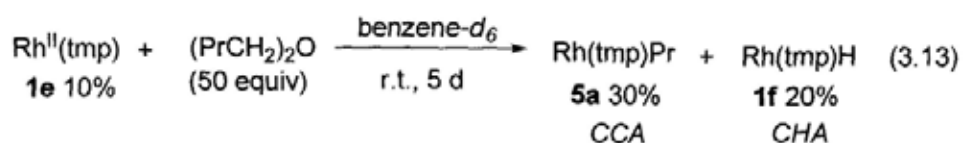


Scheme 3.2 Possible parallel CCA and CHA of ether with $\text{Rh}^{\text{II}}(\text{tmp})$

To gain further insight into the reaction mechanism, we monitored the reaction by ^1H NMR spectroscopy and attempted to identify the fate of organic coproducts.

3.4.2 NMR Monitoring of CCA Reaction

The progress of the reaction of $\text{Rh}^{\text{II}}(\text{tmp})$ with *n*-butyl ether (50 equiv) in benzene- d_6 was monitored by ^1H NMR spectroscopy. Initially, $\text{Rh}^{\text{II}}(\text{tmp})$ reacted with Bu_2O (50 equiv) to give the both $\text{Rh}(\text{tmp})\text{Pr}$ (24%) and $\text{Rh}(\text{tmp})\text{H}$ (18%) within 10 minutes at 24 °C. Prolonged reaction to 5 days did not change the amount of $\text{Rh}(\text{tmp})\text{Pr}$ (30%) and $\text{Rh}(\text{tmp})\text{H}$ (20%) significantly with 10% of $\text{Rh}^{\text{II}}(\text{tmp})$ still remained (eq 3.13).

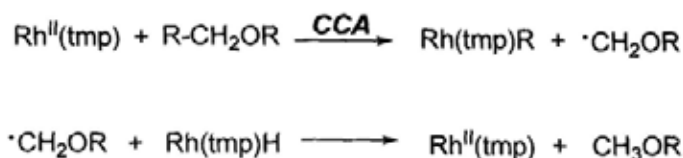


The observation of $\text{Rh}(\text{tmp})\text{H}$ suggests that the CHA of ether concurrently occurs (Scheme 3.2). While $\text{Rh}^{\text{II}}(\text{por})$ species are known to activate C-H bonds,⁹⁶⁻⁹⁷ the CHA

most probably occurs at the weakest C(α)-H bond of the ether to give Rh(tmp)H. (The strength of C(α)-H and C(β)-H bonds in the diethyl ether are 93 and 100 kcal/mol, respectively).¹⁵

3.4.3 Fate of Organic Coproducts

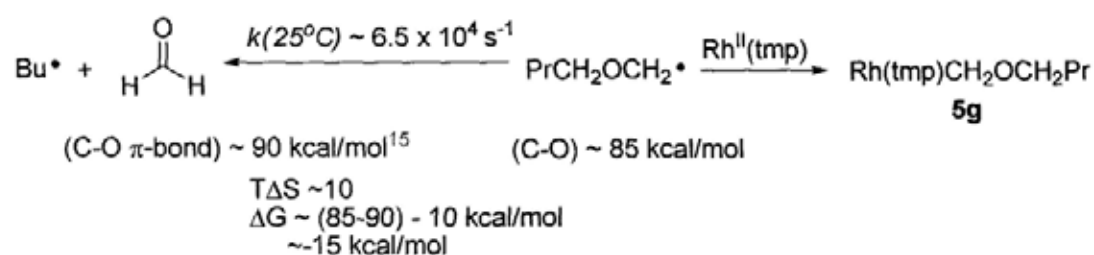
To verify whether the C-C bond cleavage of ether via S_H2 pathway by Rh^{II}(tmp), we attempted to find out the possible structure of the organic coproduct, we analyzed the reaction mixture of *n*-butyl ether by GC-MS. However, the expected organic coproduct, PrCH₂OCH₃, presumably generated from hydrogen transfer between Rh(tmp)H (formed from the CHA of ether) and the resultant alkoxy methyl radical PrCH₂OCH₂· (formed from the metalloradical cleavage of C(α)-C(β) bond of ether), was not observed even the theoretical yield should be above the detection limit of the GC-MS spectrometer used (Scheme 3.3). The detection limit of PrCH₂OCH₃ in *n*-butyl ether solvent was found to be 0.046 ppm (approximately up to 1% of PrCH₂OCH₃ in the reaction mixture of *n*-butyl ether). Therefore PrCH₂OCH₃ is less likely generated.



Scheme 3.3 Possible hydrogen atom transfer of Rh(tmp)H to ·CH₂OR

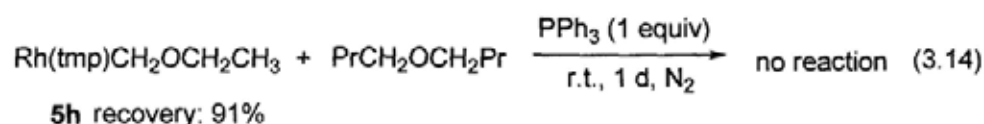
Another possible coproduct of Rh(tmp)CH₂OR, most likely generated from the coupling reaction between Rh^{II}(tmp) and alkoxy methyl radical, was also not

observed (Scheme 3.1). Alternatively, the alkoxy methyl radical if generated is presumably very reactive and may undergo rapid rearrangement to give HCHO and an alkyl radical and then alkane after hydrogen atom abstraction (Scheme 3.4).¹¹⁵ This rearrangement can provide further driving force of the reaction by around -15 kcal/mol.¹⁵ However, alkyl radical, alkane and formaldehyde were unable to be detected.



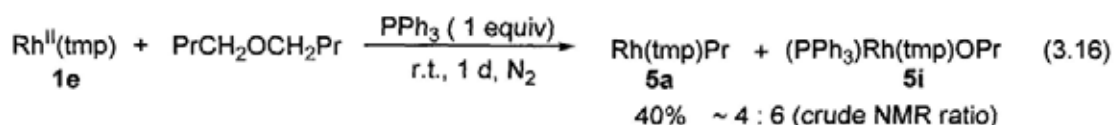
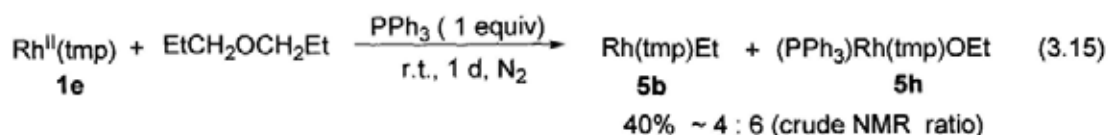
Scheme 3.4 Possible reaction pathways of the resultant alkoxy methyl radical

Since the detection of low molecular weight molecules proves to be difficult. We tested the proposed pathway by examining the stability of $\text{Rh}(\text{tmp})\text{CH}_2\text{OCH}_2\text{CH}_3$ **5h** in neat *n*-butyl ether. $\text{Rh}(\text{tmp})\text{CH}_2\text{OCH}_2\text{CH}_3$ **5h** did not react with neat *n*-butyl at 24 °C for 1 day with the recovery yield of $\text{Rh}(\text{tmp})\text{CH}_2\text{OCH}_2\text{CH}_3$ in 91% (eq. 3.14). It suggests that $\text{Rh}(\text{tmp})\text{CH}_2\text{OR}$ is stable and most likely does not form. Therefore, the C-C bond cleavage of ether via $\text{S}_{\text{H}2}$ pathway by $\text{Rh}^{\text{II}}(\text{tmp})$ is doubtful and it would be discussed in later section.



3.4.3.1 Phosphine Effect - Observation of Suspected (PPh₃)Rh(tmp)OR

On the other hand, upon addition of PPh₃, the CCA reaction of (RCH₂)₂O (R = Et and Pr) with Rh^{II}(tmp) gave Rh(tmp)R and new products that were sufficiently stable for ¹H NMR analysis in benzene-*d*₆ (eq 3.15-3.16). Though the crude reaction mixtures were not completely soluble in benzene-*d*₆, other than the CCA products of Rh(tmp)Et (Figure 3.2) and Rh(tmp)Pr (Figure 3.3), the Rh(tmp)-containing coproducts with upfield signals were also present which are assignable as (PPh₃)Rh(tmp)OEt **5h** (Figure 3.2, eq 3.15) and (PPh₃)Rh(tmp)OPr **5i** (Figure 3.3, eq 3.16) respectively. The formation of the (PPh₃)Rh(tmp)OR is not clearly understood. We attempted to isolate the suspected (PPh₃)Rh(tmp)OR through flash column chromatography but without success. Instead approximately 50% yield of (PPh₃)Rh(tmp)Cl was isolated after flash column chromatography eluting with hexane and CH₂Cl₂. It could be due to the conversion of (PPh₃)Rh(tmp)OR to Rh^{II}(tmp) and Rh(tmp)H which further react with CH₂Cl₂ to give (PPh₃)Rh(tmp)Cl.



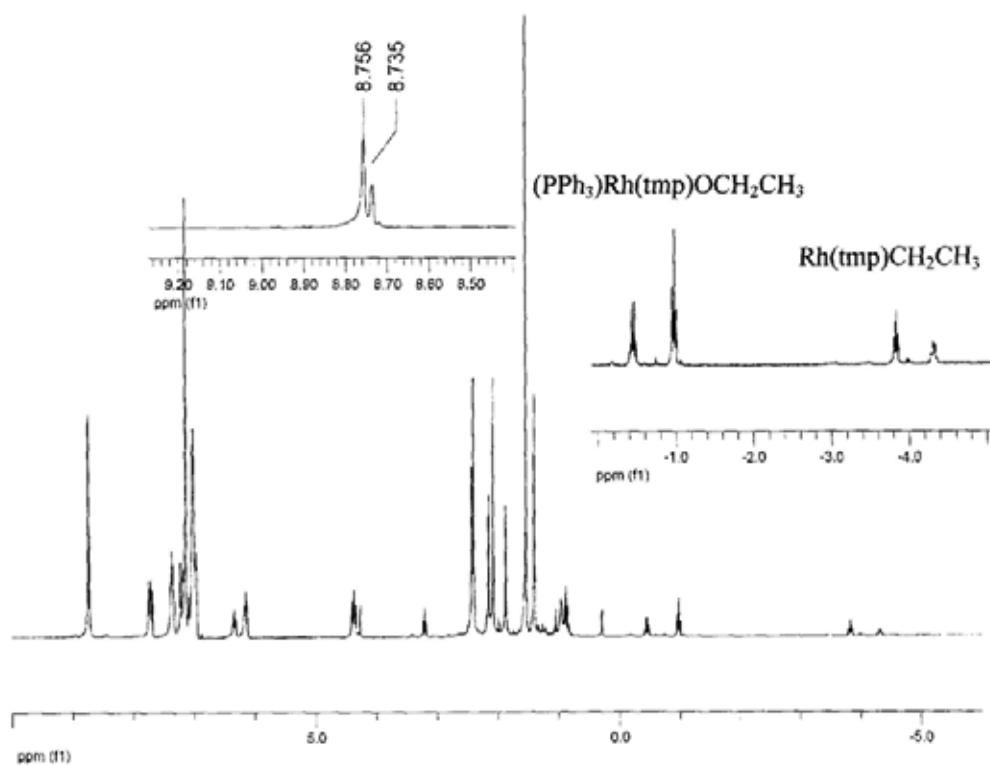


Figure 3.2 Crude ¹H NMR of eq 3.15

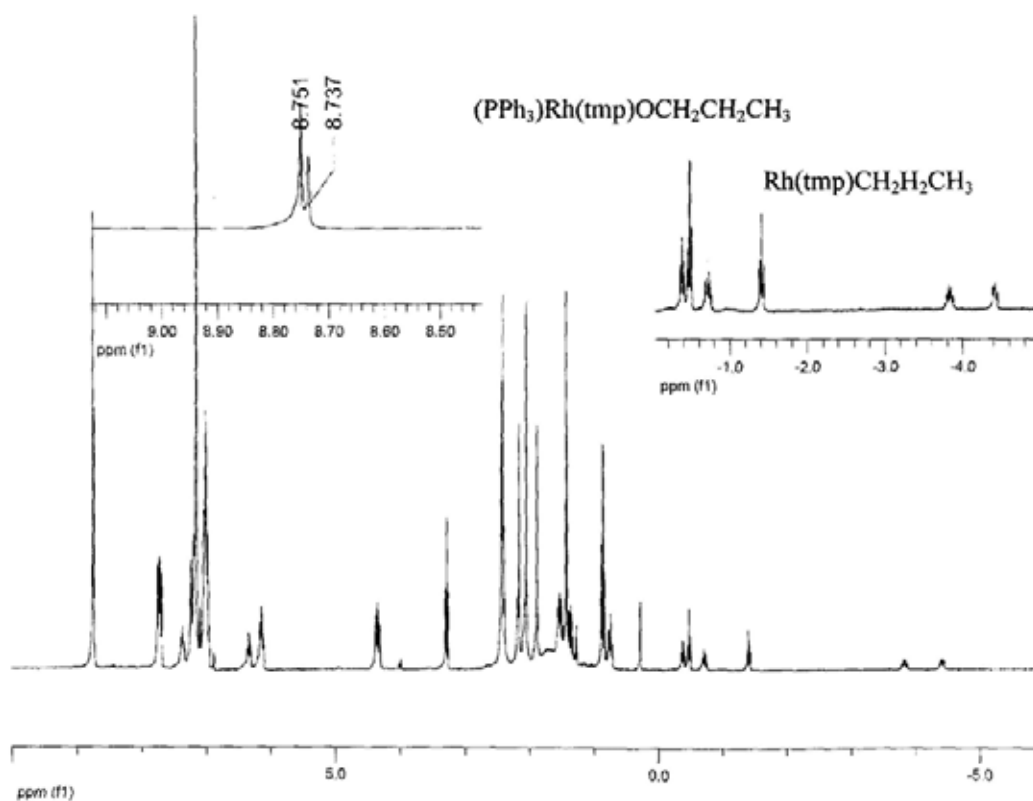
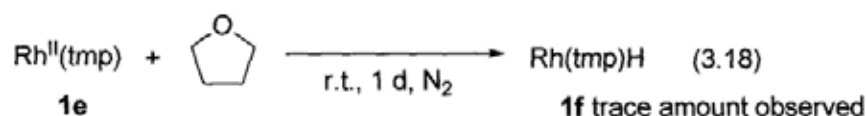
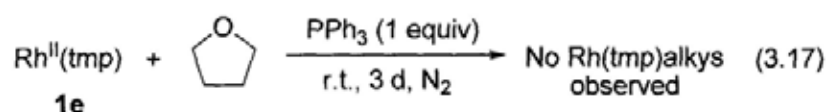


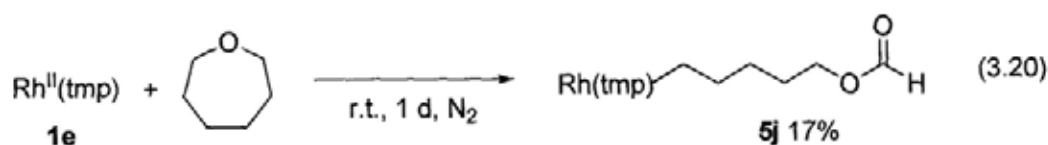
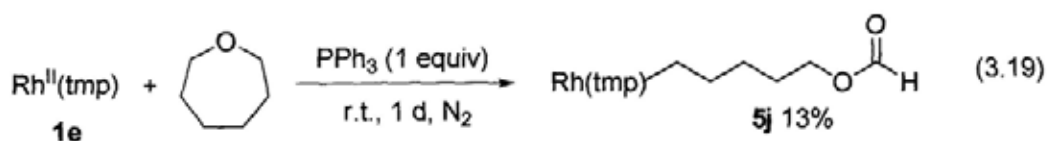
Figure 3.3 Crude ¹H NMR of eq 3.16

3.4.3.2 Intramolecular Trapping with Cyclic Ether

To assist the identification of organic coproduct, we designed intramolecular trapping experiments with cyclic ethers (eq 3.17 – 3.18). Initially, $\text{Rh}^{\text{II}}(\text{tmp})$ was reacted with THF, no corresponding CCA product was observed (eq 3.17-3.18). Indeed, only a trace amount of $\text{Rh}(\text{tmp})\text{H}$ was observed with mainly $\text{Rh}^{\text{II}}(\text{tmp})$ remained unreacted (eq 3.18).



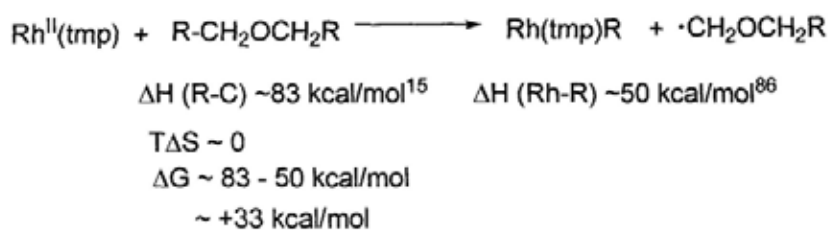
$\text{Rh}^{\text{II}}(\text{tmp})$ was then reacted with the more strained, 7-membered oxepane (ring strain energy ~ 6 kcal/mol)¹¹⁶ at 24 °C in 1 day. The unexpected formate product, $\text{Rh}(\text{tmp})(\text{CH}_2)_5\text{OCHO}$ were isolated in 13% and 17% yields in both the presence and absence of PPh_3 respectively (eq 3.19 – 3.20). Additionally, $\text{Rh}^{\text{II}}(\text{tmp})$ reacted with neat *n*-butyl ether in the presence of PPh_3 to give 40% yield of $\text{Rh}(\text{tmp})\text{Pr}$ (eq 3.12, entry 3) with approximately 1% yield of *n*-butyl formate was also detected from the GC-MS analysis. Although formates were detected in low yields, it still provides some important mechanistic insight on what the key rhodium porphyrin species responsible for the C-C bond cleavage step. The detail will be discussed in the Section 3.4.5, Alternative CCA Mechanism.



Although C-C bond cleavage of a variety of substrates by $\text{Rh}^{\text{II}}(\text{tmp})$ have been proposed via the $\text{S}_{\text{H}}2$ pathway (Scheme 3.1),⁶² the expected coproduct of $\text{CH}_3\text{OCH}_2\text{R}$ (Scheme 3.3) and $\text{Rh}(\text{tmp})\text{CH}_2\text{OCH}_2\text{R}$ (Scheme 3.4) were not detected. Moreover, the formation of formate product from the oxepane is inconsistent with $\text{Rh}^{\text{II}}(\text{tmp})$ chemistry (eq 3.19-3.20). Therefore, $\text{Rh}^{\text{II}}(\text{tmp})$ alone is less likely the direct intermediate in the C-C bond cleavage step.

3.4.4 Energetic Consideration of C-C Bond Cleavage by $\text{Rh}^{\text{II}}(\text{tmp})$

Furthermore, cleavage of a saturated C-C bond of ether *via* a $\text{S}_{\text{H}}2$ pathway is improbable because it has an overwhelmingly disfavored energetical barrier by around +33 kcal/mol even though the subsequent fragmentation of the alkoxy methyl radical can provide extra driving force by around -15 kcal/mol (Schemes 3.4-3.5, Figure 3.4). An activation energy of +33 kcal/mol would require a long half life to be 5.7×10^3 years at 25 °C which is inconsistent with the observed reaction rate. Therefore, the C-C bond cleavage step is less likely occurred via $\text{S}_{\text{H}}2$ pathway.



Scheme 3.5 Proposed mechanism of CCA of ether by $\text{Rh}^{\text{II}}(\text{tmp})$

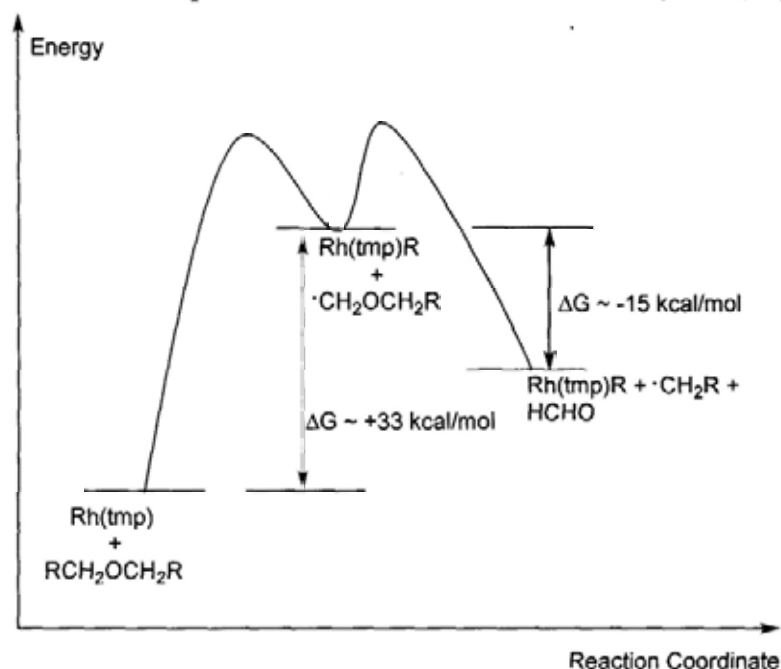
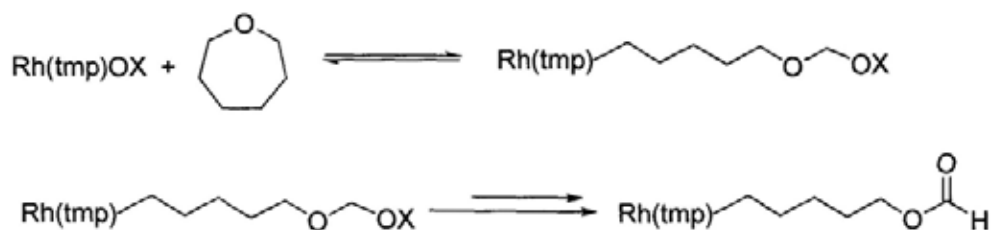


Figure 3.4 Energetic consideration of C-C bond cleavage with $\text{Rh}^{\text{II}}(\text{tmp})$

3.4.5 Alternative CCA Mechanism

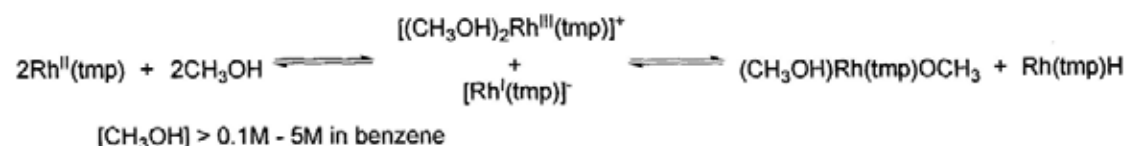
We then considered other possible $\text{Rh}(\text{tmp})$ intermediates that are responsible for the C-C bond cleavage. Since the formate product bears one more O-atom, likely, it is the result of an oxidation process probably from $\text{Rh}(\text{tmp})\text{OX}$ (Scheme 3.7).



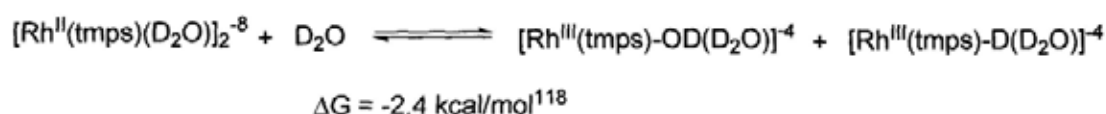
Scheme 3.7 Proposed mechanism for the formation of formate product with $\text{Rh}(\text{tmp})\text{OX}$

3.4.5.1 Disproportionation of Rh^{II}(tmp)

Previously, disproportionation of Rh(II) porphyrin complexes with CH₃OH (Scheme 3.8)¹¹⁷ and H₂O (Scheme 3.9)¹¹⁸ have been reported by Wayland *et al.*

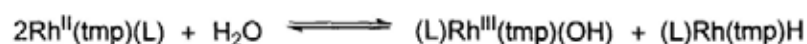


Scheme 3.8 Proposed mechanism for the disproportionation of Rh^{II}(tmp) by methanol



Scheme 3.9 Proposed mechanism for the disproportionation of water-soluble Rh^{II}(tmp) complexes in D₂O

Since a small residue of H₂O, estimated to be about 1-2 equiv with respect to Rh^{II}(tmp) in benzene-*d*₆ (eq 3.7), is present even after distillation from sodium. We reasoned that both the H₂O and PPh₃ ligand can cause Rh^{II}(tmp) to disproportionate into Rh(tmp)OH and Rh(tmp)H in ethers (Scheme 3.10). The disproportionation reaction of Rh^{II}(tmp) induced by H₂O to give Rh(tmp)OH and Rh(tmp)H is estimated to be thermodynamically favorable by around -4 kcal/mol (Scheme 3.10).

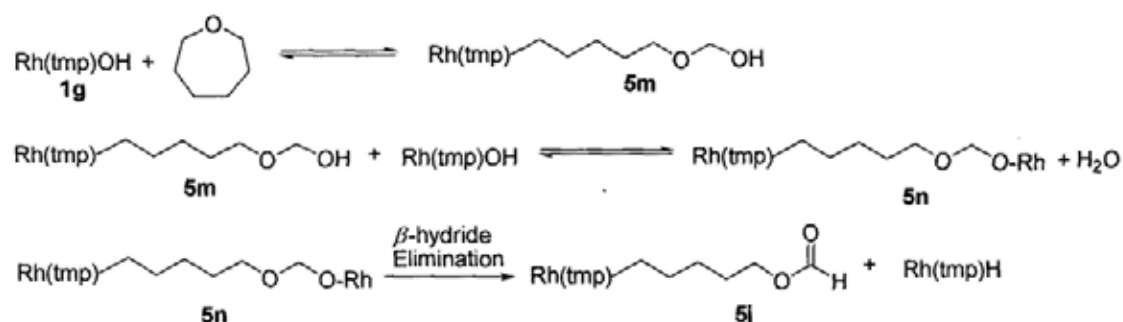


$$\Delta G^\circ(\text{H}-\text{OH}) 116 \text{ kcal/mol}^{110} \quad \Delta G^\circ(\text{Rh}-\text{OH}) 60 \text{ kcal/mol}^{110} \quad \Delta G^\circ(\text{Rh}-\text{H}) 60 \text{ kcal/mol}^{110}$$

$$\Delta G^\circ = 116 - (60 + 60) \text{ kcal/mol} = -4 \text{ kcal/mol}$$

Scheme 3.10 Plausible mechanism for the generation of Rh(tmp)OH

Therefore, Rh(tmp)OH is proposed to form from the disproportionation between Rh^{II}(tmp) with H₂O and reacts rapidly with oxepane to give the corresponding formate product. Scheme 3.11 illustrates the proposed mechanism for the formation of Rh(tmp)(CH₂)₅OCHO **5j**. Initially, Rh(tmp)OH **1g** reacts with oxepane to give the acetal **5m**. Then, **5m** reacts with Rh(tmp)OH to give the ether Rh(tmp)(CH₂)₅OCH₂ORh **5n** and H₂O. **5n** undergoes a β -hydride elimination to give the formate **5j**. Rh(tmp)H recycles back to Rh^{II}(tmp) and then Rh(tmp)OH by dehydrogenation either thermally or assisted by hydroxide (see Chapter 4, Section 4.5.4.3).



Scheme 3.11 Proposed mechanism for the formation of formate product with Rh(tmp)OH

3.4.5.2 Energetic Consideration of C-C Bond Cleavage with Rh(tmp)OH

In contrast to Rh^{II}(tmp), the C-C bond cleavage step of ether by Rh(tmp)OH is thermodynamically feasible by approximately -2 kcal/mol (Figure 3.5). Further conversion of the acetal **5m** to formate provides the extra driving force for the overall reaction system by around -19 kcal/mol (Figures 3.5-3.6).

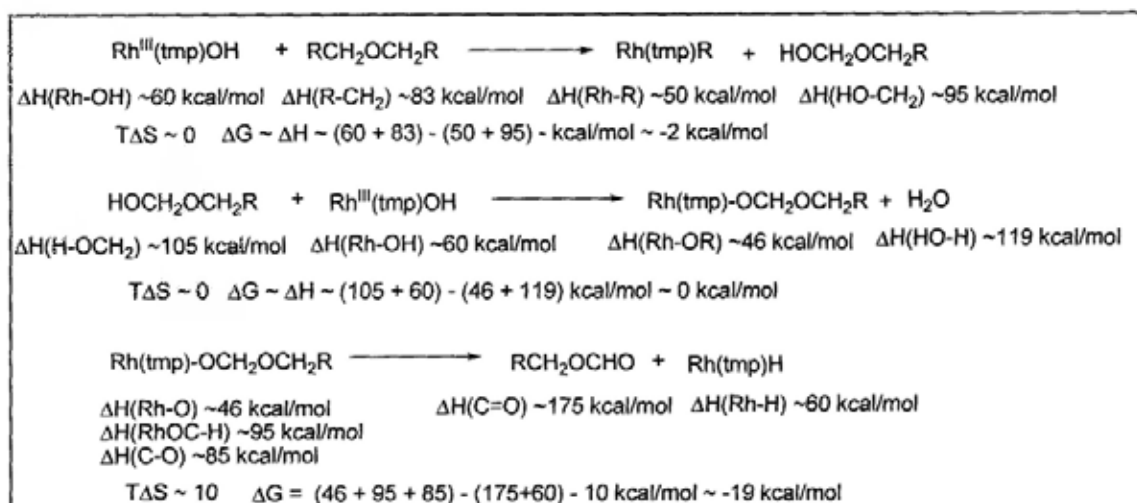


Figure 3.5 Energetic estimation of the CCA of ether by Rh(tmp)OH

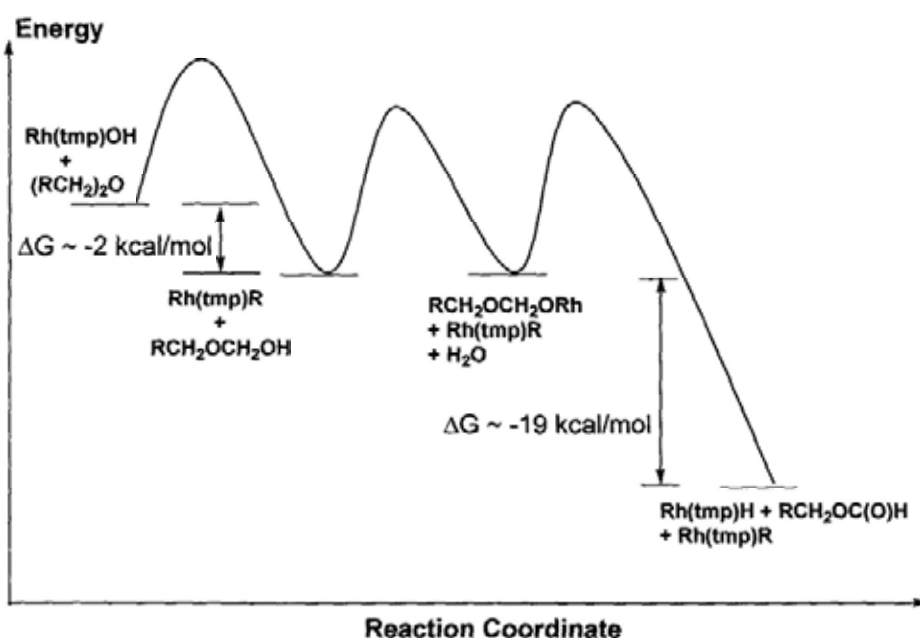
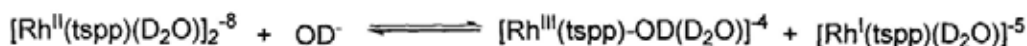


Figure 3.6 Energetic consideration of the CCA of ether by Rh(tmp)OH

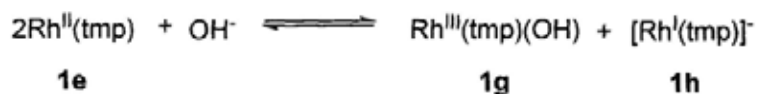
3.4.5.3 Base Effects

Since Rh(tmp)OH was proposed to be generated from the disproportionation of Rh^{II}(tmp) with H₂O. Furthermore, hydroxide ion has also been reported to cause the disproportionation of [Rh^{II}(tspp)(D₂O)]₂⁻⁸ to [Rh^{III}(tspp)-OD(D₂O)]⁻⁴ and [Rh^I(tspp)(D₂O)]₂⁻⁵ (Scheme 3.12).¹¹⁰



Scheme 3.12 Proposed Proposed Mechanism for OH⁻ induced disproportionation of [Rh^{II}(tspp)(D₂O)]₂⁻⁸

The above proposed pathways were then tested by the based-promoted CCA reaction of Rh^{II}(tmp) with ethers (Scheme 3.13, Table 3.4, eq 3.19).



Scheme 3.13 Proposed mechanism for hydroxide-induced disproportionation of Rh^{II}(tmp)

Upon addition of bases, the corresponding (PPh₃)Rh(tmp)OPr (Figure 3.3, eq 3.16) was not observed in the crude reaction mixture of the reaction of Rh^{II}(tmp) with *n*-butyl ether (eq 3.21). Likely (PPh₃)Rh(tmp)OPr is unstable under basic conditions. The addition of KOH alone did not promote the product yield (Table 3.4, entry 2) likely due to its poor solubility in *n*-butyl ether at 24 °C. Further addition of 50 equiv H₂O promoted the product yield to 62% (Table 3.4, entry 3) due to the enhanced solubility KOH in *n*-butyl ether/water. Other stronger and more soluble bases such as KO^tBu and CsOH.H₂O gave higher product yields of 56% and 59% respectively (Table 3.4, entries 4-5). These results further suggest that Rh(tmp)OH intermediate is likely generated and cleaves the C-C bond rapidly.

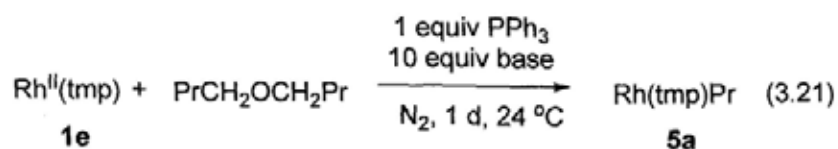


Table 3.4 Base and H₂O Effect

Entry	Base	H ₂ O/ equiv	Rh(tmp)Pr 5a / Yield%
1	Nil		40
2	KOH		40
3	KOH	50	62
4	KO ^t Bu		56
5	CsOH.H ₂ O		59

Table 3.5 Solubility of Inorganic Bases in *n*-Butyl Ether Solvent at 25 °C

Base	Solubility	Solubility with H ₂ O added (50 equiv)	Reported solubility in H ₂ O (g/g) ¹¹⁹
KOH	Sparingly soluble	Soluble	1.2
KO ^t Bu	Soluble	Soluble	-
CsOH.H ₂ O	Soluble	Soluble	3.0

3.5 Summary

Mild, selective carbon(α)-carbon(β) bond activation of ethers with rhodium(II) porphyrin complexes have been discovered. Triarylphosphines were found to be the promoter ligands in enhancing the reactivity of CCA with PPh₃ being the best ligand. The sterics of porphyrin also affect the reactivity of CCA. The sterically hindered, monomeric rhodium(II) porphyrin radical, Rh^{II}(tmp), gave the highest CCA product yield. Rh(tmp)OH has been proposed as the key intermediate plausibly generated from the PPh₃- OH⁻- and H₂O-assisted disproportionation of Rh^{II}(tmp). The CCA yields were further improved with the addition of strong bases and H₂O, so as to promote the more facile generation of the reactive Rh(tmp)OH for further CCA reaction. Further mechanistic investigation and the preparation of Rh(tmp)OH for subsequent C-C bond activation of ethers will be discussed in the next chapter.

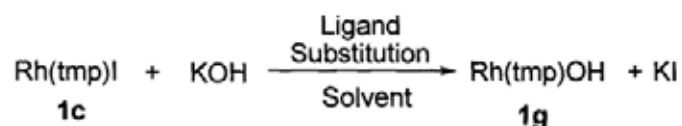
Chapter 4 Base-Promoted Carbon-Carbon Bond Activation of Ethers by Rhodium(III) Porphyrins

4.1 Introduction

In chapter 3, Rh(tmp)OH has been proposed as the key intermediate in the carbon-carbon bond activation of ethers. In this chapter, we present the results of the attempted synthesis, detection of Rh(tmp)OH as well as the systematic investigation of the CCA of ethers with *in-situ* prepared Rh(tmp)OH from rhodium(III) porphyrin halides with KOH. The promoting roles of KOH in the interconversions of Rh(tmp)-species will also be presented.

4.2 Attempted Synthesis of Rhodium(III) Porphyrin Hydroxide, (Rh(tmp)OH).

Initially, we attempted to synthesize and isolate rhodium porphyrin hydroxide by means of ligand substitution reaction between Rh(tmp)I with KOH in different solvents (Scheme 4.1, Table 4.1).



Scheme 4.1 Attempted synthesis of Rh(tmp)OH

Interestingly, the unexpected chemical transformations in three different solvents were discovered; (1) the reduction of Rh(III) porphyrin with KOH to give Rh(II) porphyrin radical in benzene (Table 4.1, entries 1-2), (2) the reduction of Rh(III) porphyrin with KOH to give Rh(I) porphyrin anion in THF (Table 4.1, entry 3), and (3)

the formation of Rh(tmp)Et via carbon(α)-carbon(β) bond cleavage in neat *n*-propyl ether solvent (Table 4.1, entry 4).

Table 4.1 Reaction between Rh(tmp)I and KOH in Different Solvents

Entry	Solvent	Temp/ °C	Time/d	Products/ (Yield/%)
1	Benzene	100	1	Rh(tmp)I 1c (70)
2 ^a	Benzene- <i>d</i> ₆	100	1	Rh(tmp)I 1c (75) Rh ^{II} (tmp) 1e (20)
3 ^a	THF- <i>d</i> ₈	100	5	[Rh ^I (tmp)] ⁻ 1h (quantitative)
4	Propyl ether	80	1	Rh(tmp)Et 5b (34)

^a NMR yield.

In non polar solvent such as benzene, only a small amount of Rh(tmp)I reacted and 70% yield of Rh(tmp)I was recovered after 1 day at 100 °C (Table 4.1, entry 1). The reaction was then carried out at benzene-*d*₆ in a sealed NMR tube and was monitored by ¹H NMR spectroscopy. After 1 day, ~75% yield of Rh(tmp)I remained unreacted and ~20% yield of Rh^{II}(tmp) formed (Table 4.1, entry 2). In the polar THF-*d*₈ solvent, Rh(tmp)I reacted with KOH at 100 °C for 5 days to give [Rh^I(tmp)]⁻ quantitatively (Table 4.1, entry 3). The base-promoted reduction of the rhodium(III) porphyrin species is strongly dependent on the solvent polarity (Table 4.2) which will be discussed in the later section (Section 4.5, Mechanistic Investigation). When neat *n*-propyl ether was used as the solvent, Rh(tmp)I and KOH were found to react with *n*-propyl ether at 80 °C to give Rh(tmp)Et in 34% yield as the selective

carbon(α)-carbon(β) bond activation product (Table 4.1, entry 4). As the reactivity patterns are strongly dependent on solvent polarity, further studies in the reactivity patterns between rhodium porphyrin halides and KOH in different solvents and ethers will aid to design the preparation of rhodium porphyrin hydroxide. Since Rh(tmp)OH proved hard to be synthesized, the objectives of my work are (1) to explore the scope of carbon-carbon bond activation of ethers with in-situ prepared Rh(tmp)OH; (2) to investigate the mechanism of carbon-carbon bond activation of ethers; and (3) to understand the reactivity patterns of rhodium porphyrin complexes in basic media.

Table 4.2 Polarity of Some Common Solvents¹²⁰

Solvent	Dielectric constant	Donor Number (kcal/mol)
Benzene	2.27	0.1
Diethyl ether	4.19	19.2
<i>n</i> -propyl ether	3.38	
<i>n</i> -butyl ether	3.08	18.1
<i>n</i> -pentyl ether	2.80	
Tetrahydrofuran	7.52	20.0
Tetrahydropyran	5.66	
Oxepane	4.97	

4.3 Carbon-Carbon Bond Activation of Ethers

4.3.1 Base Effects

The base effects for the CCA of ethers were then examined. Initially, the control experiment was carried out, Rh(tmp)I reacted with neat *n*-butyl ether at 40 °C in 1 day to give a low yield of 4% Rh(tmp)Pr as the selective C(α)-C(β) bond activated product (Table 4.3, entry 1).

Several inorganic bases were then investigated (Table 4.3, eq 4.1). Weaker bases of K₂CO₃ and Cs₂CO₃ (Table 4.3, entries 2-3) were found not to be advantageous with a little increase of product yields. Stronger bases such as NaOMe, NaOH, KO^tBu and KOH (Table 4.3, entries 3-10) were much more effective in promoting the selective C(α)-C(β) bond cleavage with KOH producing the highest product yield (Table 4.3, entry 8). A lower loading of KOH (5 equiv) (Table 4.3, entry 7) gave a lower yield while a higher loading (20 equiv) (Table 4.3, entry 9) resulted in little enhancement over the use of 10 equivalents (Table 4.3, entry 8). KOH gave the highest reactivity probably due to the more facile formation of reactive rhodium porphyrin hydroxide. In benzene or THF solvent with the addition of 50 equiv of *n*-butyl ether, less than 1% of Rh(tmp)Pr was obtained at 40 °C in 1 day. Therefore, basic and solvent-free conditions are necessary.

Table 4.3 CCA of *n*-Butyl Ether with Rh(tmp)I with Various Inorganic Bases
$$\text{Rh(tmp)I} + \text{PrCH}_2\text{OCH}_2\text{Pr} \xrightarrow[\text{N}_2, 40^\circ\text{C}]{10 \text{ equiv base}} \text{Rh(tmp)Pr} \quad (4.1)$$

1c **5a**

Entry	Bases	Time/d	5a/Yield/%
1	--	1	4
2	K ₂ CO ₃	3	7
3	Cs ₂ CO ₃	2	4
4	NaOH	1	18
5	NaOMe	1	20
6	KO ^t Bu	1	22
7 ^a	KOH	1	17
8	KOH	1	33
9 ^b	KOH	1	35
10 ^c	KOH	1	53

^a 5 equiv of KOH; ^b 20 equiv of KOH, ^c 80 °C

4.3.2 Counter Anion Effects

We then investigated the counter anion effects of the rhodium(III) porphyrin complexes, Rh(tmp)Cl, Rh(tp)Cl, Rh(tmp)I, Rh(tp)I, and Rh(tmp)BF₄. The reactions were carried out at a slightly higher reaction temperature (80 °C) in order to enhance the CCA reaction (Table 4.4, eq 4.2). The counter anion of (por)Rh-X (X = I, Cl, BF₄) strongly affected the yield of CCA. In the presence of KOH (10 equiv), Rh(tmp)Cl and Rh(tp)Cl gave Rh(tmp)Pr and Rh(tp)Pr in lower yields of only 23% and 19%

respectively (Table 4.4, entries 1-2) while Rh(tmp)I and Rh(tpp)I gave Rh(tmp)Pr and Rh(tpp)Pr in higher yields of 53% and 60% respectively (Table 4.4, entries 3-4). Likely, Rh(por)I undergoes much more facile ligand substitution with KOH for further CCA reaction. Moreover, Rh(por)Cl being less soluble than Rh(por)I in ether, gave a lower CCA yield. However, the more electrophilic Rh(tmp)BF₄, reacted with *n*-butyl ether in the presence of KOH to give Rh(tmp)Pr in only 30% yield (Table 4.4, entry 5). Therefore, rhodium(III) porphyrin iodide was chosen for further studies.

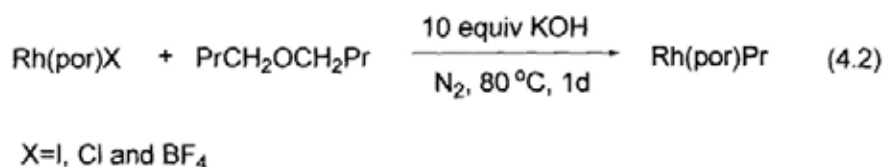


Table 4.4 Anion Effects of CCA of Ether

Entry	Rh(por)X	Product/Yield%
1	Rh(tmp)Cl	Rh(tmp)Pr 5a / 23%
2	Rh(tpp)Cl	Rh(tpp)Pr 3f / 19%
3	Rh(tmp)I	Rh(tmp)Pr 5a / 53%
4	Rh(tpp)I	Rh(tpp)Pr 3f / 60%
5 ^a	Rh(tmp)BF ₄	Rh(tmp)Pr 5a / 29%

^a prepared *in-situ*

4.3.3 Porphyrin Effects

We then examined the steric and electronic effects of various porphyrin ligands (Table 4.5, eq 4.3). Generally, Rh(*ttp*)I and Rh(*t*₄-CF₃pp)I reacted poorly with ethers comparing with Rh(*tmp*)I (Table 4.5, entries 1, 3, and 5 vs entries 2 and 4). The higher yields were obtained from Rh(*tmp*)I can be explained by two reasons. First, Rh(*tmp*)I are much more soluble than Rh(*ttp*)I and Rh(*t*₄-CF₃pp)I in ethers. Secondly, the sterically hindered *tmp* porphyrin prevents the formation of dimeric Rh₂(por)₂ and possibly other μ -oxo rhodium porphyrin.^{91,105}

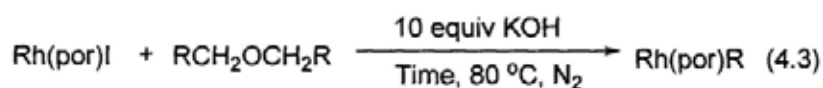


Table 4.5 Porphyrin Effects in CCA

Entry	Rh(por)I	Ether	Time	Product/Yield%
1	Rh(<i>ttp</i>)I	PrCH ₂ OCH ₂ Pr	3d	Rh(<i>ttp</i>)Pr 3f / 65
2	Rh(<i>tmp</i>)I	PrCH ₂ OCH ₂ Pr	3d	Rh(<i>tmp</i>)Pr 5a / 84
3	Rh(<i>ttp</i>)I	BuCH ₂ OCH ₂ Bu	1d	Rh(<i>ttp</i>)Bu 3i / 16
4	Rh(<i>tmp</i>)I	BuCH ₂ OCH ₂ Bu	1d	Rh(<i>tmp</i>)Bu 5c / 88
5	Rh(<i>t</i> ₄ -CF ₃ pp)I	BuCH ₂ OCH ₂ Bu	1d	Rh(<i>t</i> ₄ -CF ₃ pp)Bu 2d / 58

4.3.4 Temperature Effects

The reaction temperature for CCA of the straight chain ethers with Rh(*tmp*)I was varied from 40 °C to 100 °C (Table 4.6, eq 4.4). The lower yields for *n*-propyl ether than *n*-butyl ether (Table 4.6, entries 1-3 vs 4-5) were due to the poorer solubility of

Rh(tmp)I in *n*-propyl ether. The highest product yield was obtained for the more soluble *n*-butyl ether in 86% yield at 100 °C (Table 4.6, entry 5).

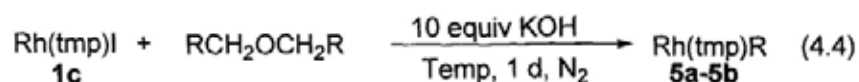


Table 4.6 Temperature Effects in CCA

Entry	Ethers	Temp/°C	Product/Yield/%
1	EtCH ₂ OCH ₂ Et	40	Rh(tmp)Et 5b / 23
2	EtCH ₂ OCH ₂ Et	80	Rh(tmp)Et 5b / 34
3	EtCH ₂ OCH ₂ Et	100	Rh(tmp)Et 5b / 30
4	PrCH ₂ OCH ₂ Pr	80	Rh(tmp)Pr 5a / 53
5	PrCH ₂ OCH ₂ Pr	100	Rh(tmp)Pr 5a / 86

4.3.5 Scope of Symmetrical Ethers

To explore the substrate scope, various ethers were then investigated using the optimal conditions at 100 °C for 1 day with KOH (10 equiv) (Table 4.6, eq 4.5).

The reactions were highly selective in the cleavage of C(α)-C(β) bonds of ethers to give Rh(tmp)R. In general, linear ethers were more reactive than branched ethers (Table 4.7, entries 2-5 vs 1 and 6) likely due to sterics. The steric effect is also evident in the activation of 2-ethoxyethyl ether (Table 4.7, entry 7). Even though the internal C(α)-C(β) bond is weaker than the terminal one by around 10 kcal/mol,¹⁵ only the terminal, least hindered C(α)-C(β) bond was cleaved to give Rh(tmp)Me, though in lower yield of 19% (Table 4.7, entry 7). For dibenzyl ether (Table 4.7, entry 8), no

corresponding Rh(tmp)Ph was obtained as this much stronger C(α)-C(β) bond is hard to cleave (BDE ~ 102 kcal/mol).¹⁵

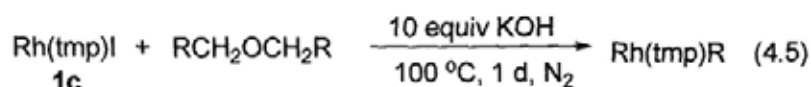


Table 4.7 CCA of Ethers with Rh(tmp)I

Entry	Ether	Product /Yield %
1	(Me) ₂ CHOCH(Me) ₂	Rh(tmp)Me 1d / 32%
2	EtCH ₂ OCH ₂ Et	Rh(tmp)Et 5b / 30%
3	PrCH ₂ OCH ₂ Pr	Rh(tmp)Pr 5a / 86%
4	BuCH ₂ OCH ₂ Bu	Rh(tmp)Bu 5c / 88%
5	PentCH ₂ OCH ₂ Pent	Rh(tmp)Pent 5e / 58%
6	ⁱ BuCH ₂ OCH ₂ ⁱ Bu	Rh(tmp) ⁱ Bu 5d / trace
7 ^a	(MeCH ₂ OCH ₂) ₂	Rh(tmp)Me 1d / 19%
8	PhCH ₂ OCH ₂ Ph	Nil

^a reaction temperature was 80 °C

4.3.6 Scope of Unsymmetrical Ethers

Rh(tmp)I reacted poorly with a branched chain ether such as isoamyl ether to give CCA product in low yield (Table 4.7, entry 7) likely due to the sterically less-accessible C(α)-C(β) bond of those substrates than that of the linear ethers. A sterically less hindered rhodium porphyrin complex Rh(ttp)I was then examined (Table 4.8, eq 4.6). However, Rh(ttp)I did not react with branched chain ethers efficiently. Therefore, the CCA reactivity is strongly dependent on the sterics of the

ethers.

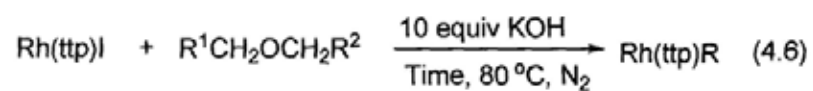


Table 4.8 CCA of Branched Chain Ethers with Rh(tp)I

Entry	Ether	Time	Product	Yield/%
1	(Me) ₂ CHOCH ₂ Pr	1d	Rh(tp)Me 16c	19
2 ^a	^t BuOCH ₂ Me	3d	Rh(tp)Me 16c	5
			Rh(tp)CH ₂ O ^t Bu 16f	5
3	^t BuOCH ₂ Pr	3d	Nil	0
4	^t BuCH ₂ OCH ₂ ^t Bu	3d	Rh(tp) ^t Bu 16e	trace
5	(CH ₂ O) ₂ CHBu	2d	Rh(tp)Bu 16d	21
6	(CH ₂ O) ₂ CHPr	1d	Rh(tp)Pr 16a	10

^a NMR yield of the reaction mixture

4.4 X-Ray Structures of Selected CCA Products, Rh(tmp)^tBu 5d, Rh(ttp)^tBu 3k and Rh(t₄-CF₃pp)Bu 2d

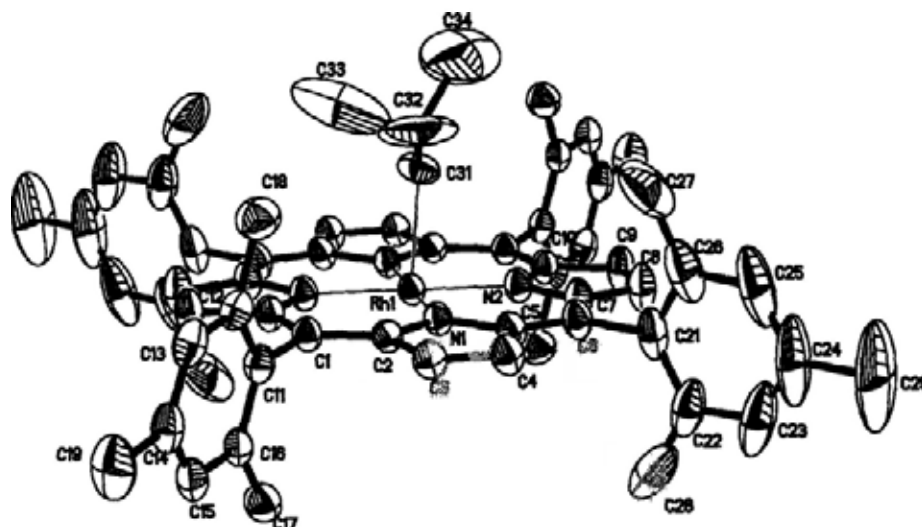


Figure 4.1 ORTEP drawing of Rh(tmp)^tBu 5d, showing the atomic labeling scheme and 30% probability displacement ellipsoids.

Table 4.9 Selected Bond Lengths (Å) and Angles (°) of Rh(tmp)^tBu

Bond length (Å)			
Rh(1)-N(1)	2.010 (3)	Rh(1)-N(1)#1	2.010 (3)
Rh(1)-N(2)	2.022 (3)	Rh(1)-N(2)#1	2.022 (3)
Rh(1)-C(31)	2.158 (9)	C(31)-C(32)	1.515 (10)
C(32)-C(33)	1.518 (10)	C(32)-C(34)	1.517 (10)
Bond angle (°)			
N(1)-Rh(1)-C(31)	94.1 (3)	N(2)-Rh(1)-C(31)	86.8 (3)
N(1)#1-Rh(1)-C(31)	85.9 (3)	N(2)#-Rh(1)-C(31)	93.2 (3)
C(32)-C(31)-Rh(1)	121.9 (8)	C(31)-C(32)-C(34)	97.1 (14)
C(31)-C(32)-C(33)	81.0 (16)	C(34)-C(32)-C(33)	97.5 (17)

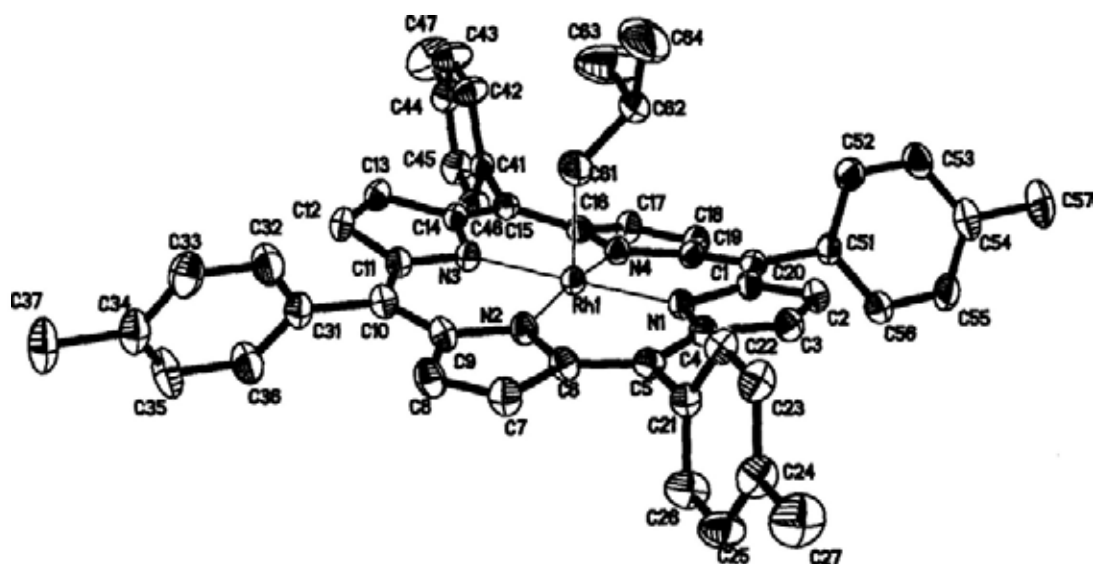


Figure 4.2 ORTEP drawing of Rh(tp)^tBu **3k** with solvent molecules omitted for clarity, showing the atomic labeling scheme and 30% probability displacement ellipsoids.

Table 4.10 Selected Bond Lengths (Å) and Angles (°) of Rh(tp)^tBu

Bond length (Å)			
Rh(1)-N(1)	2.020 (5)	Rh(1)-N(2)	2.019 (6)
Rh(1)-N(3)	2.027 (5)	Rh(1)-N(4)	2.012 (5)
Rh(1)-C(61)	2.061 (8)	C(61)-C(62)	1.461 (12)
C(62)-C(64)	1.479 (14)	C(62)-C(63)	1.526 (16)
Bond angle (°)			
N(1)-Rh(1)-C(61)	106.6 (5)	N(2)-Rh(1)-C(61)	87.8 (3)
N(3)-Rh(1)-C(61)	90.1 (3)	N(4)-Rh(1)-C(61)	99.9 (3)
C(62)-C(61)-Rh(1)	122.4 (6)	C(61)-C(62)-C(64)	113.3 (9)
C(61)-C(62)-C(63)	109.1 (9)	C(64)-C(62)-C(63)	104.8 (10)

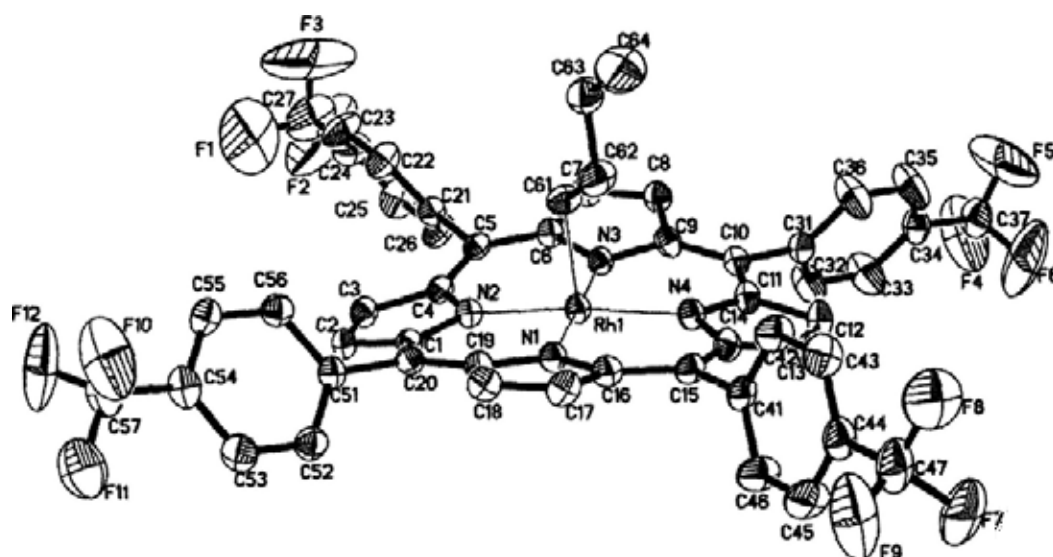


Figure 4.3 ORTEP drawing of Rh(t_4 -CF₃pp)Bu **2d**, showing the atomic labeling scheme and 30% probability displacement ellipsoids.

Table 4.11 Selected Bond Lengths (Å) and Angles (°) of Rh(t_4 -CF₃pp)Bu **2d**

Bond length (Å)			
Rh(1)-N(1)	2.030 (5)	Rh(1)-N(2)	2.004 (5)
Rh(1)-N(3)	2.024 (5)	Rh(1)-N(4)	2.019 (5)
Rh(1)-C(61)	2.051 (7)	C(61)-C(62)	1.474 (9)
C(62)-C(63)	1.461 (11)	C(63)-C(64)	1.504 (12)
Bond angle (°)			
N(1)-Rh(1)-C(61)	90.9 (2)	N(2)-Rh(1)-C(61)	90.8 (2)
N(3)-Rh(1)-C(61)	88.3 (2)	N(4)-Rh(1)-C(61)	94.8 (3)
C(62)-C(61)-Rh(1)	119.5 (5)	C(63)-C(62)-C(61)	116.0 (7)
C(62)-(63)-C(64)	116.6 (8)		

The structures of Rh(tmp)ⁱBu **5d**, Rh(tp)ⁱBu **3k**, and Rh(4-CF₃pp)Bu **2d** were confirmed by single crystal X-ray diffraction studies (Figures 4.1, 4.2 and 4.3, 30% thermal ellipsoids). Crystals were grown from dichloromethane-methanol solution. Details of data collection and processing parameters are listed in Appendix.

In Rh(tmp)ⁱBu **5d**, the Rh-C bond length is 2.158 Å which is similar to the reported Rh-C bond length of Rh(tmp)Me **1d** (2.136 Å)¹²¹ but is longer than that of analogous Rh-C bond of Rh(tp)ⁱBu **3k** (2.061 Å) likely due to steric bulkiness of the mesitylporphyrin. The porphyrin ring is nearly planar. The Rh atom is displaced at the mean plane of porphyrin ring. The individual NC₄ pyrrole rings are also nearly planar. The largest deviation relative to the mean plane of four pyrrole rings is at C₁₃ (0.072 Å). The dihedral angles between mesityl plane and the mean porphyrin plane are 84.7.5°, 86.8°, 84.7°, 86.8°, respectively. The dihedral angles between NC₄ pyrroles and mean plane are 1.58°, 1.75°, 1.58°, 1.75°, respectively.

The Rh-C bond length of Rh(tp)ⁱBu **3k** is 2.061 Å as previously mentioned. The porphyrin ring deviates slightly from planarity. The Rh atom is displaced 0.061 Å from the mean plane of porphyrin ring. The largest deviation relative to the mean plane of four pyrrole rings is at C₁₈ (0.495 Å), where as N₂ lies approximately above the mean plane by about 0.075 Å. The dihedral angles between toly plane and the mean porphyrin plane are 63.9°, 82.8°, 60.5°, 80.8°, respectively. The dihedral angles

between NC₄ pyrroles and mean plane are 9.77°, 5.59°, 11.39°, 11.46°, respectively.

The Rh-C bond length of Rh(t₄-CF₃pp)Bu **2d** is 2.051 Å. The porphyrin ring deviates slightly from planarity. The Rh atom is displaced 0.042 Å from the mean plane of porphyrin ring. The largest deviation relative to the mean plane of four pyrrole rings is at C₁₈ (0.570 Å), where as N₂ lies approximately above the mean plane by about 0.057 Å. The dihedral angles between 4-CF₃-Ph plane and the mean porphyrin plane are 76.4°, 54.0°, 56.8°, 61.9°, respectively. The dihedral angles between NC₄ pyrroles and mean plane are 13.20°, 9.07°, 12.81°, 10.14°, respectively.

4.5 Mechanistic Investigation

4.5.1 NMR Monitoring of CCA of Ether

To gain further details of the reaction mechanism, the progress of the reactions of Rh(tmp)I with *n*-butyl ether (50 equiv) and KOH (10 equiv) at 100 °C in benzene-*d*₆ and THF-*d*₈ were monitored separately by ¹H NMR spectroscopy.

In benzene-*d*₆, after the complete consumption of Rh(tmp)I in 14 hours, Rh(tmp)H (10%), Rh^{II}(tmp) (8%), Rh(tmp)Pr (10%) and some precipitate were formed (Figures 4.4a-d). Prolonged heating led to the disappearance of Rh(tmp)H and Rh^{II}(tmp) with the concomitant increase of Rh(tmp)Pr and Rh(tmp)-OO-Rh(tmp)^{94c} to 37% and 7% yields in 6 days, respectively (Figures 4.4a-d, Table 4.12). Therefore, Rh(tmp)H and Rh^{II}(tmp) are plausible intermediates. The precipitate could be

$[\text{Rh}^{\text{I}}(\text{tmp})]^+$ which is known to be insoluble in benzene- d_6 . The formation of $\text{Rh}(\text{tmp})\text{-OO-Rh}(\text{tmp})$ will be discussed in later section (Section 4.5.4.1).

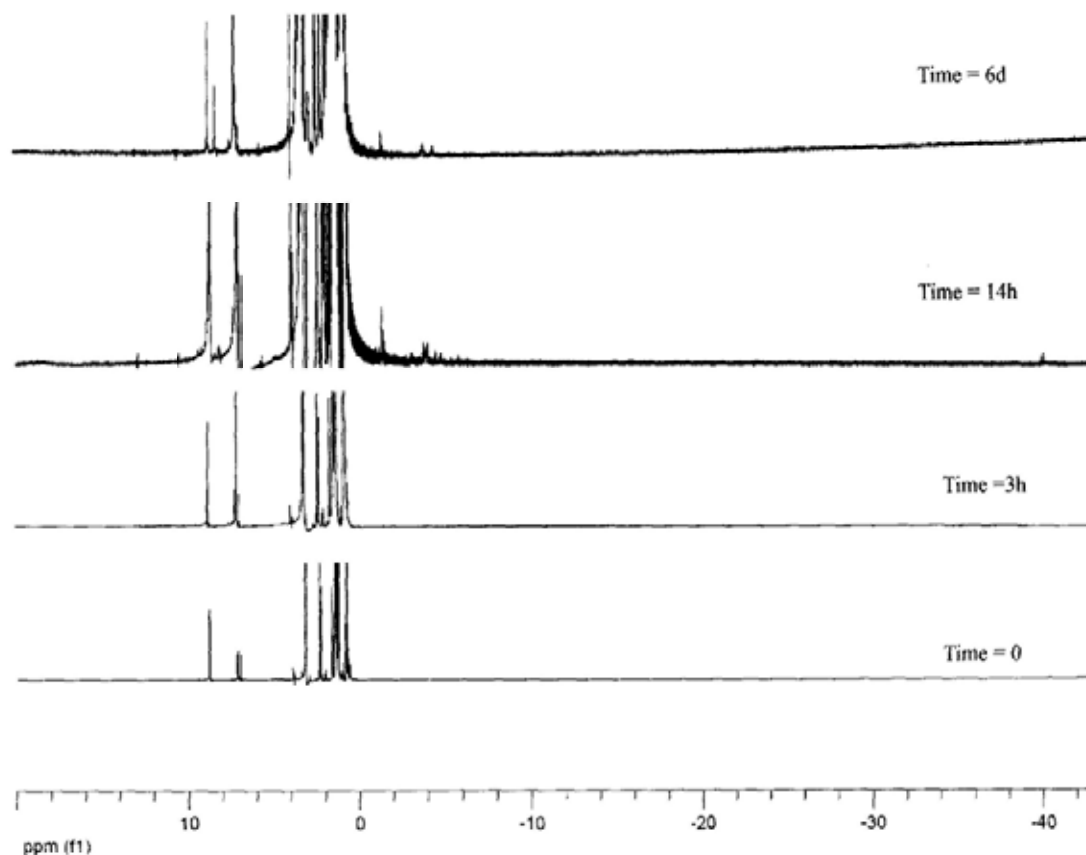


Figure 4.4a ^1H NMR spectra for the progress of reaction between $\text{Rh}(\text{tmp})\text{I}$, *n*-butyl ether(50 equiv) and KOH (10 equiv) in benzene- d_6 at $100\text{ }^\circ\text{C}$

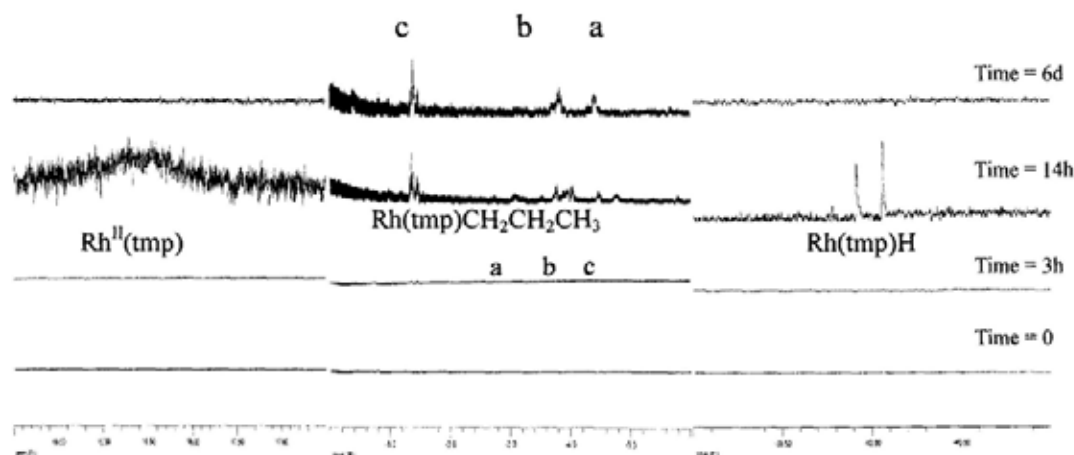


Figure 4.4b. Selected NMR region for $\text{Rh}^{\text{II}}(\text{tmp})$ signal

Figure 4.4c. Selected NMR region for $\text{Rh}(\text{tmp})\text{CH}_2\text{CH}_2\text{CH}_3$ signal

Figure 4.4d Selected NMR region for $\text{Rh}(\text{tmp})\text{H}$ signal

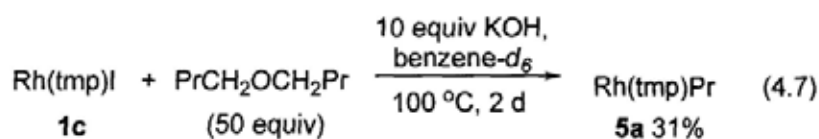
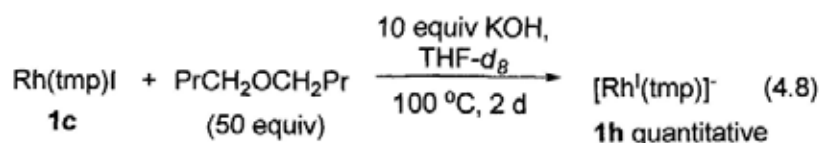


Table 4.12 Progress of the CCA of *n*-Butyl Ether with Rh(tmp)I in Benzene-*d*₆

Entry	Time	Yield/ %				
		Rh(tmp)I	Rh(tmp)H	Rh ^{II} (tmp)	Rh(tmp)Pr	Rh(tmp)-OO-Rh(tmp)
1	0	100	0	0	0	0
2	3h	82	0	0	0	0
3	14h	0	10	8	10	0
4	2d	0	0	0	31	6
5	6d	0	0	0	37	7

In THF-*d*₈, only [Rh^I(tmp)]⁺ was observed as the sole product after heating at 100 °C for 2 days (Figures 3.5a-b, eq 3.14). Most likely, the CHA of both *n*-butyl ether and THF occurs to give Rh(tmp)H which then undergoes rapid deprotonation with KOH in THF to yield [Rh^I(tmp)]⁺. Indeed, Rh(tmp)H was found to be deprotonated with KOH (10 equiv) at 100 °C to give [Rh(tmp)]⁺ quantitatively (Also see section 4.5.4, Role of base). Moreover, some other rhodium porphyrins were also observed and are suspected to be Rh(tmp)-alkyls species (Figure 4.5b, unknown c and unknown d). However, these species could not be further identified.



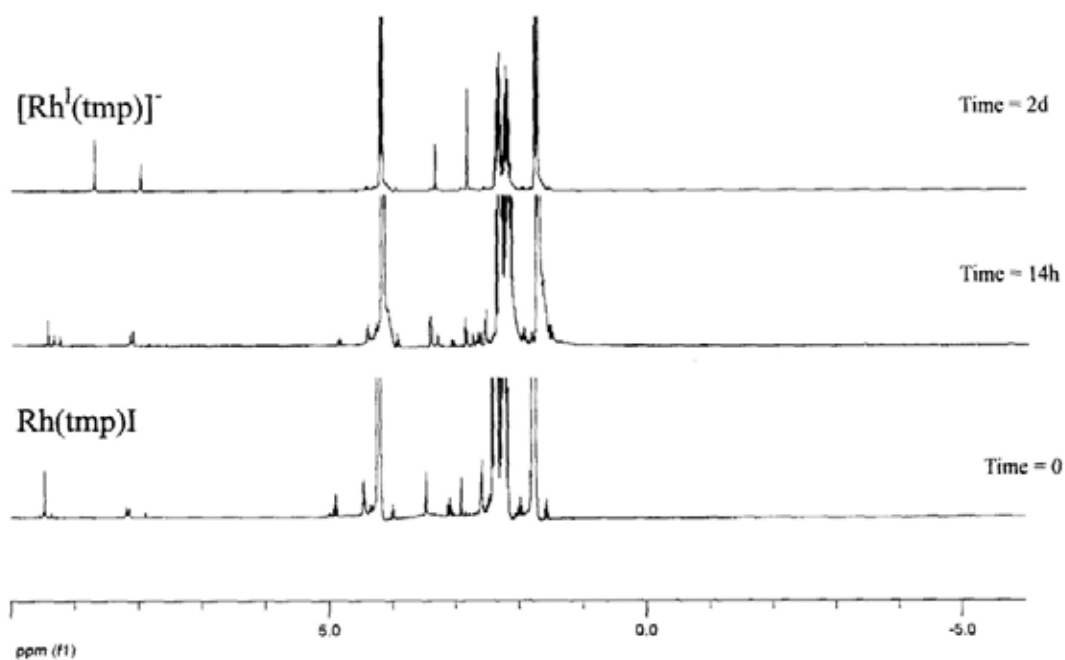


Figure 4.5a ^1H NMR spectra for the progress of reaction between $\text{Rh}(\text{tmp})\text{I}$, *n*-butyl ether(50 equiv) and KOH (10 equiv) in $\text{THF-}d_8$ at 100°C

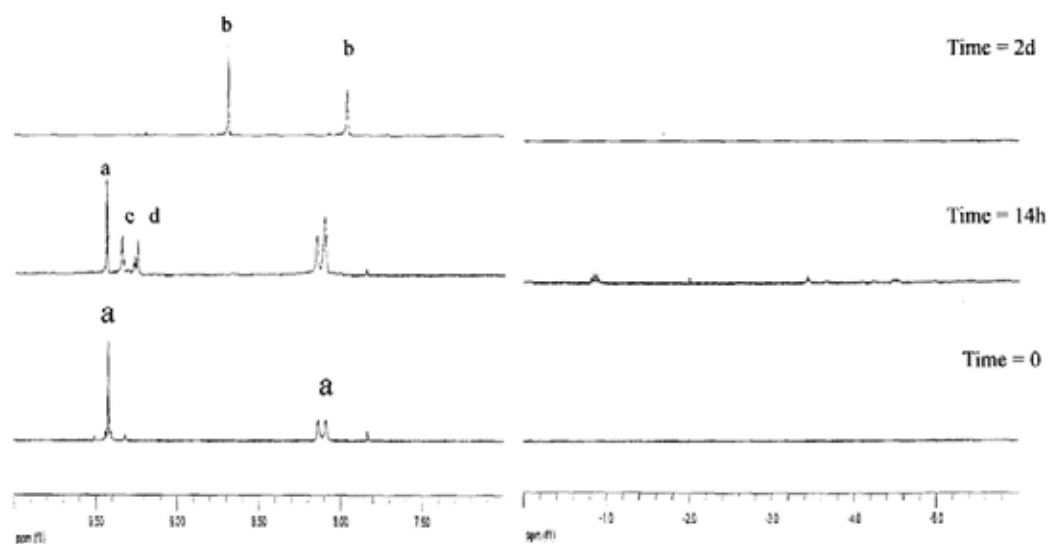


Figure 4.5b Expanded region for pyrrolic signal of rhodium porphyrin species
(a) $\text{Rh}(\text{tmp})\text{I}$; (b) $[\text{Rh}^{\text{I}}(\text{tmp})]^-$;
(c) & (d) unidentified rhodium porphyrins

Figure 4.5c Expanded upfield region of the NMR analysis

Table 4.13 Selected Characteristic ^1H NMR Signals (ppm) of Rhodium Porphyrin Complexes in the Reaction Between $\text{Rh}(\text{tmp})\text{I}$, *n*-Butyl Ether, and KOH in THF- d_8 at 100 °C (eq 4.7).

Rhodium Complexes	Pyrrole/ δ ppm	Phenyl/ δ ppm	Methyl group/ δ ppm
$\text{Rh}(\text{tmp})\text{I}$ 1c	8.70	7.41, 7.37	2.70, 2.41, 1.82
$[\text{Rh}^{\text{I}}(\text{tmp})]^-$ 1h	8.01	7.29	2.66, 2.15
Unknown c	8.61	unresolved	unresolved
Unknown d	8.51	unresolved	unresolved

4.5.2 Reaction Intermediates: $\text{Rh}^{\text{II}}(\text{tmp})$, $\text{Rh}(\text{tmp})\text{H}$ and $[\text{Rh}^{\text{I}}(\text{tmp})]^-$

Since $\text{Rh}(\text{tmp})\text{H}$ and $[\text{Rh}^{\text{I}}(\text{tmp})]^-$, $\text{Rh}^{\text{II}}(\text{tmp})$ are possible intermediates. Therefore, we sought to identify the roles of these rhodium porphyrin species in the CCA of ether by reacting $\text{Rh}(\text{tmp})\text{H}$ and $[\text{Rh}^{\text{I}}(\text{tmp})]^-$, $\text{Rh}^{\text{II}}(\text{tmp})$ with *n*-butyl ether in either presence or absence of KOH.

4.5.2.1 $\text{Rh}(\text{tmp})\text{H}$

$\text{Rh}(\text{tmp})\text{H}$ was thus reacted with *n*-butyl ether at 100 °C (Table 4.14, eq 4.9). In the absence of base, only 10% yield of $\text{Rh}(\text{tmp})\text{Pr}$ was obtained (Table 4.14, entry 1). In the presence of KOH (10 equiv), $\text{Rh}(\text{tmp})\text{Pr}$ was obtained in 54% yield (Table 4.14, entry 2). Therefore $\text{Rh}(\text{tmp})\text{H}$ is not the direct and major intermediate.

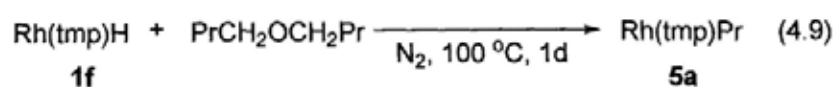


Table 4.14 Reaction of neat *n*-Butyl Ether with Rh(tmp)H **1f**

Entry	Base (10 equiv)	Rh(tmp)Pr 5a / Yield%
1	Nil	10
2	KOH	54

In order to gain a deeper understanding on how Rh(tmp)H reacted in the presence of KOH, the reaction of Rh(tmp)H and *n*-butyl ether (50 equiv) in the presence or absence of KOH in benzene-*d*₆ at 100 °C were then monitored by ¹H NMR (eq 4.10). Without KOH, no Rh(tmp)Pr was observed from the NMR analysis and about 85% of Rh(tmp)H remained unreacted even after 3 days. In the presence of KOH, Rh(tmp)H did react. After 34 hours, Rh^{II}(tmp) (14%), Rh(tmp)Pr (10%) and 23% yield of Rh(tmp)H were found (Figure 4.6, Table 4.15). Some insoluble rhodium porphyrin precipitate was also observed and suspected to be [Rh^I(tmp)]⁺. These results further suggested that Rh(tmp)H is not the direct intermediate and is converted to other rhodium porphyrin species that are responsible for the C-C bond cleavage. Since Rh^{II}(tmp) has been observed as the intermediate. Likely, Rh(tmp)H can convert to Rh^{II}(tmp) under basic conditions for further reaction.

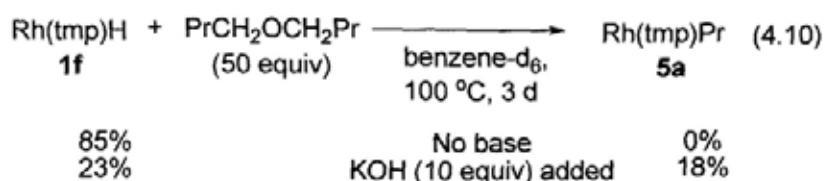
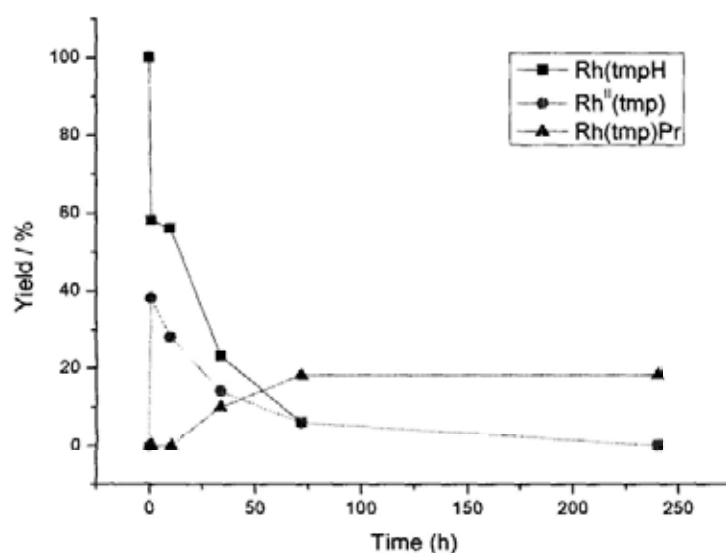


Table 4.15 Progress of CCA of *n*-Butyl Ether by Rh(tmp)H with KOH in Benzene-*d*₆

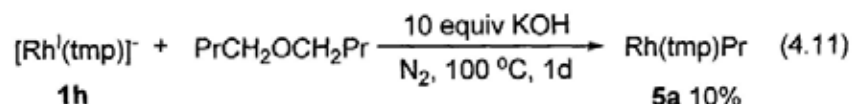
Entry	Time	Yield/%		
		Rh(tmp)H	Rh ^{II} (tmp)	Rh(tmp)Pr
1	0	100	0	0
2	1h	58	39	0
3	34h	23	14	10
4	3d	5	5	18
5	10d	0	0	18

**Figure 4.6** Progress of the reaction between Rh(tmp)H **1f**, KOH (10 equiv) and *n*-butyl ether in benzene-*d*₆.

4.5.2.2 [Rh^I(tmp)]⁻

Since insoluble rhodium porphyrin of [Rh^I(tmp)]⁻ was likely formed from the deprotonation of Rh(tmp)H in the reaction mixture of benzene-*d*₆ in basic media,¹¹⁸ its intermediacy was then examined. However, [Rh^I(tmp)]⁻ reacted with neat *n*-butyl ether to give only 10% yield of Rh(tmp)Pr even in the presence of KOH (10 equiv)

(eq 4.11). Therefore, $[\text{Rh}^{\text{I}}(\text{tmp})]^{-}$ is unlikely the intermediate.



4.5.2.3 $\text{Rh}^{\text{II}}(\text{tmp})$

To find out the role of $\text{Rh}^{\text{II}}(\text{tmp})$ in the CCA reaction, $\text{Rh}^{\text{II}}(\text{tmp})$ was reacted with *n*-butyl ether (Table 4.16, eq 4.12). $\text{Rh}(\text{tmp})\text{Pr}$ was isolated in 37% yield (Table 4.16, entry 1). Furthermore, in the presence of KOH (10 equiv) in 1 day at 100 °C, $\text{Rh}^{\text{II}}(\text{tmp})$ gave $\text{Rh}(\text{tmp})\text{Pr}$ in a higher yield of 56% (Table 4.16, entry 2). Most likely, KOH can promote the reactivity of $\text{Rh}^{\text{II}}(\text{tmp})$ towards CCA of ethers.

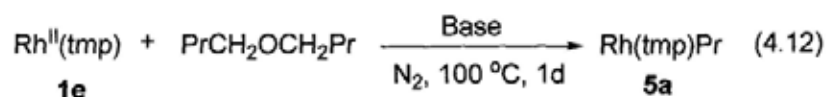


Table 4.16 CCA of neat *n*-Butyl Ether with $\text{Rh}^{\text{II}}(\text{tmp})$

Entry	Base (10 equiv)	$\text{Rh}(\text{tmp})\text{Pr}$ 5a / Yield%
1	Nil	37
2	KOH	56

Besides, a NMR tube experiment of the reaction of $\text{Rh}^{\text{II}}(\text{tmp})$ with Bu_2O (50 equiv) in benzene- d_6 gave both $\text{Rh}(\text{tmp})\text{Pr}$ (24%) and $\text{Rh}(\text{tmp})\text{H}$ (18%) within 10 minutes even at 25 °C with 20% of $\text{Rh}^{\text{II}}(\text{tmp})$ remained (eq 4.13). Prolonged reaction at 100 °C for 4 days gave $\text{Rh}(\text{tmp})\text{Pr}$ (25%) and $\text{Rh}(\text{tmp})\text{H}$ (23%) with 12% of $\text{Rh}^{\text{II}}(\text{tmp})$ remained (Table 4.17, eq 4.13). While in the presence of KOH, $\text{Rh}^{\text{II}}(\text{tmp})$ reacted with Bu_2O (50 equiv) in benzene- d_6 gave both $\text{Rh}(\text{tmp})\text{Pr}$ (24%) and

Rh(tmp)H (15%) initially at 25 °C with 24% of Rh^{II}(tmp) remaining. Prolonged reaction at 100 °C for 4 days gave 51% yield of Rh(tmp)Pr with some precipitate being observed in the bottom of the NMR tube.

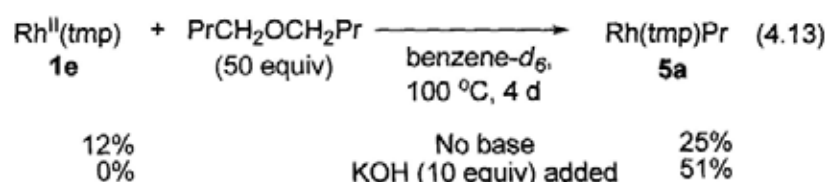
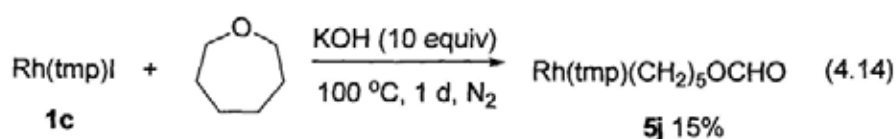


Table 4.17 Progress of CCA of *n*-Butyl Ether by Rh^{II}(tmp) with KOH in Benzene-*d*₆

Entry	Time	Yield/%		
		Rh ^{II} (tmp)	Rh(tmp)H	Rh(tmp)Pr
1	0	24	15	24
2	2h	21	23	35
3	14h	0	10	41
4	4d	0	0	51

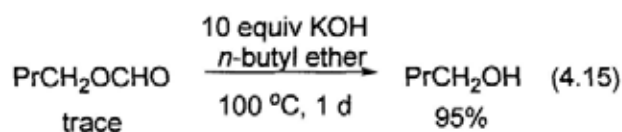
4.5.3 Rh(tmp)OH

As concluded previously in Chapter 3, Rh^{II}(tmp) alone is not the active intermediate. KOH can convert Rh^{II}(tmp) to Rh(tmp)OH that is responsible for the subsequent CCA reaction (Chapter 3, Section 3.4.4.3). To test the proposal, Rh(tmp)I was reacted with oxepane in the presence of KOH (10 equiv) at 100 °C for 1 day and Rh(tmp)(CH₂)₅OCHO was isolated in 15% yield (eq 4.14).



This result strongly suggests that Rh(tmp)OH is most likely the intermediate in the C-C bond cleavage step (see Chapter 3, Scheme 3.10). Additionally, we also detected *n*-butyl formate (<1%) from the crude reaction mixture of the reaction

between Rh(tmp)I and *n*-butyl ether in the presence of KOH at 100 °C for 1 day (Table 4.6, entry 4). The low yield of the formate product is probably due to its instability in basic media as the formate could be hydrolyzed to alcohol (eq 4.15).



4.5.4 Promoting Roles of KOH in Interconversion of Rhodium Porphyrin Species

Since Rh(tmp)I, Rh^{II}(tmp) and Rh(tmp)H reacted poorly with ether in the absence of KOH. Therefore, the promoting roles of bases are important and mechanistically interesting to study. Further experiments have been done to support the intermediacy of Rh(tmp)OH.

4.5.4.1 Ligand Substitution

The first role of a hydroxide is probably to undergo ligand substitution with Rh(tmp)I to give Rh(tmp)OH. We thus monitored the reaction between Rh(tmp)I and KOH (10 equiv) in benzene-*d*₆ at 100 °C (Figure 4.7). As the reaction progressed, the NMR peaks were broadened indicating the presence of paramagnetic species. Indeed, the paramagnetic diagnostic pyrrole signal at δ 18.1 ppm of Rh^{II}(tmp) was observed in 1 day in 20% yield together with other upfield-shifted pyrrole signals at around 8.23 ppm assignable to be the known Rh(tmp)-OO-Rh(tmp)^{94c} in 5% yield (eq 4.16). The reaction proceeded much faster at a higher temperature of 120 °C to give 54% yield of Rh^{II}(tmp) in just 2 hours (eq 4.16). These results showed that Rh(tmp)OH is

presumably very reactive and rapidly equilibrate with $\text{Rh}^{\text{II}}(\text{tmp})$ under basic media

(Scheme 4.3).

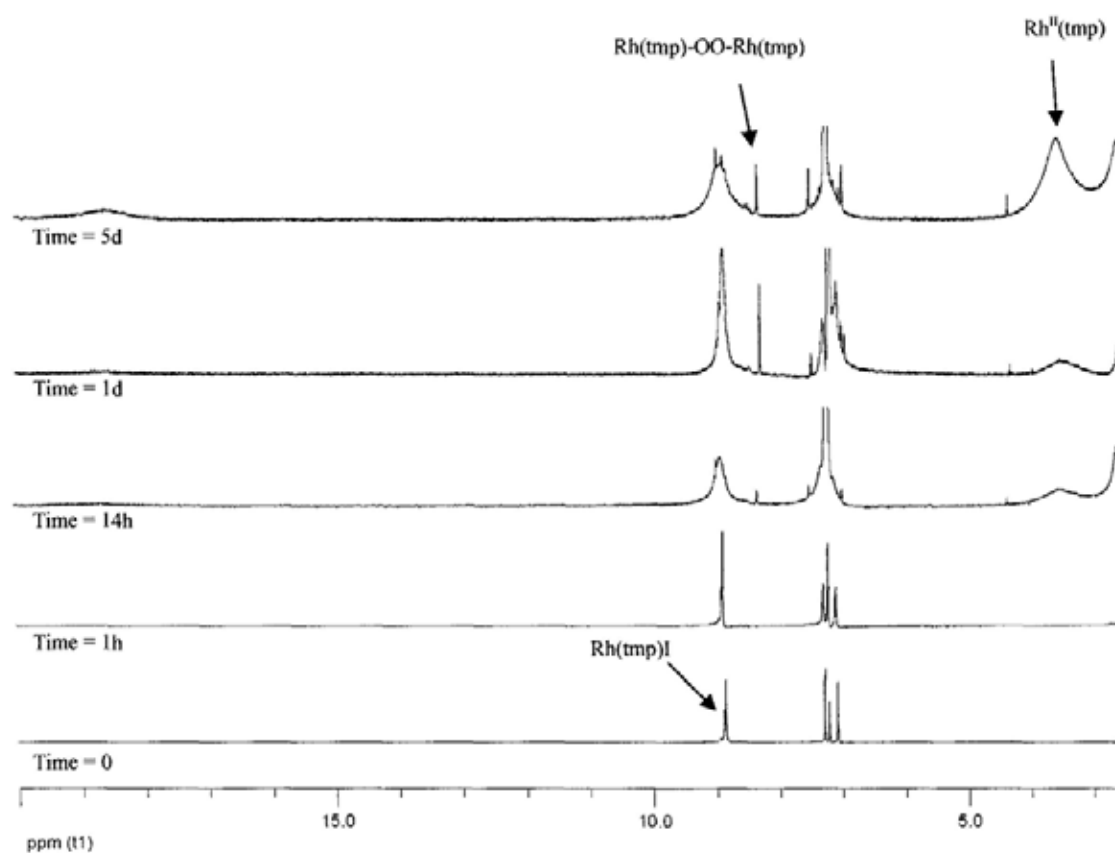
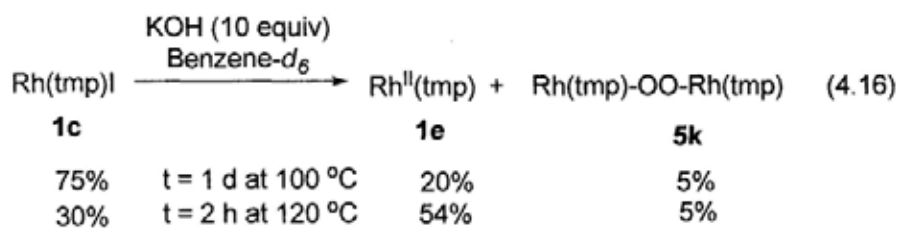
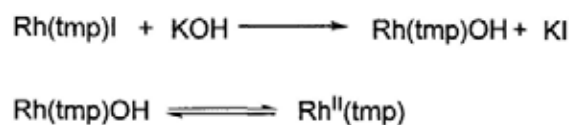


Figure 4.7 Reaction time profile of the reaction between $\text{Rh}(\text{tmp})\text{I}$ and KOH (10 equiv) in $\text{benzene-}d_6$ at 100 °C.



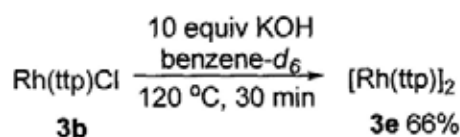
Scheme 4.3 Proposed ligand substitution of $\text{Rh}(\text{tmp})\text{I}$ with KOH

Table 4.18 The selected characteristic ¹H NMR shifts (ppm) of Rh(tmp)I and Rh(tmp)OORh(tmp) **5k**

Complexes	Pyrrole/ δ ppm	Phenyl/ δ ppm
Rh(tmp)I	8.81	7.22, 7.01
Rh(tmp)-OO-Rh(tmp)	8.23 (8.27) ^a	7.22 (7.21) ^a , 6.93 (6.93) ^a

^a Wayland's reported result^{94c}

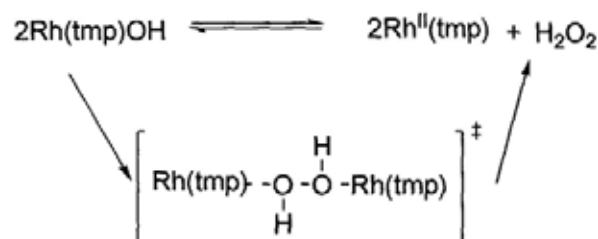
Analogous result has also been demonstrated by Mr K. S. Choi in Professor K. S. Chan's group. Rh(ttp)Cl reacted with KOH to give Rh₂(ttp)₂ via the proposed Rh(ttp)OH intermediate under similar reaction conditions (Scheme 4.4).¹²²



Scheme 4.4 Base-promoted reduction of Rh(ttp)Cl

4.5.4.2 Reducing Agent

The mechanism for the reduction of rhodium(III) porphyrins to the more reactive rhodium(II) porphyrins with KOH is mechanistically interesting and important because a hydroxide plays the role of a reducing agent. Rh(tmp)OH can undergo bimolecular reductive elimination via the concerted pathway to give Rh^{II}(tmp) and hydrogen peroxide (Scheme 4.5).¹²³ The reduction of Rh(tmp)OH to Rh^{II}(tmp) via this pathway is thermodynamically unfavorable by around +60 kcal/mol. However, further decomposition of H₂O₂ can provide extra driving force by around -29 kcal/mol and shifts the equilibrium to the side of Rh^{II}(tmp).



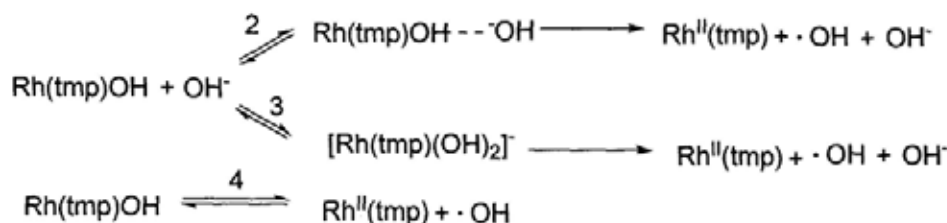
Scheme 4.5 Generation of Rh^{II}(tmp) via concerted pathway

Alternatively, the reduction process can be explained by electron transfer, the reduction of iron(III) porphyrin hydroxide¹⁰⁸ and manganese(III) porphyrin hydroxide¹¹⁰ with hydroxide ion have been reported. Hydroxide ion is a known efficient one-electron reducing agent in aprotic solvent,¹²⁰ the hydroxide anion possibly transfer an electron to rhodium metal center *via* (1) outer sphere electron transfer (Scheme 4.6, pathway 1), (2) inner sphere electron transfer (Scheme 4.6, pathways 2-4), and (3) nucleophilic attack on rhodium-bound hydroxide by free OH⁻ (Scheme 4.6, pathway 5).¹¹⁰

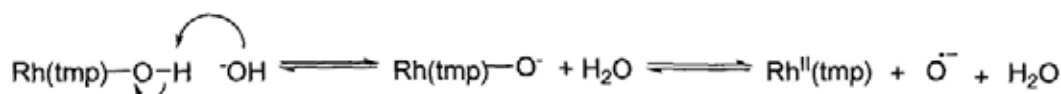
Pathway 1 – Outer Sphere Electron Transfer



Pathway 2 - 4 – Inner Sphere Electron Transfer of Rh-bound hydroxide



Pathway 5 – Nucleophilic attack on Rh-bound hydroxide¹⁰⁸

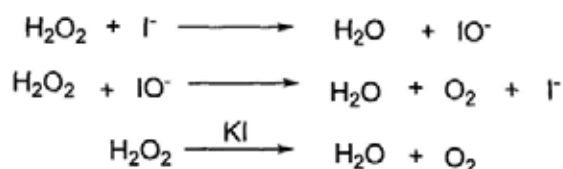


Scheme 4.6 Possible pathways for base reduction of Rh(III) to Rh(II) porphyrin

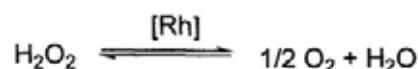
An outer-sphere electron-transfer oxidation of a free hydroxide to a hydroxyl radical (Scheme 4.6, pathway 1) is kinetically less accessible.¹⁰⁸ Therefore, the reduction of the rhodium(III) porphyrin by OH⁻ likely involves an inner sphere electron transfer from a rhodium(III)-bound OH⁻ (Scheme 4.6, pathways 2-4) or by a nucleophilic attack with a free OH⁻ (Scheme 4.6, pathway 5).

For the inner-sphere electron transfer pathways (Scheme 4.6, pathways 2-4), [Rh^{II}(tmp)••OH(OH)]/[Rh^{II}(tmp)••OH] presumably formed and then transforms into Rh^{II}(tmp) and •OH.

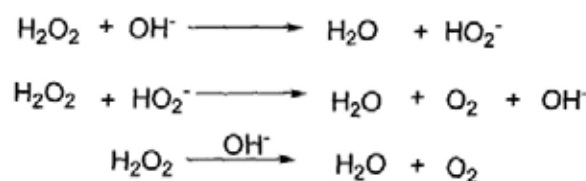
The coproduct hydroxide radicals can self-couple to give H₂O₂ providing the extra driving force of a HO-OH bond by around 50 kcal/mol.¹⁵ H₂O₂ probably undergoes catalytic decomposition in the presence of potassium iodide (Scheme 4.7),^{124a} rhodium porphyrin complexes (Scheme 4.8)^{124b-c} or hydroxide ion (Scheme 4.9),^{124d} to give oxygen and H₂O. Competing reaction of •OH and O^{•-} with solvent may also happen, however, no corresponding Ph-OH was observed.¹²⁵



Scheme 4.7 Catalytic decomposition of H₂O₂ by KI

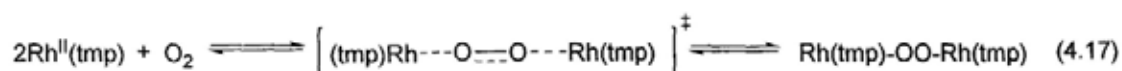


Scheme 4.8 Catalase-type reaction with rhodium porphyrin complexes



Scheme 4.9 Catalytic decomposition of H_2O_2 by OH^-

The observation of the reported $\text{Rh}(\text{tmp})\text{-OO-Rh}(\text{tmp})$ ^{94c} (Figure 4.8) strongly supports that a trace amount of dioxygen, generated from the decomposition of H_2O_2 and further reacts with $\text{Rh}^{\text{II}}(\text{tmp})$ to give the known $\text{Rh}(\text{tmp})\text{-OO-Rh}(\text{tmp})$ (eq 4.17) as reported by Wayland *et al.*^{94c}



4.5.4.3 Base-Promoted Dehydrogenation of $\text{Rh}(\text{tmp})\text{H}$

Since $\text{Rh}(\text{tmp})\text{H}$ also reacted with *n*-butyl ether to give $\text{Rh}(\text{tmp})\text{Pr}$ in the presence of KOH . The thermal and base-promoted dehydrogenation of $\text{Rh}(\text{tmp})\text{H}$ to give $\text{Rh}^{\text{II}}(\text{tmp})$ and then $\text{Rh}(\text{tmp})\text{OH}$ are also viable. While the dehydrogenation of $\text{Rh}(\text{oep})\text{H}$ (*oep* = octaethylporphyrin) is reported to slowly give $[\text{Rh}^{\text{II}}(\text{oep})]_2$ at 60-70 °C in toluene,^{91a,d} the base-promoted dehydrogenation of $\text{Rh}(\text{ttp})\text{H}$ to $[\text{Rh}(\text{ttp})]_2$ ^{90b} and $\text{Ir}(\text{ttp})\text{H}$ to $[\text{Ir}(\text{ttp})]_2$ ¹²⁶ have been reported recently. Initially, $\text{Rh}(\text{tmp})\text{H}$ did not give any $\text{Rh}^{\text{II}}(\text{tmp})$ at 100 °C in 3 days (Table 4.19, entry 1) while it was converted to $\text{Rh}^{\text{II}}(\text{tmp})$ in 10% yield at 180 °C for 2 hours (Table 4.19, entry 2). When 10 equiv of KOH was added to $\text{Rh}(\text{tmp})\text{H}$ in benzene-*d*₆, 30% of $\text{Rh}^{\text{II}}(\text{tmp})$ was observed in 1 hour (Table 4.19, entry 3).

To gain some idea on the base strength effect, Rh(tmp)H was then treated with a variety of inorganic bases to investigate the base-promoted dehydrogenation of Rh(tmp)H in benzene-*d*₆ (Table 4.19, eq 4.18).

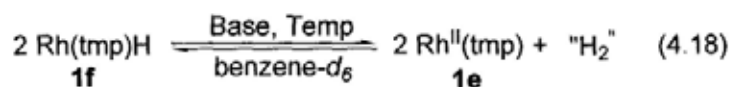
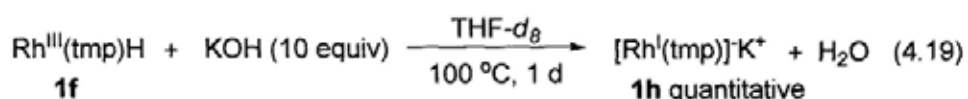


Table 4.19 Base-Promoted Dehydrogenation of Rh(tmp)H **1f** to Rh^{II}(tmp) **1e**

Entry	Base	Equiv	Temp/ °C	Time	Rh(tmp)H / yield%	Rh ^{II} (tmp) / yield%
1	Nil		100	3 d	quantitative	0
2	Nil		180	2 h	85	10
3	KOH	10	100	1 h	60	30
4	KOH	0.05	100	3 d	quantitative	0
5	KOH	0.5	100	3 d	quantitative	0
6	KOH	100	100	30 min	40	50
7	KOAc	10	100	1 h	85	10
8	KO ^t Bu	10	24	5 min	71	20

A lower base loading (0.5 or 0.05 equiv of KOH) did not promote the dehydrogenation process (Table 4.19, entries 4-5) while a higher base loading (100 equiv of KOH) promoted the yield and rate of the dehydrogenation process (Table 4.19, entry 6). Weak base such as KOAc also worked but gave lower yield (Table 4.19, entry 7) while strong base such as KO^tBu induced the dehydrogenation of Rh(tmp)H even at room temperature to give 20% yield of Rh^{II}(tmp) within 5 minutes (Table 4.19, entry 8). However, Rh^{II}(tmp) completely decomposed in 2 days at room temperature to give an insoluble reaction mixture, likely the [Rh^I(tmp)]⁺K⁺.

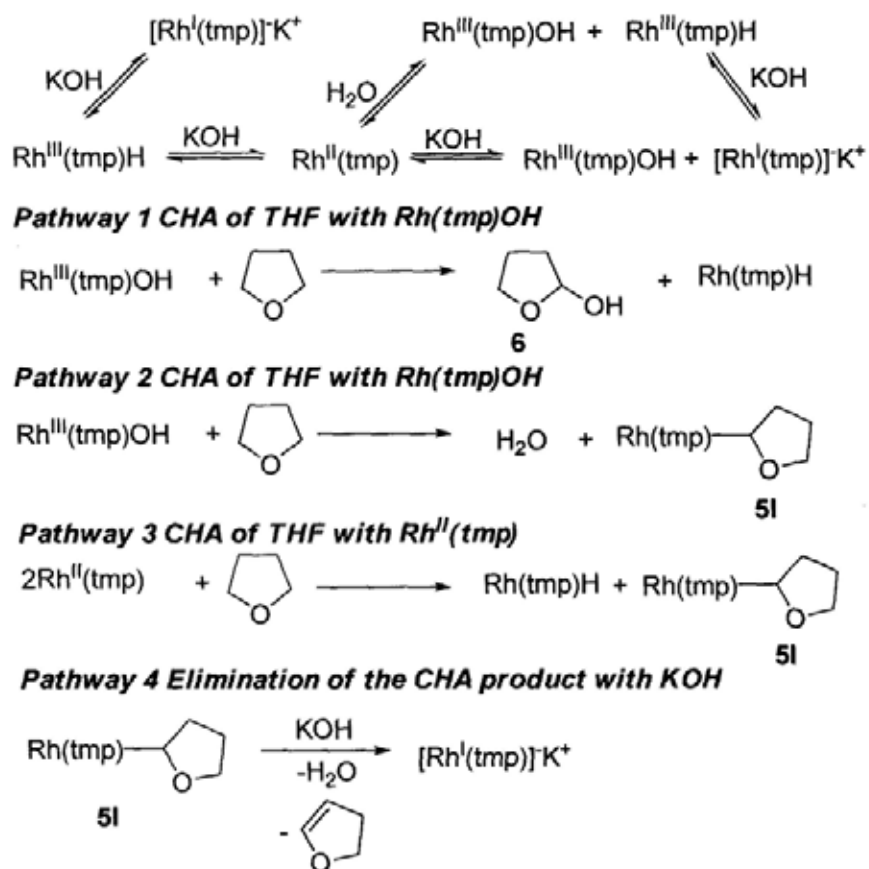
On the other hand, Rh(tmp)H reacted with KOH in THF- d_8 at 100 °C for 1 day to give $[\text{Rh}^{\text{I}}(\text{tmp})]^- \text{K}^+$ quantitatively (eq 4.19). Solvent strongly affects the reactivity pattern.



The possible pathways for the reduction of Rh(tmp)H in THF is illustrated in Scheme 4.10. Firstly, Rh(tmp)H can react with KOH to give the deprotonated product of $[\text{Rh}^{\text{I}}(\text{tmp})]^-$ directly. Alternatively, Rh(tmp)H can also react with KOH to give dehydrogenated product of $\text{Rh}^{\text{II}}(\text{tmp})$ and then Rh(tmp)OH, Rh(tmp)OH can further react with THF to give Rh(tmp)H and **6** (Scheme 4.10, pathway 1) or Rh(tmp)(2-tetrahydrofuranyl) **5I** and H_2O (Scheme 4.10, pathway 2). Besides, $\text{Rh}^{\text{II}}(\text{tmp})$ may also react with THF to give Rh(tmp)H and **5I** (Scheme 4.10, pathway 3). Finally, Rh(tmp)H undergoes deprotonation and **5I** undergoes E_2 elimination with KOH respectively to give $[\text{Rh}^{\text{I}}(\text{tmp})]^-$ as the final stable product (Scheme 4.10, pathways 4).

The different reactivity patterns of Rh(tmp)H and KOH in benzene and THF are mainly due to two reasons: Firstly, the difference in the C-H bond strengths of benzene and THF (BDE of Ph-H = 112 kcal/mol while C(α)-H bond of THF = 92 kcal/mol).¹⁵ Therefore, the CHA of THF by Rh(tmp)OH and $\text{Rh}^{\text{II}}(\text{tmp})$ is more competitive (Scheme 4.10, pathways 1-3); Secondly, THF (dielectric constant = 7.52)

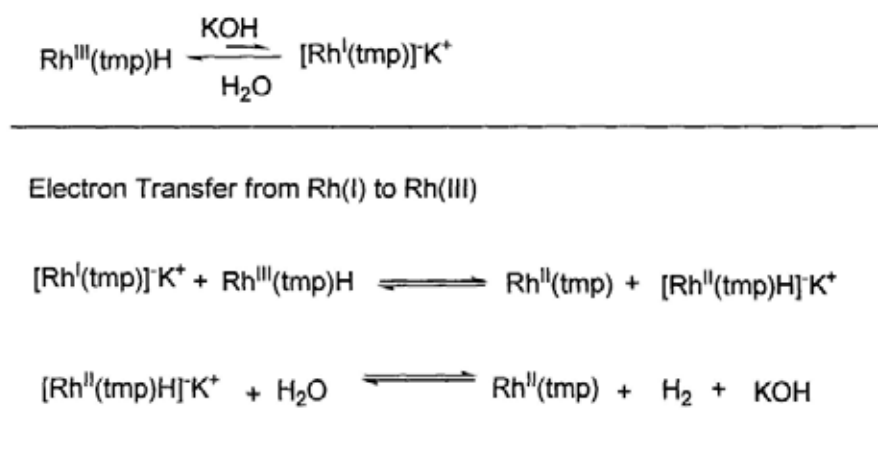
is much more polar than benzene (dielectric constant = 2.27) in which the formation of anionic $[\text{Rh}^{\text{I}}(\text{tmp})]^-$, from the deprotonation of $\text{Rh}(\text{tmp})\text{H}$ and E_2 elimination of **5l**, would be more favorable. Therefore, the interconversion of $\text{Rh}(\text{tmp})\text{H}$ to $\text{Rh}^{\text{II}}(\text{tmp})$, $\text{Rh}(\text{tmp})\text{OH}$ and $[\text{Rh}^{\text{I}}(\text{tmp})]^-$ with OH^- is strongly solvent dependent and the generation of $[\text{Rh}^{\text{I}}(\text{tmp})]^-$ is favored in THF.



Scheme 4.10 Possible mechanism for the generation of $[\text{Rh}^{\text{I}}(\text{tmp})]^- \text{K}^+$ **1h** from $\text{Rh}(\text{tmp})\text{H}$ **1f** in THF.

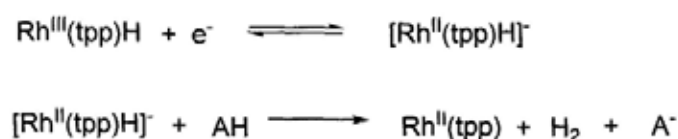
Furthermore, the deprotonation of $\text{Rh}(\text{por})\text{H}$ has been reported to be dependent on the acidity of $\text{Rh}(\text{por})\text{H}$. The pK_a of $\text{Rh}(\text{F}_{28}\text{tpp})\text{H}$ (F_{28}tpp = 5,10,15,20-tetrakis-(pentafluorophenyl)-2,3,7,8,12,13,17,18-octafluoroporphyrin) in DMSO is 2.1 while the pK_a of $\text{Rh}(\text{tpp})\text{H}$ is 11.0.¹²⁷

Therefore, for the base-promoted dehydrogenation of Rh(tmp)H to Rh^{II}(tmp) in benzene, we propose that [Rh^I(tmp)]⁻ is initially formed from the deprotonation of Rh(tmp)H. [Rh^I(tmp)]⁻ is unstable in benzene and undergoes electron transfer reaction with unreacted Rh^{III}(tmp)H to give Rh^{II}(tmp) and [Rh^{II}(tmp)(H)]⁺K⁺. [Rh^{II}(tmp)(H)]⁺K⁺ then further reacts with a water molecule to give another Rh^{II}(tmp), dihydrogen and KOH (Scheme 4.11).



Scheme 4.11 Possible pathways of the base-promoted dehydrogenation of Rh(tmp)H in benzene-*d*₆

Indeed, the analogous electrochemical generation of rhodium(II) porphyrin hydrides and subsequent hydrogen evolution, from the reaction between [Rh^{II}(tpp)H]⁻ and solvent (CH₃COOH in DMSO), has been suggested by Savéant *et al.*¹²⁸ (Scheme 4.12).



Scheme 4.12 Hydrogen evolution from the electroreduction of Rh(tpp)H

However, no dihydrogen was detected by the ^1H NMR analysis in the vacuum-sealed NMR tube experiment. The maximum concentration for 100% yield of dihydrogen in benzene- d_6 solution is estimated as $4.52 \times 10^{-3}\text{M}$ only. However, the hydrogen solubility in benzene at 30°C was estimated to be only 0.0026 mole fraction at around 1 MPa and the mole fraction decreases as the pressure decreases.¹²⁹ The unsuccessful detection of H_2 is likely due to much poorer hydrogen solubility in benzene under vacuum conditions (5×10^{-3} mmHg/ 7×10^{-7} MPa). Therefore, the concentration of hydrogen in benzene was too low to be observed in NMR.

4.5.4.4 Hydroxide-Induced Disproportionation of $\text{Rh}^{\text{II}}(\text{tmp})$

Finally, hydroxide ion can also act as a ligand to induce the disproportionation of $\text{Rh}^{\text{II}}(\text{tmp})$ to give $\text{Rh}^{\text{III}}(\text{tmp})\text{OH}$ and $[\text{Rh}^{\text{I}}(\text{tmp})]^-$ as discussed previously (see Chapter 3, Section 3.4.4.3, Scheme 3.12). The equilibration between $\text{Rh}(\text{tmp})\text{OH}$ and $\text{Rh}^{\text{II}}(\text{tmp})$ with KOH is still not fully established. Presumably, the rate of disproportionation of $\text{Rh}^{\text{II}}(\text{tmp})$ to $\text{Rh}(\text{tmp})\text{OH}$ and the stability of $\text{Rh}(\text{tmp})\text{OH}$ are solvent dependent. The higher the polarity and donicity of the solvent, the faster the rate of disproportionation of $\text{Rh}^{\text{II}}(\text{tmp})$. Further works in the relationship between $\text{Rh}(\text{tmp})\text{OH}$ and $\text{Rh}^{\text{II}}(\text{tmp})$ in different solvents and KOH would be fruitful.

4.6 Thermodynamic and Kinetic Consideration of Selective CCA on Bu₂O

The selective C(α)-C(β) bond cleavage over other C-C bonds and C-O bond can be explained by the following three considerations. Firstly, the C(α)-C(β) bond is the weakest C-C bond (~83 kcal/mol) over other C-C bonds (~88-89 kcal/mol) of ether. Therefore, the cleavage of C(α)-C(β) bond is thermodynamically more favorable (Figure 4.8).

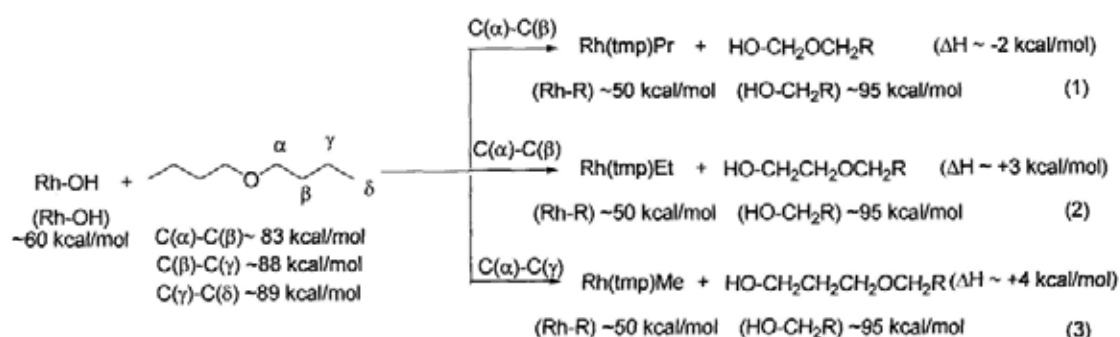


Figure 4.8 Thermodynamic estimation of C-C bonds cleavage of ether¹⁵

Secondly, the C(α)-C(β) bond cleavage of ether is thermodynamically more favorable over the C(α)-O bond as more stable products are formed from the CCA than that in COA (Figure 4.9, eq 1-2 vs 3-4).

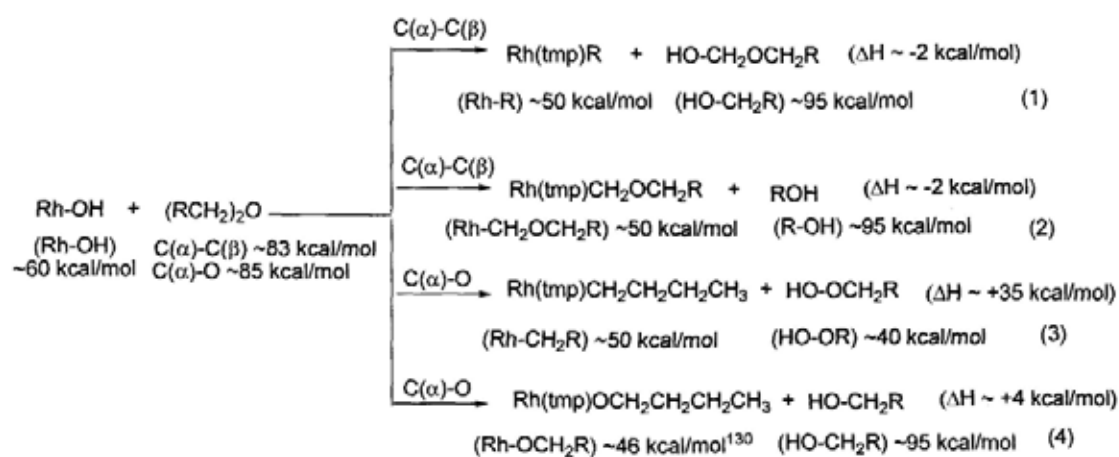


Figure 4.9 Thermodynamic estimation of CCA and COA of ether^{15,86,110}

Thirdly, the selective formation of C(β)-substituent of Rh(tmp)R rather than the C(α)-substituent of Rh(tmp)CH₂OR can be explained by the sterically less hindered transition state (Figure 4.10). On the other hand, the O-atom of ether can facilitate the pre-organization of the C(α)-C(β) bond of ether in close proximity to Rh-OH bond via hydrogen bonding (Figure 4.11).

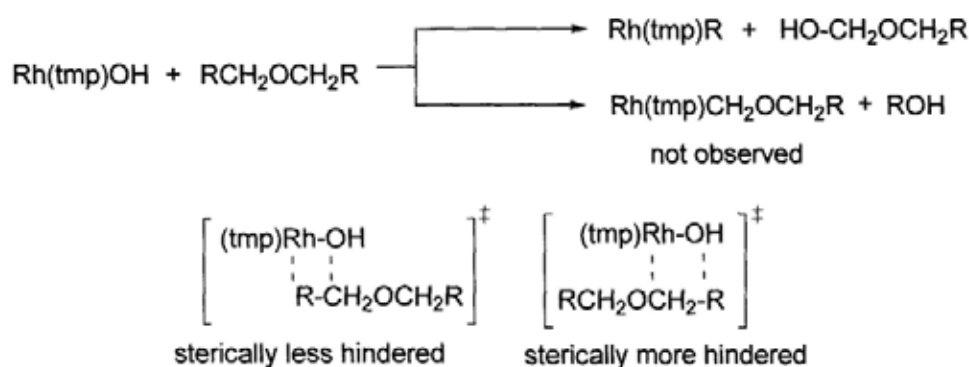


Figure 4.10 Selective generation of Rh(tmp)R

Based on the previous explanation, a possible mechanism for the selective CCA is (1) the pre-organization of the ether and Rh(tmp)-OH into a 6-membered-ring-like structure, with neighboring atoms featuring opposite polarities (Figure 4.11); (2) the conversion of the pre-organized molecules into a 4-membered-cycle transition state in which the cleavage of C-C bond occurred. Indeed, the formation of Rh-C(β) bond is more preferable when comparing with the Rh-C(α) bond due to their electrostatic interaction (Figure 4.11).

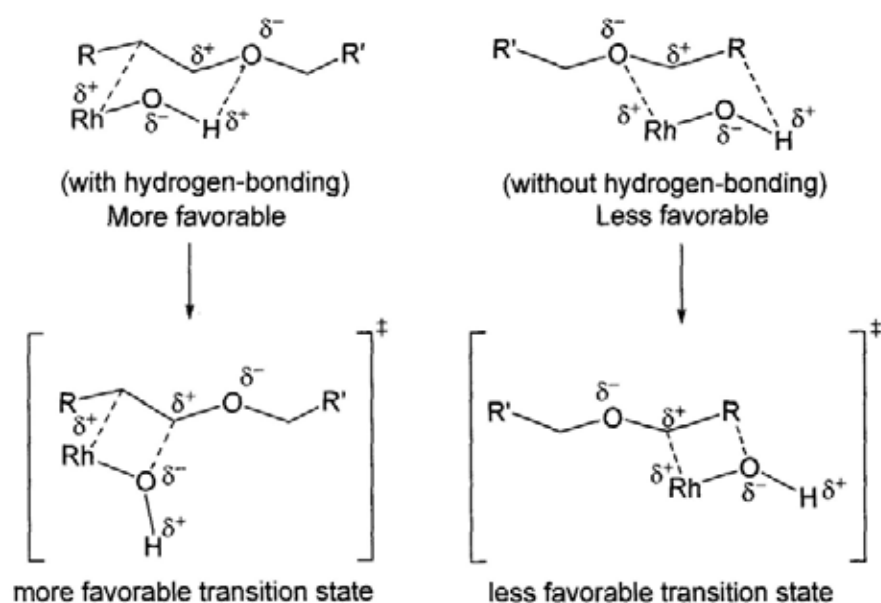
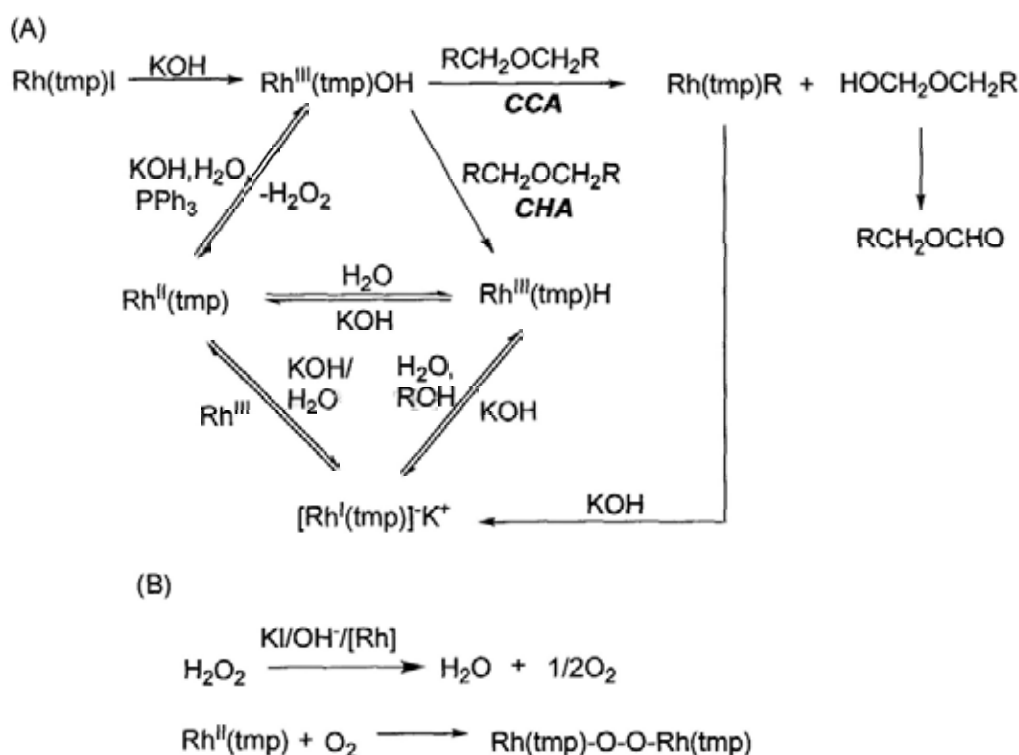


Figure 4.11 Pre-organization of ether to Rh-OH bond via hydrogen bonding

4.7 Summary of Reaction Mechanism

Scheme 4.13 illustrates the overall view of the proposed mechanism of CCA of ethers based on the above data. Initially, Rh(tmp)I reacts with KOH to generate Rh(tmp)OH via a ligand substitution. The formation of Rh(tmp)OH is supported by the observation of Rh(tmp)-OO-Rh(tmp). Then, Rh(tmp)OH reacts at least in three pathways, (1) the C(α)-C(β) bond cleavage of ether; (2) the formation of Rh^{II}(tmp) and H₂O₂; (3) the C-H bond activation of ether solvent to form Rh(tmp)H. Rh(tmp)H then undergoes base-promoted dehydrogenation to give Rh^{II}(tmp) and then recycles back to Rh(tmp)OH. These rhodium porphyrin species probably exist in equilibrium. The observation of Rh^{II}(tmp) and Rh(tmp)H does not mean that they are the active intermediates for CCA, they are in fact the non-productive intermediates.¹³¹



Scheme 4.13 Proposed mechanism of CCA of ethers with Rh(tmp)I

4.8 Potential of Catalytic CCA of Ethers

It is important to find out whether the rhodium porphyrin alkyls are stable or not in basic conditions. It was found that several Rh(tmp)R reacted with ethers in the presence of KOH (Table 4.20, eq 4.20). Rh(tmp)R, with KOH added, was found to cleave the C(α)-C(β) bond of R¹CH₂OCH₂R¹ to give Rh(tmp)R¹ (Table 4.20, entries 1, 2 and 4). No reaction was observed in the absence of KOH (Table 4.20, entry 3). A trace amount of Rh^{II}(tmp) was identified in the crude reaction mixture of the reaction between Rh(tmp)Pr with *n*-pentyl ether (Table 4.20, entry 4) by ¹H NMR analysis. Presumably, Rh^{II}(tmp) and the unobserved [Rh^I(tmp)]⁻ and Rh(tmp)OH were generated in the course of reaction for further reaction.

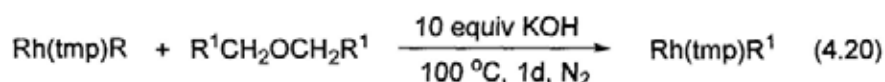
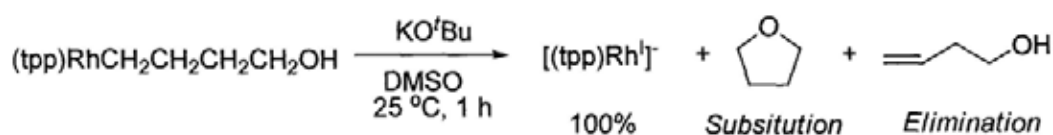


Table 4.20 CCA of Ethers with Rh(tmp)-alkyls

Entry	R =	Base (10 equiv)	R ¹ CH ₂ OCH ₂ R ¹	Product/ Yield/%	
				Recovered Rh(tmp)R	Product Rh(tmp)R ¹
1	Me	KOH	PrCH ₂ OCH ₂ Pr	Rh(tmp)Me (30)	Rh(tmp)Pr (30)
2	Et	KOH	PrCH ₂ OCH ₂ Pr	Rh(tmp)Et (40)	Rh(tmp)Pr (40)
3	Pr	Nil	BuCH ₂ OCH ₂ Bu	Rh(tmp)Pr (95)	Rh(tmp)Bu (0)
4 ^a	Pr	KOH	BuCH ₂ OCH ₂ Bu	Rh(tmp)Pr (48)	Rh(tmp)Bu (32)

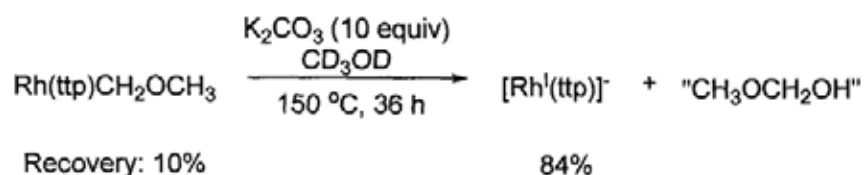
^a trace amount of Rh^{II}(tmp) was observed in crude mixture

Groves and Sanford *et al.* reported the conversion of Rh(tpp)R complexes into [Rh(tpp)]⁻ under basic media at room temperature conditions by nucleophilic substitution and elimination¹³² (Scheme 4.14).



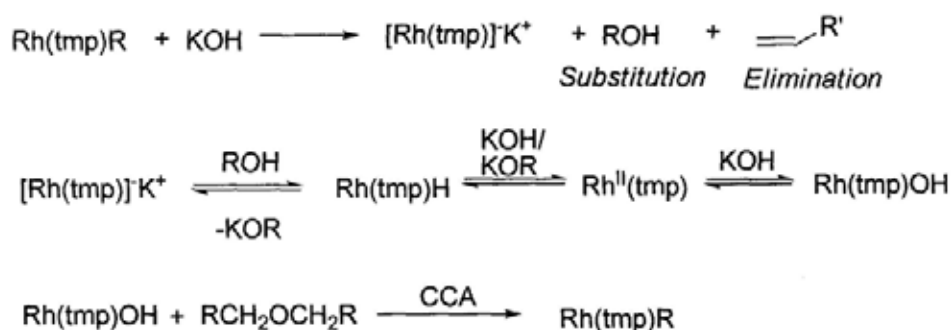
Scheme 4.14 Carbon-oxygen bond forming reductive elimination

Chan *et al.* have also recently reported the conversion of Rh(tpp)CH₂OCH₃ by K₂CO₃ into [Rh(tpp)]⁻ in methanol-*d*₄ at 150 °C,¹³³ a nucleophilic substitution mechanism was proposed (Scheme 4.15).



Scheme 4.15 Base-promoted elimination of Rh(tpp)CH₂OCH₃

In the ether substrates, we reason that Rh(tmp)R reacts with KOH to give [Rh^I(tmp)]⁻K⁺ and an alcohol. Then [Rh^I(tmp)]⁻K⁺ undergoes rapid proton abstraction from alcohol to generate Rh(tmp)H followed by base-promoted dehydrogenation to regenerate Rh^{II}(tmp) and then Rh(tmp)OH for subsequent CCA reaction (Scheme 4.16). Base on these results, a catalytic CCA of ethers can be feasible.



Scheme 4.16 Plausible mechanism for the base-promoted E₂ elimination of Rh(tmp)R

4.9 Conclusion

The selective, aliphatic carbon(α)-carbon(β) bond of a series of ethers have been successfully activated with Rh(tmp)I to give Rh(tmp)-alkyls from moderate to good yields under mild and basic reaction conditions. KOH is the best promoter. The reactivity of CCA of ethers decreases with increasing sterics of ether substrates.

Mechanistic investigation reveals that Rh^{II}(tmp) and Rh(tmp)H are the observable intermediates but non-productive intermediates. The key intermediate for the C-C cleavage is consolidated to be Rh(tmp)OH. Also, the hydroxide-promoted dehydrogenation of Rh(tmp)H to Rh^{II}(tmp), and the reduction of Rh(tmp)I by hydroxide to Rh^{II}(tmp) have also been discovered.

Chapter 5 Experimental Section

Physical and Analytical Measurements

^1H and ^{13}C NMR spectra were recorded on a Bruker DPX-300 at 300 and 75 MHz, respectively or on a Bruker AvanceIII 400 at 400 and 100 MHz, respectively. Chemical shifts for ^1H NMR were referenced with the residual solvent protons in C_6D_6 (δ 7.15 ppm), CDCl_3 (δ 7.26 ppm) and $\text{THF-}d_8$ (δ 3.74 ppm) while for ^{13}C NMR, chemical shifts were referenced to the residual solvent peak of CDCl_3 (δ 77.15 ppm).

Mass spectra were recorded on a ThermoFinnigan MAT 95 XL in fast atom bombardment mode using 3-nitrobenzyl alcohol (NBA) as the matrix and ESI ($\text{MeOH}:\text{CH}_2\text{Cl}_2 = 1:1$ as solvent) modes.

GC-MS analysis was conducted on a Shimadzu GCMS-2010Plus using Rtx-5MS column (30 m x 0.25 mm).

General Procedures

Unless otherwise mentioned, all reagents were purchased from the commercial suppliers and used without purification. Benzene and tetrahydrofuran (THF) were distilled from sodium under nitrogen. Hexane was distilled from calcium chloride. Ethers were distilled from sodium under nitrogen and stored in a Teflon screw-head

stoppered flask under nitrogen. Triphenylphosphine was recrystallized in hexane and dried under higher vacuum.

All preparative reactions were carried out in a Teflon screw-head stoppered tube under N₂ conditions with the apparatus protected from light by wrapping with aluminum foil. The reactions were carried out at least in duplicate and the yields were the average.

Thin layer chromatography was performed on Merck precoated silica gel 60 F₂₄₅ plates. Column chromatography was performed on silica gel (70-230 mesh).

Preparation of 5,10,15,20-Tetrakis(mesityl)porphyrin (H₂tmp) (1a).¹¹³ To a 2 L 3-necked round-bottomed flask that was connected with N₂ inlet, a condenser and charged with CHCl₃ (distilled over CaCl₂ under nitrogen, 1 L), mesitylaldehyde (1.5 mL, 10 mmol) and pyrrole (0.7 mL, 10 mmol) were added. After the reaction was purged with N₂ for 15 min, boron trifluoride etherate (0.5 mL, 3.3 mmol) was added. The reaction mixture gradually turned from colorless to brown in color. After 1 hour, chlorinil (1.8 g, 7.5 mmol) was added and the reaction was heated to reflux for 1 hour. The reaction mixture was turned to dark purple in color. Solvent was then removed by rotary evaporation. The crude product was purified by chromatography on silica gel by CHCl₃. The first red band was collected. After removal of solvent by rotary

evaporation, purple crystalline solids (673 mg, 0.86 mmol, 34%) were obtained after recrystallization from CH₂Cl₂/MeOH, R_f = 0.35 (hexane:CH₂Cl₂ = 4:2); ¹H NMR(CDCl₃) δ-2.51 (s, 2 H), 1.85 (s, 24 H), 2.62 (s, 12 H), 7.61 (s, 8 H).

Preparation of 5,10,15,20-Tetrakis[4-(trifluoromethyl)phenyl]porphyrin

(H₂t₄-CF₃pp) (2a).¹³⁴ To a 2 L 3-necked round-bottomed flask that was connected with N₂ inlet, a condenser and charged with CHCl₃ (distilled over CaCl₂ under nitrogen, 1 L), 4-(trifluoromethyl)benzaldehyde (1.74 g, 10 mmol) and pyrrole (0.7 mL, 10 mmol) were added. After the reaction was purged with nitrogen for 15 minutes, boron trifluoride etherate (0.5 mL, 3.3 mmol) was added. The reaction mixture gradually turned from colorless to brown in color. After 1 hour, chlorinil (1.8 g, 7.5 mmol) was added and the reaction was heated to reflux for 1 hour. The reaction mixture was turned to dark purple in color. Solvent was then removed by rotary evaporation. The crude product was purified by chromatography on silica gel by CHCl₃. The first red band was collected. After removal of solvent by rotary evaporation, purple crystalline solids (210 mg, 0.24 mmol, 11%) were obtained after recrystallization from CH₂Cl₂/MeOH, R_f = 0.67 (hexane:CH₂Cl₂ = 2:1); ¹H NMR(300 MHz, CDCl₃) δ-2.85 (s, 2 H), 8.04 (d, 8 H, *J* = 8.1 Hz), 8.33 (d, 4 H, *J* = 8.0 Hz), 8.81 (s, 8 H).

Preparation of (5,10,15,20-Tetramesitylporphyrinato)chloro Rhodium(III)

Rh(tmp)Cl (1b).⁸⁹ To a 150 mL 3-necked round-bottomed flask that was connected with a condenser, PhCN (distilled over P₂O₅, 40 mL), H₂tmp (320 mg, 0.41 mmol) and RhCl₃·xH₂O (215 mg, 0.82 mmol) were added. The reaction mixture was heated to refluxing temperature for 1 day. The PhCN solvent was vacuum evaporated. The crude product was then purified by chromatography on silica gel using a solvent mixture of CH₂Cl₂: ethyl acetate (100:3). The slow moving red band was collected and the solvent was evaporated off to give red solids of Rh(tmp)Cl⁸⁹ **1b** (293 mg, 318 mmol, 78%) The product was further purified from recrystallization from CH₂Cl₂/MeOH. R_f = 0.60 (CH₂Cl₂:EA = 100:3). ¹H NMR (300 MHz, C₆D₆) δ 1.67 (s, 12 H), 2.20 (s, 12 H), 2.43 (s, 12 H), 7.02 (s, 4 H), 7.22 (s, 4 H), 8.93 (s, 8 H).

Preparation of (5,10,15,20-Tetratolylporphyrinato)chloro Rhodium(III)

(Rh(ttp)Cl) (3b).¹¹⁴ To a 150 mL 3 necked round-bottomed flask that was connected with a condenser PhCN (distilled over P₂O₅, 30 mL), H₂ttp (356 mg, 0.53 mmol) and RhCl₃·xH₂O (209 mg, 1 mmol) were added. The reaction mixture was heated to refluxing temperature for 4 hours. The PhCN solvent was vacuum evaporated. The crude product was then purified by chromatography on silica gel using a solvent of CH₂Cl₂ as the eluent. The slow moving red band was collected and the solvent was

evaporated off to give red solids of Rh(ttp)Cl **3b** (285 mg, 0.35 mmol, 66%). The product was further purified from recrystallization from CH₂Cl₂/methanol. $R_f = 0.30$ (CH₂Cl₂). ¹H NMR(300 MHz, CDCl₃) δ 2.71 (s, 12 H), 7.54 (d, 8 H, $J = 7.8$ Hz), 8.09 (d, 4 H, $J = 6.6$ Hz), 8.13 (d, 4 H, $J = 7.2$ Hz), 8.95 (s, 8 H).

Preparation of [5,10,15,20-Tetra(4-fluoromethyl)phenylporphyrinato]chloro Rhodium(III) (Rh(t₄-CF₃pp)Cl) (2b**).¹¹⁴**

To a 150 mL 3-necked round-bottomed flask that was connected with a condenser, PhCN (20 mL), H₂t₄-CF₃pp (190 mg, 0.21 mmol) and RhCl₃·xH₂O (84.7 mg, 0.32 mmol) were added. The reaction mixture was heated to refluxing temperature for 4 hours. The PhCN solvent was vacuum evaporated. The crude product was then purified by chromatography on silica gel using a solvent of CH₂Cl₂ as the eluent. The slow moving red band was collected and the solvent was evaporated off to give red solids of Rh(t₄-CF₃pp)Cl **2b** (150 mg, 0.15 mmol, 68%). The product was further purified from recrystallization from CH₂Cl₂/methanol. $R_f = 0.35$ (CH₂Cl₂). ¹H NMR(300 MHz, CDCl₃) δ 8.05 (d, 8 H, $J = 8.4$ Hz), 8.35 (d, 4 H, $J = 6.6$ Hz), 8.37 (d, 4 H, $J = 6.6$ Hz), 8.90 (s, 8 H). HRMS (FABMS): Calcd for (C₄₈H₂₄F₁₂N₄Cl₁Rh₁)⁺: m/z 987.0859. Found: m/z 987.0839.

Preparation of (5,10,15,20-Tetramesitylporphyrinato)iodydo Rhodium(III)

(Rh(tmp)I) (1c).^{81a}

A red suspension of Rh(tmp)Cl **1b** (57 mg, 0.061 mmol) in EtOH (30 mL) and a solution of NaBH₄ (4.6 mg, 0.122 mmol) in aqueous NaOH (0.5 M, 6.0 mL) was deoxygenated with nitrogen for 15 minutes. The solution of NaBH₄ was added slowly to the suspension of Rh(tmp)Cl via a cannular. The reaction was heated at 60 °C for 1 hour and the color changed to deep brown in color. The reaction mixture was then cooled down to around 0 °C and excess degassed aqueous HCl was added through a cannular. Once the reaction mixture became orange, excess I₂ (210 mg, 0.827 mmol) was added and reaction mixture turned dark brown immediately and stirred for further 5 minutes. Solvent was then removed by rotary evaporation. The residue was then purified by chromatography on silica gel using a solvent mixture of hexane:CH₂Cl₂ (5:1) to hexane:CH₂Cl₂ (5:3). The slow moving orange band was collected and the solvent was evaporated off to give purple solids of Rh(tmp)I^{81a} (50.3 mg, 0.05 mmol, 82%). The product was further purified from recrystallization from CH₂Cl₂/methanol. R_f = 0.20 (Hexane:CH₂Cl₂ = 3:2). ¹H NMR(300 MHz, CDCl₃) δ 1.72 (s, 12 H), 2.03 (s, 12H), 2.60 (s, 12 H), 7.22 (s, 4 H), 7.27 (s, 4 H), 8.60 (s, 8 H).

Preparation of (5,10,15,20-Tetratolylporphyrinato)iodo Rhodium(III) (Rh(ttp)I)

(3c).^{91a}

A red suspension of Rh(ttp)Cl **3b** (79 mg, 0.098 mmol) in EtOH (30 mL) and a solution of NaBH₄ (7.46 mg, 0.196 mmol) in aqueous NaOH (0.5 M, 6.0 mL) was deoxygenated with nitrogen for 15 minutes. The solution of NaBH₄ was added slowly to the suspension of Rh(ttp)Cl via a cannular. The reaction was heated at 60 °C for 1 hour and the color changed to deep brown in color. The reaction mixture was then cooled down to around 0 °C and excess degassed aqueous HCl was added through a cannular. Once the reaction mixture became orange, excess I₂ (210 mg, 0.827 mmol) was added and reaction mixture turned dark brown immediately and stirred for further 5 minutes. Solvent was then removed by rotary evaporation. The residue was then purified by chromatography on silica gel using a solvent mixture of hexane:CH₂Cl₂ (5:1) to hexane:CH₂Cl₂ (5:3). The slow moving orange band was collected and the solvent was evaporated off to give purple solids of Rh(ttp)I^{91a} **3c** (68.5 mg, 0.076 mmol, 82%). The product was further purified from recrystallization from CH₂Cl₂/methanol. R_f = 0.35 (CH₂Cl₂). ¹H NMR(300 MHz, CDCl₃) δ 2.70 (s, 12H), 7.53 (d, 4 H, *J* = 6.9 Hz), 7.55 (d, 4 H, *J* = 7.2 Hz), 8.05 (d, 4 H, *J* = 7.8 Hz), 8.10 (d, 4 H, *J* = 7.8 Hz), 8.89 (s, 8 H).

Preparation of [5,10,15,20-Tetra(4-trifluoromethyl)porphyrinato]iodo Rhodium(III) (Rh(t₄-CF₃pp)I) (2c).

A red suspension of Rh(t₄-CF₃pp)Cl **2b** (52 mg, 0.051 mmol) in EtOH (20 mL) and a solution of NaBH₄ (19.2 mg, 0.51 mmol) in aqueous NaOH (0.5 M, 2.0 mL) was deoxygenated with nitrogen for 15 minutes. The solution of NaBH₄ was added slowly to the suspension of Rh(t₄-CF₃pp)Cl via a cannular. The reaction was heated at 60 °C for 1 hour and the color changed to deep brown in color. The reaction mixture was then cooled down to around 0 °C and excess degassed aqueous HCl was added through a cannular. Once the reaction mixture became orange, excess I₂ (210 mg, 0.827 mmol) was added and reaction mixture turned dark brown immediately and stirred for further 5 min. Solvent was then removed by rotary evaporation. The residue was then purified by chromatography on silica gel using a solvent mixture of hexane:CH₂Cl₂ (5:1) to hexane:CH₂Cl₂ (5:3). The slow moving orange band was collected and the solvent was evaporated off to give purple solids of Rh(t₄-CF₃pp)I **2c** (30.1 mg, 0.027 mmol, 53%). The product was further purified from recrystallization from CH₂Cl₂/methanol. R_f = 0.65 (CH₂Cl₂). ¹H NMR(300 MHz, CDCl₃) δ 8.02 (d, 8 H, J = 7.8 Hz), 8.05 (d, 8 H, J = 7.8 Hz) 8.30 (d, 4 H, J = 7.5 Hz), 8.36 (d, 4 H, J = 7.5 Hz), 8.84 (s, 8 H). HRMS (FABMS): Calcd for (C₄₈H₂₄F₁₂N₄I₁Rh₁)⁺: m/z 1113.9904. Found: m/z 1113.9894.

Preparation of (5,10,15,20-tetramesitylporphyrinato)methyl Rhodium(III)

[Rh(tmp)CH₃] (1d).^{81a} A red suspension of Rh(tmp)Cl **1b** (200 mg, 0.150 mmol) in EtOH (100 mL) and a solution of NaBH₄ (28 mg, 0.74 mmol) in aqueous NaOH (0.5 M, 8 mL) were purged with nitrogen separately for about 15 minutes. The solution of NaBH₄ was added slowly to the suspension of **1b** via a cannular in a period of 30 minutes under N₂. The reaction mixture was heated at 70 °C for 3 hours and the color changed to deep brown in color. The reaction mixture was then cooled down to 0 °C under nitrogen and MeI (0.4 mL, 6.4 mmol) was added via syringe. An orange suspension formed immediately and was stirred for 2 hours. The reaction mixture was worked up by addition with CH₂Cl₂/H₂O (1/1). The crude product was extracted with CH₂Cl₂ (200 mL), washed with H₂O (25 mL × 3), dried over MgSO₄, filtered and rotary evaporated off to dryness. After purification by chromatography on silica gel eluting with a solvent mixture of hexane: CH₂Cl₂ (10:1) and slowly increasing to hexane: CH₂Cl₂ (5:1), an orange solid (153 mg, 0.17 mmol, 86%) was obtained which was further purified by recrystallization from CH₂Cl₂/hexane. R_f = 0.47 (hexane: CH₂Cl₂ = 5:1); ¹H NMR (CDCl₃, 300 MHz) δ -5.76 (d, 3 H, ²J_{Rh-H} = 2.7 Hz), 1.75 (s, 12 H), 1.95 (s, 12 H), 2.59 (s, 12 H), 7.22 (s, 4 H), 7.24 (s, 4 H), 8.45 (s, 8 H); ¹H NMR (C₆D₆, 300 MHz) δ -5.26 (d, 3 H, ²J_{Rh-H} = 2.7 Hz), 1.72 (s, 12 H), 2.25 (s, 12 H), 2.43 (s, 12 H), 7.07 (s, 4 H), 7.20 (s, 4 H), 8.75 (s, 8 H).

Preparation of [5,10,15,20-tetrakis(3,5-di-*tert*-butylphenyl)porphyrinato]methyl Rhodium(III) [Rh(tdbpp)CH₃] (4c). A red suspension of Rh(tdbpp)Cl **4a** (100 mg, 0.083 mmol) in EtOH (50 mL) and a solution of NaBH₄ (32 mg, 0.83 mmol) in aqueous NaOH (0.5 M, 8 mL) were purged with nitrogen separately for about 15 minutes. The solution of NaBH₄ was added slowly to the suspension of **4a** via a cannular in a period of 30 minutes under N₂. The reaction mixture was heated at 70 °C for 3 hours and the color changed to deep brown in color. The reaction mixture was then cooled down to 0 °C under N₂ and MeI (0.4 mL, 6.4 mmol) was added via syringe. An orange suspension formed immediately and was stirred for 2 hours. The reaction mixture was worked up by addition with CH₂Cl₂/H₂O (1/1). The crude product was extracted with CH₂Cl₂ (200 mL), washed with H₂O (25 mL × 3), dried over MgSO₄, filtered and rotary evaporated off to dryness. After purification by chromatography on silica gel eluting with a solvent mixture of hexane: CH₂Cl₂ (5:1) to obtain an orange solid of Rh(tdbpp)Me **4c** (83 mg, 0.071 mmol, 85%) which was further purified by recrystallization from CH₂Cl₂/hexane. R_f = 0.63 (hexane: CH₂Cl₂ = 5:1); ¹H NMR(300 MHz, C₆D₆) δ -5.38 (d, 3 H, *J* = 2.4 Hz), 1.45 (s, 36 H), 1.50 (s, 36 H), 7.96 (s, 4 H), 8.28 (s, 4 H), 8.46 (s, 4 H), 9.11 (s, 8 H). HRMS (FAB): Calcd for (C₇₇H₉₅N₄Rh+H)⁺: *m/z* 1179.6685. Found: *m/z* 1179.6685. Anal. Calcd. For C₇₇H₉₅N₄Rh: C, 78.41; H, 8.12; N, 4.75. Found: C, 78.19; H, 7.92; N, 4.80.

Preparation of 5,10,15,20-Tetramesitylporphyrinato Rhodium(II) [Rh(tmp)]

(1e).^{81a} To a Teflon screw-head stoppered flask, Rh(tmp)CH₃ **1d** (10.0 mg, 0.011 mmol) was dissolved in C₆H₆ (4.0 mL) to form a clear orange solution. The reaction mixture was then degassed by the freeze-pump-thaw method (3 cycles) and refilled with nitrogen. The reaction mixture was irradiated under a 400 W Hg-lamp at 6-10 °C until complete Rh(tmp)CH₃ **1d** consumption was confirmed by TLC analysis (10 - 11 hours). Addition of excess iodine to the mixture yielded Rh(tmp)I **1e** in 80 % average yield after column chromatography. ¹H NMR of Rh(tmp) (C₆D₆, 300 MHz) δ 3.55 (bs, 24 H), 3.50 (s, 12 H), 8.87 (bs, 8 H), 18.2 (bs, 8 H). If assuming the yield was 100 % in the reaction between Rh(tmp) **1e** and I₂, the yield of photolysis was estimated to be 80%.

Preparation of [5,10,15,20-tetrakis(3,5-di-tert-butylphenyl)porphyrinato]

Rhodium(II) [Rh^{II}(tdbpp)] (4d).^{81a} To a Teflon screw-head stoppered flask, Rh(tdbpp)CH₃ **4c** (14.2 mg, 0.011 mmol) was dissolved in C₆H₆ (4.0 mL) to form a clear orange solution. The reaction mixture was then degassed by the freeze-pump-thaw method (3 cycles) and refilled with nitrogen. The reaction mixture was irradiated under a 400 W Hg-lamp at 6-10 °C until complete Rh(tdbpp)CH₃ **4c** consumption was confirmed by TLC analysis (10 - 11 hours). Selected ¹H NMR

signal of Rh(tdbpp) (C_6D_6 , 400 MHz) δ 2.39 (bs, 72 H), 9.44 (bs, 12 H), 12.31 (bs, 8 H), 18.19 (bs, 8 H). Indeed, some other 1H NMR signal was observed which was possibly the dimeric form of Rh(tdbpp). Addition of excess iodine to the mixture yielded Rh(tdbpp)I **4b** in 81% average yield after column chromatography. $R_f = 0.61$ (hexane: $CH_2Cl_2 = 1:1$); 1H NMR(400 MHz, $CDCl_3$) δ 1.50 (s, 36 H), 1.52 (s, 36 H), 1.50 (s, 36 H), 7.78 (t, 4 H, $J = 1.4$ Hz), 8.07 (t, 8 H, $J = 1.4$ Hz), 8.94 (s, 8 H). ^{13}C NMR ($CDCl_3$, 100 MHz) δ 31.94, 35.21, 121.01, 123.64, 129.14, 129.25, 131.74, 141.43, 143.39, 148.77, 148.83. HRMS (FAB): Calcd for $(C_{76}H_{92}I_1N_4Rh)^+$: m/z 1290.5422. Found: m/z 1290.5401. If assuming the yield was 100% in the reaction between Rh(tdbpp) **4d** and I_2 , the yield of photolysis was estimated to be 81%.

Preparation of (5,10,15,20-Tetramesitylporphyrinato)rhodium(III) Hydride (Rh(tmp)H) **1f.**^{81a} A red suspension of Rh(tmp)Cl **1b** (2.6 mg, 0.0028 mmol) in EtOH (2 mL) and a solution of $NaBH_4$ (1.1 mg, 0.028 mmol) in aqueous NaOH (0.5 M, 0.5 mL) were purged with nitrogen separately for about 15 minutes. The solution of $NaBH_4$ was added slowly to the suspension of **1b** via a cannular. The reaction mixture was heated at 55 °C for 3 hours and the color changed to deep brown in color. The reaction mixture was then cooled down to 0 °C under nitrogen and excess degassed aqueous solution of HCl (1 M) was added via a cannular with an orange

precipitate formed immediately indicating the formation of Rh(tmp)H. The solvent was then removed through a cannular adapted with a filter paper and washed 2 times with degassed water (3 mL/each). The orange precipitate was further dried at 60 °C under vacuum evaporation for 1 hour to obtain a pure Rh(tmp)H.^{81d} ¹H NMR (300 MHz, C₆D₆) δ -40.06 (d, 1 H, *J* = 33 Hz), 1.78 (s, 12 H), 2.13 (s, 12H), 2.43 (s, 12 H), 7.09 (s, 4 H), 7.18 (s, 4 H), 8.77 (s, 8 H).

Reaction of Rh^{II}(tmp) (1e) and *n*-Butyl Ether. Degassed *n*-butyl ether (2.0 mL) was added to neat Rh^{II}(tmp) **13a** (0.0088 mmol) and the mixture was then stirred at 25 °C under nitrogen for 1 day. Excess *n*-butyl ether was removed, the dark red crude product was then purified by column chromatography on silica gel eluting with hexane/CH₂Cl₂(5:1) to give the reddish purple solid of Rh(tmp)Pr^{51b} **5a** (1.2 mg, 0.0013 mmol, 15% yield). *R_f* = 0.61 (hexane:CH₂Cl₂ = 5:1). ¹H NMR (300 MHz, C₆D₆) δ -4.43 (dt, 2 H, ²*J*_{Rh-H} = 3.0 Hz, ³*J*_{H-H} = 7.5 Hz), -3.87 (sextet, 2 H, *J* = 7.6 Hz), -1.43 (t, 3 H, *J* = 7.5 Hz), 1.87 (s, 12 H), 2.17 (s, 12 H), 2.43 (s, 12 H), 7.09 (s, 4 H), 7.19 (s, 4 H), 8.74 (s, 8 H).

Reaction of Rh^{II}(tmp) (1e) and *n*-Butyl Ether with 1 equiv of P(^{*i*}Pr)₃. In the benzene solution of Rh^{II}(tmp) **1e** (0.0088 mmol), P(^{*i*}Pr)₃ (1.5 mg, 0.0088 mmol) was

added and the reaction mixture was stirred at 25 °C. After 10 minutes, the benzene solvent was removed by vacuum evaporation and then degassed *n*-butyl ether (2.0 mL) was added and the mixture was then stirred under nitrogen for 1 day. Excess *n*-butyl ether was removed, the dark red crude product was then purified by column chromatography on silica gel eluting with hexane/CH₂Cl₂(5:1) to give the reddish purple solid of a mixture of 1:1 ratio of Rh(tmp)Pr^{51b} **5a** (~5%) and Rh(tmp)Me^{81a} **1d** (~5%).

Reaction of Rh^{II}(tmp) (1e) and *n*-Butyl Ether with 1 equiv of P(Cy)₃. In the benzene solution of Rh^{II}(tmp) **1e** (0.0088 mmol), P(Cy)₃ (2.5 mg, 0.0088 mmol) was added and the reaction mixture was stirred at 25 °C. After 10 minutes, the benzene solvent was removed by vacuum evaporation and then degassed *n*-butyl ether (2.0 mL) was added to form the suspension and the mixture was then stirred under nitrogen for 1 day. Excess *n*-butyl ether was removed, the dark red crude product was then purified by column chromatography on silica gel eluting with hexane/CH₂Cl₂(5:1) to give the reddish purple solid of Rh(tmp)Pr^{51b} **5a** (1.5 mg, 0.0016 mmol, 18%).

Reaction of Rh^{II}(tmp) (1e) and *n*-Butyl Ether with 1 equiv of P(4-OMePh)₃. In the benzene solution of Rh^{II}(tmp) **1e** (0.0088 mmol), P(4-OMePh)₃ (3.1 mg, 0.0088 mmol)

was added and the reaction mixture was stirred at 25 °C. After 10 minutes, the benzene solvent was removed by vacuum evaporation and then degassed *n*-butyl ether (2.0 mL) was added to form the suspension and the mixture was then stirred under nitrogen for 1 day. Excess *n*-butyl ether was removed, the dark red crude product was then purified by column chromatography on silica gel eluting with hexane/CH₂Cl₂(5:1) to give the reddish purple solid of Rh(tmp)Pr^{51b} **5a** (1.3 mg, 0.0014 mmol, 16%).

Reaction of Rh^{II}(tmp) (1e) and *n*-Butyl Ether with 1 equiv of P(toly)₃. In the benzene solution of Rh^{II}(tmp) **1e** (0.0088 mmol), P(toly)₃ (2.7 mg, 0.0088 mmol) was added and the reaction mixture was stirred at 25 °C. After 10 minutes, the benzene solvent was removed by vacuum evaporation and then degassed *n*-butyl ether (2.0 mL) was added to form the suspension and the mixture was then stirred under nitrogen at 25 °C for 1 day. Excess *n*-butyl ether was removed, the dark red crude product was then purified by column chromatography on silica gel eluting with hexane/CH₂Cl₂(5:1) to give the reddish purple solid of Rh(tmp)Pr^{51b} **5a** (1.8 mg, 0.0019 mmol, 20%).

Reaction of Rh^{II}(tmp) (1e) and *n*-Butyl Ether with 1 equiv of PPh₃. In the benzene solution of Rh^{II}(tmp) **1e** (0.0088 mmol), PPh₃ (2.3 mg, 0.0088 mmol) was added and the reaction mixture was stirred at 25 °C. After 10 minutes, the benzene solvent was

removed by vacuum evaporation and then degassed *n*-butyl ether (2.0 mL) was added and the mixture was then stirred under nitrogen at 25 °C for 1 day. Excess *n*-butyl ether was removed. Rh(tmp)Pr **5a** and the suspected (PPh₃)Rh(tmp)OPr **5i** were observed from the ¹H NMR of the crude reaction mixture in benzene-*d*₆, then the dark red crude product was then purified by column chromatography on silica gel eluting with hexane/CH₂Cl₂(5:1) to give the reddish purple solid of Rh(tmp)Pr^{51b} **5a** (3.3 mg, 0.004 mmol, 40% yield) while the suspected (PPh₃)Rh(tmp)OPr **5i** was not able to be isolated. The suggestive ¹H NMR signals of (PPh₃)Rh(tmp)OPr **5i**; ¹H NMR(300 MHz, C₆D₆) -0.69 (qu, 2 H, *J* = 7.2 Hz), -0.47 (t, 3 H, *J* = 7.2 Hz), -0.39 (t, 2 H, *J* = 7.5 Hz), 1.43 (s, 12 H), 2.06 (s, 12H), 2.41 (s, 12 H), 4.36 (t, 6 H, *J* = 8.4 Hz), 6.16 (t, 6H, *J* = 7.5Hz), 6.35 (t, 3 H, *J* = 7.2 Hz), 8.75 (s, 8 H).

Reaction of Rh^{II}(tmp) (1e) and *n*-Butyl Ether with 2 equiv of PPh₃. In the benzene solution of Rh^{II}(tmp) **1e** (0.0088 mmol), PPh₃ (4.6 mg, 0.018 mmol) was added and the reaction mixture was stirred at 25 °C. After 10 minutes, the benzene solvent was removed by vacuum evaporation and then degassed *n*-butyl ether (2.0 mL) was added and the mixture was then stirred under nitrogen at 25 °C for 1 day. Excess *n*-butyl ether was removed, the dark red crude product was then purified by column chromatography on silica gel eluting with hexane/CH₂Cl₂(5:1) to give the reddish

purple solid of Rh(tmp)Pr^{51b} **5a** (3.3 mg, 0.004 mmol, 40%).

Reaction of Rh^{II}(tdbpp) (4d) and *n*-Butyl Ether with 1 equiv of PPh₃. In the benzene solution of Rh^{II}(tdbpp) **4d** (0.0089 mmol), PPh₃ (2.3 mg, 0.0089 mmol) was added and the reaction mixture was stirred at 25 °C. After 10 minutes, the benzene solvent was removed by vacuum evaporation and then degassed *n*-butyl ether (2.0 mL) was added and the mixture was then stirred under nitrogen at 25 °C for 1 day. Excess *n*-butyl ether was removed, the dark red crude product was then purified by column chromatography on silica gel eluting with hexane/CH₂Cl₂(5:1) to give the reddish purple solid of Rh(tdbpp)Pr **4e** (3.0 mg, 0.0025 mmol, 28%). $R_f = 0.57$ (hexane:CH₂Cl₂ = 3:2). ¹H NMR(300 MHz, CDCl₃) δ - 4.85 (dt, 2 H, ² $J_{Rh-H} = 2.9$ Hz, ³ $J_{H-H} = 8.1$ Hz), -4.37 (s, 2 H, $J = 7.4$ Hz), -1.63 (t, 3 H, $J = 7.3$ Hz), 1.50 (s, 36 H), 1.51 (s, 36 H), 7.76 (t, 4 H, $J = 1.7$ Hz), 8.00 (t, 4 H, $J = 1.8$ Hz), 8.02 (t, 4 H, $J = 1.8$ Hz), 8.75 (s, 8 H). ¹³C NMR (CDCl₃, 100 MHz) δ 11.11, 17.68 (d, ¹ $J_{Rh-C} = 26.7$ Hz), 20.73, 29.85, 31.88, 31.91, 35.17, 120.97, 123.74, 128.96, 129.22, 131.65, 141.43, 143.36, 148.72, 148.76. HRMS (FAB): Calcd for (C₇₉H₉₉N₄Rh+H)⁺: m/z 1207.6998. Found: m/z 1207.6990.

Reaction of $[\text{Rh}^{\text{II}}(\text{ttp})]_2$ (3e**) and *n*-Butyl Ether with 1 equiv of PPh_3 .** In the benzene solution of $[\text{Rh}^{\text{II}}(\text{ttp})]_2$ **3e** (0.0062 mmol), PPh_3 (2.7 mg, 0.012 mmol) was added and the reaction mixture was stirred at 25 °C. After 10 minutes, the benzene solvent was removed by vacuum evaporation and then degassed *n*-butyl ether (2.0 mL) was added and the mixture was then stirred under nitrogen at 25 °C for 1 day. Excess *n*-butyl ether was removed, the dark red crude product was then purified by column chromatography on silica gel eluting with hexane/ CH_2Cl_2 (5:1) to give the reddish purple solid of $\text{Rh}(\text{ttp})\text{Pr}^{135}$ **3f** (0.7 mg, 0.00086 mmol, 37%). $R_f = 0.46$ (hexane: $\text{CH}_2\text{Cl}_2 = 5:2$). $^1\text{H NMR}$ (300 MHz, CDCl_3) δ -4.98 (dt, 2 H, $^2J_{\text{Rh-H}} = 3.3$ Hz, $^3J_{\text{H-H}} = 8.3$ Hz), -4.46 (s, 2 H, $J = 8.7$ Hz), -1.75 (t, 3 H, $J = 7.2$ Hz), 2.69 (s, 12 H), 7.53 (t, 8 H, $J = 5.7$ Hz), 8.00 (dd, 4 H, $J = 2.1$ Hz, 5.7 Hz), 8.07 (dd, 4 H, $J = 2.1$ Hz, 7.5 Hz), 8.71 (d, 4 H, $J = 7.3$ Hz), 8.76 (s, 8 H).

Reaction of $\text{Rh}^{\text{II}}(\text{tmp})$ (1e**) and *n*-Propyl Ether with 1 equiv of PPh_3 .** In the benzene solution of $\text{Rh}^{\text{II}}(\text{tmp})$ **1e** (0.0088 mmol), PPh_3 (2.3 mg, 0.0088 mmol) was added and the reaction mixture was stirred at 25 °C. After 10 minutes, the benzene solvent was removed by vacuum evaporation and then degassed *n*-propyl ether (2.0 mL) was added and the mixture was then stirred under nitrogen at 25 °C for 1 day. Excess *n*-propyl ether was removed. $\text{Rh}(\text{tmp})\text{Et}$ **5b** and the suspected

(PPh₃)Rh(tmp)OEt **15o** were observed from the ¹H NMR of the crude reaction mixture in benzene-*d*₆, then the dark red crude product was then purified by column chromatography on silica gel eluting with hexane/CH₂Cl₂(5:1) to give the reddish purple solid of Rh(tmp)Et^{51b} **5b** (3.4 mg, 0.0037 mmol, 41%). R_f = 0.53 (hexane:CH₂Cl₂ = 5:1). ¹H NMR(300 MHz, C₆D₆) δ -4.31 (dq, 3 H, ²J_{Rh-H} = 3.0 Hz, ³J_{H-H} = 7.5 Hz), -3.83 (dt, 3 H, ³J_{Rh-H} = 1.5 Hz, ³J_{H-H} = 7.5 Hz), 1.88 (s, 12 H), 2.12 (s, 12 H), 2.44 (s, 12 H), 6.93 (s, 4 H), 7.19 (s, 4 H), 8.74 (s, 8 H). While the suspected (PPh₃)Rh(tmp)OEt **15h** was not able to be isolated. The suggestive ¹H NMR signals of Rh(tmp)OEt **5h**; ¹H NMR (300 MHz, C₆D₆) δ -0.98 (t, 3 H, J = 7.5 Hz), -0.45 (q, 2 H, J = 7.5 Hz), 1.40 (s, 12 H), 2.41 (s, 12H), 4.38 (t, 6 H, J = 8.4 Hz), 6.16 (t, 6 H, J = 7.5Hz), 6.35 (t, 3 H, J = 7.2 Hz), 8.76 (s, 8 H).

Reaction of Rh^{II}(tmp) (1e) and *n*-Butyl Ether with 1 equiv of PPh₃. In the benzene solution of Rh^{II}(tmp) **1e** (0.0088 mmol), PPh₃ (2.3 mg, 0.0088 mmol) was added and the reaction mixture was stirred at 25 °C. After 10 minutes, the benzene solvent was removed by vacuum evaporation and then degassed *n*-butyl ether (2.0 mL) was added and the mixture was then stirred under nitrogen at 0-3 °C for 1 day. Excess *n*-butyl ether was removed, the dark red crude product was then purified by column chromatography on silica gel eluting with hexane/CH₂Cl₂(5:1) to give the reddish

purple solid of Rh(tmp)Pr^{51b} **5a** (3.1 mg, 0.0033 mmol, 38%).

Reaction of Rh^{II}(tmp) (1e) and *n*-Pentyl Ether with 1 equiv of PPh₃. In the benzene solution of Rh^{II}(tmp) **1e** (0.0088 mmol), PPh₃ (2.3 mg, 0.0088 mmol) was added and the reaction mixture was stirred at 25 °C. After 10 minutes, the benzene solvent was removed by vacuum evaporation and then degassed *n*-pentyl ether (2.0 mL) was added and the mixture was then stirred under nitrogen at 25 °C for 5 days. Excess *n*-pentyl ether was removed, the dark red crude product was then purified by column chromatography on silica gel eluting with hexane/CH₂Cl₂(5:1) to give the reddish purple solid of Rh(tmp)Bu⁸⁸ **5c** (2.4 mg, 0.0026 mmol, 30%). $R_f = 0.63$ (hexane:CH₂Cl₂ = 5:1). ¹H NMR (300 MHz, C₆D₆) δ -4.43 (dt, 2 H, ² $J_{Rh-H} = 3.0$ Hz, ³ $J_{HH} = 8$ Hz), -3.92 (qu, 2 H, $J = 7.7$ Hz), -1.13 (sextet, 2 H, $J = 7.5$ Hz), -0.68 (t, 3 H, $J = 7.5$ Hz), 1.95 (s, 12 H), 2.17 (s, 12 H), 2.43 (s, 12 H), 7.11 (s, 4 H), 7.19 (s, 4 H), 8.74 (s, 8 H).

Reaction of Rh^{II}(tmp) (1e) and Isoamyl Ether with 1 equiv of PPh₃. In the benzene solution of Rh^{II}(tmp) **1e** (0.0088 mmol), PPh₃ (2.3 mg, 0.0088 mmol) was added and the reaction mixture was stirred at 25 °C. After 10 minutes, the benzene solvent was removed by vacuum evaporation and then degassed isoamyl ether (2.0 mL) was added

and the mixture was then stirred under nitrogen at 25 °C for 5 days. Excess isoamyl ether was removed, the dark red crude product was then purified by column chromatography on silica gel eluting with hexane/CH₂Cl₂(5:1) to give the reddish purple solid of Rh(tmp)^tBu **5d** (1.1 mg, 0.0012 mmol, 13%).

Preparation of (5,10,15,20-Tetramesitylporphyrinato)isobutyl Rhodium(III) (Rh(tmp)^tBu) (5d). A suspension of Rh(tmp)Cl **1b** (60 mg, 0.065 mmol) in EtOH (30 mL) in a Schlenk flask and a solution of NaBH₄ (10.0 mg, 0.260 mmol) in aqueous NaOH (0.5 M, 3 mL) in a conical flask were flushed with nitrogen for 15 minutes. The solution of NaBH₄ was added slowly to the suspension of Rh(tmp)Cl via a cannular. The reaction mixture was heated at 60 °C for 1 hour and the color changed to deep brown in color. The reaction mixture was then cooled down in an ice bath and upon addition of excess 1-bromo-2-methylpropane (350 μL, 3.25 mmol), reddish precipitate was formed immediately. After stirring for 10 minutes, solvent was then removed by rotary evaporation and the crude reaction mixture was then purified by column chromatography on silica gel eluting with hexane/CH₂Cl₂ (5:1) to give the reddish purple solid of Rh(tmp)^tBu **5d** (45 mg, 0.048 mmol, 74%). $R_f = 0.63$ (hexane:CH₂Cl₂ = 5:1). ¹H NMR (400 MHz, CD₂Cl₂) δ -4.43 (dd, 2 H, ² $J_{Rh-H} = 3.2$ Hz, ³ $J_{H-H} = 7.2$ Hz), -4.65 (m, 1 H), -2.18 (d, 6 H, $J = 6.7$ Hz), 1.82 (s, 12 H), 1.91 (s, 12

H), 2.59 (s, 12 H), 7.26 (s, 4 H), 7.27 (s, 4 H), 8.84 (s, 8 H). ^{13}C NMR (CD_2Cl_2 , 75 MHz) δ 20.30, 21.70, 22.05, 23.93 (d, $^1J_{\text{Rh-C}} = 27.7$ Hz), 26.41, 120.21, 128.18, 130.99, 138.04, 138.96, 139.28, 139.54, 143.17 HRMS: Calcd for $(\text{C}_{60}\text{H}_{61}\text{N}_4\text{Rh}^+)$: m/z 940.3946. Found: m/z 940.3939. Anal. Calcd. For $\text{C}_{60}\text{H}_{61}\text{N}_4\text{Rh}$: C, 76.58; H, 6.53; N, 5.95. Found: C, 76.15; H, 6.56; N, 5.81.

Reaction of $\text{Rh}^{\text{II}}(\text{tmp})$ (1e) and 2-Propyl-1,3-Dioxolane with 1 equiv of PPh_3 . In the benzene solution of $\text{Rh}^{\text{II}}(\text{tmp})$ **1e** (7.8 mg, 0.0088 mmol), PPh_3 (2.3 mg, 0.0088 mmol) was added and the reaction mixture was stirred at 25 °C. After 10 minutes, the benzene solvent was removed by vacuum evaporation and then degassed 2-propyl-1,3-dioxolane (2.0 mL) was added and the mixture was then stirred under nitrogen at 25 °C for 1 day. Excess 2-propyl-1,3-dioxolane was removed, the dark red crude product was then purified by column chromatography on silica gel eluting with hexane/ CH_2Cl_2 (5:1) to give the reddish purple solid of $\text{Rh}(\text{tmp})\text{Pr}^{51\text{b}}$ **5a** (1.8 mg, 0.0019 mmol, 22%).

Reaction of $\text{Rh}^{\text{II}}(\text{tmp})$ (1e) and 2-Ethoxyethyl Ethyl Ether with 1 equiv of PPh_3 at 25 °C. In the benzene solution of $\text{Rh}^{\text{II}}(\text{tmp})$ **1e** (0.0088 mmol), PPh_3 (2.3 mg, 0.0088 mmol) was added and the reaction mixture was stirred at 25 °C. After 10 minutes, the

benzene solvent was removed by vacuum evaporation and then degassed 2-ethoxyethyl ethyl ether (2.0 mL) was added and the mixture was then stirred under nitrogen at 25 °C for 4 days. Excess 2-ethoxyethyl ethyl ether was removed, the dark red crude product was then purified by column chromatography on silica gel eluting with hexane/CH₂Cl₂(5:1) to give two fraction, the first fraction was the reddish purple solid of Rh(tmp)Me^{81a} **1d** (1.0 mg, 0.0011 mmol, 13%), the second fraction was the reddish purple solid of Rh(tmp)CH₂OEt **5f** (1.0 mg, 0.0011 mmol, 12%). R_f = 0.57 (hexane:CH₂Cl₂ = 1:1). ¹H NMR (300 MHz, C₆D₆) δ -1.59 (d, 2 H, ²J_{Rh-H} = 3.0 Hz), -0.90 (q, 2 H, J = 6.9 Hz), -0.64 (t, 3 H, J = 6.9 Hz), 1.97 (s, 12 H), 2.08 (s, 12 H), 2.46 (s, 12 H), 7.15 (s, 4 H), 7.19 (s, 4 H), 8.76 (s, 8 H). ¹³C NMR (CDCl₃, 100 MHz) δ 12.97, 21.60, 21.68, 21.92, 62.83 (d, ¹J_{Rh-C} = 26.0 Hz), 61.14, 119.72, 127.80, 127.83, 130.66, 137.49, 138.56, 138.98, 139.30, 142.79. HRMS: Calcd for (C₅₉H₅₉N₄O₁Rh⁺): m/z 942.3738. Found: m/z 942.3730.

Preparation of (5,10,15,20-Tetramesitylporphyrinato)ethoxymethyl Rhodium(III)

(Rh(tmp)CH₂OEt) (5f). A suspension of Rh(tmp)Cl **1b** (100 mg, 0.109 mmol) in EtOH (30 mL) in a Schlenk flask and a solution of NaBH₄ (16.5 mg, 0.435 mmol) in aqueous NaOH (0.5 M, 3 mL) in a conical flask were flushed with N₂ for 15 minutes. The solution of NaBH₄ was added slowly to the suspension of Rh(tmp)Cl via a

cannular. The reaction mixture was heated at 60 °C for 1 hour and the color changed to deep brown in color. The reaction mixture was then cooled down in an ice bath and upon addition of excess chloromethyl ethyl ether (0.2 mL), reddish precipitate was formed immediately. After stirring for 10 minutes, solvent was then removed by rotary evaporation and the crude reaction mixture was then purified by column chromatography on silica gel eluting with hexane/CH₂Cl₂ (5:1) to give the reddish purple solid of Rh(tmp)CH₂OEt **5f** (76.8 mg, 0.082 mmol, 75%).

Reaction of Rh^{II}(tmp) (1e) and 2-Ethoxyethyl Ethyl Ether with 1 equiv of PPh₃ at 50 °C. In the benzene solution of Rh^{II}(tmp) **1e** (0.0088 mmol), PPh₃ (2.3 mg, 0.0088 mmol) was added and the reaction mixture was stirred at 25 °C. After 10 minutes, the benzene solvent was removed by vacuum evaporation and then degassed 2-ethoxyethyl ethyl ether (2.0 mL) was added and the mixture was then stirred under nitrogen at 50 °C for 4 days. Excess 2-ethoxyethyl ethyl ether was removed, the dark red crude product was then purified by column chromatography on silica gel eluting with hexane/CH₂Cl₂(5:1) to give two fraction, the first fraction was the reddish purple solid of Rh(tmp)Me^{81a} **1d** (1.3 mg, 0.0014 mmol, 16%), the second fraction was the reddish purple solid of Rh(tmp)CH₂OEt **5f** (1.4 mg, 0.0015 mmol, 17%).

Reaction of Rh^{II}(tmp) (1e) and Phenyl Ethyl Ether with 1 equiv of PPh₃. In the benzene solution of Rh^{II}(tmp) **1e** (0.0088 mmol), PPh₃ (2.3 mg, 0.0088 mmol) was added and the reaction mixture was stirred at 25 °C. After 10 minutes, the benzene solvent was removed by vacuum evaporation and then degassed phenyl ethyl ether (2.0 mL) was added and the mixture was then stirred under nitrogen at 25 °C for 4 days. Excess phenyl ethyl ether was removed, the dark red crude product was then purified by column chromatography on silica gel eluting with hexane/CH₂Cl₂(5:1) to give the reddish purple solid of Rh(tmp)Et^{51b} **5b** (0.8 mg, 0.00088 mmol, 10%).

Reaction of Rh^{II}(tmp) (1e) and THF with 1 equiv of PPh₃. In the benzene solution of Rh^{II}(tmp) **1e** (0.0088 mmol), PPh₃ (2.3 mg, 0.0088 mmol) was added and the reaction mixture was stirred at 25 °C. After 10 minutes, the benzene solvent was removed by vacuum evaporation and then degassed THF (2.0 mL) was added and the mixture was then stirred under nitrogen at 25 °C for 3 days. Excess THF was removed, no corresponding CCA product was observed in the crude ¹H NMR analysis.

Reaction of Rh^{II}(tmp) (1e) and THF. Degassed THF was added into the neat Rh^{II}(tmp) **1e** (0.0088 mmol) and the mixture was then stirred under nitrogen at 25 °C for 1 days. Excess THF was removed, the crude reaction mixture was then analyzed

with ^1H NMR with degassed benzene- d_6 , $\text{Rh}^{\text{II}}(\text{tmp})$ **1e** remained unreacted with only trace amount of $\text{Rh}(\text{tmp})\text{H}$ **1f** was observed.

Reaction of $\text{Rh}^{\text{II}}(\text{tmp})$ (1e**) and *n*-Butyl Ether in Benzene- d_6 .** Degassed *n*-butyl ether (37 μL , 0.22 mmol) and benzene- d_6 (500 μL) were added into $\text{Rh}^{\text{II}}(\text{tmp})$ **1e** (0.0044 mmol) in an NMR tube under nitrogen. The red solution was degassed for three freeze-thaw-pump cycles and the NMR tube was flame-sealed under vacuum. The reaction mixture was heated and was monitored with ^1H NMR spectroscopy with NMR yields measured using the residual benzene signal as the internal standard.

Reaction of $\text{Rh}(\text{tmp})\text{CH}_2\text{OEt}$ (5f**) and *n*-Butyl Ether in the presence of PPh_3 at 24 $^\circ\text{C}$.** $\text{Rh}(\text{tmp})\text{CH}_2\text{OEt}$ **1c** (10.0 mg, 0.011 mmol) and PPh_3 (2.8 mg, 0.011 mmol) were dissolved in *n*-butyl ether (2.0 mL) and stirred at 24 $^\circ\text{C}$ under nitrogen for 1 day. Excess *n*-butyl ether was removed, the dark red crude product was then purified by column chromatography on silica gel eluting with hexane/ CH_2Cl_2 (5:1) to recover the reddish purple solid of $\text{Rh}(\text{tmp})\text{CH}_2\text{OEt}^{51\text{b}}$ **5a** (9.1 mg, 0.0067 mmol, 91%).

Reaction of $\text{Rh}^{\text{II}}(\text{tmp})$ (1e**) and Oxepane in the presence of PPh_3 .** In the benzene solution of $\text{Rh}^{\text{II}}(\text{tmp})$ **1e** (0.0088 mmol), PPh_3 (2.3 mg, 0.0088 mmol) was added and

the reaction mixture was stirred at 25 °C. After 10 minutes, the benzene solvent was removed by vacuum evaporation and then degassed oxepane (2.0 mL) was added and the mixture was then stirred under nitrogen at 25 °C for 1 day. Excess oxepane was removed, the dark red crude product was then purified by column chromatography on silica gel eluting with hexane/CH₂Cl₂(1:1) to give the reddish purple solid of Rh(tmp)CH₂CH₂CH₂CH₂CH₂OCHO **5j** (1.1 mg, 0.0011 mmol, 13%). R_f = 0.7 (CH₂Cl₂). ¹H NMR (400 MHz, C₆D₆) δ -4.55 (dt, 2 H, ²J_{Rh-H} = 3.0 Hz, J = 8.2 Hz), -4.01 (qu, 2 H, J = 7.8 Hz), -1.26 (qu, 2 H, J = 7.5 Hz), -0.26 (qu, 2 H, J = 7.0 Hz), 1.90 (s, 12 H), 2.15 (s, 12 H), 2.44 (s, 12 H), 2.80 (t, 3 H, J = 6.7 Hz), 7.12 (s, 4 H), 7.19 (s, 4 H), 8.72 (s, 8 H), 8.92 (s, 1 H). ¹³C NMR (CDCl₃, 100 MHz) δ 21.61, 21.70, 21.84, 22.64 (d, ¹J_{Rh-C} = 23.0 Hz), 26.45, 27.57, 29.85, 63.04, 119.64, 127.83, 127.86, 130.70, 137.54, 138.53, 138.90, 139.13, 142.64, 160.69. HRMS: Calcd for (C₆₂H₆₃N₄O₂Rh⁺): m/z 998.4001. Found: m/z 998.3988.

Reaction of Rh^{II}(tmp) (1e) and Oxepane. Degassed oxepane was added into the neat Rh^{II}(tmp) **1e** (0.0088 mmol) to form suspension and the mixture was then stirred under nitrogen at 25 °C for 1 day. Excess oxepane was removed, the dark red crude product was then purified by column chromatography on silica gel eluting with hexane/CH₂Cl₂(1:1) to give the reddish purple solid of

Rh(tmp)CH₂CH₂CH₂CH₂CH₂OCHO **5j** (1.5 mg, 0.0015 mmol, 17%).

Reaction of Rh^{II}(tmp) (1e), *n*-Butyl Ether and PPh₃ with the addition of 10 equiv of KOH. In the benzene solution of Rh^{II}(tmp) **1e** (0.0088 mmol), PPh₃ (2.3 mg, 0.0088 mmol) was added and the reaction mixture was stirred at 25 °C. After 10 minutes, the benzene solvent was removed by vacuum evaporation and then KOH (4.9 mg, 0.088 mmol) followed by degassed *n*-butyl ether (2.0 mL) were added and the mixture was then stirred under nitrogen at 0-3 °C for 1 day. Excess *n*-butyl ether was removed, the dark red crude product was then purified by column chromatography on silica gel eluting with hexane/CH₂Cl₂(5:1) to give the reddish purple solid of Rh(tmp)Pr^{51b} **5a** (3.3 mg, 0.0036 mmol, 40%).

Reaction of Rh^{II}(tmp) (1e), *n*-Butyl Ether and PPh₃ with the addition of 10 equiv of KOH and 50 equiv of H₂O. In the benzene solution of Rh^{II}(tmp) **1e** (0.0088 mmol), PPh₃ (2.3 mg, 0.0088 mmol) was added and the reaction mixture was stirred at 25 °C. After 10 minutes, the benzene solvent was removed by vacuum evaporation and then KOH (4.9 mg, 0.088 mmol) followed by degassed H₂O (8 uL) and *n*-butyl ether (2.0 mL) were added and the mixture was then stirred under nitrogen at 0-3 °C for 1 day. Excess *n*-butyl ether was removed, the dark red crude product was then

purified by column chromatography on silica gel eluting with hexane/CH₂Cl₂(5:1) to give the reddish purple solid of Rh(tmp)Pr^{51b} **5a** (5.2 mg, 0.0056 mmol, 64%).

Reaction of Rh^{II}(tmp) (1e), *n*-Butyl Ether and PPh₃ with the addition of 10 equiv of KO^tBu. In the benzene solution of Rh^{II}(tmp) **1e** (0.0088 mmol), PPh₃ (2.3 mg, 0.0088 mmol) was added and the reaction mixture was stirred at 25 °C. After 10 minutes, the benzene solvent was removed by vacuum evaporation and then KO^tBu (9.9 mg, 0.088 mmol) followed by degassed *n*-butyl ether (2.0 mL) were added and the mixture was then stirred under nitrogen at 0-3 °C for 1 day. Excess *n*-butyl ether was removed, the dark red crude product was then purified by column chromatography on silica gel eluting with hexane/CH₂Cl₂(5:1) to give the reddish purple solid of Rh(tmp)Pr^{51b} **5a** (4.6 mg, 0.0050 mmol, 56%).

Reaction of Rh^{II}(tmp) (1e), *n*-Butyl Ether and PPh₃ with the addition of 10 equiv of CsOH.H₂O. In the benzene solution of Rh^{II}(tmp) **1e** (0.0088 mmol), PPh₃ (2.3 mg, 0.0088 mmol) was added and the reaction mixture was stirred at 25 °C. After 10 minutes, the benzene solvent was removed by vacuum evaporation and then CsOH.H₂O (13.2 mg, 0.088 mmol) followed by degassed *n*-butyl ether (2.0 mL) were added and the mixture was then stirred under nitrogen at 0-3 °C for 1 day. Excess

n-butyl ether was removed, the dark red crude product was then purified by column chromatography on silica gel eluting with hexane/CH₂Cl₂(5:1) to give the reddish purple solid of Rh(tmp)Pr^{51b} **5a** (4.8 mg, 0.0052 mmol, 59%).

Reaction of Rh(tmp)I (1c) and *n*-Butyl Ether at 40 °C. Rh(tmp)I **1c** (10.9 mg, 0.011 mmol) was dissolved in *n*-butyl ether (2.0 mL) and heated at 40 °C under nitrogen for 1 day. Excess *n*-butyl ether was removed, the dark red crude product was then purified by column chromatography on silica gel eluting with hexane/CH₂Cl₂(5:1) to give the reddish purple solid of Rh(tmp)Pr^{51b} **5a** (0.4 mg, 0.0004 mmol, 4%).

Reaction of Rh(tmp)I (1c) and *n*-Butyl Ether with 5 equiv of KOH at 40 °C. Rh(tmp)I **1c** (11.0 mg, 0.011 mmol) and KOH (3.1 mg, 0.544 mmol) were dissolved in *n*-butyl ether (2.0 mL) and heated at 40 °C under nitrogen for 1 day. Excess *n*-butyl ether was removed, the dark red crude product was then purified by column chromatography on silica gel eluting with hexane/CH₂Cl₂(5:1) to give the reddish purple solid of Rh(tmp)Pr^{51b} **5a** (1.7 mg, 0.0018 mmol, 17%).

Reaction of Rh(tmp)I (1c) and *n*-Butyl Ether with 10 equiv of KOH at 40 °C. Rh(tmp)I **1c** (10.7 mg, 0.011 mmol) and KOH (5.9 mg, 0.106 mmol) were dissolved

in *n*-butyl ether (2.0 mL) and heated at 40 °C under nitrogen for 1 day. Excess *n*-butyl ether was removed, the dark red crude product was then purified by column chromatography on silica gel eluting with hexane/CH₂Cl₂ (5:1) to give the reddish purple solid of Rh(tmp)Pr^{51b} **5a** (3.2 mg, 0.0035 mmol, 32%).

Reaction of Rh(tmp)I (1c) and *n*-Butyl Ether with 10 equiv of K₂CO₃ at 40 °C.

Rh(tmp)I **1c** (10.7 mg, 0.011 mmol) and K₂CO₃ (15.2 mg, 0.11 mmol) were dissolved in *n*-butyl ether (2.0 mL) and heated at 40 °C under nitrogen for 3 days. Excess *n*-butyl ether was removed, the dark red crude product was then purified by column chromatography on silica gel eluting with hexane/CH₂Cl₂ (5:1) to give the reddish purple solid of Rh(tmp)Pr^{51b} **5a** (0.7 mg, 0.00074 mmol, 7%).

Reaction of Rh(tmp)I (1c) and *n*-Butyl Ether with 10 equiv of Cs₂CO₃ at 40 °C.

Rh(tmp)I **1c** (11.0 mg, 0.011 mmol) and K₂CO₃ (35.4 mg, 0.11 mmol) were dissolved in *n*-butyl ether (2.0 mL) and heated at 40 °C under nitrogen for 2 days. Excess *n*-butyl ether was removed, the dark red crude product was then purified by column chromatography on silica gel eluting with hexane/CH₂Cl₂ (5:1) to give the reddish purple solid of Rh(tmp)Pr^{51b} **5a** (0.4 mg, 0.0004 mmol, 4%).

Reaction of Rh(tmp)I (1c) and *n*-Butyl Ether with 10 equiv of KO^tBu at 40 °C.

Rh(tmp)I **1c** (10.4 mg, 0.010 mmol) and KO^tBu (11.5 mg, 0.10 mmol) were dissolved in *n*-butyl ether (2.0 mL) and heated at 40 °C under nitrogen for 1 days. Excess *n*-butyl ether was removed, the dark red crude product was then purified by column chromatography on silica gel eluting with hexane/CH₂Cl₂ (5:1) to give the reddish purple solid of Rh(tmp)Pr^{51b} **5a** (2.1 mg, 0.002 mmol, 22%).

Reaction of Rh(tmp)I (1c) and *n*-Butyl Ether with 10 equiv of NaOMe at 40 °C.

Rh(tmp)I **1c** (10.6 mg, 0.010 mmol) and NaOMe (5.7 mg, 0.10 mmol) were dissolved in *n*-butyl ether (2.0 mL) and heated at 40 °C under nitrogen for 3 days. Excess *n*-butyl ether was removed, the dark red crude product was then purified by column chromatography on silica gel eluting with hexane/CH₂Cl₂ (5:1) to give the reddish purple solid of Rh(tmp)Pr^{51b} **5a** (1.9 mg, 0.002 mmol, 20%).

Reaction of Rh(tmp)I (1c) and *n*-Butyl Ether with 10 equiv of NaOH at 40 °C.

Rh(tmp)I **1c** (11.4 mg, 0.011 mmol) and NaOH (4.5 mg, 0.118 mmol) were dissolved in *n*-butyl ether (2.0 mL) and heated at 40 °C under nitrogen for 3 days. Excess *n*-butyl ether was removed, the dark red crude product was then purified by column chromatography on silica gel eluting with hexane/CH₂Cl₂ (5:1) to give the reddish

purple solid of Rh(tmp)Pr^{51b} **5a** (1.9 mg, 0.002 mmol, 18%).

Reaction of Rh(tmp)I (1c) and *n*-Butyl Ether with 20 equiv of KOH at 40 °C.

Rh(tmp)I **1c** (10.1 mg, 0.010 mmol) and KOH (11.2 mg, 0.200 mmol) were dissolved in *n*-butyl ether (2.0 mL) and heated at 40 °C under nitrogen for 1 day. Excess *n*-butyl ether was removed, the dark red crude product was then purified by column chromatography on silica gel eluting with hexane/CH₂Cl₂ (5:1) to give the reddish purple solid of Rh(tmp)Pr^{51b} **5a** (3.3 mg, 0.0036 mmol, 35%).

Reaction of Rh(tmp)I (1c) and *n*-Butyl Ether with 10 equiv of KOH in benzene

solvent at 40 °C. Rh(tmp)I **1c** (12.6 mg, 0.012 mmol), KOH (7.0 mg, 0.125 mmol), *n*-butyl ether (106 μL, 0.623mmol) were dissolved in benzene (2.0 mL) and heated at 40 °C under nitrogen for 1 day. Excess *n*-butyl ether and benzene were removed, only trace amount of Rh(tmp)Pr^{51b} **5a** was identified in the crude reaction mixture by ¹H NMR analysis.

Anion Effect

Reaction of Rh(tmp)I (1c) and *n*-Butyl Ether with 10 equiv of KOH at 80 °C.

Rh(tmp)I **1c** (10.0 mg, 0.010 mmol) and KOH (5.6 mg, 0.099 mmol) were dissolved

in *n*-butyl ether (2.0 mL) and heated at 80 °C under nitrogen for 1 day. Excess *n*-butyl ether was removed, the dark red crude product was then purified by column chromatography on silica gel eluting with hexane/CH₂Cl₂ (5:1) to give the reddish purple solid of Rh(tmp)Pr^{51b} **5a** (4.9 mg, 0.005 mmol, 53%).

Reaction of Rh(tmp)Cl (1b) and *n*-Butyl Ether with 10 equiv of KOH at 80 °C.

Rh(tmp)Cl **1b** (10 mg, 0.010 mmol) and KOH (6.7 mg, 0.120 mmol) were incompletely dissolved in *n*-butyl ether (2.0mL) and heated at 80 °C to form suspension under nitrogen in the dark for 1 day. Excess *n*-butyl ether was removed, the dark red crude product was then purified by column chromatography on silica gel eluting with hexane/CH₂Cl₂ (5:1) to give reddish purple solid of Rh(tmp)Pr^{51b} **5a** (2.6 mg, 0.003 mmol, 23%).

Reaction of Rh(ttp)I (3c) and *n*-Butyl Ether with 10 equiv of KOH at 80 °C.

Rh(ttp)I **3c** (15.0 mg, 0.017 mmol) and KOH (9.7 mg, 0.17 mmol) were dissolved in *n*-butyl ether (2.0 mL) to form a suspension and heated at 80 °C under nitrogen for 1 day. Excess *n*-butyl ether was removed, the dark red crude product was then purified by column chromatography on silica gel eluting with hexane/CH₂Cl₂ (5:1) to give the reddish purple solid of Rh(ttp)Pr¹³⁵ **3f** (8.4 mg, 0.01 mmol, 60%). $R_f = 0.46$

(hexane:CH₂Cl₂ = 5:2).

Reaction of Rh(ttp)Cl (3b) and *n*-Butyl Ether with 10 equiv of KOH at 80 °C.

Rh(ttp)Cl **3b** (10.7 mg, 0.013 mmol) and KOH (7.4 mg, 0.133 mmol) were incompletely dissolved in *n*-butyl ether (2.0mL) to form a suspension and heated at 80 °C to form suspension under nitrogen in the dark for 1 day. Excess *n*-butyl ether was removed, the dark red crude product was then purified by column chromatography on silica gel eluting with hexane/CH₂Cl₂ (5:1) to give reddish purple solid of Rh(ttp)Pr¹³⁵ **3f** (2.1 mg, 0.003 mmol, 19%).

Reaction of Rh(tmp)BF₄ (1k) and *n*-Butyl Ether with 10 equiv of KOH at 80 °C.

Rh(tmp)BF₄ **1k** was prepared in-situ from the reaction between Rh(tmp)I (10 mg, 0.010 mmol) and AgBF₄ in dichloromethane (4.0 mL) at ambient conditions for 2 hours under N₂. After complete consumption of Rh(tmp)I observed from the TLC analysis, excess dichloromethane was removed under high vacuum for 2 hours. Then KOH (6.7 mg, 0.120 mmol) was added together with degassed *n*-butyl ether (2.0 mL) and heated at 80 °C to form suspension under nitrogen in the dark for 1 day. Excess *n*-butyl ether was removed, the dark red crude product was then purified by column chromatography on silica gel eluting with hexane/CH₂Cl₂ (5:1) to give reddish purple

solid of Rh(tmp)Pr^{51b} **5a** (2.6 mg, 0.003 mmol, 23%).

Porphyrin Effect

Reaction of Rh(ttp)I (**3c**) and *n*-Propyl Ether and 10 equiv of KOH at 80 °C.

Rh(ttp)I **3c** (10.4 mg, 0.012 mmol) and KOH (6.5 mg, 0.116 mmol) were incompletely dissolved in *n*-propyl ether (2.0 mL) and heated at 80 °C to form suspension under nitrogen for 1 day. Excess *n*-propyl ether was removed, the dark red crude product was then purified by column chromatography on silica gel eluting with hexane/CH₂Cl₂ (5:1) to give the reddish purple solid of Rh(ttp)Et¹³⁶ **3g** (2.8 mg, 0.003 mmol, 30%). *R_f* = 0.53 (hexane:CH₂Cl₂ = 2:1). ¹H NMR (300 MHz, CDCl₃) δ -4.86 (dq, 3 H, ²*J*_{Rh-H} = 3.0 Hz, ³*J*_{H-H} = 6.0 Hz), -4.45 (t, 3 H, *J* = 6.0 Hz), 2.69 (s, 12 H), 7.53 (t, 8 H, *J* = 6.3 Hz), 8.08 (d, 4 H, *J* = 7.5 Hz), 8.08 (s, 8 H).

Reaction of Rh(tmp)I (**1c**) and *n*-Propyl Ether and 10 equiv of KOH at 80 °C.

Rh(tmp)I **1c** (10.0 mg, 0.010 mmol) and KOH (5.5 mg, 0.098 mmol) were incompletely dissolved in *n*-propyl ether (2.0 mL) and heated at 80 °C to form suspension under nitrogen for 1 day. Excess *n*-propyl ether was removed, the dark red crude product was then purified by column chromatography on silica gel eluting with hexane/CH₂Cl₂ (5:1) to give the reddish purple solid of Rh(tmp)Et^{51b} **5b** (3.1 mg,

0.003 mmol, 34%).

Reaction of Rh(ttp)I (3c) and *n*-butyl Ether and 10 equiv of KOH at 80 °C.

Rh(ttp)I **3c** (12.4 mg, 0.014 mmol) and KOH (5.6 mg, 0.138 mmol) were incompletely dissolved in *n*-butyl ether (2.0 mL) and heated at 80 °C under nitrogen for 3 days to form a suspension. Excess *n*-butyl ether was removed, the dark red crude product was then purified by column chromatography on silica gel eluting with hexane/CH₂Cl₂ (5:1) to give the reddish purple solid of Rh(ttp)Pr¹³⁵ **3f** (7.3 mg, 0.009 mmol, 65%).

Reaction of Rh(ttp)I (3c) and *n*-Pentyl Ether and 10 equiv of KOH at 80 °C.

Rh(ttp)I **3c** (11.1 mg, 0.012 mmol) and KOH (6.9 mg, 0.124 mmol) were poorly dissolved in *n*-pentyl ether (2.0 mL) and heated at 80 °C under nitrogen for 1 day to form a suspension. Excess *n*-pentyl ether was removed, the dark red crude product was then purified by column chromatography on silica gel eluting with hexane/CH₂Cl₂ (5:1) to give the reddish purple solid of Rh(ttp)Bu¹³⁵ **3i** (1.6 mg, 0.002 mmol, 16%). *R_f* = 0.61 (hexane:CH₂Cl₂ = 2:1). ¹H NMR (400 MHz, CDCl₃) δ -4.96 (dd, 2 H, ²*J*_{Rh-H} = 3.2 Hz, ³*J*_{H-H} = 4.9 Hz), -4.76 (m, 1 H), -2.20 (d, 6 H, *J* = 6.7 Hz), 2.72 (s, 12 H), 7.26 (s, 4 H), 7.54 (d, 4 H, *J* = 5.7 Hz), 7.56 (d, 4 H, *J* = 5.7 Hz), 8.02

(d, 4 H, $J = 7.5$ Hz), 8.12 (d, 4 H, $J = 7.5$ Hz), 8.76 (s, 8 H).

Reaction of Rh(tmp)I (1c) and *n*-Pentyl Ether and 10 equiv of KOH at 80 °C.

Rh(tmp)I **1c** (10.0 mg, 0.010 mmol) and KOH (5.6 mg, 0.099 mmol) were dissolved in *n*-pentyl ether (2.0 mL) and heated at 80 °C under nitrogen for 1 day. Excess *n*-pentyl ether was removed, the dark red crude product was then purified by column chromatography on silica gel eluting with hexane/CH₂Cl₂ (5:1) to give the reddish purple solid of Rh(tmp)Bu^{51b} **5c** (8.2 mg, 0.009 mmol, 88%).

Reaction of Rh(t₄-CF₃pp)I (2c) and *n*-Pentyl Ether and 10 equiv of KOH at 80 °C.

Rh(t₄-CF₃pp)I **2c** (11.1 mg, 0.010 mmol) and KOH (5.6 mg, 0.099 mmol) were dissolved in *n*-pentyl ether (2.0 mL) and heated at 80 °C under nitrogen for 1 day. Excess *n*-pentyl ether was removed, the dark red crude product was then purified by column chromatography on silica gel eluting with hexane/CH₂Cl₂ (5:1) to give the reddish purple solid of Rh(t₄-CF₃pp)Bu **2d** (6.0 mg, 0.006 mmol, 58%). $R_f = 0.67$ (hexane:CH₂Cl₂ = 5:1). ¹H NMR(400 MHz, CDCl₃) δ -4.94 (dt, 2 H, ² $J_{Rh-H} = 2.8$ Hz, ³ $J_{H-H} = 7.5$ Hz), -4.53 (qu, 2 H, $J = 7.5$ Hz), -1.57 (s, 2 H, $J = 7.4$ Hz), -0.81 (t, 3 H, $J = 7.3$ Hz), 8.03 (d, 8 H, $J = 7.1$ Hz) 8.04 (d, 4 H, $J = 7.1$ Hz), 8.25 (d, 4 H, $J = 7.7$ Hz), 8.33 (d, 4 H, $J = 7.7$ Hz), 8.67 (s, 8 H). ¹³C NMR (CDCl₃, 100 MHz) δ 12.30,

16.05 (d, $^1J_{\text{Rh-C}} = 26.9$ Hz), 19.39, 29.80, 120.59 (q, $^1J_{\text{C-F}} = 270.6$ Hz), 123.91, 123.95, 129.85 (q, $^2J_{\text{C-F}} = 32.4$ Hz), 131.85, 133.97, 134.25, 143.02, 145.67. HRMS (FABMS): Calcd for $(\text{C}_{53}\text{H}_{33}\text{F}_{12}\text{N}_4\text{Rh}_1)^+$: m/z 1044.1563. Found: m/z 1044.1573.

Temperature Effect

Reaction of Rh(tmp)I (**1c**) and *n*-Propyl Ether and 10 equiv of KOH at 40 °C.

Rh(tmp)I **1c** (10.0 mg, 0.010 mmol) and KOH (5.6 mg, 0.099 mmol) were incompletely dissolved in *n*-propyl ether (2.0 mL) and heated at 40 °C under nitrogen for 1 day. Excess *n*-propyl ether was removed, the dark red crude product was then purified by column chromatography on silica gel eluting with hexane/ CH_2Cl_2 (5:1) to give the reddish purple solid of Rh(tmp)Et^{51b} **5b** (2.1 mg, 0.0023 mmol, 23%).

Reaction of Rh(tmp)I (**1c**) and *n*-Propyl Ether and 10 equiv of KOH at 80 °C.

Rh(tmp)I **1c** (10.0 mg, 0.010 mmol) and KOH (5.6 mg, 0.099 mmol) were incompletely dissolved in *n*-propyl ether (2.0 mL) and heated at 80 °C under nitrogen for 1 day. Excess *n*-propyl ether was removed, the dark red crude product was then purified by column chromatography on silica gel eluting with hexane/ CH_2Cl_2 (5:1) to give the reddish purple solid of Rh(tmp)Pr^{51b} **5a** (3.1 mg, 0.003 mmol, 34%).

Reaction of Rh(tmp)I (1c) and *n*-Propyl Ether and 10 equiv of KOH at 100 °C.

Rh(tmp)I **1c** (10.4 mg, 0.010 mmol) and KOH (5.8 mg, 0.010 mmol) were incompletely dissolved in *n*-propyl ether (2.0 mL) and heated at 100 °C under nitrogen for 1 day. Excess *n*-propyl ether was removed, the dark red crude product was then purified by column chromatography on silica gel eluting with hexane/CH₂Cl₂ (5:1) to give the reddish purple solid of Rh(tmp)Et^{51b} **5b** (2.8 mg, 0.003 mmol, 30%).

Reaction of Rh(tmp)I (1c) and *n*-Butyl Ether and 10 equiv of KOH at 80 °C.

Rh(tmp)I **1c** (10.0 mg, 0.010 mmol) and KOH (5.6 mg, 0.099 mmol) were dissolved in *n*-butyl ether (2.0 mL) and heated at 80 °C under nitrogen for 1 day. Excess *n*-butyl ether was removed, the dark red crude product was then purified by column chromatography on silica gel eluting with hexane/CH₂Cl₂ (5:1) to give the reddish purple solid of Rh(tmp)Pr^{51b} **5a** (4.9 mg, 0.005 mmol, 53%).

Reaction of Rh(tmp)I (1c) and *n*-Butyl Ether with 10 equiv of KOH at 100 °C.

Rh(tmp)I **1c** (10.7 mg, 0.011 mmol) and KOH (6.0 mg, 0.106 mmol) were dissolved in *n*-butyl ether (2.0 mL) and heated at 100 °C under nitrogen for 1 day. Excess *n*-butyl ether was removed, the dark red crude product was then purified by column

chromatography on silica gel eluting with hexane/CH₂Cl₂ (5:1) to give the reddish purple solid of Rh(tmp)Pr^{51b} **5a** (8.2 mg, 0.009 mmol, 86%).

Substrate Scope of Symmetrical Ether

Reaction of Rh(tmp)I (1c**) and *n*-Propyl Ether and 10 equiv of KOH at 100 °C.**

Rh(tmp)I **1c** (10.0 mg, 0.010 mmol) and KOH (5.5 mg, 0.098 mmol) were incompletely dissolved in *n*-propyl ether (2.0 mL) and heated at 100 °C to form suspension under nitrogen for 1 day. Excess *n*-propyl ether was removed, the dark red crude product was then purified by column chromatography on silica gel eluting with hexane/CH₂Cl₂ (5:1) to give the reddish purple solid of Rh(tmp)Et^{51b} **5b** (3.1 mg, 0.003 mmol, 34%).

Reaction of Rh(tmp)I (1c**) and Isopropyl Ether with 10 equiv of KOH at 100 °C.**

Rh(tmp)I **1c** (10.0 mg, 0.009 mmol) and KOH (5.5 mg, 0.099 mmol) were incompletely dissolved in isopropyl ether (2.0 mL) and heated at 100 °C to form suspension under nitrogen for 1 day. Excess isopropyl ether was removed, the dark red crude product was then purified by column chromatography on silica gel eluting with hexane/CH₂Cl₂ (5:1) to give the reddish purple solid of Rh(tmp)Me^{81a} **1d** (3.7 mg, 0.004 mmol, 42%).

Reaction of Rh(tmp)I (1c) and *n*-Pentyl Ether with 10 equiv of KOH at 100 °C.

Rh(tmp)I **1c** (11.3 mg, 0.012 mmol) and KOH (6.3 mg, 0.11 mmol) were dissolved in *n*-pentyl ether (2.0 mL) and heated at 100 °C under nitrogen for 1 day. Excess *n*-pentyl ether was removed, the dark red crude product was then purified by column chromatography on silica gel eluting with hexane/CH₂Cl₂ (5:1) to give the reddish purple solid of Rh(tmp)Bu^{5b} **5c** (9.3 mg, 0.009 mmol, 88%).

Reaction of Rh(tmp)I (1c) and Isoamyl Ether with 10 equiv of KOH at 100 °C.

Rh(tmp)I **1c** (10.4 mg, 0.010 mmol) and KOH (5.7 mg, 0.100 mmol) were dissolved in isoamyl ether (2.0 mL) and heated at 100 °C under nitrogen in the dark for 1 day. Excess isoamyl ether was removed. Only trace amount of Rh(tmp)^tBu **5d** was observed from the ¹H NMR of the crude reaction mixture.

Reaction of Rh(tmp)I (1c) and *n*-Hexyl Ether with 10 equiv of KOH at 100 °C.

Rh(tmp)I **1c** (10.1 mg, 0.009 mmol) and KOH (5.6 mg, 0.099 mmol) were dissolved in *n*-hexyl ether (2.0 mL) and heated at 100 °C under nitrogen in the dark for 1 day. Excess *n*-hexyl ether was removed, the dark red crude product was then purified by column chromatography on silica gel eluting with hexane/CH₂Cl₂ (5:1) to give the reddish purple solid of Rh(tmp)Pent **5e** (5.3 mg, 0.005 mmol, 57%). R_f = 0.63

(hexane:CH₂Cl₂ = 5:1). ¹H NMR (300 MHz, C₆D₆) δ -4.46 (dt, 2 H, ²J_{Rh-H} = 3.0 Hz, ³J_{HH} = 7.5 Hz), -3.93 (qu, 2 H, J = 7.5 Hz), -1.15 (qu, 2 H, J = 7.5 Hz), -0.35 (m, 2 H), -0.22 (t, 3H, J = 7.5 Hz), 1.91 (s, 12 H), 2.17 (s, 12 H), 2.44 (s, 12 H), 7.12 (s, 4 H), 7.19 (s, 4 H), 8.74 (s, 8 H). HRMS (FAB): Calcd for (C₆₁H₆₃N₄Rh)⁺: m/z 954.4102. Found: m/z 954.4101. Anal. Calcd. For C₆₁H₆₃N₄Rh: C, 76.71; H, 6.65; N, 5.86. Found: C, 76.11; H, 6.74; N, 5.57. The ¹³C NMR Spectra of **5e** was not able to obtain since **5e** is not soluble enough in CD₂Cl₂, CDCl₃ and C₆D₆.

Reaction of Rh(tmp)I (1c) and 2-Ethoxyethyl Ethyl Ether with 10 equiv of KOH at 80 °C. Rh(tmp)I **1c** (10.1 mg, 0.010 mmol) and KOH (5.5 mg, 0.100 mmol) were dissolved in 2-ethoxyethyl ethyl ether (2.0 mL) and heated at 80 °C under N₂ for 1 day. Excess 2-ethoxyethyl ethyl ether was removed, the dark red crude product was then purified by column chromatography on silica gel eluting with hexane/CH₂Cl₂ (5:1) to give the reddish purple solid of Rh(tmp)Me^{81a} **1d** (1.8 mg, 0.002 mmol, 19%).

Substrate Scope of Unsymmetrical Ethers

Reaction of Rh(ttp)I (3c) and Di-isopropyl Ether with 10 equiv of KOH at 80 °C.

Rh(ttp)I **3c** (10.2 mg, 0.011 mmol) and KOH (6.4 mg, 0.114 mmol) were incompletely dissolved in di-isopropyl ether (2.0 mL) and heated at 80 °C under

nitrogen in the dark for 1 day to form a suspension. Excess di-isopropyl ether was removed, the dark red crude product was then purified by column chromatography on silica gel eluting with hexane/CH₂Cl₂ (5:1) to give the reddish purple solid of Rh(tp)Me¹³³ **3h** (5.0 mg, 0.006 mmol, 56%). *R_f* = 0.63 (hexane:CH₂Cl₂ = 2:1). ¹H NMR (300 MHz, CDCl₃) δ -5.82 (d, 3 H, *J* = 3.0 Hz), 2.70 (s, 12 H), 7.53 (d, 8 H, *J* = 7.5 Hz), 8.01 (dd, 4 H, *J* = 2.4, 8.4 Hz), 8.07 (dd, 4 H, *J* = 2.4, 8.4 Hz), 8.73 (s, 8 H).

Reaction of Rh(tp)I (3c) and Isopropyl Butyl Ether with 10 equiv of KOH at 80

°C. Rh(tp)I **3c** (15.3 mg, 0.017 mmol) and KOH (9.6 mg, 0.170 mmol) were incompletely dissolved in isopropyl butyl ether (2.0 mL) and heated at 80 °C under N₂ for 1 day. Excess 2-isopropyl butyl ether was removed, the dark red crude product was then purified by column chromatography on silica gel eluting with hexane/CH₂Cl₂ (5:1) to give the reddish purple solid of Rh(tp)Me¹³³ **3h** (2.6 mg, 0.003 mmol, 10%).

Reaction of Rh(tp)I (3c) and *t*-Butyl Ethyl Ether with 10 equiv of KOH at 80 °C.

Rh(tp)I **3c** (10.1 mg, 0.010 mmol) and KOH (5.5 mg, 0.100 mmol) were incompletely dissolved in *t*-butyl ethyl ether (2.0 mL) and heated at 80 °C under N₂ for 1 day to form a suspension. Excess *t*-butyl ethyl ether was removed, both

Rh(ttp)Me **3h** and Rh(ttp)CH₂O^tBu **3j** were observed from crude ¹H NMR analysis with 1:1 ratio, the dark red crude product was then purified by column chromatography on silica gel eluting with hexane/CH₂Cl₂ (5:1) to give the reddish purple solid of the mixture of Rh(ttp)Me¹³³ **3h** (~5% NMR yield) and Rh(ttp)CH₂O^tBu⁹⁸ (~5% NMR yield). ¹H NMR of Rh(ttp)CH₂O^tBu⁹⁸ (300 MHz, CDCl₃) δ -2.82 (d, 2 H, ²J_{Rh-H} = 3.0 Hz), -1.23 (s, 9 H), 7.44 – 7.66 (m 8 H), 7.94 – 8.00 (m, 8 H), 8.70 (s, 8 H).

Reaction of Rh(ttp)I (3c) and *t*-Butyl Butyl Ether with 10 equiv of KOH at 80 °C.

Rh(ttp)I **3c** (11.6 mg, 0.013 mmol) and KOH (7.2 mg, 0.129 mmol) were dissolved in *t*-butyl butyl ether (2.0 mL) and heated at 80 °C under N₂ for 1 day. Excess *t*-butyl butyl ether was removed; no correspondening CCA products were obtained.

Reaction of Rh(ttp)I (3c) and Di-isoamyl Ether with 10 equiv of KOH at 80 °C.

Rh(ttp)I **3c** (10.5 mg, 0.012 mmol) and KOH (6.6 mg, 0.117 mmol) were dissolved in di-isoamyl ether (2.0 mL) and heated at 80 °C under N₂ for 1 day. Excess di-isoamyl ether was removed, only trace amount of Rh(ttp)^tBu **3k** were observed.

Preparation of (5,10,15,20-Tetramesitylporphyrinato)isobutyl Rhodium(III)

(Rh(ttp)ⁱBu) (3k). A suspension of Rh(ttp)Cl **3b** (50 mg, 0.062 mmol) in EtOH (30 mL) in a Schlenk flask and a solution of NaBH₄ (9.3 mg, 0.248 mmol) in aqueous NaOH (0.5 M, 3 mL) in a conical flask were flushed with N₂ for 15 minutes. The solution of NaBH₄ was added slowly to the suspension of Rh(ttp)Cl via a cannular. The reaction mixture was heated at 60 °C for 1 hour and the color changed to deep brown in color. The reaction mixture was then cooled down in an ice bath and upon addition of excess 1-bromo-2-methylpropane (350 μL, 3.25 mmol), reddish precipitate was formed immediately. After stirring for 10 minutes, solvent was then removed by rotary evaporation and the crude reaction mixture was then purified by column chromatography on silica gel eluting with hexane/CH₂Cl₂ (5:1) to give the reddish purple solid of Rh(ttp)ⁱBu **3k** (39 mg, 0.047 mmol, 76%). *R_f* = 0.69 (hexane:CH₂Cl₂ = 2:1). ¹H NMR (400 MHz, CDCl₃) δ -4.96 (dd, 2 H, ²*J*_{Rh-H} = 3.2 Hz, ³*J*_{H-H} = 4.9 Hz), -4.76 (m, 1 H), -2.20 (d, 6 H, *J* = 6.7 Hz), 2.72 (s, 12 H), 7.26 (s, 4 H), 7.54 (d, 4 H, *J* = 5.7 Hz), 7.56 (d, 4 H, *J* = 5.7 Hz), 8.02 (d, 4 H, *J* = 7.5 Hz), 8.12 (d, 4 H, *J* = 7.5 Hz), 8.76 (s, 8 H). ¹³C NMR (CD₂Cl₂, 75 MHz) δ 19.77, 21.68, 24.92 (d, ¹*J*_{Rh-C} = 27.4 Hz), 122.63, 127.45, 127.53, 131.54, 133.72, 134.16, 137.25, 139.44, 143.44. HRMS: Calcd for (C₅₂H₄₅N₄Rh)⁺: *m/z* 829.2772. Found: *m/z* 829.2739.

Reaction of Rh(ttp)I (3c) and 2-Butyl-1,3-Dioxolane with 10 equiv of KOH at 80 °C. Rh(ttp)I **3c** (11.1 mg, 0.013 mmol) and KOH (9.2 mg, 0.128mmol) were dissolved in 2-butyl-1,3-dioxolane (2.0 mL) and heated at 80 °C under N₂ for 1 day. Excess 2-butyl-1,3-dioxolane was removed, the dark red crude product was then purified by column chromatography on silica gel eluting with hexane/CH₂Cl₂ (5:1) to give the reddish purple solid of Rh(ttp)Bu¹³⁵ **3i** (2.1 mg, 0.0023 mmol, 21%).

Reaction of Rh(ttp)I (3c) and 2-Propyl-1,3-Dioxolane with 10 equiv of KOH at 80 °C. Rh(ttp)I **3c** (10.2 mg, 0.011 mmol) and KOH (6.4 mg, 0.114 mmol) were dissolved in 2-propyl-1,3-dioxolane (2.0 mL) and heated at 80 °C under N₂ for 1 day. Excess 2-propyl-1,3-dioxolane was removed, the dark red crude product was then purified by column chromatography on silica gel eluting with hexane/CH₂Cl₂ (5:1) to give the reddish purple solid of Rh(ttp)Pr¹³⁵ **3f** (0.9 mg, 0.001 mmol, 10%).

Mechanistic Investigation

Reaction of Rh(tmp)I (1c) and *n*-Butyl Ether (50 equiv) with 10 equiv of KOH in Benzene-*d*₆. Rh(tmp)I **1c** (6.7 mg, 0.0066 mmol), KOH (3.7 mg, 0.066 mmol) and *n*-butyl ether (43 μL, 0.33 mmol) were added into benzene-*d*₆ (500 μL) in an NMR tube under nitrogen. The red solution was degassed for three freeze-thaw-pump cycles

and the NMR tube was flame-sealed under vacuum. The reaction mixture was heated at 100 °C and was monitored with ¹H NMR spectroscopy with NMR yields measured using the residual benzene signal as the internal standard.

Reaction of Rh(tmp)I (1c) and *n*-Butyl Ether (50 equiv) with 10 equiv of KOH in THF-*d*₈. Rh(tmp)I **1c** (6.7 mg, 0.0066 mmol), KOH (3.7 mg, 0.066 mmol) and *n*-butyl ether (43 μL, 0.33 mmol) were added into THF-*d*₈ (500 μL) in an NMR tube under nitrogen. The red solution was degassed for three freeze-thaw-pump cycles and the NMR tube was flame-sealed under vacuum. The reaction mixture was heated at 100 °C and was monitored with ¹H NMR spectroscopy with NMR yields measured using the residual benzene signal as the internal standard.

Reaction of Rh(tmp)H (1f) and *n*-Butyl Ether. The suspension of Rh(tmp)H (10.0 mg, 0.011 mmol) in *n*-butyl ether (2.0 mL) was heated at 100 °C to form suspension under nitrogen for 1 day. Excess *n*-butyl ether was removed, the dark red crude product was then purified by column chromatography on silica gel eluting with hexane/CH₂Cl₂(5:1) to give the reddish purple solid of Rh(tmp)Pr^{51b} **5a** (1.1 mg, 0.0011 mmol, 10%).

Reaction of Rh(tmp)H (1f) and *n*-Butyl Ether with 10 equiv of KOH. The suspension of Rh(tmp)H **1f** (10.0 mg, 0.011 mmol) and KOH (6.0 mg, 0.106 mmol) in *n*-butyl ether (2.0 mL) was heated at 100 °C to form suspension under nitrogen for 1 day. Excess *n*-butyl ether was removed, the dark red crude product was then purified by column chromatography on silica gel eluting with hexane/CH₂Cl₂ (5:1) to give the reddish purple solid of Rh(tmp)Pr^{51b} **5a** (5.9 mg, 0.0064 mmol, 54%).

Reaction of Rh(tmp)H (1f) and *n*-Butyl Ether (50 equiv) in Benzene-*d*₆. Rh(tmp)H **1f** (2.5 mg, 0.0028 mmol) and *n*-butyl ether (18 μL, 0.14 mmol) were added into benzene-*d*₆ (500 μL) in an NMR tube under nitrogen. The red solution was degassed for three freeze-thaw-pump cycles and the NMR tube was flame-sealed under vacuum. The reaction mixture was heated at 100 °C and was monitored with ¹H NMR spectroscopy with NMR yields measured using the residual benzene signal as the internal standard.

Reaction of Rh(tmp)H (1f) and *n*-Butyl Ether (50 equiv) with 10 equiv of KOH in Benzene-*d*₆. Rh(tmp)H **1f** (2.5 mg, 0.0028 mmol), KOH (1.6 mg, 0.028 mmol) and *n*-butyl ether (18 μL, 0.14 mmol) were added into benzene-*d*₆ (500 μL) in an NMR tube under nitrogen. The red solution was degassed for three freeze-thaw-pump cycles

and the NMR tube was flame-sealed under vacuum. The reaction mixture was heated at 100 °C and was monitored with ¹H NMR spectroscopy with NMR yields measured using the residual benzene signal as the internal standard.

Reaction of [Rh^I(tmp)]⁻ (1h) and *n*-Butyl Ether with 10 equiv of KOH. Degassed *n*-butyl ether (4.0 mL) and KOH (15.2 mg, 0.27 mmol) were added to [Rh^I(tmp)]⁻ **1h** (24.1 mg, 0.027 mmol) to form a suspension and heated at 100 °C under nitrogen for 1 day. Excess *n*-butyl ether was removed, the dark red crude product was then purified by column chromatography on silica gel eluting with hexane/CH₂Cl₂ (5:1) to give reddish purple solid of Rh(tmp)Pr^{51b} **5a** (2.5 mg, 0.0027 mmol, 10%).

Reaction of Rh^{II}(tmp) (1e) and *n*-Butyl Ether. Degassed *n*-butyl ether (2.0 mL) was added to Rh^{II}(tmp) **1e** (7.8 mg, 0.0088 mmol) and the mixture was then heated at 100 °C under nitrogen for 1 day. Excess *n*-butyl ether was removed, the dark red crude product was then purified by column chromatography on silica gel eluting with hexane/CH₂Cl₂(5:1) to give the reddish purple solid of Rh(tmp)Pr^{51b} **5a** (3.1 mg, 0.0033 mmol, 37%).

Reaction of Rh^{II}(tmp) (1e) and *n*-Butyl Ether with 10 equiv of KOH. Degassed *n*-butyl ether (2.0 mL) and KOH (4.9 mg, 0.088 mmol) were added to Rh^{II}(tmp) (7.8 mg, 0.0088 mmol) and the mixture was then heated at 100 °C under nitrogen for 1 day. Excess *n*-butyl ether was removed, the dark red crude product was then purified by column chromatography on silica gel eluting with hexane/CH₂Cl₂ (5:1) to give reddish purple solid of Rh(tmp)Pr^{51b} **5a** (4.7 mg, 0.005 mmol, 56%).

Reaction of Rh^{II}(tmp) (1e) and *n*-Butyl Ether (50 equiv) in Benzene-*d*₆. Degassed *n*-butyl ether (28 μL, 0.22 mmol) was added into benzene-*d*₆ (500 μL) solution of Rh(tmp) **1e** (0.0044 mmol) in an NMR tube under nitrogen. The red solution was degassed for three freeze-thaw-pump cycles and the NMR tube was flame-sealed under vacuum. The reaction mixture was heated at 100 °C and was monitored with ¹H NMR spectroscopy with NMR yields measured using the residual benzene signal as the internal standard.

Reaction of Rh^{III}(tmp) (1e) and *n*-Butyl Ether (50 equiv) with 10 equiv of KOH in Benzene-*d*₆. Degassed *n*-butyl ether (28 μL, 0.22 mmol) and KOH (2.5 mg, 0.044 mmol) were added into benzene-*d*₆ (500 μL) solution of Rh^{III}(tmp) **1e** (0.0044 mmol) in an NMR tube under nitrogen. The red solution was degassed for three

freeze-thaw-pump cycles and the NMR tube was flame-sealed under vacuum. The reaction mixture was heated at 100 °C and was monitored with ¹H NMR spectroscopy with NMR yields measured using the residual benzene signal as the internal standard.

Reaction of Rh(tmp)I (1c) and KOH in Benzene-*d*₆. Rh(tmp)I **1c** (3.5 mg, 0.0035 mmol) and KOH (1.9 mg, 0.035 mmol) were dissolved in benzene-*d*₆ (0.5 mL) and heated at 100 °C in a sealed NMR tube. The reaction mixture was monitored with ¹H NMR spectroscopy with NMR yields measured using the residual benzene signal as the internal standard.

Reaction of Rh(tmp)I (1c) and KOH in Benzene. Rh(tmp)I **1c** (10 mg, 0.010 mmol) and KOH (5.5 mg, 0.098 mmol) were dissolved in benzene (2 mL) and heated at 100 °C for 1 day. Excess benzene was removed, the dark red crude product was then purified by column chromatography on silica gel eluting with hexane/CH₂Cl₂ (2:1) to recover the reddish purple of Rh(tmp)I (8.0 mg, 0.008 mmol, 80%).

Reaction of Rh(tmp)I (1c) and KOH in THF. Rh(tmp)I **1c** (3.5 mg, 0.0035 mmol) and KOH (1.9 mg, 0.035 mmol) were dissolved in THF and heated at 100 °C to give [Rh^I(tmp)]⁻ quantitatively in 5 days.

General Procedures for the Base-Promoted Dehydrogenation of Rh(tmp)H:

Reaction of Rh(tmp)H (1f) and 10 equiv of KOH in Benzene-*d*₆ Rh(tmp)H 1f (2.5 mg, 0.0028 mmol) and KOH (1.6 mg, 0.028 mmol) were added into benzene-*d*₆ (500 μ L) in an NMR tube under nitrogen. The red solution was degassed for three freeze-thaw-pump cycles and the NMR tube was flame-sealed under vacuum. The reaction mixture was heated at 100 °C and was monitored with ¹H NMR spectroscopy with NMR yields measured using the residual benzene signal as the internal standard. Other inorganic bases as KOAc and KO^tBu were also carried out in the same reaction conditions and the result was summarized in Table 5.1.

Table 5.1 Base-Promoted Dehydrogenation of Rh(tmp)H to Rh^{II}(tmp)

Entry	Base/	Equiv	Temp/ °C	Time	Rh ^{II} (tmp)/ yield%	Remarks
1	Nil		100	3 d	0	Rh(tmp)H unreacted
2	Nil		180	2 h	10	Rh(tmp)H (85%)
3	KOH	0.05	100	3 d	0	Rh(tmp)H unreacted
4	KOH	0.5	100	3 d	0	Rh(tmp)H unreacted
5	KOH	10	100	1 h	30	Rh(tmp)H (60%)
6	KOH	100	100	30 min	50	Rh ^{II} (tmp) decomposed in prolonged heating
8	KOAc	10	100	1 h	10	Rh(tmp)H (85%)
9	KO ^t Bu	10	24	5 min	20	Rh ^{II} (tmp) completely decomposed in 2 days to give insoluble product formed

Reaction of Rh(tmp)H (1f) and 10 equiv of KOH in THF-*d*₈. Rh(tmp)H **1f** (2.5 mg, 0.0028 mmol) and KOH (1.6 mg, 0.28 mmol) were added into THF-*d*₈ (500 μL) in a NMR tube under nitrogen. The red solution was degassed for three freeze-thaw-pump cycles and the NMR tube was flame-sealed under vacuum. The reaction mixture was heated at 100 °C for 1 day and was monitored with ¹H NMR spectroscopy. [Rh^I(tmp)]⁺ **1h** was observed as the deprotonation product. ¹H NMR (300 MHz, THF-*d*₈) δ 2.16 (s, 24 H), 2.66 (s, 12 H), 7.29 (s, 8 H), 8.01 (s, 8 H).

Reaction of Rh(tmp)I (1c) and Oxepane with 10 equiv of KOH. Rh(tmp)I **1c** (11.4 mg, 0.013 mmol) and KOH (7.3 mg, 0.13 mmol) were dissolved in oxepane (1.0 mL) and heated at 100 °C under N₂ for 3 days. Excess oxepane was removed, the dark red crude product was then purified by column chromatography on silica gel eluting with hexane/CH₂Cl₂ (1:1) to give the reddish purple solid of Rh(tmp)CH₂CH₂CH₂CH₂CH₂OCHO **5j** (1.6 mg, 0.0016 mmol, 14%).

Reactivity of CCA product

Reaction of Rh(tmp)Me (1d) and *n*-Butyl Ether with 10 equiv of KOH.

Rh(tmp)Me **1d** (11.1 mg, 0.012 mmol) and KOH (6.9 mg, 0.123 mmol) were dissolved in *n*-butyl ether (2.0 mL) and heated at 100 °C under nitrogen for 1 day.

Excess *n*-butyl ether was removed, the dark red crude product was then purified by column chromatography on silica gel eluting with hexane/CH₂Cl₂ (5:1) to give the reddish purple solid of the mixture (7.5 mg) of Rh(tmp)Me **1d** (~30% NMR yield) and Rh(tmp)Pr^{51b} **5a** (~30% NMR yield) in approximately 1:1 ratio.

Reaction of Rh(tmp)Et (5b) and *n*-Butyl Ether with 10 equiv of KOH. Rh(tmp)Et **5b** (10.0 mg, 0.011 mmol) and KOH (6.1 mg, 0.11 mmol) were dissolved in *n*-butyl ether (2.0 mL) and heated at 100 °C under nitrogen for 1 day. Excess *n*-butyl ether was removed, the dark red crude product was then purified by column chromatography on silica gel eluting with hexane/CH₂Cl₂ (5:1) to give the reddish purple solid of the mixture (8.1 mg) of Rh(tmp)Et **5b** (~40% NMR yield) and Rh(tmp)Pr **5a** (~40% NMR yield).

Reaction of Rh(tmp)Pr (5a) and *n*-Pentyl Ether. Rh(tmp)Pr **5a** (11.7 mg, 0.013 mmol) was dissolved in *n*-pentyl ether (2.0 mL) and heated at 100 °C under nitrogen for 1 day. Excess *n*-pentyl ether was removed, the dark red crude product was then purified by column chromatography on silica gel eluting with hexane/CH₂Cl₂ (5:1) to recover the reddish purple solid of Rh(tmp)Pr^{51b} **5a** (11.1 mg, 0.012 mmol, 95%).

Reaction of Rh(tmp)Pr (5a) and *n*-Pentyl Ether with 10 equiv of KOH.

Rh(tmp)Pr **5a** (10.9 mg, 0.012 mmol) and KOH (6.3 mg, 0.118 mmol) were dissolved in *n*-pentyl ether (2.0 mL) and heated at 100 °C under nitrogen for 1 day. Excess *n*-pentyl ether was removed. Besides, Rh(tmp)Pr and Rh(tmp)Bu were observed in the ¹H NMR analysis of the crude mixture under degass benzene-*d*₆, trace amount of Rh^{II}(tmp) was also observed. The dark red crude product was then purified by column chromatography on silica gel eluting with hexane/CH₂Cl₂ (5:1) to give the reddish purple solid of the mixture (9.3 mg) of Rh(tmp)Pr^{51b} **5a** (~48% NMR yield) and Rh(tmp)Bu^{51b} **5c** (~32% NMR yield).

Reference

- (1) (a) Smith, M. B.; March, J. *March's Advanced Organic Chemistry; Reactions, Mechanism, Structure*, 5th Ed.; Wiley-Interscience: New York, 2001. (b) Sykes, P. *A Guidebook To Mechanism In Organic Chemistry*, 6th Ed.; Prentice Hall, Pearson: U.K., 1986. (c) Fokin, A. A.; Schreiner, P. R. *Chem. Rev.* **2002**, *102*, 1551-1593.
- (2) Anslyn, E. V.; Dougherty, D. A. *Modern Physical Organic Chemistry*; University Science Books: Sausalito, California, 2006.
- (3) (a) Olah, G. A. *Acc. Chem. Res.* **1976**, *9*, 41-52. (b) Wagner, G. J. *Russ. Phys. Chem. Soc.* **1899**, *31*, 690.
- (4) Gajewski, J. J. *Hydrocarbon Thermal Isomerizations*; Academic Press: New York, 2003.
- (5) Berson, J. A. *Angew. Chem.; Int. Ed.* **2002**, *41*, 4655-4660.
- (6) Brouwer, L. E. J. *The Petroleum Handbook*, 5th Ed; Shell Co. of Hong Kong: London, 1966.
- (7) (a) Roberts, J. D.; Dirstine, P. H. *J. Am. Chem. Soc.* **1945**, *67*, 1281-1283. (b) Della, E. W.; Head, N. J.; Mallon, P.; Walton, J. C. *J. Am. Chem. Soc.* **1992**, *114*, 10730-10738. (c) Wiberg, K. B.; Waddell, S. T.; Laidig, K. *Tetrahedron Lett.* **1986**, *27*, 1553-1556.
- (8) Fabre, R.-L.; Devynck, J.; Tremillon, B. *Chem. Rev.* **1982**, *82*, 591-614.
- (9) (a) Olah, G. A.; Molnar, A. *Hydrocarbon Chemistry*, 2nd Ed.; Wiley Interscience: New York, 2003. (b) Olah, G. A.; Prakash, G. K. S.; Sommer, J. *Science* **1979**, *206*, 13-20. (c) Olah, G. A.; Klumpp, D. A. *Acc. Chem. Res.* **2004**, *37*, 211-220.
- (10) (a) Olah, G. A.; Lukas, J. *J. Am. Chem. Soc.* **1967**, *89*, 2227-2228. (b) Olah,

- G. A.; Lukas, J. *J. Am. Chem. Soc.* **1967**, *89*, 4739-4744. (c) Fokin, A. A.; Schreiner, P. R. *Chem. Rev.* **2002**, *102*, 1551-1593.
- (11) (a) Wiberg, K. B.; Kass, S. R. *J. Am. Chem. Soc.* **1985**, *107*, 988-995. (b) Wiberg, K. B.; Kass, S. R.; Bishop, K. C., III. *J. Am. Chem. Soc.* **1985**, *107*, 996-1002. (c) Wiberg, K. B.; Kass, S. R.; de Meijere, A.; Bishop, K. C., III. *J. Am. Chem. Soc.* **1985**, *107*, 1003-1007.
- (12) (a) Pearson, R. G. *J. Am. Chem. Soc.* **1963**, *85*, 3533-3539. (b) Parr, R. G.; Pearson, R. G. *J. Am. Chem. Soc.* **1983**, *105*, 7512-7516. (c) Kubas, G. J. *J. Am. Chem. Soc.* **1988**, *21*, 120-128. (d) Pearson, R. G. *Chem. Rev.* **1985**, 41-49.
- (13) (a) Crabtree, R. H. *Chem. Rev.* **1995**, *95*, 987-1007. (b) Crabtree, R. H. *Chem. Rev.* **1985**, *85*, 245-269. (c) Jones, W. D. *Nature* **1993**, *364*, 676-677. (d) Murai, S., Ed.; *In Tropics in Organometallic Chemistry*; Springer: Berlin 1999; Vol. 3. pp 97-129. (e) Jun, C.-H. *Chem. Soc. Rev.* **2004**, *33*, 610-618. (f) Murai, S., Ed. *Activation of Unreactive Bonds and Organic Synthesis*; Springer: Berlin, 1999.
- (14) (a) Sundermann, A.; Uzan, O.; Milstein, D.; Martin, J. M. L. *J. Am. Chem. Soc.* **2000**, *122*, 7095-7104. (b) Blomberg, M. R. A.; Siegbahn, P. E. M.; Nagahima, V.; Wennerberg, J. *J. Am. Chem. Soc.* **1991**, *113*, 424-433.
- (15) (a) Luo, Y. R. *Handbook of Bond Dissociation Energies in Organic Compounds*; CRC Press: Boca Raton, FL, 2003. (b) Sanderson, R. T. *Chemical Bonds and Bond Energy*; Academic Press: New York, 1976.
- (16) (a) Bauschlicher, C. W.; Langhoff, S. R.; Partridge, H.; Barnes, L. A. *J. Chem. Phys.* **1989**, *91*, 2399-2411. (b) Simones, J. A.; Beauchamp, J. L. *Chem. Rev.* **1990**, *90*, 629-688.
- (17) Siegbahn, P. E. M. *J. Phys. Chem.* **1995**, *99*, 12723-12729.

- (18) (a) Bercaw, J. E. *Pure and Appl. Chem.* **1990**, *62*, 1151-1154. (b) Bhan, A.; Gounder, R.; Macht, J. Iglesia, E. *J. Catal.* **2008**, *253*, 221-224.
- (19) (a) Cassar, L.; Eaton, P. E.; Halpern, J. *J. Am. Chem. Soc.* **1970**, *92*, 3515-3518. (b) Cassar, L.; Eaton, P. E.; Halpern, J. *J. Am. Chem. Soc.* **1970**, *92*, 6366-6368.
- (20) Tipper, C. H. F. *J. Chem. Soc.* **1955**, 2045-2046.
- (21) Eish, J. J.; Piotrowski, A. M.; Han, K. I.; Kruger, C.; Tsay, Y. H. *Organometallics* **1985**, *4*, 224-231.
- (22) Perthuisot, C.; Edelbach, B. L.; Zubris, D. L.; Jones, W. D. *Organometallics* **1997**, *16*, 2016-2023.
- (23) Lenarda, M.; Ros, R.; Graziani, M.; Belluco, U. *J. Organomet. Chem.* **1974**, *65*, 407-416.
- (24) Atkinson, E. R.; Levins, P. L.; Dickelman, T. E. *Chem. Ind.* **1964**, 934-935.
- (25) Lu, Z.; Jun, C. H.; de Gala, S. R.; Sigalas, M.; Eisenstein, O.; Crabtree, R. *H. J. Chem. Soc., Chem. Commun.* **1993**, 1877-1880.
- (26) Fokin, A. A.; Schreiner, P. R. *Chem. Rev.* **2002**, *102*, 1551-1593.
- (27) Eilbracht, P.; Dahler, P. *Chem. Ber.* **1980**, *113*, 542-554.
- (28) Benfield, F. W. S.; Green, M. L. H. *Dalton Trans.* **1974**, 1324-1131.
- (29) Takahashi, T.; Ishikawa, M.; Huo, S. *J. Am. Chem. Soc.* **2002**, *124*, 388-389.
- (30) (a) Suggs, J. W.; Jun, C. H. *J. Am. Chem. Soc.* **1984**, *106*, 3054-3056. (b) Suggs, J. W.; Jun, C. H. *J. Am. Chem. Soc.* **1986**, *108*, 4679-4681. (c) Suggs, J. W.; Wovkulich, M. J.; Cox, S. D. *Organometallics* **1985**, *4*, 1101-1107.
- (31) (a) Murakami, M.; Amii, H.; Ito, Y. *Nature* **1994**, *370*, 541-542. (b) Murakami, M.; Tsuruta T.; Ito, Y. *Angrew. Chem., Int. Ed.* **2000**, *39*, 2484-2486.
- (32) (a) Gozin, M.; Weisman, A.; Ben-David, Y.; Milstein, D. *Nature* **1993**, *364*,

- 699-670. (b) Rybtchinski, B.; Vigalok, A.; Ben-David, Y.; Milstein, D. *J. Am. Chem. Soc.* **1999**, *118*, 12406-12415. (c) van der Boom, M. E.; Liou, S. Y.; Ben-David, Y.; Gozin, M.; Milstein, D. *J. Am. Chem. Soc.* **1998**, *120*, 13415-13421. (d) Liou, S. Y.; van der Boom, M. E.; Milstein, D. *Chem. Commun.*, **1998**, *6*, 687-688. (e) Rybtchinski, B.; Milstein, D.; *J. Am. Chem. Soc.* **1999**, *121*, 4528-4529. (f) van der Boom, M. E.; Ben-David, Y.; Milstein, D. *J. Am. Chem. Soc.* **1999**, *121*, 6652-6656. (g) Rybtchinski, B.; Vigalok, A.; Ben-David, Y.; Milstein, D. *J. Am. Chem. Soc.* **1996**, *118*, 12406-2415. (h) Rybtchinski, B.; Oevers, S.; Montag, M.; Vigalok, A.; Rozenberg, H.; Martin, J. M. L.; Milstein, D. *J. Am. Chem. Soc.* **2001**, *123*, 9064-9077.
- (33) (a) García, J. J.; Arévalo, A.; Brunkan, N. M.; Jones, W. D. *Organometallics* **2004**, *23*, 3997-4002. (b) Brunkan, N. M.; Brestensky, D. M.; Jones, W. D. *J. Am. Chem. Soc.* **2004**, *126*, 3627-3641.
- (34) (a) Park, Y. J.; Park, J.-W.; Jun, C.-H. *Acc. Chem. Res.* **2008**, *41*, 222-234. (b) Jun, C.-H. *Chem. Soc. Rev.* **2004**, *33*, 610-618. (c) Jun, C.-H.; Moon, C. W.; Lee, D.-Y. *Chem. Eur. J.* **2002**, *8*, 2420-2428. For the reference of primary amine; (d) Jun, C.-H.; Chung, K.-Y.; Hong, J.-B. *Org. Lett.* **2001**, *3*, 785-787. (e) Lim, S.-G.; Lee, J. H.; Moon, C. W.; Hong, J.-B.; Jun, C.-H. *Org. Lett.* **2003**, *5*, 2759-2761. For the references of cycloalkanone imine; (f) Jun, C.-H.; Lee, H.; Lim, S.-G. *J. Am. Chem. Soc.* **2001**, *123*, 751-752. For the reference of unstrained secondary alcohols; (g) Jun, C.-H.; Lee, H.; Moon, C. W.; Hong, H.-S. *J. Am. Chem. Soc.* **2001**, *123*, 8600-8601. For the reference of alkyne; (h) Park, Y. J.; Kwon, B.-I.; Ahn, J.-A.; Lee, H.; Jun, C.-H. *J. Am. Chem. Soc.* **2004**, *126*, 13892-13893. For the references of catalytic CCA of unstrained ketone; (i) Jun, C.-H.; Lee, H. *J. Am. Chem.*

- Soc.* **1999**, *121*, 880-881. (j) Chang, D.-H.; Lee, D.-Y.; Hong, B.-S.; Choi, J.-H.; Jun, C.-H. *J. Am. Chem. Soc.* **2004**, *126*, 424-425.
- (35) Watson, P. L.; Roe, D. C. *J. Am. Chem. Soc.* **1982**, *104*, 6471-6473.
- (36) (a) Bunel, E.; Burger, B. J.; Bercaw, J. E. *J. Am. Chem. Soc.* **1988**, *110*, 976-978. (b) Hajela, S.; Bercaw, J. E. *Organometallics* **1994**, *13*, 1147-1154.
- (37) Nishimura, T.; Ohe, K.; Uemura, S. *J. Am. Chem. Soc.* **1999**, *121*, 2645-2646.
- (38) Murakami, M.; Makino, M.; Ashida, S.; Matsuda, T. *Bull. Chem. Soc. Jpn.* **2006**, *79*, 1315-1321.
- (39) (a) Vidal, V.; Theolier, A.; Thivolle-Cazat, J.; Basset, J.-M. *Science* **1997**, *276*, 99-102. (b) Basset, J.-M.; Copéret, C.; Lefort, L.; Maunders, B. M.; Maury, O.; Roux, E. Le. ; Saggio, G. ; Soignier, S. ; Soulivong, D. ; Sunley, G. J.; Taoufik, M.; Thivolle-Cazat, J. *J. Am. Chem. Soc.* **2005**, *127*, 8604-8605. (c) Roux, E. Le.; Taoufik, M.; Copéret, C.; de Mallmann, A.; Thivolle-Cazat, J.; Basset, J.-M.; Maunders, B. M.; Sunley, G. J. *Angew. Chem., Int. Ed.* **2005**, *44*, 6755-6758.
- (40) Goldman, A. S.; Roy, A. H.; Huang, Z.; Ahuja, R.; Schinski, W.; Brookhart, M. *Science* **2006**, *312*, 257-261.
- (41) (a) Eisch, J. J.; Dutta, S.; Gitua, J. N. *Organometallics* **2005**, *24*, 6291-6294. (b) Eisch, J. J.; Gitua, J. N. *Organometallics* **2007**, *26*, 778-779.
- (42) (a) Taw, F. L.; White, P. S.; Bergman, R. G.; Brookhart, M. *J. Am. Chem. Soc.* **2002**, *124*, 4192-4193. (b) Taw, F. L.; Mueller, A. H.; Bergman, R. G.; Brookhart, M. *J. Am. Chem. Soc.* **2003**, *125*, 9808-9813.
- (43) Anstey, M. R.; Yung, C. M.; Bu, J.; Bergman, R. G. *J. Am. Chem. Soc.* **2007**, *129*, 776-777.

- (44) (a) Kumar, V. S.; Floreancig, P. E. *J. Am. Chem. Soc.* **2001**, *123*, 3842-3843.
(b) Baciocchi, E.; Bietti, M.; Putignani, L.; Steenken, S. *J. Am. Chem. Soc.* **1996**, *118*, 5952-5956. (c) Selders, J. R. II; Wang, L.; Floreancig, P. E. *J. Am. Chem. Soc.* **2003**, *125*, 2406-2407.
- (45) Moreira, R. F.; Tshuva, E. Y.; Lipard, S. J. *Inorg. Chem.* **2004**, *43*, 4427-4434.
- (46) Yeung, S. K. *Ph.D Thesis*, The Chinese University of Hong Kong, **2005**.
- (47) Suginome, H.; Wang, J. B. *J. Chem. Soc. Perkin Trans. I*, **1990**, 2825-2529.
- (48) Black, D. S. C.; Doyle, J. E. *Aust. J. Chem.* **1978**, *31*, 2323-2326.
- (49) Suresh, J. R.; Barun, O.; Ila, H.; Junjappa, H. *Tetrahedron* **2000**, *56*, 8153-8160.
- (50) Berkoff, C. E.; Rivard, D. E.; Kirkpatrick, D.; Ives, J. L. *Synth. Commun.* **1980**, *10*, 939
- (51) (a) Chan, K. S.; Li, X. Z.; Fung, C. W.; Zhang, L. *Organometallics* **2007**, *26*, 20-21. (b) Chan, K. S.; Li, X. Z.; Zhang, L.; Fung, C. W. *Organometallics* **2007**, *26*, 2679-2687.
- (52) Smith, P. A. S.; Horwitz, J. P. *J. Am. Chem. Soc.* **1950**, *72*, 3718-3722.
- (53) Fuson, R. C.; Bull, B. A. *Chem. Rev.* **1934**, *15*, 275-309.
- (54) Krapcho, A. P.; Glynn, G. A.; Gernon, B. J. *Tetrahedron Lett.* **1967**, *3*, 215-217.
- (55) (a) Zhang, L.; Chan, K. S. *J. Organomet. Chem.* **2006**, *691*, 3782-3787. (b) Zhang, L.; Chan, K. S. *J. Organomet. Chem.* **2007**, *692*, 2021-2027.
- (56) Datta, S. K.; Grundmann, C.; Bhattacharyya, N. K. *J. Chem. Soc. C*, **1970**, 2058-2059.
- (57) Meyers, A. I.; Fleming, M. P. *J. Org. Chem.* **1979**, *44*, 3404-3405.
- (58) Pearson, W. H.; Fang, W. *J. Org. Chem.* **1995**, *60*, 4960-4961.

- (59) Bunton, C. A.; Hadwick, T.; Llewellyn, D. R.; Pocker, Y. *J. Chem. Soc.* **1958**, 403-408.
- (60) Huang, X.; Keillor, J. W. *Tetrahedron Lett.* **1997**, *38*, 313-316.
- (61) Kondo, T.; Kodoi, K.; Nishinaga, E.; Okada, T.; Morisaki, Y.; Watanabe, Y.; Mitsudo, T. *J. Am. Chem. Soc.* **1998**, *120*, 5587-5588.
- (62) (a) Tse, M. K.; Chan, K. S. *Dalton Trans.* **2001**, 510-511. (b) Chan, K. S.; Li, X. Z.; Dzik, W. I.; De Bruin, B. *J. Am. Chem. Soc.* **2008**, *130*, 2051-2061.
- (63) Fleischer, E. B. *Acc. Chem. Res.* **1970**, *3*, 105-112.
- (64) Kadish, K. M., Smith, K. M., Guillard, R., Eds.; *The Porphyrin Handbook Volume 3*; Academic Press: Boston, 2000.
- (65) Smith, K. M., Ed. *Porphyrins and Metalloporphyrins*; Elsevier Scientific Pub. Co.: New York, 1975.
- (66) Ogoshi, H.; Mizutani, A. *Acc. Chem. Res.* **1998**, *31*, 81-89.
- (67) Shanmugathan, S.; Edwards, C.; Boyle, R. W. *Tetrahedron* **2000**, *56*, 1025-1046.
- (68) Dolphin, D. Ed.; *B₁₂*; Wiley-Interscience: New York, 1982.
- (69) Banerjee, R. Ed.; *Chemistry and Biochemistry of B₁₂*; John Wiley: New York, 1999.
- (70) Hodgkin, D. C.; Kamper, J.; Mackay, M.; Pickworth, J. *Nature* **1956**, *178*, 64-66.
- (71) (a) Schrauzer, G. N. *Angew. Chem., Int. Ed. Engl.* **1976**, *15*, 414-426. (b) Schrauzer, G. N. *Acc. Chem. Res.* **1968**, *1*, 97-103.
- (72) (a) Groves, J. T.; Nemo, T. E. *J. Am. Chem. Soc.* **1983**, *105*, 5786-5791. (b) Groves, J. T.; Quinn, R. *J. Am. Chem. Soc.* **1985**, *107*, 5790-5792.
- (73) Collman, J. P.; Zhang, X.; Lee, V. J.; Uffelman, E. S.; Brauman, J. I. *Science* **1993**, *261*, 1404-1411.

- (74) Liang, J. L.; Huang, J.-S.; Yu, Z.-Q.; Zhu, N.; Che, C. M. *Chem. Eur. J.* **2002**, *8*, 1563-1572.
- (75) Zhang, R.; Yu, W. Y.; Wong, K. Y.; Che, C. M. *J. Org. Chem.* **2001**, *66*, 8145-8153.
- (76) Traylor, T. G.; Hill, K. W.; Fann, W.-P.; Tsuchiya, S.; Bunlap, B. E. *J. Am. Chem. Soc.* **1992**, *114*, 1308-1312.
- (77) Liang, J. L.; Yuan, S. X.; Huang, J. S.; Yu, W. Y.; Che, C. M. *Angew. Chem., Int. Ed.* **2002**, *41*, 3468-3468.
- (78) Yu, Z.-Q.; Huang, J.-S.; Zhou, Z.-G.; Che, C. M. *Org. Lett.* **2000**, *15*, 2233-2236.
- (79) Del Rossi, K. J.; Wayland, B. B. *J. Am. Chem. Soc.* **1985**, *107*, 7941-7944.
- (80) Collman, J. P.; Boulatov, R. *Inorg. Chem.* **2001**, *40*, 560-563.
- (81) (a) Wayland, B. B.; Sherry, A. E.; Poszmik, G.; Bunn, A. G. *J. Am. Chem. Soc.* **1992**, *114*, 1673-1681.
- (82) Mak, K. W.; Chan, K. S. *J. Am. Chem. Soc.* **1998**, *120*, 9686-9687.
- (83) (a) Callot, H. J.; Piechocki, C. *Tetrahedron Lett.* **1980**, *21*, 3489-3492. (b) Bartley, D. W.; Kodadek, T. *J. Am. Chem. Soc.* **1993**, *115*, 1656-1660.
- (84) Aoyama, Y.; Tanaka, Y.; Yoshida, T.; Toi, H.; Ogoshi, H. *J. Organomet. Chem.* **1987**, *329*, 251-266.
- (85) Tagliatesta, P.; Floris, B.; Galloni, P.; Leoni, A.; D'Arcangelo, G. *Inorg. Chem.* **2003**, *42*, 7701-7703.
- (86) (a) Li, G.; Zhang, F. F.; Pi, N.; Chen, H. L.; Zhang, S. Y.; Chan, K. S. *Chem. Lett.* **2001**, 284-285. (b) Wayland, B. B.; Feng, Y.; Ba, S. *Organometallics* **1989**, *8*, 1438-1441. (c) Wayland, B. B.; Ba, S.; Sherry, A. E. *J. Am. Chem. Soc.* **1991**, *113*, 5305-5311. (d) Bakac, A. *Dalton Trans.* **2006**, 1589-1596. (e) Wayland, B. B.; Coffin, V. L.; Farnos, M. D. *Inorg. Chem.* **1988**, *27*,

2745-2747.

- (87) Aoyama, Y.; Yoshida, T.; Sakurai, K.; Ogoshi, H. *Organometallics* **1986**, *5*, 168-173.
- (88) Zhang, L.; Chan, K. S. *Organometallics* **2006**, *25*, 4822-4829.
- (89) Chan, K. S.; Lau, C. M. *Organometallics* **2006**, *25*, 260-265.
- (90) (a) Chan, K. S.; Chiu, P. F.; Choi, K. S. *Organometallics* **2007**, *26*, 1117-1119. (b) Chan, Y. W.; Chan, K. S. *Organometallics* **2008**, *27*, 4625-4635.
- (91) (a) Wayland, B. B.; Van Voorhees, S. L.; Wilker, C. *Inorg. Chem.* **1986**, *25*, 4039-4042. (b) Del Rossi, K. J.; Wayland, B. B. *J. Am. Chem. Soc.* **1985**, *107*, 7941-7944. (c) Ogoshi, H.; Setsume, J.; Yoshida, Z. *J. Am. Chem. Soc.* **1977**, *99*, 3869-3870. (d) Wayland, B. B.; Coffin, V. L.; Farnos, M. D. *Inorg. Chem.* **1988**, *27*, 2745-2747. (e) Wayland, B. B. *Polyhedron* **1988**, *7*, 1545-1555.
- (92) Wayland, B. B.; Sherry, A. E.; Bunn, A. G. *J. Am. Chem. Soc.* **1993**, *115*, 7675-7684.
- (93) (a) Zhang, X.-X.; Wayland, B. B. *J. Am. Chem. Soc.* **1994**, *116*, 7879-7898. (b) Bunn, A. G.; Wei, M.; Wayland, B. B. *Organometallics* **1994**, *13*, 3390-3392.
- (94) Wayland, B. B.; Newman, A. R. *J. Am. Chem. Soc.* **1979**, *101*, 6472-6473. (b) Wayland, B. B.; Newman, A. R. *Inorg. Chem.* **1981**, *20*, 3093-3097. (c) Cui, W.; Wayland, B. B. *J. Am. Chem. Soc.* **2006**, *128*, 10350-10351.
- (95) (a) Farnos, M. D.; Woods, B. A.; Wayland, B. B. *J. Am. Chem. Soc.* **1986**, *108*, 3659-3663. (b) Wayland, B. B.; Woods, B. A.; Pierce, R. J. *J. Am. Chem. Soc.* **1982**, *104*, 302-303. (c) Zhang, X. X.; Parks, G. F.; Wayland, B. B. *J. Am. Chem. Soc.* **1997**, *119*, 7938-7944.

- (96) (a) Sherry, A. E.; Wayland, B. B. *J. Am. Chem. Soc.* **1990**, *112*, 1259-1261.
- (97) (a) Del Rossi, K. J.; Zhang, X. X.; Wayland, B. B. *J. Organomet. Chem.* **1995**, *504*, 47-56. (b) Del Rossi, K. J.; Zhang, X.-X.; Wayland, B. B. *J. Organomet. Chem.* **1995**, *504*, 47-56. (c) Del, Rossi, K. J.; Wayland, B. B. *J. Chem. Soc., Chem. Commun.* **1986**, 1653-1655.
- (98) Wayland, B. B.; Ba, S.; Sherry, A. E. *J. Am. Chem. Soc.* **1991**, *113*, 5305-5311.
- (99) Fulton, J. R.; Holland, A. W.; Fox, D. J.; Bergman, R. G. *Acc. Chem. Res.* **2002**, *35*, 44-56.
- (100) (a) Newman, L. J.; Bergman, R. G. *J. Am. Chem. Soc.* **1985**, *107*, 5314-5315. (b) Simpson, R. D.; Bergman, R. G. *Organometallics* **1992**, *11*, 3980-3993. (c) Kaplan, A. W.; Bergman, R. G. *Organometallics* **1998**, *17*, 5072-5085.
- (101) Caulton, K. G. *New J. Chem.* **1994**, *18*, 25-41.
- (102) Woerpel, K. A.; Bergman, R. G. *J. Am. Chem. Soc.* **1993**, *115*, 7888-7889.
- (103) Tenn, W. J., III; Young, K. J. H.; Oxgaard, J.; Nielsen, R. J.; Goddard, W. A., III; Periana, R. A. *Organometallics* **2006**, *25*, 5173-5175.
- (104) Kloek, S. M.; Heinekey, D. M.; Goldberg, K. I. *Angew. Chem., Int. Ed.* **2007**, *46*, 4736-473.
- (105) Cheng, R.-J.; Latos-Grazynski, L.; Balch, A. L. *Inorg. Chem.* **1982**, *21*, 2412-2418.
- (106) Shin, K.; Kraner, S. K.; Goff, H. M. *Inorg. Chem.* **1987**, *26*, 4103-4106.
- (107) Groves, J. T.; Stern, M. K. *J. Am. Chem. Soc.* **1988**, *110*, 8628-8638.
- (108) Arasasingham, R. D.; Bruice, T. C. *Inorg. Chem.* **1990**, *29*, 1422-1427.
- (109) Del Rossi, K. J.; Wayland, B. B. *J. Am. Chem. Soc.* **1985**, *107*, 7941-7944.
- (110) (a) Fu, X.; Wayland, B. B. *J. Am. Chem. Soc.* **2004**, *126*, 2623-2631. (b) Fu, X.; Li, S.; Wayland, B. B. *J. Am. Chem. Soc.* **2006**, *128*, 8979-8954. (c) Fu,

- X.; Basicckes, L.; Wayland, B. B. *Chem. Commun.* **2003**, 520-521.
- (111) Tsang, P. K. S.; Cofre, P.; Sawyer, D. T. *Inorg. Chem.* **1987**, *26*, 3604-3609.
- (112) (a) Kadish, K. M.; Hu, Y.; Boschi, T.; Tagliatesta, R. *Inorg. Chem.* **1993**, *32*, 2996-3002. (b) Kadish, K. M.; Yao, C. L.; Anderson, J. E.; Cocolios, P. *Inorg. Chem.* **1985**, *24*, 4515-20. (c) Kadish, K. M.; Araullo, C.; Yao, C. L. *Organometallics* **1988**, *7*, 1583-1587.
- (113) (a) Wagner, R. W.; Lawrence, D. S.; Lindsey, J. S. *Tetrahedron Lett.* **1987**, *28*, 3069-3070. (b) Chan, K. S.; Chen, X. M.; Mak, T. C. W. *Polyhedron* **1992**, *11*, 2703-2716.
- (114) (a) Zhou, X.; Li, Q.; Mak, T. C. W.; Chan, K. S. *Inorg. Chim. Acta.* **1998**, *270*, 551-554. (b) Zhou, X.; Wang, R.-J.; Xue, F.; Mak, T. C. W.; Chan, K. S. *J. Organomet. Chem.* **1999**, *580*, 22-25.
- (115) (a) Wallace, T. J.; Gritter, R. J. *J. Org. Chem.* **1961**, *26*, 5256. (b) Walling, C.; Mintz, M. J. *J. Am. Chem. Soc.* **1967**, *89*, 1515-1519. (c) Steenken, S.; Schuchmann, H, P.; von Sonntag, C. *J. Phys. Chem.* **1975**, *79*, 763-764. (d) Griller, P.; Ingold, K. M. *Acc. Res. Res.* **1980**, *13*, 317-323.
- (116) Dudev, T.; Lim, C. *J. Am. Chem. Soc.* **1998**, *120*, 4450-4458.
- (117) Li, S.; Cui, W.; Wayland, B. B. *Chem. Commun.*, **2007**, 4024-4025.
- (118) Li, S.; Wayland, B. B. *Inorg. Chem.* **2006**, *45*, 9884-9889.
- (119) Lide, D. R., Ed. *CRC Handbook of Chemistry and Physics*, 84th ed.; CRC Press: Boca Raton, FL, 2003.
- (120) Lide, D. R. *Handbook of Organic Solvents*; CRC Press: Boca Raton, FL, 1995.
- (121) Li, X. Z. *Ph.D Thesis*, The Chinese University of Hong Kong, **2006**.
- (122) Choi, K. S. Unpublished result, 2009.
- (123) (a) Chock, P. B.; Dewar, R. B. K.; Halpern, J.; Wong, L.-Y. *J. Am. Chem.*

- Soc.* **1969**, *91*, 82-84. (b) Halpern, J.; Goodall, B. L.; Khare, G. P.; Lim, H. S.; Pluth, J. J. *J. Am. Chem. Soc.* **1975**, *97*, 2301-2303.
- (124) (a) Harned, H. S. *J. Am. Chem. Soc.* **1918**, *40*, 1461-1481. (b) Zhang, J.; Li, S.; Fu, X.; Wayland, B. B. *Dalton Trans.* **2009**, *19*, 3661-3663. (c) Walling, C. *Acc. Chem. Res.* **1975**, *8*, 125-131. (d) Kumar, A.; McCluskey, R. J. *Ind. Eng. Chem. Res.* **1987**, *26*, 1323-1329.
- (125) Kunai, A.; Hata, S.; Ito, S.; Sasaki, K. *J. Am. Chem. Soc.* **1986**, *108*, 6012-6016.
- (126) Cheung, C. W.; Chan, K. S. *Organometallics* **2008**, *27*, 3043-3055.
- (127) Nelson, A. P.; Dimango, S. G. *J. Am. Chem. Soc.* **2000**, *122*, 8569-8570.
- (128) (a) Grass, V.; Lexa, D.; Saveant, J.-M. *J. Am. Chem. Soc.* **1997**, *119*, 7526-7532. (b) Grass, V.; Lexa, D.; Momenteau, M.; Saveant, J.-M. *J. Am. Soc.* **1997**, *119*, 3536-3542.
- (129) Tsuji, T.; Shinya, Y.; Hiaki, T.; Itoh, N. *Fluid Phase Equilibria.* **2005**, *228*, 499-503.
- (130) Wayland, B. B. Private Communication, 2008.
- (131) Landis, C. R.; Halpern, J. *J. Am. Chem. Soc.* **1987**, *109*, 1746-1754.
- (132) Sanford, M. S.; Groves, J. T. *Angew. Chem., Int. Ed.* **2004**, *43*, 588-590.
- (133) Fung, H. S.; Chan, Y. W.; Cheung, C. W.; Choi, K. S.; Lee, S. Y.; Qian, Y. Y.; Chan, K. S. *Organometallics* **2009**, *28*, 3981-3989.
- (134) Eaton, S. S.; Eaton, G. R. *J. Am. Chem. Soc.* **1975**, *97*, 3660-3666.
- (135) Mak, K. W.; Xue, F.; Mak, T. C. W.; Chan, K. S. *Dalton Trans.* **1999**, 3333-3334.
- (136) Chan, K. S.; Mak, K. W.; Tse, M. K.; Yeung, S. K.; Li, B. Z.; Chan, Y. W. *J. Organomet. Chem.* **2008**, *693*, 399-407.

Table of Content of Appendix

No	Appendix I – X-ray crystallography data	Page
1	X-ray data of Rh(tmp) ^t Bu (5d), Rh(ttp) ^t Bu (3k) and Rh(t ₄ -CF ₃ pp)Bu (2d)	174-187
	Appendix II --- List of NMR spectra	
1	¹ H NMR Spectrum of Rh(t ₄ -CF ₃ pp)Cl (2b)	188
2	¹ H NMR Spectrum of Rh(t ₄ -CF ₃ pp)I (2c)	188
3	¹ H NMR Spectrum of Rh(t ₄ -CF ₃ pp)CH ₂ CH ₂ CH ₂ CH ₃ (2d)	189
4	¹³ C NMR Spectrum of Rh(t ₄ -CF ₃ pp)CH ₂ CH ₂ CH ₂ CH ₃ (2d)	189
5	¹ H NMR Spectrum of Rh(ttp) ^t Bu (3k)	190
6	¹³ C NMR Spectrum of Rh(ttp) ^t Bu (3k)	190
7	¹ H NMR Spectrum of Rh(tdbpp)I (4b)	191
8	¹³ C NMR Spectrum of Rh(tdbpp)I (4b)	191
9	¹ H NMR Spectrum of Rh(tdbpp)CH ₃ (4c)	192
10	¹ H NMR Spectrum of Rh(tdbpp)CH ₂ CH ₂ CH ₃ (4e)	192
11	¹³ C NMR Spectrum of Rh(tdbpp)CH ₂ CH ₂ CH ₃ (4e)	193
12	¹ H NMR Spectrum of Rh(tmp) ^t Bu (5d)	193
13	¹³ C NMR Spectrum of Rh(tmp) ^t Bu (5d)	194
14	¹ H NMR Spectrum of Rh(tmp)Pent (5e)	194
15	¹ H NMR Spectrum of Rh(tmp)CH ₂ OEt (5f)	195
16	¹³ C NMR Spectrum of Rh(tmp)CH ₂ OEt (5f)	195
17	¹ H NMR Spectrum of Rh(tmp)(CH ₂) ₅ OCHO (5j)	196
18	¹³ C NMR Spectrum of Rh(tmp)(CH ₂) ₅ OCHO (5j)	196
19	Appendix III --- List of Publications	197

X-Ray Structure of Rh(tmp)^tBu (5d)

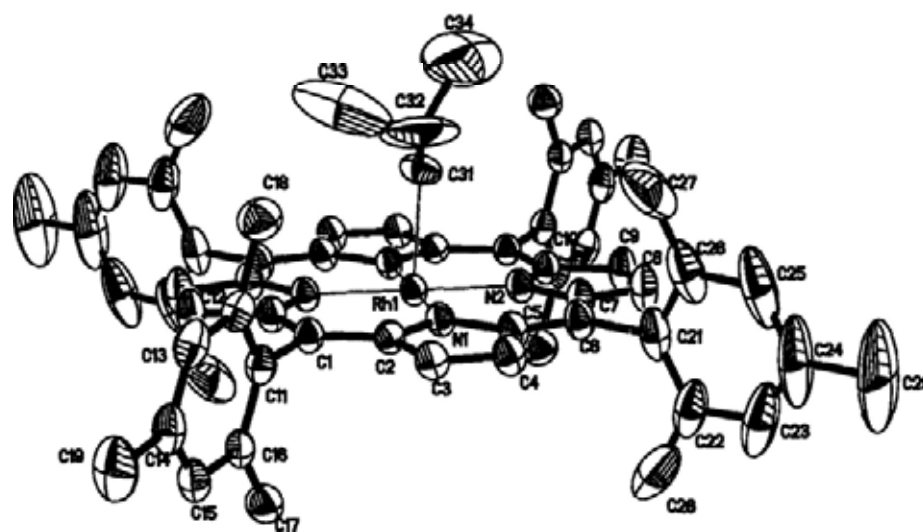


Figure 1 ORTEP drawing of Rh(tmp)^tBu **5d**, showing the atomic labeling scheme and 30% probability displacement ellipsoids.

Table 1. Crystal data and structure refinement for Rh(tmp)^tBu (**5d**)

Identification code	THL394
Empirical formula	C ₆₀ H ₆₁ N ₄ Rh
Formula weight	941.04
Temperature	293(2) K
Wavelength	0.71073 Å
Crystal system, space group	Tetragonal, I ₄ (1)/a
Unit cell dimensions	a = 27.870(3) Å alpha = 90° b = 27.870(3) Å beta = 90° c = 14.412(3) Å gamma = 90°
Volume	11195(3) Å ³
Z, Calculated density	8, 1.117 Mg/m ³

Absorption coefficient	0.343 mm ⁻¹
F(000)	3952
Crystal size	0.50 x 0.40 x 0.30 mm
Theta range for data collection	1.46 to 28.04 deg.
Limiting indices	-36<=h<=36, -30<=k<=36, -15<=l<=19
Reflections collected / unique	37210 / 6774 [R(int) = 0.0771]
Completeness to theta = 28.04	99.70%
Absorption correction	SADABS
Max. and min. transmission	1.000 and 0.530556
Refinement method	Full-matrix least-squares on F ²
Data / restraints / parameters	6774 / 3 / 313
Goodness-of-fit on F ²	1.067
Final R indices [I>2sigma(I)]	R1 = 0.0522, wR2 = 0.1312
R indices (all data)	R1 = 0.1194, wR2 = 0.1807
Largest diff. peak and hole	0.935 and -0.645 e.A ⁻³

Table 2 Bond lengths [Å] and angles [deg] for Rh(tmp)^tBu **5d**

Rh(1)-N(1)#1	2.010(3)	C(11)-C(12)	1.392(6)
Rh(1)-N(1)	2.010(3)	C(11)-C(16)	1.397(6)
Rh(1)-N(2)	2.022(3)	C(12)-C(13)	1.404(6)
Rh(1)-N(2)#1	2.022(3)	C(12)-C(18)	1.495(7)
Rh(1)-C(31)	2.158(9)	C(13)-C(14)	1.365(7)
Rh(1)-C(31)#1	2.158(9)	C(14)-C(15)	1.373(7)
N(1)-C(2)	1.370(5)	C(14)-C(19)	1.519(7)
N(1)-C(5)	1.383(5)	C(15)-C(16)	1.401(6)
N(2)-C(10)	1.376(5)	C(16)-C(17)	1.507(6)
N(2)-C(7)	1.382(5)	C(21)-C(26)	1.391(10)
C(1)-C(10)#1	1.387(5)	C(21)-C(22)	1.392(10)
C(1)-C(2)	1.399(5)	C(22)-C(23)	1.401(10)

C(1)-C(11)	1.500(5)	C(22)-C(28)	1.487(11)
C(2)-C(3)	1.431(5)	C(23)-C(24)	1.355(18)
C(3)-C(4)	1.345(6)	C(24)-C(25)	1.347(18)
C(4)-C(5)	1.436(6)	C(24)-C(29)	1.545(10)
C(5)-C(6)	1.384(6)	C(25)-C(26)	1.412(10)
C(6)-C(7)	1.384(6)	C(26)-C(27)	1.499(12)
C(6)-C(21)	1.515(6)	C(31)-C(32)	1.515(10)
C(7)-C(8)	1.429(6)	C(32)-C(34)	1.517(10)
C(8)-C(9)	1.345(6)	C(32)-C(33)	1.518(10)
C(9)-C(10)	1.436(6)		
C(10)-C(1)#1	1.387(5)		
N(1)#1-Rh(1)-N(1)	180.00(18)	C(9)-C(8)-C(7)	108.0(4)
N(1)#1-Rh(1)-N(2)	90.05(13)	C(8)-C(9)-C(10)	107.0(4)
N(1)-Rh(1)-N(2)	89.95(13)	N(2)-C(10)-C(1)#1	125.8(4)
N(1)#1-Rh(1)-N(2)#1	89.95(13)	N(2)-C(10)-C(9)	109.5(4)
N(1)-Rh(1)-N(2)#1	90.05(13)	C(1)#1-C(10)-C(9)	124.7(4)
N(2)-Rh(1)-N(2)#1	180.00(16)	C(12)-C(11)-C(16)	120.4(4)
N(1)#1-Rh(1)-C(31)	85.9(3)	C(12)-C(11)-C(1)	120.9(4)
N(1)-Rh(1)-C(31)	94.1(3)	C(16)-C(11)-C(1)	118.7(4)
N(2)-Rh(1)-C(31)	86.8(3)	C(11)-C(12)-C(13)	118.2(4)
N(2)#1-Rh(1)-C(31)	93.2(3)	C(11)-C(12)-C(18)	121.3(4)
N(1)#1-Rh(1)-C(31)#1	94.1(3)	C(13)-C(12)-C(18)	120.4(4)
N(1)-Rh(1)-C(31)#1	85.9(3)	C(14)-C(13)-C(12)	122.3(5)
N(2)-Rh(1)-C(31)#1	93.2(3)	C(13)-C(14)-C(15)	118.8(4)
N(2)#1-Rh(1)-C(31)#1	86.8(3)	C(13)-C(14)-C(19)	121.7(5)
C(31)-Rh(1)-C(31)#1	180.0(4)	C(15)-C(14)-C(19)	119.5(5)
C(2)-N(1)-C(5)	106.3(3)	C(14)-C(15)-C(16)	121.5(5)
C(2)-N(1)-Rh(1)	126.8(2)	C(11)-C(16)-C(15)	118.8(4)
C(5)-N(1)-Rh(1)	126.9(3)	C(11)-C(16)-C(17)	121.4(4)
C(10)-N(2)-C(7)	106.4(3)	C(15)-C(16)-C(17)	119.8(4)
C(10)-N(2)-Rh(1)	126.8(3)	C(26)-C(21)-C(22)	121.1(6)
C(7)-N(2)-Rh(1)	126.8(3)	C(26)-C(21)-C(6)	118.0(6)
C(10)#1-C(1)-C(2)	124.3(4)	C(22)-C(21)-C(6)	120.7(6)
C(10)#1-C(1)-C(11)	118.9(3)	C(21)-C(22)-C(23)	116.8(9)
C(2)-C(1)-C(11)	116.6(3)	C(21)-C(22)-C(28)	121.0(6)
N(1)-C(2)-C(1)	126.1(3)	C(23)-C(22)-C(28)	122.2(9)
N(1)-C(2)-C(3)	109.9(3)	C(24)-C(23)-C(22)	124.0(11)
C(1)-C(2)-C(3)	124.0(4)	C(25)-C(24)-C(23)	117.7(7)

C(4)-C(3)-C(2)	107.3(4)	C(25)-C(24)-C(29)	120.2(14)
C(3)-C(4)-C(5)	107.6(4)	C(23)-C(24)-C(29)	122.0(14)
N(1)-C(5)-C(6)	125.8(4)	C(24)-C(25)-C(26)	122.8(11)
N(1)-C(5)-C(4)	109.0(3)	C(21)-C(26)-C(25)	117.5(10)
C(6)-C(5)-C(4)	125.2(4)	C(21)-C(26)-C(27)	121.8(6)
C(5)-C(6)-C(7)	125.0(4)	C(25)-C(26)-C(27)	120.7(9)
C(5)-C(6)-C(21)	116.4(4)	C(32)-C(31)-Rh(1)	121.9(8)
C(7)-C(6)-C(21)	118.6(4)	C(31)-C(32)-C(34)	97.1(14)
N(2)-C(7)-C(6)	125.6(4)	C(31)-C(32)-C(33)	81.0(16)
N(2)-C(7)-C(8)	109.1(4)	C(34)-C(32)-C(33)	97.5(17)
C(6)-C(7)-C(8)	125.4(4)		

Symmetry transformations used to generate equivalent atoms: #1 -x+1,-y+1,-z

X-Ray Structure of Rh(*ttp*)^tBu (**3k**)

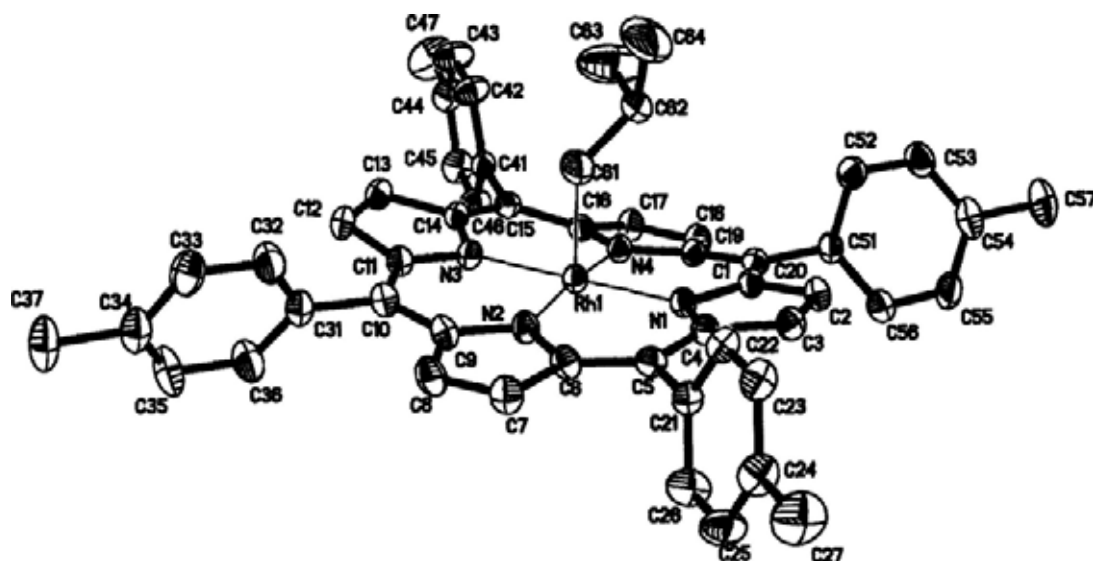


Figure 1 ORTEP drawing of Rh(*ttp*)^tBu **3k**, showing the atomic labeling scheme and 30% probability displacement ellipsoids.

Table 3 Crystal data and structure refinement for Rh(*ttp*)^tBu **3k**

Identification code	THL471
Empirical formula	C ₅₂ H ₄₉ N ₄ O ₂ Rh
Formula weight	864.86
Temperature	293(2) K
Wavelength	0.71073 Å
Crystal system, space group	Monoclinic, P2(1)/n
Unit cell dimensions	a = 15.6573(19) Å alpha = 90° b = 18.565(2) Å beta = 107.531°(3) c = 16.1046(19) Å gamma = 90°
Volume	4463.8(9) Å ³

Z, Calculated density	4, 1.287 Mg/m ³
Absorption coefficient	0.427 mm ⁻¹
F(000)	1800
Crystal size	0.40 x 0.30 x 0.20 mm
Theta range for data collection	1.59 to 25.00 deg.
Limiting indices	-18<=h<=13, -21<=k<=22, -19<=l<=19
Reflections collected / unique	23925 / 7850 [R(int) = 0.0440]
Completeness to theta = 25.00	99.80%
Absorption correction	SADABS
Max. and min. transmission	1.000 and 0.800330
Refinement method	Full-matrix least-squares on F ²
Data / restraints / parameters	7850 / 0 / 532
Goodness-of-fit on F	1.15
Final R indices [I>2sigma(I)]	R1 = 0.0677, wR2 = 0.2149
R indices (all data)	R1 = 0.0934, wR2 = 0.2427
Largest diff. peak and hole	2.066 and -0.438 e.A ⁻³

Table 4 Bond lengths [Å] and angles [deg] for Rh(ttp)^tBu **3k**

Rh(1)-N(4)	2.012(5)	C(19)-C(20)	1.404(9)
Rh(1)-N(2)	2.019(6)	C(20)-C(51)	1.498(9)
Rh(1)-N(1)	2.020(5)	C(21)-C(26)	1.374(11)
Rh(1)-N(3)	2.027(5)	C(21)-C(22)	1.395(10)
Rh(1)-C(61)	2.061(8)	C(22)-C(23)	1.379(10)
N(1)-C(4)	1.366(8)	C(23)-C(24)	1.399(11)
N(1)-C(1)	1.393(8)	C(24)-C(25)	1.387(12)
N(2)-C(9)	1.375(9)	C(24)-C(27)	1.512(11)
N(2)-C(6)	1.380(9)	C(25)-C(26)	1.403(12)
N(3)-C(14)	1.368(8)	C(31)-C(32)	1.368(11)

N(3)-C(11)	1.371(8)	C(31)-C(36)	1.383(11)
N(4)-C(16)	1.372(8)	C(32)-C(33)	1.378(11)
N(4)-C(19)	1.378(8)	C(33)-C(34)	1.387(13)
C(1)-C(20)	1.398(9)	C(34)-C(35)	1.346(13)
C(1)-C(2)	1.447(9)	C(34)-C(37)	1.527(11)
C(2)-C(3)	1.333(10)	C(35)-C(36)	1.395(11)
C(3)-C(4)	1.442(9)	C(41)-C(42)	1.365(10)
C(4)-C(5)	1.392(9)	C(41)-C(46)	1.373(10)
C(5)-C(6)	1.396(10)	C(42)-C(43)	1.395(11)
C(5)-C(21)	1.498(9)	C(43)-C(44)	1.360(13)
C(6)-C(7)	1.429(10)	C(44)-C(45)	1.363(12)
C(7)-C(8)	1.343(11)	C(44)-C(47)	1.519(12)
C(8)-C(9)	1.442(10)	C(45)-C(46)	1.378(10)
C(9)-C(10)	1.389(10)	C(51)-C(56)	1.364(10)
C(10)-C(11)	1.412(10)	C(51)-C(52)	1.397(10)
C(10)-C(31)	1.495(9)	C(52)-C(53)	1.377(10)
C(11)-C(12)	1.426(9)	C(53)-C(54)	1.384(12)
C(12)-C(13)	1.344(10)	C(54)-C(55)	1.369(12)
C(13)-C(14)	1.450(9)	C(54)-C(57)	1.500(10)
C(14)-C(15)	1.390(9)	C(55)-C(56)	1.383(11)
C(15)-C(16)	1.400(9)	C(61)-C(62)	1.461(12)
C(15)-C(41)	1.509(9)	C(62)-C(64)	1.479(14)
C(16)-C(17)	1.450(9)	C(62)-C(63)	1.526(16)
C(17)-C(18)	1.342(9)		
C(18)-C(19)	1.436(10)		
N(4)-Rh(1)-N(2)	172.2(2)	N(4)-C(16)-C(15)	125.3(6)
N(4)-Rh(1)-N(1)	90.5(2)	N(4)-C(16)-C(17)	108.9(5)
N(2)-Rh(1)-N(1)	89.9(2)	C(15)-C(16)-C(17)	125.5(6)
N(4)-Rh(1)-N(3)	89.6(2)	C(18)-C(17)-C(16)	107.5(6)
N(2)-Rh(1)-N(3)	90.2(2)	C(17)-C(18)-C(19)	107.2(6)
N(1)-Rh(1)-N(3)	179.2(2)	N(4)-C(19)-C(20)	125.0(6)
N(4)-Rh(1)-C(61)	99.9(3)	N(4)-C(19)-C(18)	109.6(6)
N(2)-Rh(1)-C(61)	87.8(3)	C(20)-C(19)-C(18)	125.3(6)
N(1)-Rh(1)-C(61)	89.1(3)	C(1)-C(20)-C(19)	124.4(6)
N(3)-Rh(1)-C(61)	90.1(3)	C(1)-C(20)-C(51)	117.5(6)
C(4)-N(1)-C(1)	106.6(5)	C(19)-C(20)-C(51)	118.1(6)
C(4)-N(1)-Rh(1)	127.0(4)	C(26)-C(21)-C(22)	117.5(7)

C(1)-N(1)-Rh(1)	125.5(4)	C(26)-C(21)-C(5)	120.8(6)
C(9)-N(2)-C(6)	106.9(6)	C(22)-C(21)-C(5)	121.7(6)
C(9)-N(2)-Rh(1)	126.7(5)	C(23)-C(22)-C(21)	121.8(7)
C(6)-N(2)-Rh(1)	126.4(5)	C(22)-C(23)-C(24)	120.7(7)
C(14)-N(3)-C(11)	107.1(5)	C(25)-C(24)-C(23)	117.7(7)
C(14)-N(3)-Rh(1)	125.6(4)	C(25)-C(24)-C(27)	121.7(8)
C(11)-N(3)-Rh(1)	126.1(4)	C(23)-C(24)-C(27)	120.6(8)
C(16)-N(4)-C(19)	106.4(5)	C(24)-C(25)-C(26)	120.9(8)
C(16)-N(4)-Rh(1)	126.6(4)	C(21)-C(26)-C(25)	121.3(8)
C(19)-N(4)-Rh(1)	126.8(4)	C(32)-C(31)-C(36)	117.5(7)
N(1)-C(1)-C(20)	125.4(6)	C(32)-C(31)-C(10)	120.9(7)
N(1)-C(1)-C(2)	108.7(6)	C(36)-C(31)-C(10)	121.6(7)
C(20)-C(1)-C(2)	125.8(6)	C(31)-C(32)-C(33)	121.3(8)
C(3)-C(2)-C(1)	107.3(6)	C(32)-C(33)-C(34)	121.2(8)
C(2)-C(3)-C(4)	108.1(6)	C(35)-C(34)-C(33)	117.6(7)
N(1)-C(4)-C(5)	124.9(6)	C(35)-C(34)-C(37)	120.9(9)
N(1)-C(4)-C(3)	109.2(6)	C(33)-C(34)-C(37)	121.5(9)
C(5)-C(4)-C(3)	125.8(6)	C(34)-C(35)-C(36)	121.7(9)
C(4)-C(5)-C(6)	125.0(6)	C(31)-C(36)-C(35)	120.7(8)
C(4)-C(5)-C(21)	117.3(6)	C(42)-C(41)-C(46)	118.1(7)
C(6)-C(5)-C(21)	117.7(6)	C(42)-C(41)-C(15)	120.3(6)
N(2)-C(6)-C(5)	125.5(6)	C(46)-C(41)-C(15)	121.6(6)
N(2)-C(6)-C(7)	109.2(6)	C(41)-C(42)-C(43)	120.3(8)
C(5)-C(6)-C(7)	125.1(7)	C(44)-C(43)-C(42)	121.2(8)
C(8)-C(7)-C(6)	107.5(7)	C(43)-C(44)-C(45)	118.2(7)
C(7)-C(8)-C(9)	107.8(6)	C(43)-C(44)-C(47)	121.0(9)
N(2)-C(9)-C(10)	126.3(6)	C(45)-C(44)-C(47)	120.8(9)
N(2)-C(9)-C(8)	108.5(6)	C(44)-C(45)-C(46)	121.1(8)
C(10)-C(9)-C(8)	125.1(6)	C(41)-C(46)-C(45)	121.0(7)
C(9)-C(10)-C(11)	123.9(6)	C(56)-C(51)-C(52)	117.8(6)
C(9)-C(10)-C(31)	117.5(6)	C(56)-C(51)-C(20)	122.2(6)
C(11)-C(10)-C(31)	118.6(6)	C(52)-C(51)-C(20)	120.0(6)
N(3)-C(11)-C(10)	125.9(6)	C(53)-C(52)-C(51)	120.8(7)
N(3)-C(11)-C(12)	109.5(6)	C(52)-C(53)-C(54)	121.2(8)
C(10)-C(11)-C(12)	124.6(6)	C(55)-C(54)-C(53)	117.3(7)
C(13)-C(12)-C(11)	107.6(6)	C(55)-C(54)-C(57)	121.8(9)
C(12)-C(13)-C(14)	107.1(6)	C(53)-C(54)-C(57)	120.9(9)
N(3)-C(14)-C(15)	126.0(6)	C(54)-C(55)-C(56)	122.1(8)

N(3)-C(14)-C(13)	108.6(6)	C(51)-C(56)-C(55)	120.8(7)
C(15)-C(14)-C(13)	125.2(6)	C(62)-C(61)-Rh(1)	122.4(6)
C(14)-C(15)-C(16)	123.4(6)	C(61)-C(62)-C(64)	113.3(9)
C(14)-C(15)-C(41)	118.9(6)	C(61)-C(62)-C(63)	109.1(9)
C(16)-C(15)-C(41)	117.7(6)	C(64)-C(62)-C(63)	104.8(10)

Symmetry transformations used to generate equivalent atoms: #1 -x+1,-y+1,-z

X-Ray Structure of Rh(t₄-CF₃pp)Bu (2d)

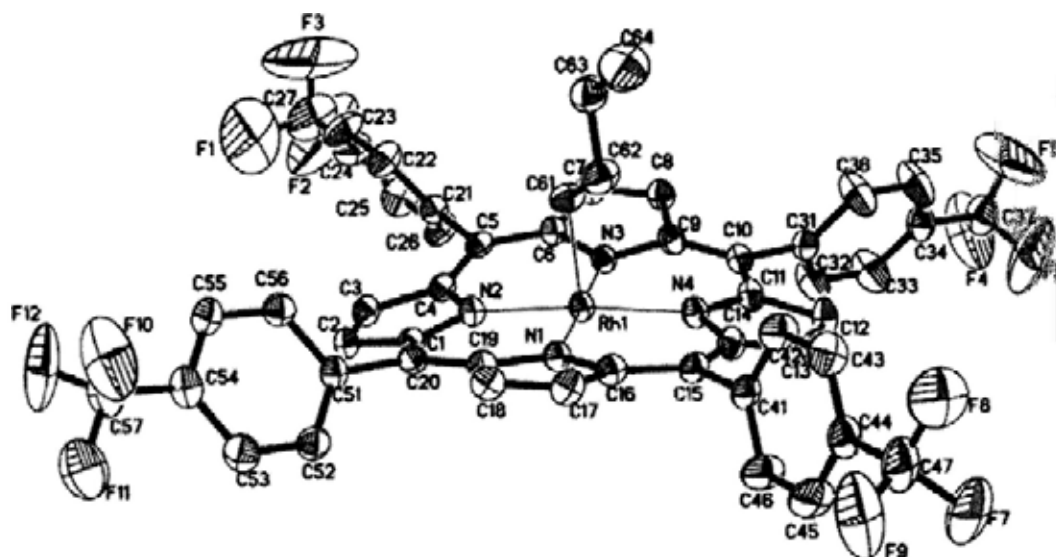


Figure 3 ORTEP drawing of Rh(t₄-CF₃pp) Bu **2d**, showing the atomic labeling scheme and 30% probability displacement ellipsoids.

Table 5 Crystal data and structure refinement for Rh(t₄-CF₃pp)Bu **2d**

Identification code	THL514
Empirical formula	C ₅₂ H ₃₃ F ₁₂ N ₄ Rh
Formula weight	1044.73
Temperature	293(2) K
Wavelength	0.71073 Å
Crystal system, space group	Triclinic, P-1
Unit cell dimensions	a = 9.729(4) Å alpha = 87.118 ^o (7) b = 15.530(6) Å beta = 72.788 ^o (7) c = 16.150(6) Å gamma = 77.894 ^o (8)
Volume	2278.9(15) Å ³
Z, Calculated density	2, 1.522 Mg/m ³

Absorption coefficient	0.466 mm ⁻¹
F(000)	1052
Crystal size	0.40 x 0.30 x 0.30 mm
Theta range for data collection	1.32 to 25.00 deg.
Limiting indices	-11<=h<=11, -17<=k<=18, -19<=l<=17
Reflections collected / unique	12063 / 7941 [R(int) = 0.0352]
Completeness to theta = 25.00	98.80%
Absorption correction	SADABS
Max. and min. transmission	1.0000 and 0.097403
Refinement method	Full-matrix least-squares on F ²
Data / restraints / parameters	7941 / 0 / 622
Goodness-of-fit on F ²	1.073
Final R indices [I>2sigma(I)]	R1 = 0.0669, wR2 = 0.1835
R indices (all data)	R1 = 0.0830, wR2 = 0.1970
Largest diff. peak and hole	1.075 and -1.051 e.A ⁻³

Table 6 Bond lengths [Å] and angles [deg] for Rh(t₄CF₃pp)Bu **2d**

Rh(1)-N(2)	2.004(5)	C(24)-C(25)	1.363(12)
Rh(1)-N(4)	2.019(5)	C(24)-C(27)	1.473(12)
Rh(1)-N(3)	2.024(5)	C(25)-C(26)	1.398(10)
Rh(1)-N(1)	2.030(5)	C(27)-F(3)	1.166(18)
Rh(1)-C(61)	2.051(7)	C(27)-F(2)	1.192(17)
N(1)-C(19)	1.371(7)	C(27)-F(1)	1.26(2)
N(1)-C(16)	1.378(7)	C(31)-C(32)	1.333(10)
N(2)-C(1)	1.377(7)	C(31)-C(36)	1.374(10)
N(2)-C(4)	1.379(7)	C(32)-C(33)	1.380(11)
N(3)-C(9)	1.376(7)	C(33)-C(34)	1.348(11)
N(3)-C(6)	1.379(7)	C(34)-C(35)	1.349(12)
N(4)-C(14)	1.378(8)	C(34)-C(37)	1.481(10)

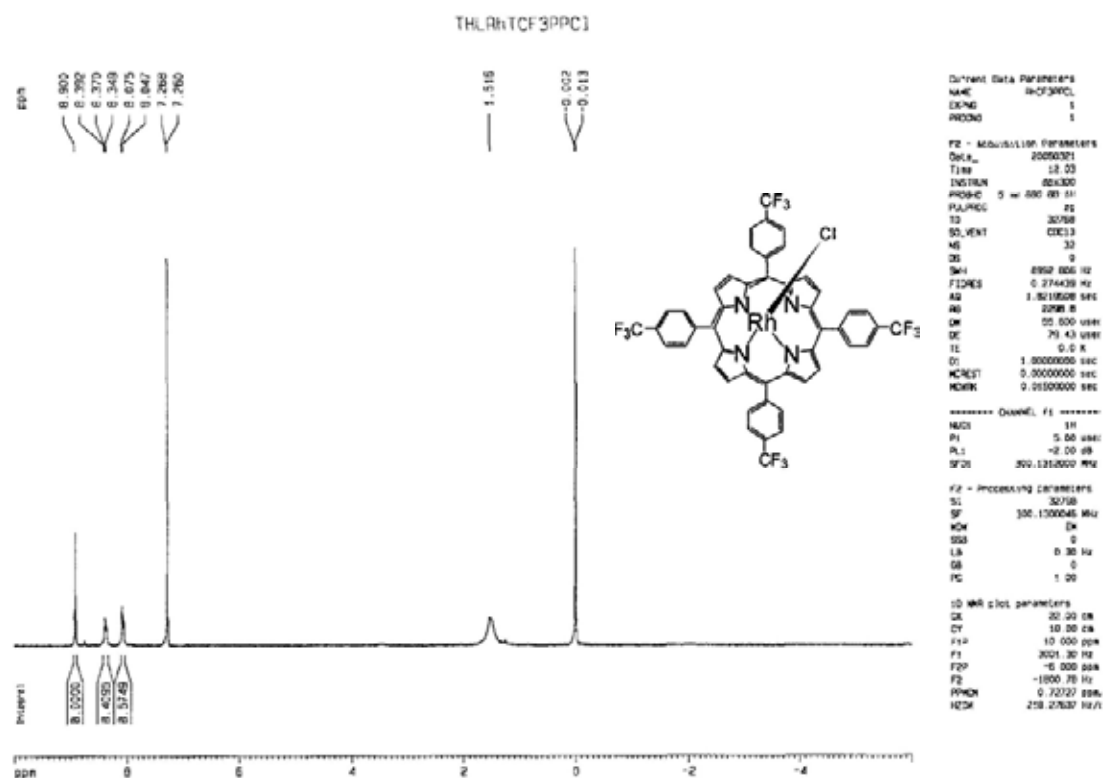
N(4)-C(11)	1.379(8)	C(35)-C(36)	1.389(11)
C(1)-C(20)	1.391(8)	C(37)-F(5)	1.214(12)
C(1)-C(2)	1.440(8)	C(37)-F(6)	1.215(12)
C(2)-C(3)	1.335(8)	C(37)-F(4)	1.250(12)
C(3)-C(4)	1.443(8)	C(41)-C(46)	1.362(10)
C(4)-C(5)	1.400(8)	C(41)-C(42)	1.378(10)
C(5)-C(6)	1.389(8)	C(42)-C(43)	1.397(9)
C(5)-C(21)	1.502(8)	C(43)-C(44)	1.347(11)
C(6)-C(7)	1.439(8)	C(44)-C(45)	1.370(12)
C(7)-C(8)	1.348(9)	C(44)-C(47)	1.509(10)
C(8)-C(9)	1.439(9)	C(45)-C(46)	1.400(10)
C(9)-C(10)	1.394(9)	C(47)-F(9)	1.276(11)
C(10)-C(11)	1.392(9)	C(47)-F(8)	1.307(12)
C(10)-C(31)	1.501(8)	C(47)-F(7)	1.322(11)
C(11)-C(12)	1.447(9)	C(51)-C(52)	1.376(9)
C(12)-C(13)	1.341(10)	C(51)-C(56)	1.394(9)
C(13)-C(14)	1.449(9)	C(52)-C(53)	1.358(10)
C(14)-C(15)	1.376(9)	C(53)-C(54)	1.402(11)
C(15)-C(16)	1.392(9)	C(54)-C(55)	1.368(10)
C(15)-C(41)	1.509(7)	C(54)-C(57)	1.480(10)
C(16)-C(17)	1.430(9)	C(55)-C(56)	1.368(9)
C(17)-C(18)	1.331(9)	C(57)-F(10)	1.270(10)
C(18)-C(19)	1.396(8)	C(57)-F(12)	1.280(11)
C(20)-C(51)	1.498(8)	C(57)-F(11)	1.299(12)
C(21)-C(22)	1.363(10)	C(61)-C(62)	1.474(9)
C(21)-C(26)	1.380(9)	C(62)-C(63)	1.461(11)
C(22)-C(23)	1.386(10)	C(63)-C(64)	1.504(12)
C(23)-C(24)	1.366(12)		
N(2)-Rh(1)-N(4)	174.4(2)	C(26)-C(21)-C(5)	121.3(6)
N(2)-Rh(1)-N(3)	90.21(18)	C(21)-C(22)-C(23)	121.0(7)
N(4)-Rh(1)-N(3)	89.96(19)	C(24)-C(23)-C(22)	119.9(8)
N(2)-Rh(1)-N(1)	89.50(18)	C(25)-C(24)-C(23)	119.8(7)
N(4)-Rh(1)-N(1)	90.41(19)	C(25)-C(24)-C(27)	119.7(10)
N(3)-Rh(1)-N(1)	179.12(19)	C(23)-C(24)-C(27)	120.5(10)
N(2)-Rh(1)-C(61)	90.8(2)	C(24)-C(25)-C(26)	120.6(7)
N(4)-Rh(1)-C(61)	94.8(3)	C(21)-C(26)-C(25)	119.4(7)
N(3)-Rh(1)-C(61)	88.3(2)	F(3)-C(27)-F(2)	105.2(18)
N(1)-Rh(1)-C(61)	90.9(2)	F(3)-C(27)-F(1)	105.5(18)

C(19)-N(1)-C(16)	107.1(5)	F(2)-C(27)-F(1)	95.9(16)
C(19)-N(1)-Rh(1)	125.8(4)	F(3)-C(27)-C(24)	117.2(14)
C(16)-N(1)-Rh(1)	125.4(4)	F(2)-C(27)-C(24)	118.3(14)
C(1)-N(2)-C(4)	106.6(5)	F(1)-C(27)-C(24)	112.1(15)
C(1)-N(2)-Rh(1)	127.1(4)	C(32)-C(31)-C(36)	117.6(7)
C(4)-N(2)-Rh(1)	126.3(4)	C(32)-C(31)-C(10)	120.6(6)
C(9)-N(3)-C(6)	106.9(5)	C(36)-C(31)-C(10)	121.8(6)
C(9)-N(3)-Rh(1)	126.3(4)	C(31)-C(32)-C(33)	122.0(8)
C(6)-N(3)-Rh(1)	125.8(4)	C(34)-C(33)-C(32)	120.4(8)
C(14)-N(4)-C(11)	106.9(5)	C(33)-C(34)-C(35)	118.9(7)
C(14)-N(4)-Rh(1)	126.2(4)	C(33)-C(34)-C(37)	120.2(8)
C(11)-N(4)-Rh(1)	126.5(4)	C(35)-C(34)-C(37)	120.8(8)
N(2)-C(1)-C(20)	124.9(5)	C(34)-C(35)-C(36)	120.4(8)
N(2)-C(1)-C(2)	108.8(5)	C(31)-C(36)-C(35)	120.5(8)
C(20)-C(1)-C(2)	125.8(5)	F(5)-C(37)-F(6)	103.7(12)
C(3)-C(2)-C(1)	108.0(5)	F(5)-C(37)-F(4)	105.9(11)
C(2)-C(3)-C(4)	107.3(5)	F(6)-C(37)-F(4)	98.4(11)
N(2)-C(4)-C(5)	125.2(5)	F(5)-C(37)-C(34)	116.3(9)
N(2)-C(4)-C(3)	108.9(5)	F(6)-C(37)-C(34)	115.0(8)
C(5)-C(4)-C(3)	125.7(5)	F(4)-C(37)-C(34)	115.4(9)
C(6)-C(5)-C(4)	124.5(5)	C(46)-C(41)-C(42)	119.0(6)
C(6)-C(5)-C(21)	118.4(5)	C(46)-C(41)-C(15)	121.1(6)
C(4)-C(5)-C(21)	117.1(5)	C(42)-C(41)-C(15)	119.9(6)
N(3)-C(6)-C(5)	124.9(5)	C(41)-C(42)-C(43)	120.2(7)
N(3)-C(6)-C(7)	109.0(5)	C(44)-C(43)-C(42)	120.0(7)
C(5)-C(6)-C(7)	126.0(6)	C(43)-C(44)-C(45)	120.8(6)
C(8)-C(7)-C(6)	107.3(6)	C(43)-C(44)-C(47)	119.6(8)
C(7)-C(8)-C(9)	107.7(6)	C(45)-C(44)-C(47)	119.6(8)
N(3)-C(9)-C(10)	125.8(6)	C(44)-C(45)-C(46)	119.0(8)
N(3)-C(9)-C(8)	108.8(5)	C(41)-C(46)-C(45)	120.8(7)
C(10)-C(9)-C(8)	125.4(6)	F(9)-C(47)-F(8)	110.2(9)
C(11)-C(10)-C(9)	124.3(6)	F(9)-C(47)-F(7)	105.1(9)
C(11)-C(10)-C(31)	117.7(5)	F(8)-C(47)-F(7)	102.7(8)
C(9)-C(10)-C(31)	117.9(5)	F(9)-C(47)-C(44)	113.3(7)
N(4)-C(11)-C(10)	125.6(6)	F(8)-C(47)-C(44)	114.0(8)
N(4)-C(11)-C(12)	108.9(6)	F(7)-C(47)-C(44)	110.7(8)
C(10)-C(11)-C(12)	125.4(6)	C(52)-C(51)-C(56)	118.2(6)
C(13)-C(12)-C(11)	107.6(6)	C(52)-C(51)-C(20)	122.5(6)

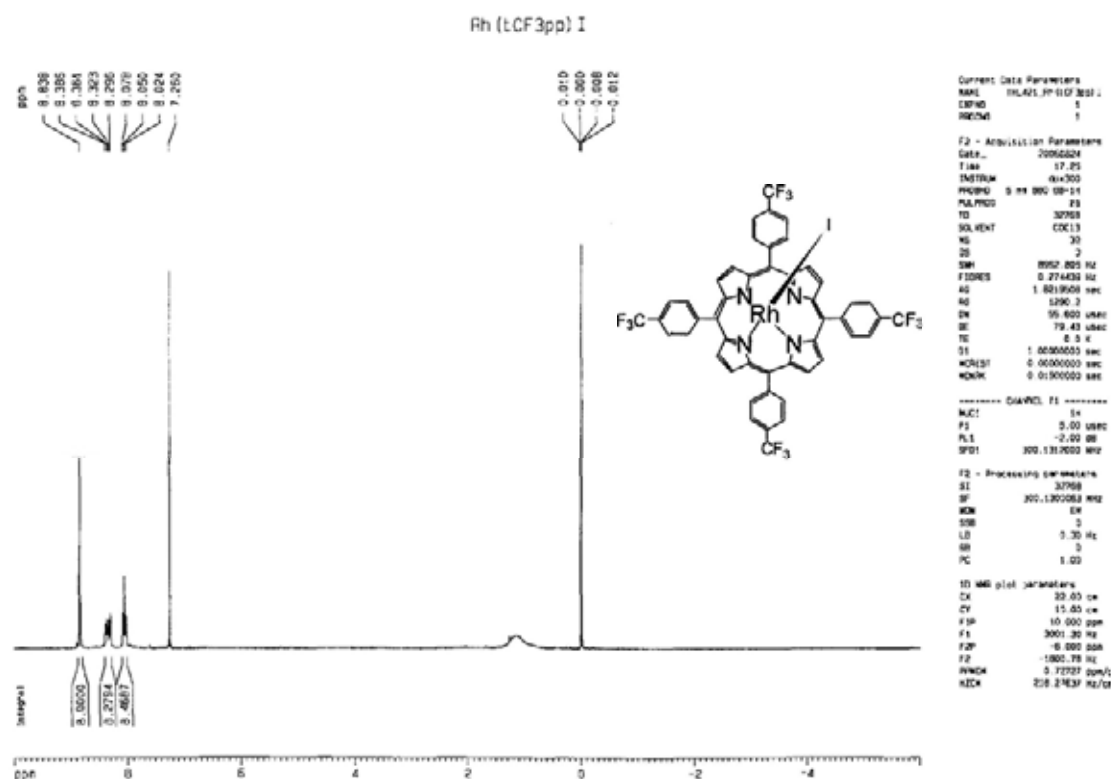
C(12)-C(13)-C(14)	107.5(6)	C(56)-C(51)-C(20)	119.2(6)
C(15)-C(14)-N(4)	125.7(5)	C(53)-C(52)-C(51)	121.7(7)
C(15)-C(14)-C(13)	125.4(6)	C(52)-C(53)-C(54)	119.7(7)
N(4)-C(14)-C(13)	108.9(5)	C(55)-C(54)-C(53)	119.0(6)
C(14)-C(15)-C(16)	125.5(5)	C(55)-C(54)-C(57)	119.7(8)
C(14)-C(15)-C(41)	118.4(5)	C(53)-C(54)-C(57)	121.3(7)
C(16)-C(15)-C(41)	116.0(5)	C(54)-C(55)-C(56)	120.9(7)
N(1)-C(16)-C(15)	125.3(5)	C(55)-C(56)-C(51)	120.4(6)
N(1)-C(16)-C(17)	108.7(5)	F(10)-C(57)-F(12)	111.1(10)
C(15)-C(16)-C(17)	126.0(5)	F(10)-C(57)-F(11)	100.6(8)
C(18)-C(17)-C(16)	107.9(5)	F(12)-C(57)-F(11)	102.3(9)
C(17)-C(18)-C(19)	107.9(6)	F(10)-C(57)-C(54)	113.7(8)
N(1)-C(19)-C(20)	125.4(5)	F(12)-C(57)-C(54)	114.7(7)
N(1)-C(19)-C(18)	108.4(5)	F(11)-C(57)-C(54)	113.1(8)
C(20)-C(19)-C(18)	126.2(6)	C(62)-C(61)-Rh(1)	119.5(5)
C(1)-C(20)-C(19)	123.9(5)	C(63)-C(62)-C(61)	116.0(7)
C(1)-C(20)-C(51)	118.4(5)	C(62)-C(63)-C(64)	116.6(8)
C(19)-C(20)-C(51)	117.6(5)		
C(22)-C(21)-C(26)	119.3(6)		
C(22)-C(21)-C(5)	119.3(6)		

Symmetry transformations used to generate equivalent atom: #1 -x+1,-y+1,-z

^1H NMR of $\text{Rh}(\text{t-CF}_3\text{pp})\text{Cl}$ (2b) in CDCl_3

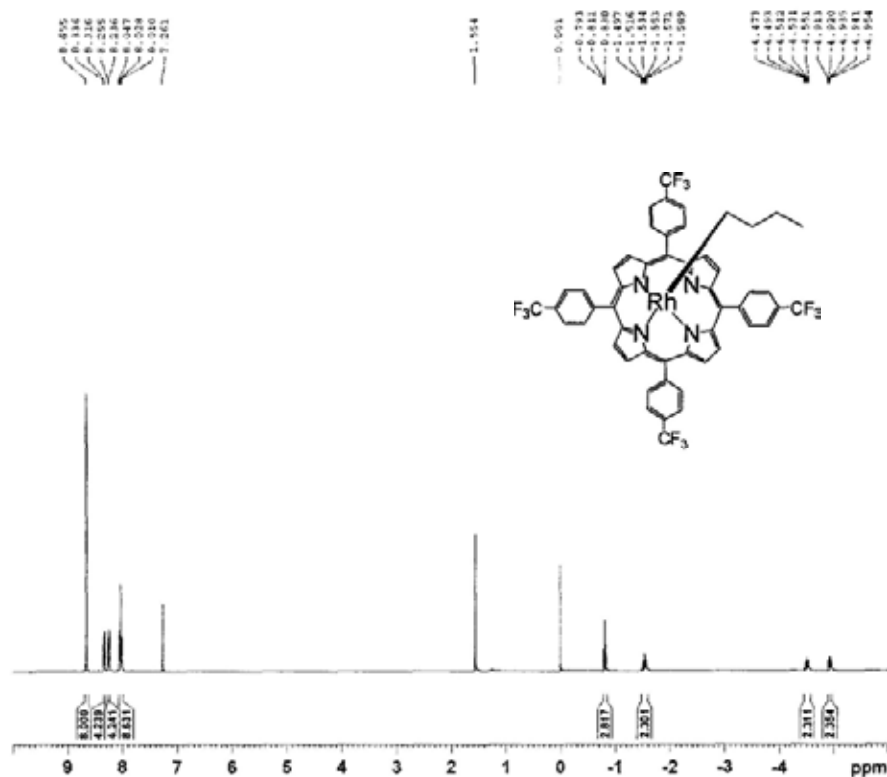


^1H NMR of $\text{Rh}(\text{t-CF}_3\text{pp})\text{I}$ (2c) in CDCl_3



¹H NMR of Rh(t₄-CF₃pp)Bu (2d) in CDCl₃

THL514_Rh(t-CF3pp)(CDCl2/CH2Cl)



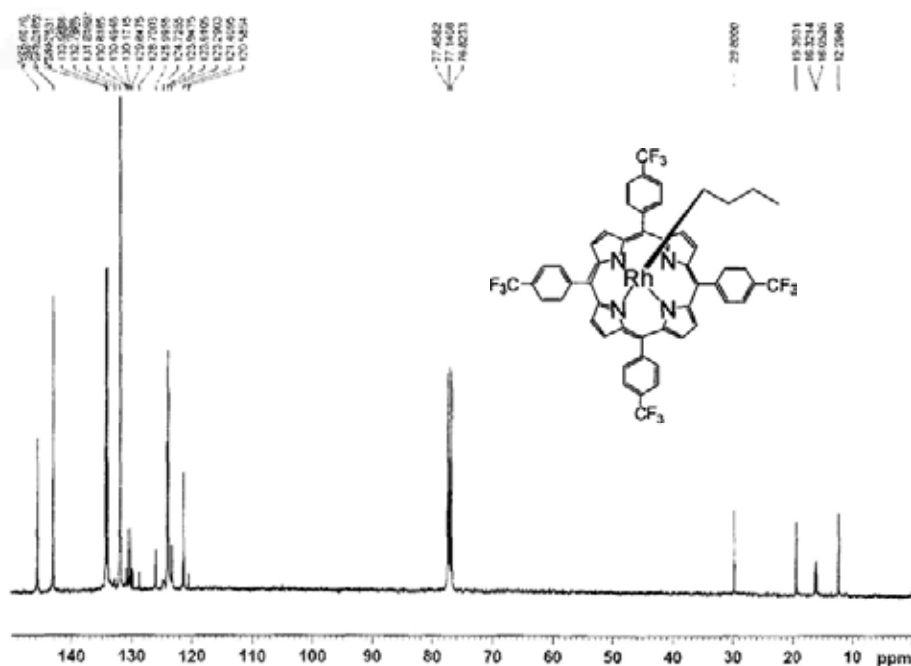
Bruker Advance III 400 NMR

NAME	THL514
EXPNO	1
PROCNO	1
DATE_	20090525
TIME	16.07
PROBHD	5mm BBO1 HX
PULPROG	zgpg30
TD	65536
F2	CC13
RG	64
SD	0
SWH	34282.539 Hz
FIDRES	0.635527 Hz
AQ	0.6258281 sec
RG	201
SI	12.000 MHz
OR	6.50 mmol
TE	281.4 K
D1	1.0500000 sec
TD0	1

***** CHANNEL f1 *****	
NUC1	13C
P1	7.10 mmol
PL1	-2.00 dB
PL1F	13.1719412 Hz
RF1	400.126200 MHz
SI	45036
DF	400.126200 MHz
WDW	EM
SSB	0
LB	9.30 Hz
GB	0
PC	1.00

¹³C NMR of Rh(t₄-CF₃pp)Bu (2d) in CDCl₃

THL_514_C13

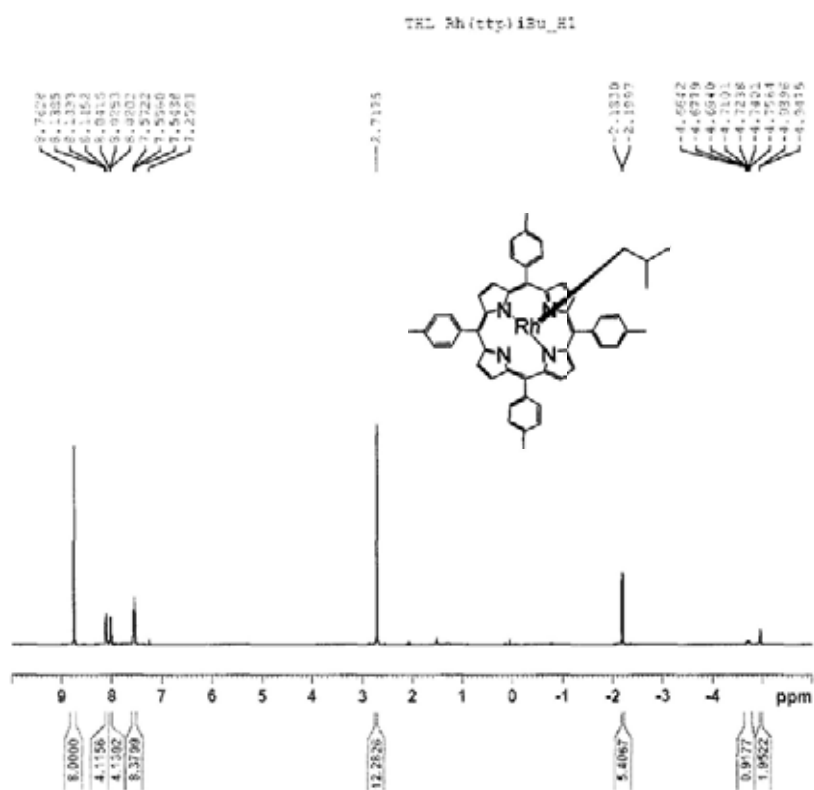


Bruker Advance III 400

NAME	THL_514_C13
EXPNO	1
PROCNO	1
DATE_	20090525
TIME	17.50
PROBHD	5 mm BBO1 HX
PULPROG	zgpg30
TD	65536
F2	CC13
RG	64
SD	0
SWH	25282.539 Hz
FIDRES	0.132641 Hz
AQ	2.182781 sec
RG	201
SI	10.000 MHz
OR	6.50 mmol
TE	281.4 K
D1	1.0500000 sec
TD0	1

***** CHANNEL f1 *****	
NUC1	13C
P1	14.00 mmol
PL1	-2.00 dB
PL1F	10.1319412 Hz
RF1	100.626100 MHz
SI	45036
DF	100.626100 MHz
WDW	EM
SSB	0
LB	9.30 Hz
GB	0
PC	1.00

¹H NMR of Rh(ttp)^tBu (3k) in CDCl₃



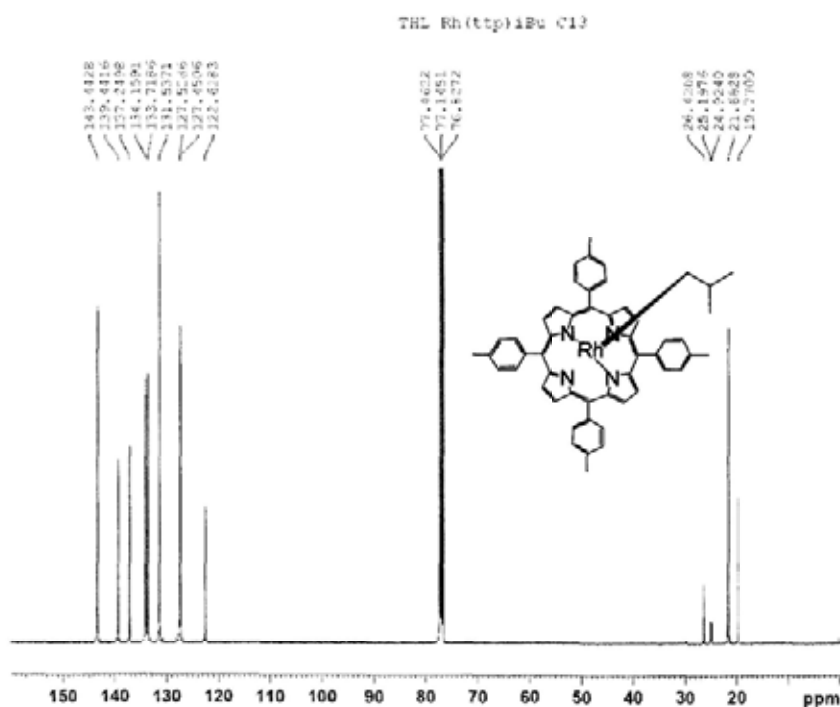
===== CHANNEL 1 =====
NAME THL Rh(ttp)^tBu_H1
EXPNO 1
PROCNO 1

F2 - Acquisition Parameters
Date_ 20090712
Time 19.31
INSTRUM spect
PROBHD 5 mm QNP1H 13C
PULPROG zgpg30
TD 65536
SOLVENT CDCl3
NS 32
DS 4
SWH 10019.230 Hz
FIDRES 0.180399 Hz
AQ 2.7248471 sec
RG 50.8
DM 41.400 usec
DE 4.50 usec
TE 298.2 K
SE 1.0000000 sec
SI 1.0000000 sec
TD 1

===== CHANNEL 2 =====
NUC1 1H
P1 14.67 usec
PC1 0 dB
PL1 -1.4000000 W
RF1 400.1500000 MHz

F2 - Processing parameters
SI 4096
SF 400.1500000 MHz
WDW EM
SSB 0
GB 0.31 Hz
CB 0
PC 1.01

¹³C NMR of Rh(ttp)^tBu (3k) in CDCl₃



===== CHANNEL 1 =====
NAME THL Rh(ttp)^tBu_C13
EXPNO 1
PROCNO 1

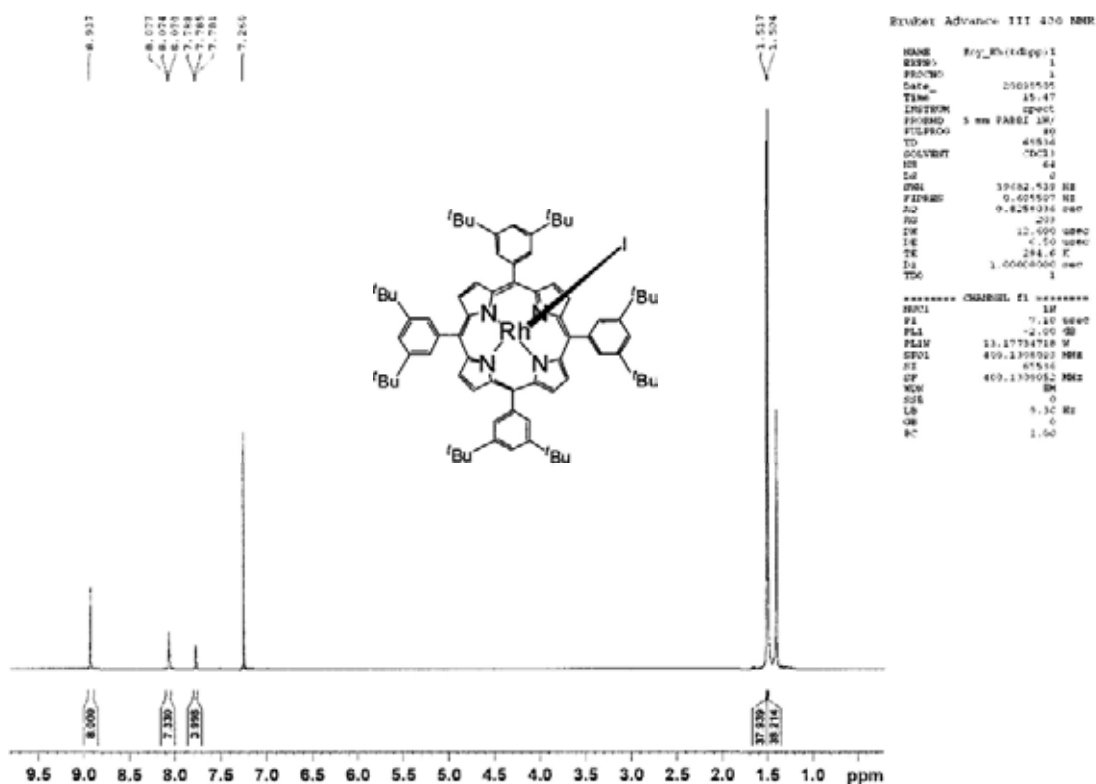
F2 - Acquisition Parameters
Date_ 20090712
Time 19.43
INSTRUM spect
PROBHD 5 mm QNP1H 13C
PULPROG zgpg30
TD 65536
SOLVENT CDCl3
NS 32
DS 4
SWH 10019.461 MHz
FIDRES 0.180734 MHz
AQ 2.7253584 sec
RG 50.8
DM 41.400 usec
DE 4.50 usec
TE 298.2 K
SE 1.0000000 sec
SI 1.0000000 sec
TD 1

===== CHANNEL 2 =====
NUC1 13C
P1 9.00 usec
PC1 0 dB
PL1 -1.4000000 W
RF1 100.6200000 MHz

F2 - Processing parameters
SI 4096
SF 100.6200000 MHz
WDW EM
SSB 0
GB 1.00 Hz
CB 0
PC 1.40

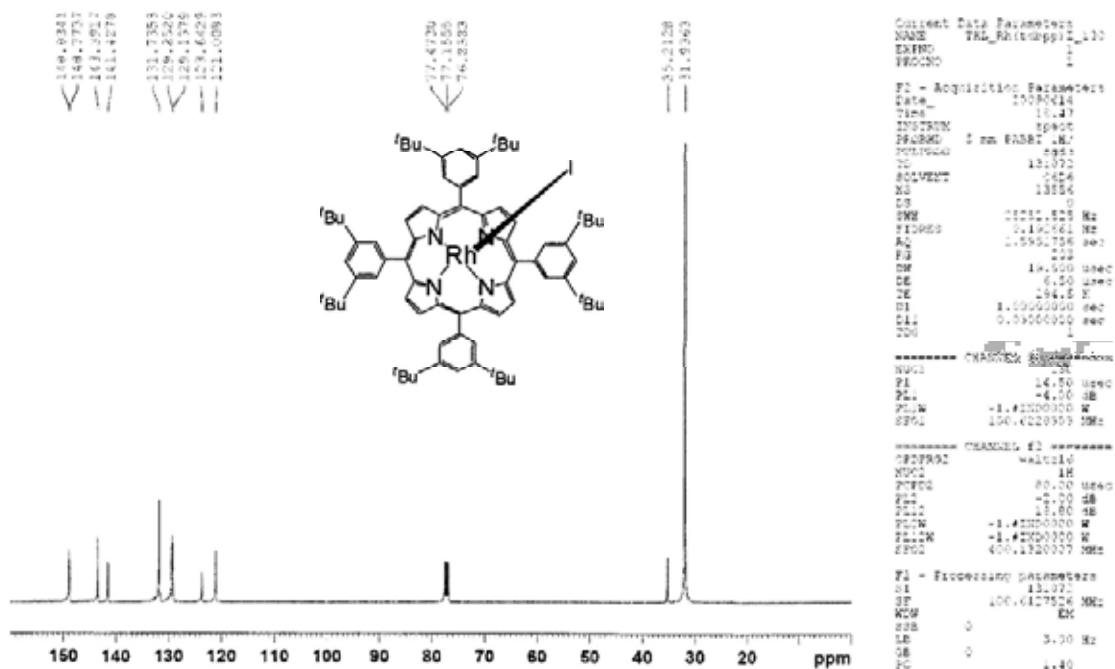
¹H NMR of Rh(tdbpp)I (4b) in CDCl₃

Roy_Rh(tdbpp)I

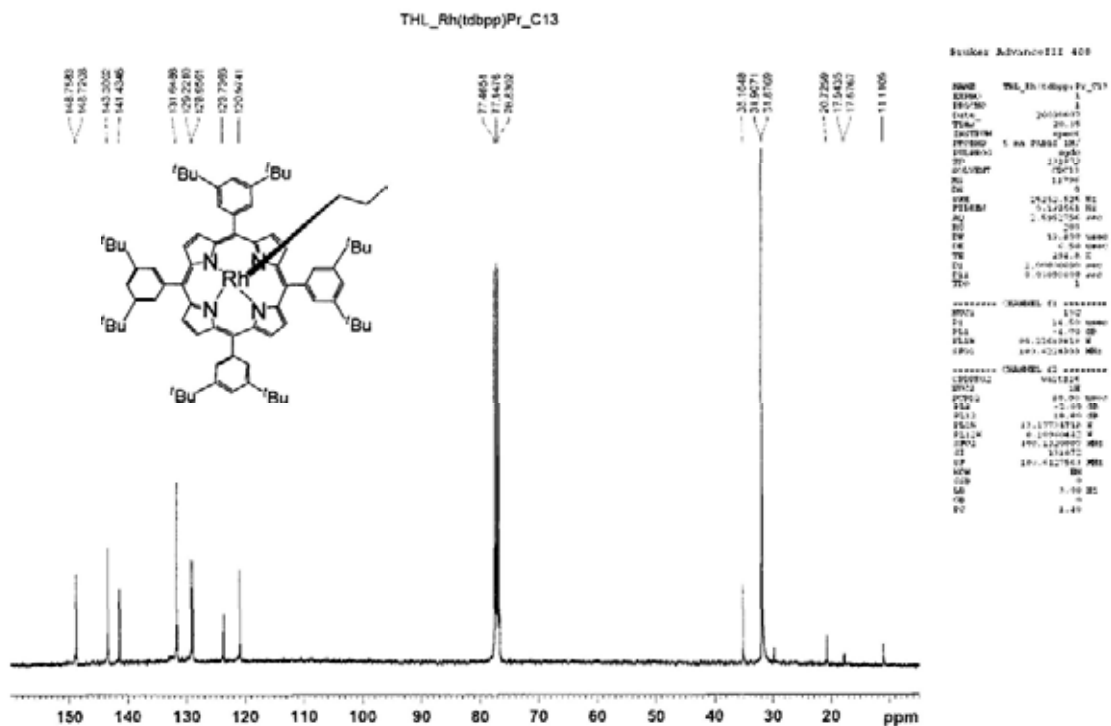


¹³C NMR of Rh(tdbpp)I (4b) in CDCl₃

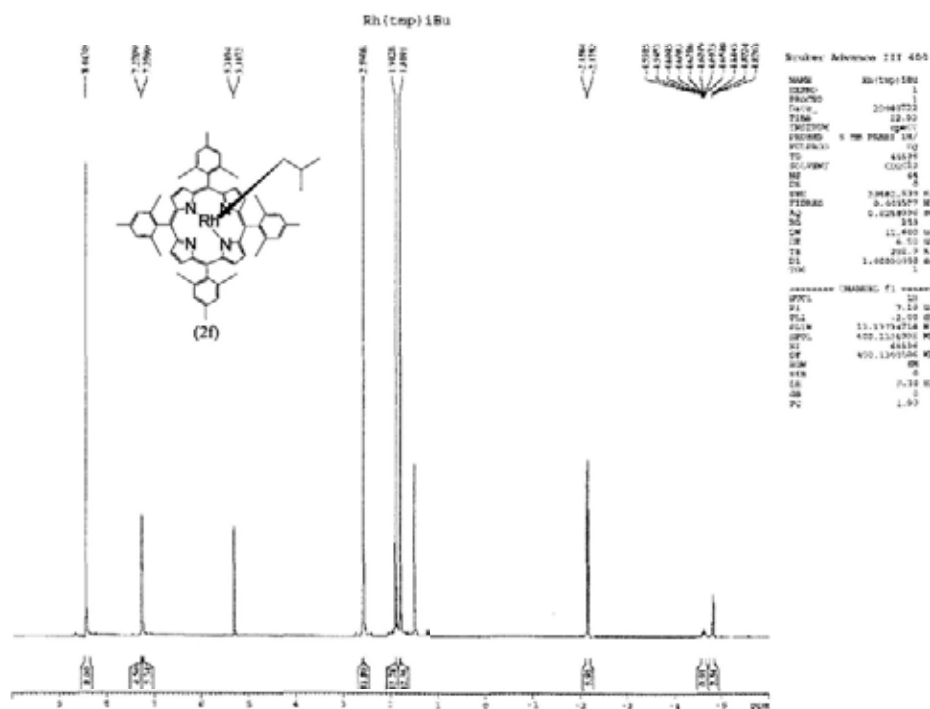
Rh(tdbpp)I_1



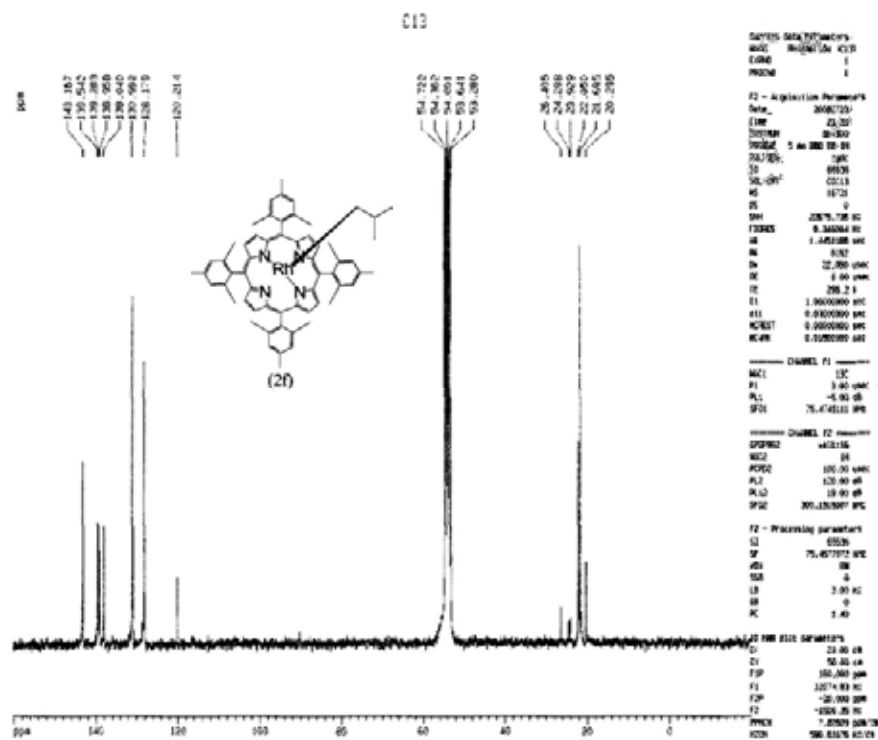
^{13}C NMR of $\text{Rh}(\text{tdbpp})\text{CH}_2\text{CH}_2\text{CH}_3$ (4e) in CDCl_3



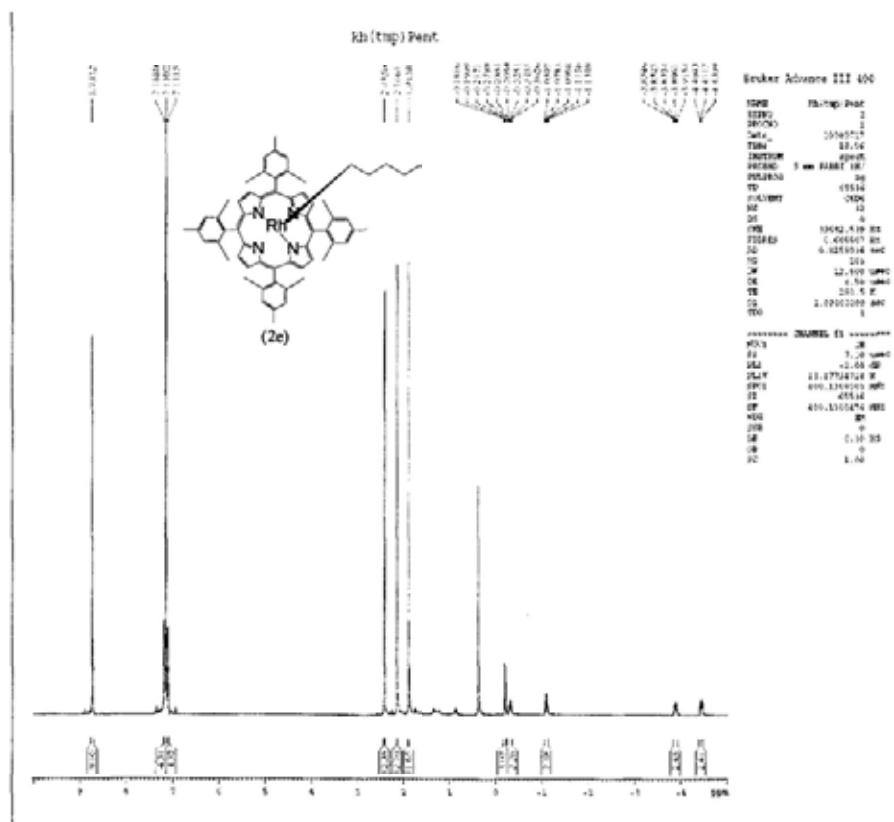
^1H NMR of $\text{Rh}(\text{tmp})^i\text{Bu}$ (5d) in CD_2Cl_2 .



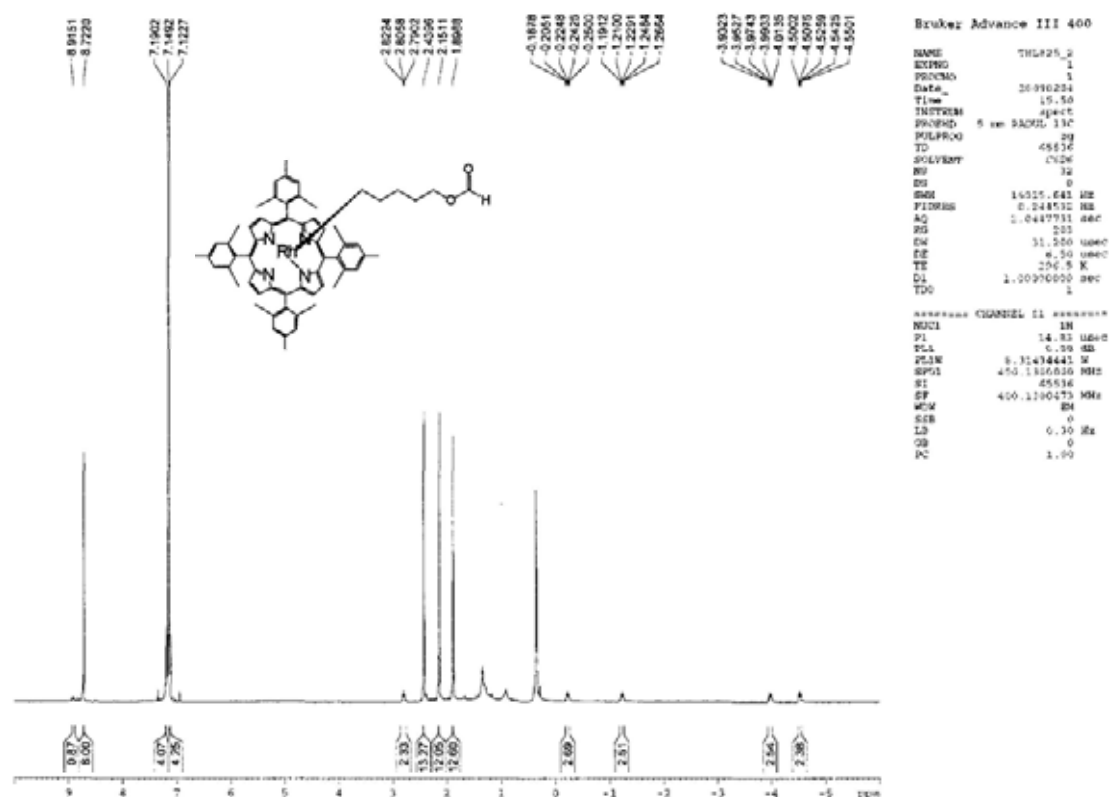
^{13}C NMR of $\text{Rh}(\text{tmp})^t\text{Bu}$ (5d) in CD_2Cl_2



^1H NMR of $\text{Rh}(\text{tmp})\text{Pent}$ in C_6D_6 (5e).



¹H NMR of Rh(tmp)CH₂CH₂CH₂CH₂CH₂OCHO (5j) in C₆D₆



¹³C NMR of Rh(tmp)CH₂CH₂CH₂CH₂CH₂OCHO (5j) in CDCl₃

